The role of *LRRK2* in the pathogenesis of Parkinson's disease

Stavroula Petridi

PhD

University of York

Biology

June 2017

Abstract

The *G2019S* mutation within the *LRRK2* gene, is the most common genetic cause of Parkinson's, being responsible for 20-40% of all familial PD cases, depending on the population under study. The actual function of the LRRK2 protein is not yet clear, although it has been implicated in several pathways including synaptic vesicle regulation, endocytosis and membrane trafficking. The gain of function *G2019S* mutation increases the kinase activity of the LRRK2 protein, contributing to the pathogenesis of PD. Several hypotheses exist on how *G2019S* contributes to PD, including regulation of dopamine metabolism and/or several Rab proteins, which have been identified as binding LRRK2, but the exact Rab is not consistent. Using the *Drosophila* visual system as an *in vivo* model, these hypotheses were addressed. HPLC analysis established that young flies expressing *LRRK2-G2019S* in their dopaminergic neurons (*TH>G2019S* flies) have lower levels of dopamine than control flies. In addition, inhibition of dopamine release by tetanus toxin showed an increase in visual sensitivity in control and old *TH>G2019S* flies, while young *TH>G2019S* flies showed a decrease in visual responses. Furthermore, new transgenic flies were generated, *LexAop-LRRK2* and *LexAop-G2019S*, giving us the opportunity to use the *Gal4* and *LexA* binary expression systems simultaneously at the same animal. Additionally, the expression protein levels of LRRK2 and G2019S were examined, indicating that LRRK2 is consistently expressing at higher levels than G2019S. That indicates that the kinase activity of the LRRK2 protein plays a vital role on the protein levels expression. Finally, the genetic screening that was performed in order to identify LRRK2-substrates *in vivo* identified six Rab proteins. Among those were *Rab3*, *Rab5*, *Rab9*, *Rab10*, *Rab18* and *Rab40*, while *Rab1* and *Rab19* were identified interacting with the dopaminergic neurons of the flies. Overall, this study confirms the early hyperactivity in young *TH>G2019S* flies that could trigger the beginning of neurodegeneration, which is the hallmark of Parkinson's.

Table of Contents

List of Tables and Figures

Tables

Figures

Acknowledgments

I would like to take this opportunity to thank everyone that has supported me throughout the course of my PhD.

Firstly, I would like to thank my supervisor Dr Chris Elliott for his constant support, patience, encouragement and expert guidance throughout my PhD. Secondly, I would like to thank the members of my Thesis Advisory Panel, Dr Sangeeta Chawla and Prof Antony Morland for their constructive advice and discussions of my work. I would also like to thank Dr Sean Sweeney, who was always available with his support and advice.

I would also like to extend my thanks to all the members of both the Elliott and Sweeney labs, who were always there to offer advice, willing to discuss and make the PhD life much easier. More specifically, I would like to mention Dr Ryan West, Amy Cording, Dr Rebecca Furmston, Dr Nathan Garnham and Laura Fort, to each one of them I am really grateful.

Moreover, I would like to thank my friends, especially those in York, and more specifically Konstantinos and Paolina, who have made my time here a very enjoyable experience. They were always there to listen to my moaning and help me out on days that weren't going so well. Moreover, I am grateful to all the friends I have made from the Latin American Society at the University of York, and especially Ivan and Kuntal, who were always there reminding me that there is also life besides the PhD.

Finally, I would like to thank my family, my mum, my sister and Leonidas, for supporting me in all of my decisions, believing in me and always being by my side even though we were many miles away. On a more personal note, I would like to dedicate this PhD to the memory of my dad, who even though is not around me anymore to see me finishing my PhD, he helped me become the person I am today and I hope he would be proud of me.

Declaration

I declare that this thesis is a presentation of original work and I am the sole author. This work has not previously been presented for an award at this, or any other, University. All sources are acknowledged as References.

1. Introduction

A major problem in Parkinson's disease (PD) is to understand the mechanism(s), which lead to neuropathology and loss of brain function. This thesis focuses on the most common known cause of Parkinson's, mutations in the *LRRK2* (leucine rich repeat kinase) gene. Although this gene was identified nearly 15 years ago, its cellular location, function and binding partners are all still unknown. Here I explore how mutations in *LRRK2* regulate dopamine, a neurotransmitter affected in PD, and Rab proteins, proposed as a possible target of the LRRK2 enzyme. To facilitate this, the fly model of *LRRK2* was deployed, as this has been shown to recapitulate many of the features of PD.

1.1 Parkinson's disease (PD)

1.1.1 Overview of PD:

"Neurodegenerative disorder" is an umbrella term for a wide variety of conditions, in which the neurons in the human brain are lost. PD is the second most common neurodegenerative disease in the developed world after Alzheimer disease, with its prevalence estimated being 6.3 million people worldwide. In the UK alone, more than 120,000 people have been reported suffering from PD, and this prevalence is set to rise in the years to come because of our ageing population.

PD was first described in 1817 by the physician James Parkinson as 'the shaking palsy' based on the motor symptoms of the disorder. Over time, a more well rounded picture of the clinical phenotype of the disease emerged, revealing that it actually is a multisystem disorder (Archibald et al., 2009).

1.1.2 Clinical presentation of PD

Clinically PD is heterogeneous and many subtypes may be recognised on the basis of age of onset, predominant clinical features and progression rate. There are two major clinical subtypes existing including a tremor-predominant form that is mostly observed in younger people, and a "postural imbalance and gait

disorder" (PIGD) that is usually observed in older people (>70 years old) (Obeso et al., 2010). It is widely accepted that people with PD suffer both from motor and non-motor symptoms, as described in further detail below.

1.1.3 Motor symptoms

The main clinical manifestations of the disease include tremor, rigidity, bradykinesia and postural instability. As the most apparent symptom, patients afflicted with PD present with tremor. This is typically evident at rest (resting tremor), when the limb is relaxed and usually disappears with voluntary movement and sleep. Bradykinesia, also known as slowness of movement, is another manifestation of the disease, which appears being the most disabling symptom in the early stages of the disease, as well as rigidity, which is resistance to limb movements. Postural instability, leading to impaired balance, festinating gait, which mostly includes abnormal walking pattern and stiffness in walk, and facial motion are less common characteristics of the disease (Andalib et al., 2014).

1.1.4 Non-motor symptoms

Even though the motor symptoms of PD are well defined, the non-motor features are most of the time under-estimated and subsequently under-treated. Non-motor symptoms and their management have been recognized by the UK National Institute for Clinical Excellence as an important unmet need in PD (Parkinson's Disease, 2006). It has been estimated that 62% of non-motor symptoms of PD might remain undeclared to health-care professionals because the patients might be embarrassed or even unaware that these symptoms can be linked to PD (Mitra et al., 2008). The lack of recognition and treatment of those symptoms have important therapeutic and societal implications, as when they are left untreated they have a huge effect on the quality of life. A large range of symptoms comprise the non-motor symptom complex of PD, as they are summarized on Table 1.1 (Chaudhuri et al., 2009).

Table 1.1: Non-motor symptoms of Parkinson's disease

Neuropsychiatric symptoms	Depression, Apathy, Anxiety Cognitive dysfunction Dementia Attention deficit Hallucinations, Illusions Panic attacks
Sleep disorders	Insomnia Restless legs and periodic limb movements REM behavior disorder Vivid dreaming
Autonomic symptoms	Bladder disturbances Sweating Orthostatic hypotension Erectile impotence
Gastrointestinal symptoms	Dribbling of saliva Ageusia Nausea Constipation
Sensory symptoms	Pain Olfactory disturbance Visual dysfunction (contrast sensitivity, colour vision)

The non-motor symptoms of PD occur not only in advanced stages of the disease but also in early stages, and include olfactory deficits, constipation, rapid-eye movement (REM) and depression. These might precede the expression of the motor symptoms even by a whole decade (Chaudhuri et al., 2006, Naidu and Chaudhuri 2008).

1.1.5 Pathophysiology of PD

The hallmark of PD is the progressive loss of the melanised dopaminergic neurons in the substantia nigra pars compacta (SNpc) with an intact striatum, the area to which the SNpc normally project. Other sets of neurons are also lost, but the loss of SNpc is extremely dramatic and is the major pathological event linked to the movement disorder seen in PD clinically. However, cell death alone is not sufficient for pathological diagnosis. This pathology is usually accompanied by the presence of Lewy bodies and Lewy neurites, with the Lewy bodies being intracellular accumulations of the protein alpha-*synuclein*, in a fibrillar form. Lewy bodies themselves are not truly diagnostic for PD as they are found in other disorders as well. For example, Lewy bodies are also present in cognitive disorders such as Alzheimer's disease. However, we have a two-part, additive logic for the neuropathology of PD; Lewy bodies and nigral cell loss are both required. Although, there are overlaps in the syndromes, the definitional approach cleanly delimits what PD is and what it isn't. The loss of dopaminergic neurons leads to the loss of dopamine release in the striatal projection areas of these neurons. That has as a result the typical motor dysfunction, which only becomes evident when approximately 80% of striatal dopamine and 50% of nigral neurons are lost (Cookson et al., 2008). In contrast, PD is very poorly understood from an etiological viewpoint.

1.1.6 Medical treatment of PD

Over the past half century, an enormous progress has been made in the treatment of PD, but levodopa (L-DOPA) remains the most potent drug for controlling PD symptoms (Jankovic 2008). Each patient's therapy can be individualized, and diverse drugs other than levodopa are presently available. Among these drugs are dopamine agonists, catechol-o-methyl-transferase (COMT) inhibitors and nondopaminergic agents. Head-to-head comparisons of drugs within classes are rare, and the differences that have emerged are related to the effects on motor fluctuations, dyskinesias, on/off times and adverse effects of the specific agents within each class (Jankovic and Aguilar 2008).

At the moment, L-DOPA, is mainly used in order to alleviate the symptoms of the disorder, but is frequently associated with motor complications, such as fluctuations and dyskinesias or other complications after 5 years of treatment (Jankovic 2005). For that reason, there is currently a debate on when in the course of PD is more appropriate to initiate levodopa therapy (Stern 2004; Weiner 2004). The addition of carbidopa, which is a peripheral dopa decarboxylase inhibitor, enhances the therapeutic benefits of levodopa. In patients who are sensitive to peripheral side effects, including vomiting and nausea, additional carbidopa can be added to the conventional carbidopa/levodopa preparation. The most common problem in patients taking levodopa is delayed onset of response after injecting a dose of levodopa. Another problem is different types of levodopa-induced dyskinesias including "peak-dose dyskinesias" and "wearing-off" dyskinesias (Fahn 2000; Jankovic 2002). That raises concern, as young-onset PD patients seem particularly likely to develop levodopa-induced dyskinesias.

Due to these side-effects of levodopa experts recommend the delay of levodopa until the symptoms of parkinsonism are affecting the quality of every day life of the patients. Indeed, many clinicians recommend using dopamine (DA) agonists as the initial dopaminergic therapy (Jankovic 2000). DA agonists exert their pharmacologic effect by directly activating DA receptors, bypassing the presynaptic synthesis of DA (Jankovic and Aguilar 2008).

In addition to the dopaminergic drugs, nondopaminergic drugs are being prescribed as well, such as anticholinergics and amantadine, as they can provide satisfactory symptoms relief at the early stages of the disease. The anticholinergic drugs are very useful in younger patients who are primary bothered by tremor. Even though they are quite effective, their usefulness is limited by the anticholinergic side effects including cognitive impairment, dry mouth and urinary problems.

Finally, there are several surgical options in order to treat the movement symptoms. Besides thalamotomy and pallidotomy, another promising surgical approach for the treatment of tremors and other movement disorders is high-

frequency deep brain stimulation (DBS) via electrodes implanted in the ventral intermediate (VIM) nucleus of the thalamus, globus pallidus (GPi), subthalamic nucleus (STN) or other subcortical nuclei. DBS surgery improves parkinsonian symptoms and prolongs the "on" time (Linazasaro 2003), along with other aspects of the quality of life (Diamond and Jankovic 2005).

1.1.7 Epidemiology of PD

PD was commonly considered to be "simply" an environmentally caused disorder in the 1970s and 1980s, although its pattern of familial inheritance has been recognized since the time of the French physician, Charcot. In recent years, several monogenic mutations were identified causing PD, but these mutations likely count only for a small proportion of PD cases. The large majority of cases are sporadic in nature with the most common risk factor being ageing. Insights into non-genetic causes are needed in order to advance our knowledge and understanding of the pathogenesis of the disease so more effective therapeutic interventions can been discovered. The global burden of PD is set to rise in the years to come because of our ageing population. In a recent study on the world's 10 and Western Europe's 5 most populous nations, it was estimated that the number of people with PD will rise from 4.1 to 4.6 million in 2005 by two times to 8.7 to 9.3 million in the year 2030. Moreover, six of the most populous countries are in Asia (China, India, Indonesia, Pakistan, Bangladesh and Japan) and the number of PD patients is expected to rise from 2.57 million in 2005 to 6.17 million in 2030 (Dorsey et al., 2007).

Many epidemiological studies are undertaken nowadays in order to explore the association between PD and various demographic and environmental factors as is indicated in the following summary table (Table 1.2).

Table 1.2: Epidemiological factors associated with PD (Tan 2013)

	Factors	Risk of PD
Demographic factors	Age	↑
	Gender	Male ↑
Lifestyle factors	Smoking	↓
	Caffeine	↓
	Alcohol	↓
	Tea	↓
	Physical activity	↓
	Obesity	↑
Occupational factors	Pesticide	↑
	Heavy metal exposure	↑
	Head injury	↑
Dietary factors	Diary products/milk	↑
	Uric acid	↓
	Carbohydrates	↑
	Fat	↑
	Cholesterol	↑
	Iron	↑
Pharmacological factors	Oestrogens	↓
	Statins	↓

Tan et al. (2013) summarized the convincing evidence that alcohol, smoking and increased caffeine intake, are associated with a reduced risk of developing PD. Moreover, pesticide use and increased intake of dairy products are associated with increased risk of PD. However, it is important to bear in mind that the association of epidemiological factors with PD does not equate to causation or protection. These factors however provide important clues to direct further clinical and basic science studies so that the underlying pathogenic mechanisms behind PD can be unraveled.

1.2 Genetic background of PD

Although studies based on these environmental factors are beginning to illuminate the mechanisms of idiopathic PD, more tremendous progress has been made with modeling the genetic forms of PD. This began with a linkage analysis study in 1996, with an Italian family with an autosomal dominant form of early onset PD (Polymeropoulos et al., 1996). In this, α-*synuclein* (*SNCA*) was identified as the causative gene of PD. This was supported by immunocytochemical studies, which identified α-*synuclein* as a component of the Lewy Bodies (Spillantini et al., 1998). Following this, and the recognition of early-onset, familial forms of the disease, and the identification of gene mutations that cause rare familial forms of PD (Table 1.3), more common highly penetrant mutations were identified in late onset PD. Most recently, Genome Wide Association Studies (GWAS) approaches identified moderate risk variants, and mapped multiple low risk conferring loci (Houlden & Singleton 2012). GWAS is considered as a breakthrough in human genetics as it marked the end of wholescale candidate gene association studies and linkage analysis studies, which were based on function. GWAS provide a very efficient method to identify common genetic loci in a genome-wide manner.

Table 1.3 Monogenic loci for Parkinson's disease

Locus	Gene	Chromosomal location	Inheritance	Type of parkinsonism	Reference
PARK1/PARK4	*SNCA*	4q21	AD	LOPD/EOPD	Polymeropoulos et al., 1996; Polymeropoulos et al., 1997 Singleton et al., 2003
PARK2	*Parkin*	6q25-q27	AR	EOPD	Kitada et al., 1998
PARK5	*UCHL1*	4p14	AD	LOPD	Wintermeyer et al., 2000
PARK6	*PINKI*	1p36	AR	EOPD	Valente et al., 2004
PARK7	*DJ1*	1p36	AR	EOPD	Bonifati et al., 2003
PARK8	*LRRK2*	12q12	AD	LOPD	Funayama et al., 2002; Paisan-Ruiz et al., 2004, Zimprich et al., 2004)
PARK9	*ATP13A2*	1p36	AR	EOPD	Di Fonzo et al., 2007
PARK13	*HTRA2*	2p12	AD	LOPD	Alnemri 2007
PARK15	*FBX07*	22q12-q13	AR	EOPD	Shojaee et al., 2008; Paisan-Ruiz et al., 2010
PARK17	*VPS35*	16q11.2	AD	LOPD	Vilarino Guell et al., 2011
	PANK2		AR	EOPD	Johnson et al., 2004

AD: Autosomal dominant, AR: Autosomal recessive, LOPD: Late onset PD, EOPD: Early onset PD

Various hereditary forms of PD that present similar clinical phenotypes to the sporadic ones have been recognized. In 2002, based on a genome-wide linkage analysis of a large Japanese family (the Sagamihara family) with autosomal dominant PD, a new locus linked to PD was identified, *PARK8* (12p11.2-q13.1) (Funayama et al., 2002; Funayama et al., 2005).

Although this confirmed the original hypothesis (that there is a genetic contribution to PD), the family demonstrated some unusual features. For instance, even though the disease had an autosomal dominant mode of inheritance, penetrance was incomplete. Despite the fact that some people had inherited the chromosomal region which tracked with disease, they did not always exhibit signs of PD. Furthermore, when autopsies were carried out on members of the family, no Lewy bodies were found, despite neurodegeneration in the substantia nigra, the main characteristic of PD (Hasegawa and Kowa, 1997). It was concluded that this family represented an unusual, possibly even private disease that resembled PD.

However, only 2 years later, several families were identified worldwide that were linked to the same chromosomal locus (Zimprich et al., 2004). In particular, several mutations at this locus were found to be within *LRRK2* (leucine-rich repeat kinase 2) (Zimprich et al., 2004; Paisan-Ruiz et al., 2004). Further research on *LRRK2* gene showed that mutations within this gene are relatively common, occurring with a prevalence ranging from 1-30% of all PD depending on the population under study (Cookson et al., 2005). This frequency is very high for a disease that until 1996 was considered to have no genetic background.

Importantly, it was confirmed that the original Japanese family was also carrying a *LRRK2* mutation, verifying the correct identification of the gene (Funayama et al., 2005). The penetrance of the mutations within the *LRRK2* gene is age dependent, but incomplete (Hulihan et al., 2008; Latourelle et al., 2008), meaning that a proportion of mutation carriers survive until their late 80s without developing any of the PD symptoms (Kay et al., 2005), in contrast to the typical age of onset, which is around 50 years old. Confirmation of this gene as a cause

of PD was supported by further investigations of the Sagamihara kindred, when some family members did indeed have Lewy bodies (Hasegawa et al., 2008).

1.3 Leucine-rich repeat kinase 2 (*LRRK2*)

Leucine-rich repeat kinase 2 (LRRK2), once also known as dardarin, is a large multidomain protein that belongs to the ROCO superfamily. ROCO, a combined term of Roc (Ras of complex proteins) and COR (C-terminal of Roc), is characterized by the presence of conserved Ras-related GTPase or Roc domain followed by a COR domain. The human *LRRK2* gene consists of 51 exons and encodes a large 2,527 amino acid protein. This multidomain protein contains an ankyrin-like (ANK) domain, several leucine-rich repeats (LRR), a Ras-like GTPase domain (ROC) along with its C-terminal domain (COR), a kinase domain and a WD40 motif (Figure 1.1). The presence of all these protein-protein interaction motifs within LRRK2 protein indicates that it may act as a scaffold for several other proteins, with an important role in cellular signalling. WD40 domains in other proteins can also interact with lipids, raising the possibility that LRRK2 might be present at the intracellular membranes (McArdle and Hoffmann, 2008). In a few words, LRRK2 is a large protein with a central catalytic GTPase/kinase region, surrounded by protein-protein interaction motifs, forming homo- and possibly hetero-dimers (Greggio et al., 2009).

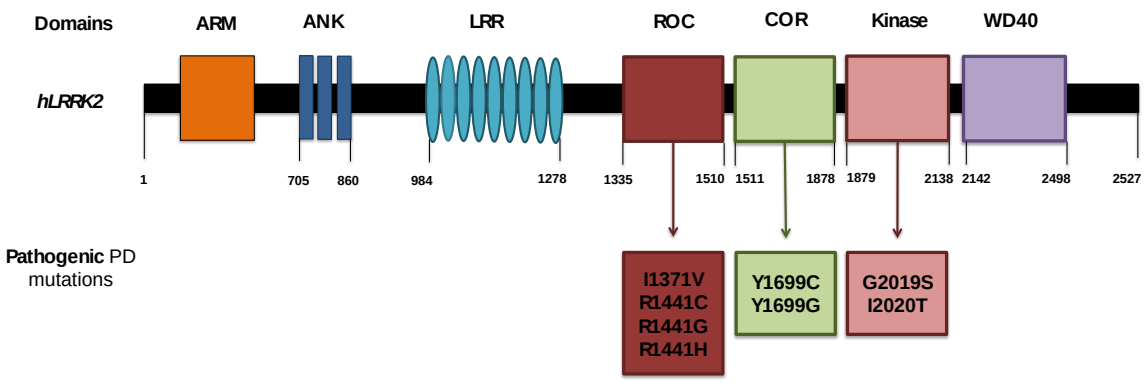

Figure 1.1: Schematic diagram of the human *LRRK2* domains and the PD pathogenic mutations. The human *LRRK2* is composed of several independent domains including armadillo repeats (ARM), ankyrin-like repeats (ANK), leucine-rich repeats (LRR), Ras of complex proteins (ROC) GTPase, C-terminal of ROC (COR), Kinase and WD40. This gene includes the ROC and the kinase domains, which are enzymatic, whilst the rest are protein-protein binding domains. Several PD pathogenic mutations have been identified within *LRRK2*, with the most common being the *G2019S* mutation lying within the kinase domain.

More than 75 *LRRK2* nucleotide substitutions (some of them are summarised in Table 1.4) have been identified but not all of them contribute to the risk of Parkinsonism to the same degree. That is rather surprising given its large size. Genetic evidence for pathogenicity is only proven for p.R1441C, p.R1441G, p.Y1699C, p.G2019S, and p.I2020T substitutions (by linkage) and for p.R1628P and p.G2385R (by association). While some of these sequence variants may be pathogenic, some might only be benign or polymorphisms. This is a critical distinction in patient diagnosis and in interpreting LRRK2 function (Dachsel and Farrer, 2010).

Table 1.4: Neuropathology of *LRRK2* forms of Parkinson's disease (Bardien et al., 2011)

Mutation	Domain	Substantia nigra neuronal loss	Lewy bodies	Ubiquitin staining	Enzymatic impact	References
p.G2019S	Kinase	Yes	Yes	Yes	Kinase ↑ GTPase ↓	Khan et al., 2005; Ross et al., 2006; Gaig et al., 2007; Giasson et al., 2008
p.R1441C	ROC	Yes	Yes	Yes	GTPase ↓	Zimprich et al., 2004
p.R1441G	ROC	Yes	No	No	GTPase ↓	Marti-Masso et al., 2009
p.I2020T	Kinase	Yes	Yes	No	None	Funayama et al., 2002
p.Y1699C	COR	Yes	Yes	Yes	GTPase ↓	Khan et al., 2005; Zimprich et al., 2004
p.I1371V	ROC	Yes	Yes	Limited	GTPase ↓	Di Fonzo et al., 2006

Epidemiological studies indicate the non-synonymous *G2019S* mutation as the most common genetic cause of late onset PD (Richecko et al., 2014). This mutation is relatively common across several populations, being responsible for PD in ~2% of sporadic and ~5% of familial PD cases in Northern European and North American populations; certain groups are being enriched by the presence of this mutation with reported frequencies of ~10% in Portuguese PD patients, ~20% in PD patients of Ashkenazi Jewish descent, and ~40% of North African Berber Arab PD patients (Houlden & Singleton 2012). It is very likely that the p.G2019S mutation has arisen on multiple occasions, but for the majority of the carriers, this mutation is believed to have been inherited from a common founder dating back 4,500-9,100 years, with the suggestion being that it arose in the Near East and then moved throughout the World with the Ashkenazi Diaspora (Bardien et al., 2011).

This mutation lies within the activation loop of the kinase domain of the LRRK2 protein leading to stabilization of the enzyme in the active form, causing enhanced phosphorylation activity (Mata et al., 2006). A 2-3-fold increase in the kinase activity of the G2019S-LRRK2 compared with the wild type protein has been consistently seen by many groups (West et al., 2005, Greggio et al., 2006, Smith et al., 2006, Guo et al., 2007).

The reduced penetrance of *LRRK2-G2019S* mutation means that a lot of mutation carriers do not manifest the disease even in their eighties, and the variability in the age of onset indicate that *LRRK2* induced PD is probably modified by a combination of environmental and genetic factors (Guo et al., 2006). Moreover, *LRKK2* mutations seem to have a true dominant effect, as individuals heterozygous for the mutation have the same risk of disease compared to those who are homozygous (Cookson et al., 2010).

The actual function and how mutations within *LRKK2* gene contribute to the pathogenesis of PD is not clear yet. The isolated LRRK2 kinase domain has been shown to be catalytically inactive, indicating that the Roc and COR domains clearly are essential for control of the kinase activity (Greggio et al., 2008). Ras-GTPases act as molecular switches, and depending on whether the GTPase is

active, will turn signal transduction cascades on or off. Typically, GTPases act to control the phosphorylation of a kinase, as appears to be the case for LRRK2. Moreover, autophosphorylation plays an important role in the regulation of kinase function, and autoregulatory interactions between the kinase and Roc-GTPase domains are highly probable (Gloeckner et al., 2010). Given that the Roc-GTP domain is the region containing the majority of autoregulation sites, it is presumably regulated by the kinase domain, and may even be the major output of LRRK2 (Taymans and Cookson 2010). LRRK2 may exist as an oligomeric complex with minimal kinase activity, which upon GTP binding, dissociates to form an intermediate structure, which phosphorylates itself, forming a homodimer with activation of the kinase (Webber et al., 2009). Since the ROC domain is a molecular switch, if GTPase activity decreases as a result of mutations, turnover of GTP to GDP will diminish, with the consequence that the activating effect of GTP on the Roc domain will be of longer duration. As the Roc-COR domain has an excitatory effect on the kinase domain, a prolonged activation of the Roc domain will lead to an increase in kinase activity. Mutations that affect GTP binding or delete the GTPase domain will bring about loss of kinase activity (Bardien et al., 2011).

This protein has been implicated in several cellular processes, including vesicle sorting and trafficking, autophagy, dopamine homeostasis, dopamine receptor activation, synaptogenesis, miRNA processing and cytoskeletal remodelling (Paisan-Ruiz et al., 2013; Migheli et al. 2013). Moreover, LRRK2 has been demonstrated being involved in the negative regulation of normal levels of dopamine. The over expression of selected mutants of *LRRK2* cause a severe reduction in the dopamine levels of the brain (Liu et al., 2014). Liu et al. (2008) reported that L-DOPA causes improvement in movement, but not in the survival of dopaminergic neurons, indicating that changes in dopamine levels might be due to defects in metabolism or processing and handling of dopamine.

1.4 Dopamine and its involvement in PD

Dopamine (DA) is a catecholamine neurotransmitter that is widely distributed in the central nervous system (CNS) and some peripheral areas including cardiovascular and renal system. The first time DA was found to occur in an organism was as a pigment-building metabolite in the plant *Sarothamnus scoparius* (Schmalfuss et al., 1931). Later on it was identified to be a substrate of aromatic amino acid decarboxylase (AADC) (Blaschko, 1942) and prevalent in invertebrates (Cottrell, 1967). At first DA was only considered being a precursor of the catecholamin neurotransmitters epinephrine (E) and norephinephrine (NE) or assumed to only be an intermediate in tyrosine degradation (Blaschko, 1942). Only later DA was recognized as an independent neurotransmitter (Hornykiewicz, 2002; Carlsson, 2003).

Calabresi et al. (2007) reported the importance of DA in the modulation of behavior and cognition; voluntary movement; motivation; punishment and reward; inhibition of prolactin production; sleep; dreaming; mood; attention; working memory; and learning. Impairment of DA transmission has been implicated in several diseases such as neuropsychiatric disorders, including attention deficit hyperactivity disorder (ADHD), Tourette syndrome (TS), schizophrenia, psychosis and depression. It has also been linked to neurodegenerative disorders including PD, Huntington disease (HD) and multiple sclerosis (MS) (Rangel-Barajas et al., 2014).

The importance of the DAergic system in the brain was highlighted in PD, because of the degeneration of the DAergic neurons of the substantia nigra pars compacta. There are three main sources of DA in the CNS all involved in different neurophysiological features (shown in Figure 1.2): the nigrostriatal pathway, which is related with motor function, the mesocorticolimbic pathway, which is related with the cognitive function, motivation and emotion and finally the tuberoinfundibular pathway, which is involved to the secretion of prolactin (Ben-Jonathan, 1985; Jackson and Westlind-Danielsson, 1994).

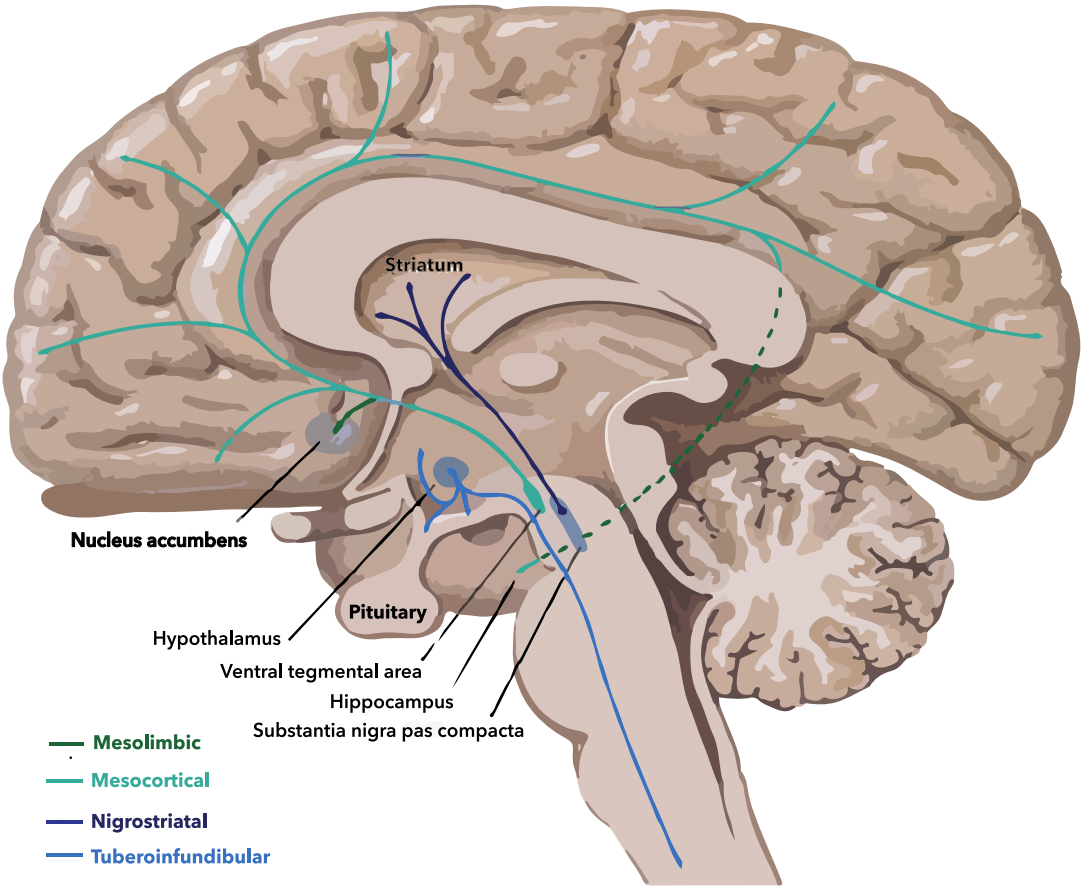

Figure 1.2: Schematic presentation of the human central dopaminergic systems. Adapted from Felten and Shetty, 2010.

The physiological effects of DA are mediated by dopaminergic receptors, which have widespread expression throughout the brain. The DA receptors belong to the G protein coupled receptors family (GPCRs), with five subtypes of mammalian DA receptors existing, which are divided in two families according to their structure and biological response. The D1-like family includes D1 and D5 receptors, while D2-like family consists of D2, D3 and D4 receptors. The D1-like family are positively coupled to adenylyl cyclase (AC) inducing the intracellular cyclic 3,5 adenine-monophosphate (cAMP) accumulation leading to the activation of the protein kinase dependent of cAMP (PKA) in contrast to the D2-like family that are negatively coupled to AC, which decreases the cAMP accumulation.

The DA receptors are the main target of several drugs including psychostimulants and antipsychotics. What is interesting is that DA receptors expression and intracellular signal transduction pathways change during degenerative process and neurotoxicity worsening the symptoms and the progression (Rangel-Barajas et al., 2015).

Although DA is an important neurotransmitter in the brain, a substantial part of the overall DA in the body is produced outside the brain by mesenteric organs (Eisenhofer et al., 1997). The classical pathway for DA biosynthesis was already postulated by Blaschko in 1939 (Blaschko, 1939). The two-step biosynthesis of DA takes place in the cytosol of DAergic neurons and starts with the hydroxylation of L-tyrosine at the phenol ring by tyrosine hydroxylase (TH) to yield DOPA. This oxidation is strongly regulated and depends on tetrahydrobiopterin (BH4) as a co-factor, which is synthesized from guanosine triphosphate (GTP) by GTP cyclohydrolase (GTPCH). DOPA is then decarbozylated to DA by aromatic amino acid decarboxylase (DDC) as shown in Figure 1.3.

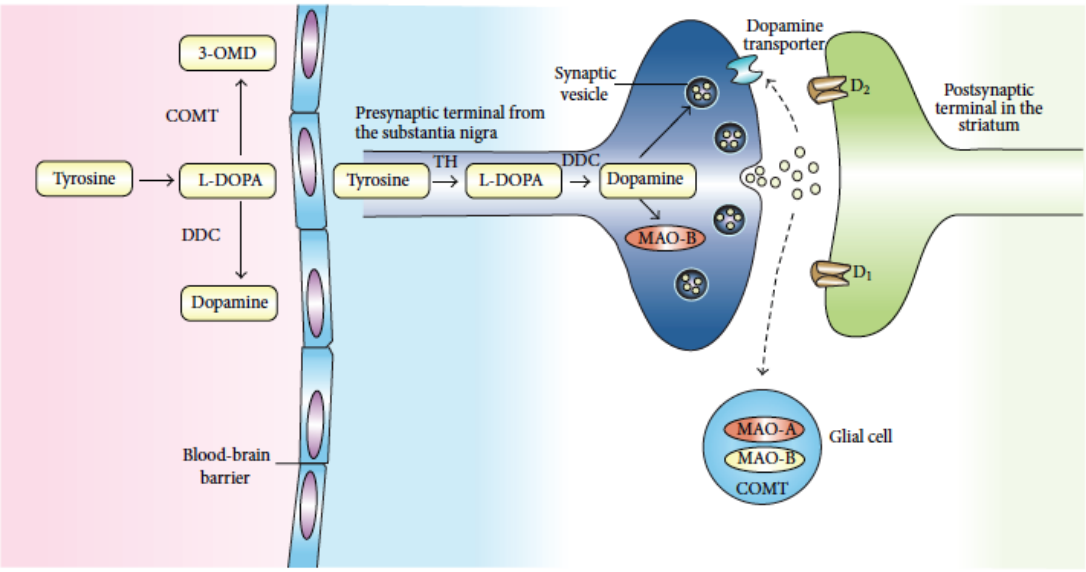

Figure 1.3: Dopamine biosynthesis pathway. Dopamine is synthesized by tyrosine via tyrosine hydroxylase (TH) catalysis to levodopa (L-DOPA), followed by decarboxylation by dopa decarboxylase (DDC) to dopamine. Responsible for dopamine metabolism are the intraneuronal monoamine oxidase A (MAOA) and glial and astrocyte MAOA and MAOB. Adapted by Youdim et al., 2006.

At physiological concentrations DA does not exhibit toxicity, however malfunction of DA release and/or metabolism could lead to neurotoxicity. The underlying mechanisms are not clear yet but several evidences have shown that it can be caused by oxidative stress, neuroinflammation and apoptosis. The enzymatic breakdown of DA to its inactive metabolites is carried out by catechol-O-methyl transferase (COMT) and monoamine oxidase (MAO). The biosynthesis of DA and other catecholamines can be limited by the action of the enzyme tyrosine hydroxylase (TH). After the biosynthesis of DA, it is incorporated into synaptic vesicles by the action of vesicular monoamine transporter 2 (VMAT2) where it is stored. DA is discharged by exocytosis into the cell membrane and dumped into the synapse (Juarez-Olguin et al., 2015).

Dopamine metabolism is considered critical for the preferential susceptibility of ventrolateral SNc cells to damage in PD. It produces highly reactive species that oxidize lipids and other compounds, increasing oxidative stress and leading to

impaired mitochondrial function. At neutral pH, DA can auto-oxidize. Therefore, reduced sequestration of dopamine into synaptic vesicles, where the pH is lower and dopamine is more stable without being auto-oxidize, may represent a vulnerability factor for neurons. That means that dopamine neurons with low dopamine transporter activity in the cell membrane are less sensitive to oxidative stress induced by dopamine or neurotoxins and are also less affected in PD (Obeso et al., 2010).

1.5 Retinal dopamine in PD

Dopaminergic neurons are not only found in the *substantia nigra*, but also in the retina. Consequently, it may be no surprise that patients with PD frequently report problems with visual tasks, such as navigating around everyday environments and using maps (Bowen et al., 1972). In questionnaire studies, 78% of patients with PD report at least one visual symptom, including difficulties in reading, double vision, and misjudging objects and distances (Archibald et al., 2011; Urwyler et al., 2014). Visual hallucinations are also very common, with a frequency of 74% after 20 years of disease (Fenelon et al., 2000; Hely et al., 2008).

Neurochemical evidence for dopaminergic deficiency in the human retina was first advanced with reports of reduced tyrosine hydroxylase immunoreactivity of dopaminergic cells in five patients with PD (Nguyen-Legros, 1988). Tyrosine hydroxylase (TH) is uniquely required for the synthesis of dopamine and hence identifies DA-containing cells in the retina. Harnois and Di Paolo (1990) examined PD patients post-mortem and found that subjects not receiving L-DOPA therapy at the time of the death had significantly lower retinal dopamine concentrations than controls. That also occurred for those whose death occurred less than 15h after their last dose. Tatton et al. (1990) treated monkeys with MPTP, a neurotoxin that destroys dopaminergic neurons, and showed that causes a dose-dependent, but reversible, reduction in TH immunoreactivity in amacrine cells. These studies confirmed the previously reported retinal dysfunction in

patients with PD and that it was dopaminergic deficiency itself that mediated these changes (Archibald et al., 2009).

Deeper understanding of the underlying mechanisms leading to visual problems will shed new light on our understanding of the pathways leading to PD (Weil et al., 2016). The presence of dopaminergic neurons in the fly retina emphasizes the importance of using *Drosophila* as an animal model to test the connection between PD and the visual problems.

1.6 *Drosophila* as an animal model

Over 100 years of innovative experimentation with the "common fruit fly" or *Drosophila melanogaster* has placed this remarkable organism at the front line of contemporary biological research. The reasons why the small fruit fly is such a successful animal model are manifold. First of all, *Drosophila* is very easy and cheap to maintain in the lab; it can give rise to a large number of genetically identical progeny; it has a rather short life span ranging from 40 to 120 days depending on diet and stress (Piper et al., 2005; Pletcher et al., 2005); it shows complex behaviour, including learning and memory (McGuire et al., 2005; Margulies et al., 2005); driven by a sophisticated brain and nervous system (Nichols, 2006). *Drosophila* is encoded by approximately 13,600 genes as compared to 27,000 human genes, located on only 4 pairs of chromosomes as compared to 23 pairs in human (Adams et al., 2000). Indeed, many of these genes and processes are conserved between *Drosophila* and other organisms, notably humans. For example, it has been estimated that two-thirds of known human disease-causing genes are also present in the fly (Rubin et al., 2000; Reiter et al., 2001). Comparative analysis of whole genome sequencing revealed striking similarities in the structural composition of individual genes of Homo sapiens and *Drosophila* (Rubin et al., 2000). Moreover, the molecules and mechanisms underlying core modules of cell biology are also conserved: homologous genes mediate homologous pathways. Furthermore, fundamental cellular processes related to neurobiology are similar in *Drosophila* and humans, including synapse formation, neuronal communication, membrane trafficking

and cell death; the neurobiological bases of behaviour are of the same origin in flies and humans, including sensory perception, integration and motor output (Hirth, 2010).

Thanks to very well-characterized anatomy, development (Campos-Ortega, 1997; Technau, 2008) and the availability of molecular genetic tools (Ashburner et al., 2004; Greenspan, 2004; Dahmann, 2008), *Drosophila* is one of the most extensively used genetic model organisms to study complex biological processes. While less complicated than the mammalian brain, *Drosophila* has a complex central nervous system, which is composed of neurons and glia, it is protected by the blood-brain barrier, and shares striking organization similarities with the vertebrate brain. In comparison to other model organisms like *C. elegans* and the mouse, *Drosophila* provides a very powerful genetic model system for the analysis of brain and behavioural disorders related to human disease: its brain is complex enough in contrast to *C. elegans* and relevant to humans but it is still small enough compared to mouse for an in-depth structural and functional analysis (Heisenberg, 1997). Functional, developmental, and molecular similarities between these systems further testify that basic principles of neural circuitry are conserved from flies to humans (McGurk et al., 2015).

Experimental manipulations and observations of cells and tissues are relatively easy in *Drosophila*, as the organs are of low complexity and size and can be often studied live or through straightforward fixation and staining protocols in the whole organism. More importantly, we can take advantage of the extensive fly genetic toolbox in order to create transgenic flies containing the sequence of interest, as is being described below.

1.7 The *Drosophila* visual system

Despite of its miniature body and tiny brain, *Drosophila* can survive in almost any corner of the world. It can find food, court mate, fight rival conspecific, avoid predators and amazingly fly without crashing into trees. *Drosophila* vision and its underlying neuronal machinery has been a key research model for at least half century for neurogeneticists.

The first mutant in *Drosophila*, which was identified by Morgan in 1910, was *white*, an ABC transporter, which when missing leads to white-eyed flies instead of the wild-type red-eyed flies (Morgan, 1910). This led to the conclusion that *white* is responsible for carrying precursors of the eye colour pigments into the developing eye (Morgan, 1910). Since then the fly eye continues to be the focus of research not only because adult eye phenotypes are very easy to detect but also because, unlike most organs in the fly, the eye is tolerant of genetic disruption of basic biological processes and is even dispensable for survival of the fly (Zhu, 2013). Versatile technologies can be used to generate, identify, and characterize mutations in the retina and have elevated the eye to a system with unrivalled potential for deciphering gene function. The fly eye has been used to study cell cycle control, cell proliferation and differentiation, neuronal connectivity, apoptosis, programmed cell death and tissue patterning (Kang Sang and Jackson, 2005).

The fruit fly has two compound eyes, each of which is composed of regularly arranged ommatidia, also known as facets (approximately 750) (Figure 1.4). Each facet has its own little lens that focuses light onto eight photoreceptors, which are arranged in such a way that six outer photoreceptors (R1-R6) surround two central ones (R7 stacked on top of R8). In contrast to vertebrate photoreceptors, insect photoreceptors depolarize in response to illumination (Borst, 2014). Spatial vision is conveyed by R1-R6. These photoreceptors are a homologous group of cells, each of which possesses the opsin Rhodopsin 1 (Rh1), which shows broad spectral sensitivity. The different photoreceptors in one ommatidium have different optical axes, but corresponding photoreceptors within neighbouring ommatidia have parallel optical axes. Colour vision is enabled by R7 and R8 (Borst, 2014).

Primary visual information is further processed in a part of the fly's brain called the 'optic lobe'. In each hemisphere, the optic lobe comprises more than 60% of all neurons. It consists of four layers of neuropil called the lamina, medulla, lobula and lobula plate, each of which is built from 750 repetitive, retinotopically arranged columns that reflect the spatial layout of the facet eye. Even though the

axons of photoreceptors R1-R6 connect to large monopolar cells of the lamina (L1-L5), the axons of photoreceptors R7 and R8 run through the lamina and terminate in specific layers of the medulla (Meinertzhagen and O'Neil, 1991). Photoreceptors release the neurotransmitter histamine (Hardie, 1989). Histamine-gated chloride channels are expressed on the postsynaptic cells and mediate signal-inverting synaptic communication: a strong, transient hyperpolarisation upon illumination onset of the eye, which is followed by a sustained component. When the light is switched off, a rebound excitation occurs in the postsynaptic cells (Laughlin et al., 1987; Zheng et al., 2009).

Each medulla column consists of more than 60 different cells, which can be grouped into medulla intrinsic (Mi) and trans-medulla neurons; with the latter connecting the medulla to the lobula complex (Strausfeld, 1976; Cajal and Sanchez, 1915; Fischbach and Dittrich, 1989). The terminals of all lamina neurons ramify in distinct, specific layers of the medulla (Takemura et al., 2008; Takemura et al., 2011). This layout suggests a splitting of photoreceptor signals into several parallel pathways that might subserve different functions.

From the optic lobe, visual information takes three major routes: from columnar neurons of the lobula complex to various glomeruli in the central brain (Mu et al., 2012); from large-field tangential neurons of the lobula plate, to descending neurons that connect, via the cervical connective, to the motor centres in the thoracic ganglion (Strausfeld and Bassemir, 1985); and from tangential cells to neck motor neurons that directly control head movements (Strausfeld and Seyan, 1985; Gronenberg et al., 1995).

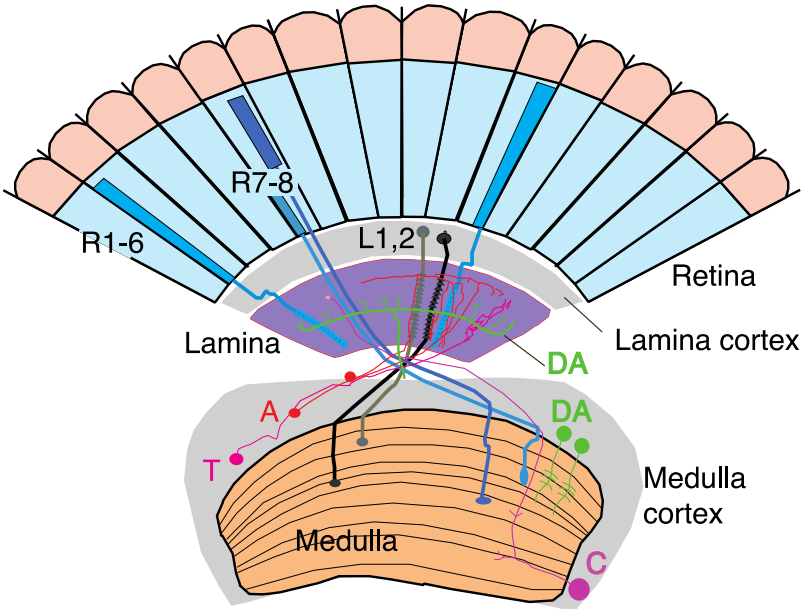

Figure 1.4: Diagram of the structure of the *Drosophila* visual system. That includes the photoreceptors and the second-order amacrine (A) and lamina neurons (L1,L2). It also presents two types of medulla neurons (C and T) that project to the lamina. The visual lobes also include dopaminergic cells (DA), some intrinsic to the medulla, others projecting from the CNS to the lamina. Adapted from Afsari et al., 2014.

1.8 Similarities between the *Drosophila* and the human visual system

As first described by the great neuroscientist Ramon Y. Cajal (1915), one of the greatest similarities between vertebrates and *Drosophila* are the neuronal circuits of vision. This was confirmed later by Sanes and Zipursky (2010). Cajal turned to the fly hoping to find a simple circuitry to allow easier tracing of neuronal connectivity. Instead, he found a complicated system rivaling that of vertebrates.

Cajal argued that fly and vertebrate visual systems were essentially identical in key aspects (Cajal and Sanchez, 1915). What he actually said was "If from the visual organ of the insect we discount the crucial fact of the dislocation of the soma…then the analogy between the visual apparatus converts almost in identity". In one of the most remarkable drawings from that early era, after he used silver staining, he made his point by translocating the fly somata to a vertebrate position without altering the neuropil, this is known as the "Flertebrate" arrangement (Figure 1.5).

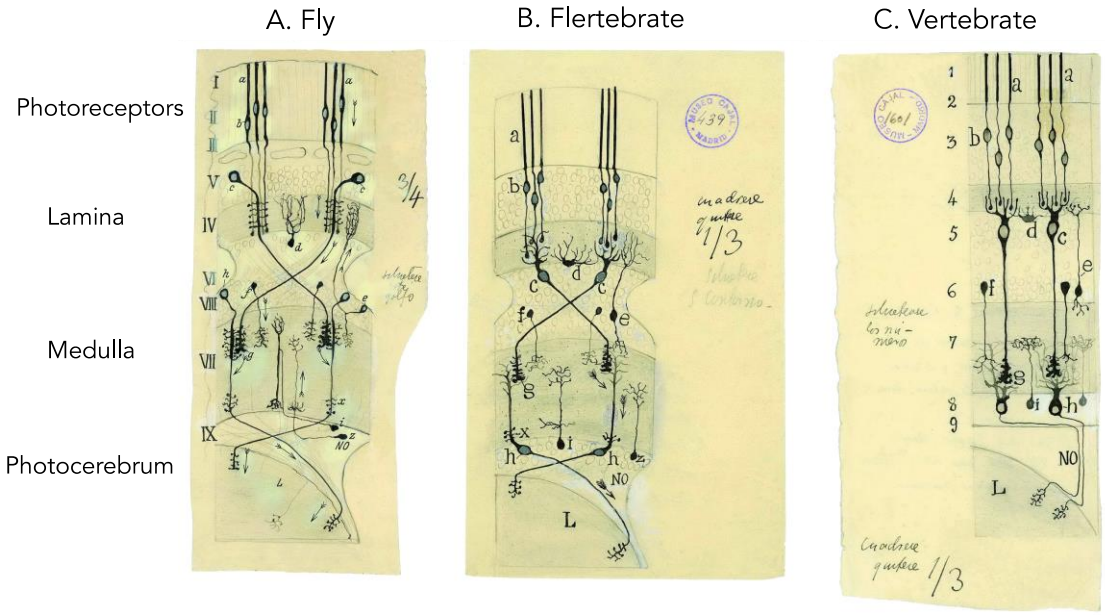

Figure 1.5: The similarities between the fly and the vertebrate visual systems. Cajal fisrt described the similarities between the fly (A) and the vertebrate (C) visual systems. A) The fly visual system, where the somas appear in their natural position. B) In this drawing of the insect visual system Cajal "moved" the cell bodies to correspond to their positions in vertebrates, without making any changes of the positions of the synaptic contacts. That is referred as the "Flertebrate" arrangement. C) Schematic presentation of the main cell types in the vertebrate retina and their connections. Adapted from Sanes and Zimpursky, 2010.

Later on modern cytochemical and ultrastructural techniques have been utilised in order to compare the fly and the vertebrate visual system providing strong evidence in support of Cajal's view (Figure 1.6). Some of the similarities between the two systems include; there are a small number of main neuronal types (five in the vertebrate and six in the fly retina), divided into numerous subtypes; multiple contact synapses with a single presynaptic terminal abutting multiple postsynaptic elements; multiple cellular layers with regular arrangement of neurons in each layer; orderly mapping of neuronal arrays at each level onto those at the next level; segregation of synapses made by specific subtypes into parallel sublaminae within soma-free neuropil (Sanes and Zipursky, 2010).

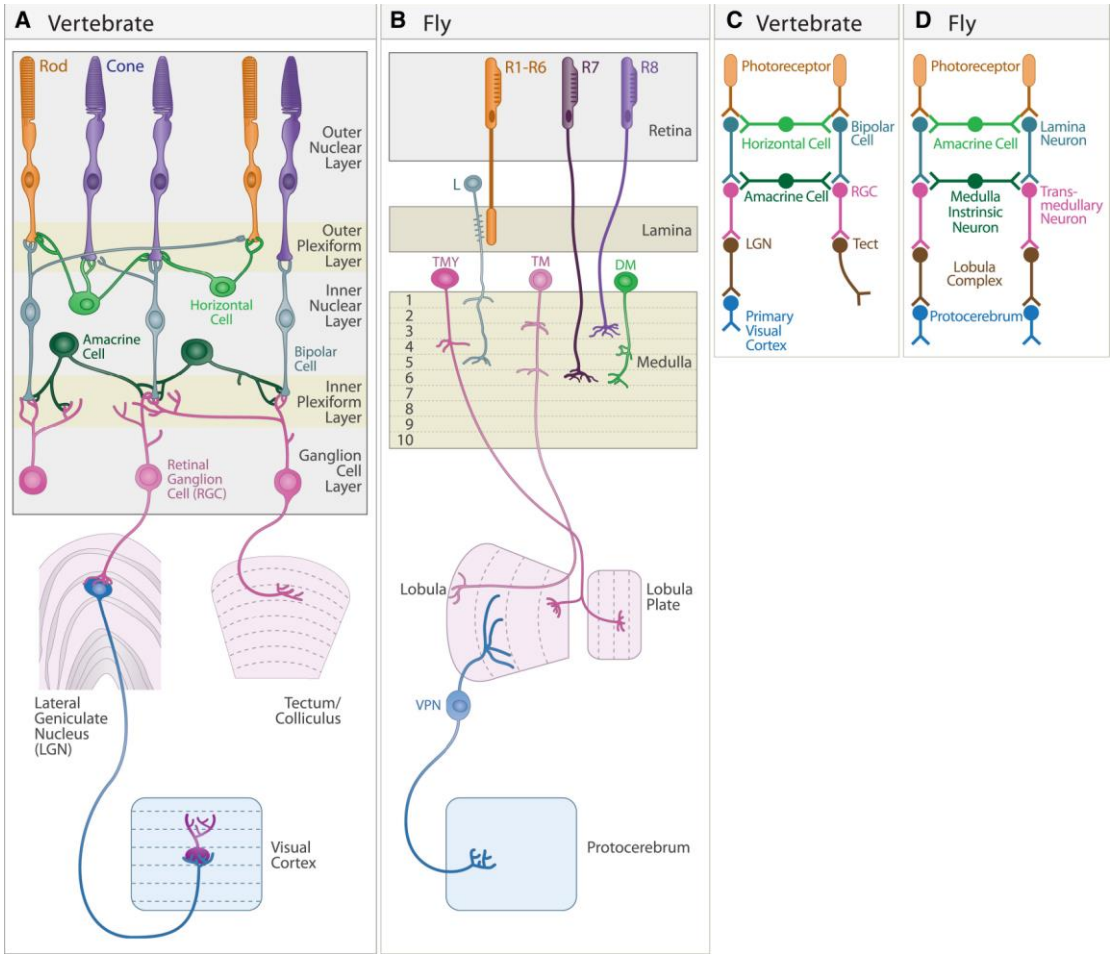

Figure 1.6: Structures underlying the first stages of visual processing in the fly and mammalian visual systems. A) Mammalian visual system, showing retina, dorsal lateral geniculate nucleus (LGN), superior colliculus, and primary visual cortex. B) The *Drosophila* visual system, showing retina, lamina, medulla, and the lobula complex, which comprises the lobula and the lobula plate. C) and D) represent similar steps in transfer of information through early stages of vertebrate and *Drosophila* visual systems. (Adapted from Sanes and Zimpursky, 2010).

Moreover, similarly to humans, *Drosophila* contains dopaminergic neurons, which actually branch in their visual system (Hindle et al., 2013). The principal DA cell in the human retina is an amacrine subtype called A18 although a second, less well defined DA cell has also been identified in primate and rodent retinas (Mariani, 1990; Mariani, 1991; Kolb et al., 1992; Witkovsky et al., 2005).

1.9 *Drosophila* as an animal model for neurodegenerative diseases

Neurodegenerative diseases represent a subset of human diseases with certain features in common. These disorders are usually characterized by the progressive loss of specific neuronal populations depending on the disease type. Most of the times they are of adult onset and generally are asymptomatic during the development and maturation of the nervous system. Even though neurodegenerative diseases were once considered being one of the most obscure and intractable of all human illnesses, this situation is changing, due to breakthroughs in human genetics that help pinpoint genes associated with familial forms of diseases including Alzheimer's disease and PD (Bonini et al., 2003; Muqit and Feany, 2002; Driscoll et al., 2003). The identification of these genes has helped investigators to characterize the mechanisms of neurodegeneration at the molecular level. New light will be shed in our understanding of the underlying pathogenic mechanisms thanks to the identification of these disease-associated mutations.

Despite the contribution of human genetics in disease understanding, studies on human subjects are of very limited use for elucidating the signalling pathways and cellular processes underlying the neurodegenerative process. This is because of both ethical and technical limitations. Moreover, most human neuropathological studies are based on post-mortem tissues that almost never reflect the earliest pathologic events at the presymptomatic stage. To overcome this problem the most powerful approach for studying disease has always been the use of animal models. Invertebrate animals, especially *Drosophila*, have proven to be an excellent model for human neurodegenerative diseases (Lu et al., 2009; Cauchi and Van den Heuvel 2006).

Apart from all the other advantages of *Drosophila* as an animal model that have been described above, it has been proven that most of the genes implicated in familial forms of disease have a fly homolog (Reiter et al., 2001). The key approaches used in order to study the underlying mechanisms of human disease in *Drosophila* include the mis-expression of a human disease gene, in its wild type or mutant form, loss and gain of function of the *Drosophila* homolog of a

human disease gene and finally genetic screens to identify enhancers and suppressors that are able to modify a phenotype caused by the mis-expression of the human version of a disease related gene or the *Drosophila* homolog.

For a model system to functionally approach a condition as complex as PD, changes to specific tissues that can result in recapitulation of phenotypes that resemble symptoms of the disease are key. The *Drosophila* adult brain has been characterised to contain clusters of dopaminergic neurons (Nassel and Elekes, 1992). Feeding of flies with various toxins has led to degeneration of dopaminergic neurons indicating that there is a susceptibility of dopamine-producing neurons to toxins that is conserved between mammals and flies (Coulom and Birman 2004).

1.10 Genetic toolbox in *Drosophila*

The genetic power and tractability of *Drosophila* is optimized by the extensive genetic toolbox available for their manipulation. Traditionally, prior to the sequencing of the *Drosophila* genome in 2000, genetic manipulation relied, predominantly, upon forward genetic approaches (St Johnston, 2002). By using this approach we can identify genes (or set of genes) responsible for a particular phenotype of an organism.

DNA-damaging agents, such as chemical mutagents, have been widely used in order to induce mutations in forward genetic studies. The chemical mutagenesis offers the advantages of a relatively high mutation rate and broad target range. Ethyl methanesulphonate (EMS) was first introduced by Lewis and Bacher (1968) and since then has been the most commonly used chemical mutagen in *Drosophila*. EMS is an alkylating agent that induces single-base changes (point mutations), which disrupts gene function by causing missense and nonsense mutations (Adams and Sekelsky, 2002).

An alternative means of creating novel mutants is the use of transposable element insertions, which is an extremely powerful mean of gene disruption.

The P-element of *Drosophila* has been engineered to suit various purposes. The fastest and easiest way to use a P-element in *Drosophila* is to order a stock that carries an insertion in the gene of interest. The mutated gene can be rapidly and easily identified using the P-element as a tag. P-elements are very inefficient mutagens, however, the most common approach is to screen the large collection of P-element insertions existing, rather than generating new insertions by mobilizing the P-element oneself (Johnston, 2002). Forward genetics remain important due to their ability to generate allelic series of mutations, ranging from nulls (amorphs) to weak partial loss of function mutations (hypomorphs) (St Johnston, 2002). Whilst forward genetics has proven highly successful in the study of gene function, the sequencing of the *Drosophila* genome has led to an expansion of the *Drosophila* genetic toolbox through more favourable reverse genetic approaches (Adams and Sekelsky, 2002). In contrast to forward genetics, reverse genetics is based on the principle of mutating specific, known genes and observing the resultant phenotypes, thus allowing elucidation of gene function. Some reverse genetic approaches also rely upon forward genetic approaches, such as chemical or transposon mediated mutagenesis, that have been modified to allow targeting of specific genes. For example, *P*-elements inserted near to a known gene of interest can be mobilized, allowing excision of the *P*-element and the generation of a double stranded DNA break (Adams and Sekelsky, 2002). Inaccurate repair of such breaks will often occur, allowing deletion of the gene sequence flanking the *P*-element insertion site and generating a specific null mutant. In order to prevent loss of such mutations through homologous recombination Drosophilist's utilise what are known as balancer chromosomes. The use of transposable elements has proven highly versatile in *Drosophila* genetics with them also being utilized to allow misexpression of genes, using *P*[EP]-elements, or to characterize the temporal and spatial expression of genes through enhancer trapping (O'Kane and Gehring, 1987). They also allow for the generation of transgenic fly lines via transposon-mediated transformation (Rubin and Spradling, 1982). This process involves the insertion of a gene of interest into a plasmid between two P-element ends followed by the microinjection of this construct, along with a transposase, into syncytial blastoderm embryos. Typically, the gene of interest will be inserted into a construct containing an Upstream Activator Sequence (UAS), allowing implementation of the

Drosophila tissue specific expression system known as the *UAS/Gal4* system. This system can also be used to implement alternative reverse genetic approaches, as opposed to those that rely upon modifications to classical forward genetic methods, for example RNA interference (RNAi) (Hammond et al., 2001). Based upon known gene sequences it is now possible to design double stranded RNAs against specific genes, allowing for target silencing of homologous genes through RNAi mediated degradation of cognate messenger RNA (mRNA) (Dietzl et al., 2007).

Another way that allow us to selectively mutagenize specific regions of the genome, allowing us to perform detailed mechanistic studies in a variety of organisms including *Drosophila* is the CRISPR/CAS9 system. Cas9 is an endonuclease that is targeted to sequences from the invading pathogen by a crRNA (CRISPR RNA), that provides specificity to the endonyclease by base repairing with a 20 nt complimentary sequence within the DNA (Brouns et al., 2008; Gasiunas et al., 2012; Jinek et al., 2012). Endogenously, another component, that is known as tracrRNA (trans-acting crRNA) forms a complex with the crRNA and targets its incorporation into the Cas9 complex. Fusion of the crRNA and the tracrRNA forms a chimeric RNA (sgRNA or chiRNA), which is composed of a 100 nt synthetic single guide, making this system even more simple that only requires two components to be expressed (Dahlem et al., 2012; Jinek et al., 2012; Cong et al., 2013; Mali et al., 2013). The specificity of the system is then determined by a 20 nt sequence at the 5' end of the sgRNA, which can be altered to match any desired sequence in the DNA. In *Drosophila* this system has been engineered by the co-injection of two plasmids into syncytial blastoderm stage *Drosophila* embryos (Gratz et al., 2013). The one plasmid is expressing the *Cas9* gene under the *Hsp70* promoter and the second produces the sgRNA driven by a *pol III* promoter from the *U6* gene. Another technique involves the co-injection of *in vitro* transcribed *Cas9* mRNA and sgRNA into early stage embryos, which achieves much higher mutagenesis rates compared to the other method (Bassett et al., 2013; Yu et al., 2013).

1.10.1 Balancer chromosomes

Balancer chromosomes are essential for the maintenance of fly stocks as well as for mating scheme design. Balancer chromosomes carry multiple inversions through which the relative positions of genes have been significantly rearranged. They segregate normally during meiosis, but they supress recombination with a normal sequence chromosome and the products of any recombination that does occur are lethal due to duplications and deletions of chromosome fragments (aneuploidy). Moreover, most of the balancer chromosomes are lethal in homozygosis. Together these properties are essential for stock maintenance, since they eliminate all genotypes that differ from the parental combination. Another key feature of balancer chromosomes is the presence of dominant and recessive marker mutations. Through their dominant marker mutations, balancer chromosomes are easy to follow in mating schemes (Figure 1.7). For instance, by making sure that a recessive mutant allele of interest is always kept over dominantly marked chromosomes, the presence of this allele can be "negatively traced" over the various generations of a mating scheme; especially since recombination with the balancer chromosomes can be excluded. There are many balancer chromosomes existing, including some on the X chromosome (*FM7a*, *FM7c*), on the 2nd chromosome (*CyO*, *SM6a*) and on the 3rd chromosome (*TM3*, *TM6B*). There are no balancer chromosomes on the 4th chromosome, as there is no recombination happening (Roote and Prokop 2013).

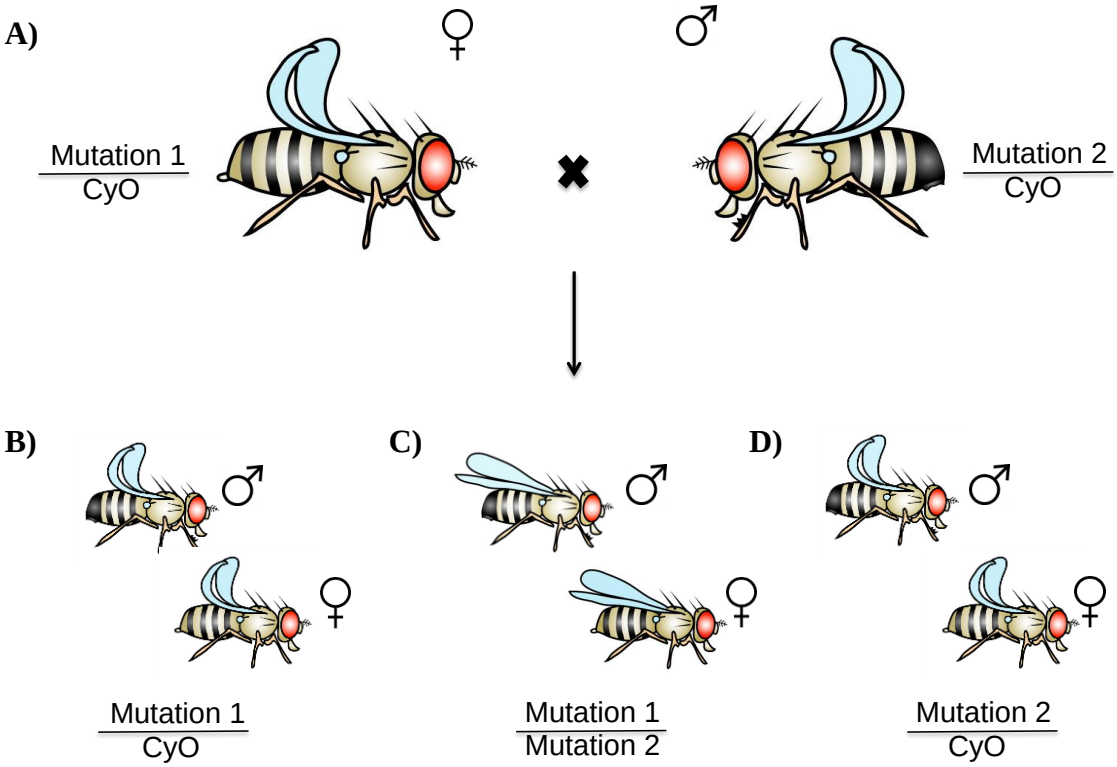

Figure 1.7: Balancer chromosomes allow following of mutations during chromosomal segregation. Balancer chromosomes allow researchers to select flies of the desired genotype during crossing schemes. In this example parent flies carrying the mutations of interest are crossed together (A) with the aim of obtaining offspring processing both of the mutations (C). Each one of the parents are carrying one of the mutations of interest on the 2nd chromosome with the balancer chromosome *CyO* on the alternative allele, which carries a dominant marker that gives a phenotype of curly wings. Following crossing of the parent flies produces progeny possessing either curly (B and D) or straight (C) wings. Those with the curly wings should possess the balancer chromosome while equally those with straight wings must have the genotype of interest carrying both of the mutations (one on each allele of chromosome 2). That allows researchers to follow alleles and obtain flies of the desired genotype during mating schemes.

1.10.2 The *Gal4-UAS* binary system

The introduction of the *Gal4/UAS* binary system in *Drosophila* (Brand and Perrimon, 1993) revolutionised our ability to achieve gene expression in a tissue-specific and time-dependent manner. One fly contains the Gal4 component, which generates the yeast protein Gal4 under the control of a *Drosophila* enhancer/promotor. The second fly contains the 'Upstream Activating Sequence' (UAS), which binds Gal4 and transcribes the gene of interest. As there is no *Drosophila* equivalent of the Gal4 transcription factor that binds to this UAS sequence, in the absence of Gal4 these fusion transgenes are mostly inactive. Once mated, such flies express the gene of interest in the pattern of the enhancer/promotor. Thus, this binary system gives the opportunity to express the desired gene where Gal4 determines the expression pattern in which the gene downstream of the UAS is going to be expressed (Figure 1.8). In practice, the Gal4 and UAS constructs are contained in a P-element, along with markers (e.g. *w+*), so that, once the transgene has been injected into an egg, successful transformants can be identified (in this case by orange eyes).

Many choices of Gal4 lines are available, including ubiquitous (*Actin*-5c), pan-neuronal (*elav*), in the dopaminergic neurons (*tyrosine hydroxylase*), early or late in eye development, and those inducible by heat-shock. Equally, many validated UAS stocks are available, including *UAS-hLRRK2*, *UAS-G2019S*, *UAS-R1441C* and RNAi lines.

The utility of the Gal4-UAS system led to the generation of another independent binary system for *Drosophila*, the *LexA-LexAop* system (Lai and Lee, 2006). LexA binds to and activates the LexA operator (LexAop). The *LexA-lexAop* system uses the LexA DNA-binding domain from a bacterial transcription factor that can be linked to the Gal4 activation domain. Usually that system is combined with Gal4 for simultaneous gene manipulations and alone for high levels of gene over- or mis-expression.

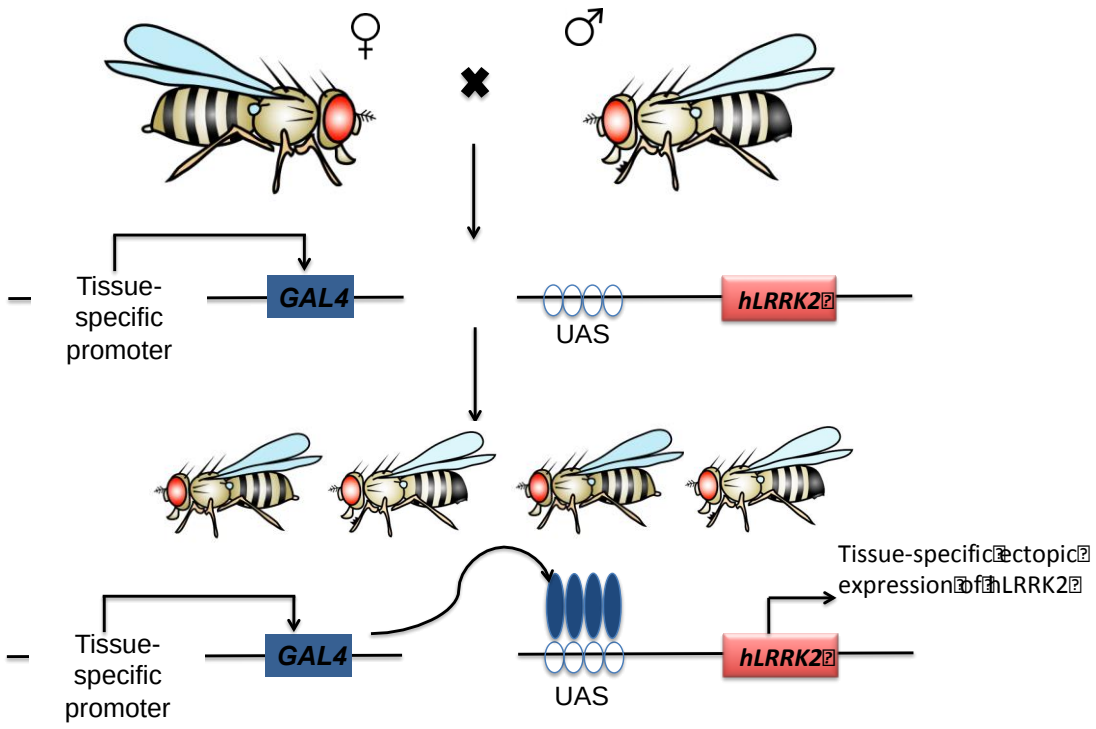

Figure 1.8: Directed gene expression in *Drosophila.*

In order to achieve this cell or tissue specific expression of a gene of interest a fly line that expresses Gal4 under the control of a tissue specific promoter is crossed to a second line that the gene of interest has been inserted downstream of the UAS, which is the binding site of Gal4. Once these two components are together in a mating scheme, progeny will be generated in which that gene of interest is only expressed in that cell or tissue specific pattern. Fly images generated using the Genotype Builder from Roote and Prokop (2013).

1.11 Modelling PD

As described above, a key goal in PD is to discover the underlying mechanism of the degeneration of the dopaminergic neurons. The discovery of genetic causes of PD (Section 1.2) allowed the creation of transgenic rats, mice, flies and worms as model organisms. Although rodent models of *α-synuclein*, *Parkin*, *DJ-1* or *Pink1* exhibit various pathological and behavioral phenotypes, the cardinal feature of PD, namely selective degeneration of dopaminergic neurons, has not been readily reproduced (Beal and Thomas, 2007). It is possible that the short

lifespan of mice may have precluded observation of the late-onset dopaminergic degeneration phenotype. Alternatively, various fundamental differences in dopaminergic neuron physiology between mice and humans could make mice less vulnerable to the dysfunction of the individual PD genes (Lu and Vogel, 2009). In contrast, many researchers that used *Drosophila* as an animal model for PD managed to recapitulate the PD symptoms (reduced movement, DA neuron loss).

The synthesis pathway for DA (outlined above Figure 1.3) is conserved in *Drosophila* and humans with distinct clusters of DA neurons detectable in the developing and adult fly brain (Monastirioti, 1999).

Comparable to the human condition, the *Drosophila* DA system is also involved in the locomotor control. Therefore, it is considerable to assume that loss of DA neurons can also affect locomotion in *Drosophila* comparable to the situation in PD. Indeed, loss of subsets of DA neurons in the brain as well as locomotion defects are the two principal parkinsonian-like phenotypes used to characterise fly models of PD. Both phenotypes have been induced by mis-expression of the wild type and/or mutant forms of human PD genes, including *α-synuclein* (Feany and Bender 2000; Seugnet et al., 2009), *PINK1* (Todd and Staveley 2008; Wang et al., 2006; Yang et al., 2008), *Parkin* (Yang et al., 2003; Haywood and Staveley 2004; Haywood and Staveley 2006; Wang et al., 2007; Sang et al., 2007) and *LRRK2* (Lee et al., 2007; Liu et al., 2008; Imai et al., 2008; Ng et al., 2009; Venderova et al., 2009). A major contribution to our understanding of the way cellular pathways provide a link, leading to a common phenotype was provided by the discovery of the interaction of *PINK1* and *Parkin* at the mitochondria (Pickrell and Youle, 2015).

1.12 *LRRK2 Drosophila* models of PD

Since *LRRK2-G2019S* is the most common cause of PD, and is a gain of function mutation, it is straightforward to create a fly model using the *Gal4-UAS* system to provide the ectopic expression of this mutation.

Lee at al. (2007) created a fly model for the fly homolog of *LRRK2* (*dLRRK*) by generating and characterising *LRRK* transgenic alleles and loss of function mutants in *Drosophila*, and clearly demonstrated an endogenous role of *LRRK2* in preventing the degeneration of DA neurons. This study shows no loss of dopaminergic neurons or deficits in climbing ability. Transgenic expression of pathogenic mutants and wild type *dLRRK* did not exhibit any significant defects, while *dLRRK* loss-of-function mutants show severely impaired locomotive activity. Moreover, dopaminergic neurons in *dLRRK* mutants showed severe reduction in tyrosine hydroxylase immunostaining and shrunken morphology, implicating a degeneration in the mutants.

Liu et al. (2008) created a gain-of-function *LRRK2 Drosophila* model by overexpressing the human wild-type *LRRK2* and the mutant form *LRRK2-G2019S*. Expression of both forms of *LRRK2* led to retinal degeneration, selective loss of DA neurons in the brain, early mortality, and locomotor impairment. Moreover, *LRRK2-G2019S* caused a more severe parkinsonism-like phenotype than wild-type *LRRK2*. Treatment with L-DOPA improved the mutant *LRRK2*-induced locomotor impairment but did not prevent the loss of TH-positive neurons, similar to *LRRK2*-linked human PD.

Imai et al. (2008) used *Drosophila* in order to understand the normal physiological function of *LRRK2* and how its dysfunction leads to DA neurodegeneration. They provided genetic and biochemical evidence that *dLRRK* modulates the maintenance of DA neuron by regulating protein synthesis. Moreover, they came to the conclusion that *LRRK2* primes phosphorylation of 4E-BP and that event has an important function in mediating the pathogenic effects of mutant *dLRRK*. Their final conclusion was that there is loss of dopamine and of dopaminergic neurons accompanied by behavioural deficits.

Ng et al. (2009) reported that their transgenics, *G2019S*, *Y1699C* and *G2385R* variants, all exhibited late-onset loss of DA neurons in selected clusters that are accompanied by locomotion deficits compared with their *hLRRK2*-expressing flies. This finding is consistent with the report by Imai et al. (2008), as the

mutant *LRRK2*-mediated degeneration occurs only towards the terminal age of the fly and is restricted to selected clusters of DA neurons, whereas transgenic flies expressing wild-type *LRRK2* are spared from this age-associated phenotype. This study completely matches the findings of other investigators (Lee et al., 2007; Imai et al., 2008) which are in contrast to the report by Liu et al (2007) where degeneration in *Drosophila* expressing either the wild-type or *LRRK2-G2019S* was observed to occur non-selectively across all the DA neuronal clusters. Moreover, no retinal degeneration was observed in this study, even at flies aged 20 or 60 day old, in contrast to Liu et al. (2007) that detected significant retinal degeneration at as early as 3 weeks of age post-eclosion.

Venderova et al. (2009) developed and characterised independent lines of WT and mutant *LRRK2*-expressing *Drosophila*. These flies displayed no overt developmental defects, notably a lack of nervous system pathology. This was probably unexpected given the association of *LRRK2* with axonal development and outgrowth. These results indicate that expression of any of the human or other *LRRK2* mutants result in loss of dopaminergic neurons. That is consistent with the notion that *LRRK2* expression results in selective dopaminergic loss in *Drosophila* without overt effects on other neuronal subpopulations.

Hindle et al. (2013) investigated the effect of *LRRK2* mutations using *Drosophila* electroretinograms (ERGs). They demonstrated progressive loss of photoreceptor function in flies expressing the *LRRK2-G2019S* mutation in their dopaminergic neurons. The photoreceptors showed increased autophagy, apoptosis and mitochondrial disorganisation and also loss of vision was determined after 28 days. Moreover, fly head dissections revealed extensive neurodegeneration throughout the visual system, even in regions not directly innervated by dopaminergic neurons. The other PD-related mutations that were tested didn't reveal any photoreceptor deficits and there was no loss of vision with kinase-dead transgenics. Furthermore, they manipulated the levels of *dLRRK*, which suggested that the *G2019S* mutation is a gain of function rather than dominant negative.

1.13 LRRK2 and its interacting proteins

As a kinase, one of the key questions is which proteins are phosphorylated by LRRK2? In order to identify binding partners of LRRK2, many different research groups tested for specific protein interactions. LRRK2 has been implicated in several cellular processes including mitochondrial function (Smith et al., 2005), regulation of transcription (Kanao et al., 2010), and translation (Imai et al., 2008; Gehrke et al., 2010), Golgi protein sorting (Sakaguchi-Nakashima et al., 2007), apoptosis (Ho et al., 2009) and dynamics of actin (Jaleel et al., 2007; Parisiadou et al., 2009) and microtubules (Gandhi et al., 2008; Gillardon 2009; Lin et al., 2009). As far as the localisation of LRRK2 is concerned, there is evidence that it localises to mitochondria (West et al., 2005; Biskup et al., 2006; Gloeckner et al., 2006; Hatano et al., 2007), the endoplasmic reticulum (Gloeckner et al., 2006; Vitte et al., 2010), Golgi (Biskup et al., 2006; Gloeckner et al., 2006; Hatano et al., 2007), and microtubule structures (Gandhi et al., 2008; Gloeckner et al., 2006). Moreover, LRRK2 has been associated with intracellular membranes (Biskup et al., 2006; Gloeckner et al., 2006; Hatano et al., 2007; Alegre-Abarrategui et al., 2009; Berger et al., 2010) and with vesicles in the endolysosomal pathway (Biskup et al., 2006; Hatano et al., 2007; Alegre-Abarrategui et al., 2009; Shin et al., 2008; Higashi et al., 2009) implicating LRRK2 in intracellular membrane transport and lysosomal function. Some of these conflicting results may be the result of unphysiological extraction buffers, or to damage of cells during extraction. The characterisation of LRRK2 still remains of paramount importance in understanding the underlying mechanisms of PD pathogenesis. Nonetheless, it has been proposed LRRK2 has several protein binding domains, indicating that it may act as a scaffold for multiple interaction partners. Identification of its interacting proteins may provide important clues about its functional role(s).

Shin et al. (2008) identified Rab5a as a LRRK2-interacting protein by using a yeast two-hybrid screening. By performing GST pull down and co-immunoprecipitation assays they confirmed that LRRK2 interacts with Rab5a. Moreover, subcellular fractionation and immunocytochemical analyses confirmed that a fraction of both proteins co-localise in synaptic vesicles. Rab5 is

a key regulator of endocytic vesicular transport from plasma membrane to early endosomes (Carney et al., 2006). That confirms the original hypothesis that LRRK2 probably modulates synaptic function by regulating clathrin-mediated endocytosis of synaptic vesicles.

Dodson et al. (2012) indicated that the fly homolog of *LRRK2*, *dLRRK*, plays a crucial role in regulating Rab7-dependent lysosomal positioning. hLRRK2 has been previously found to localise to Rab5-positive early endosomes and to physically interact with Rab5 (Shin et al., 2008) but an interaction between LRRK2 and Rab7 had not been described before. They described a physical interaction between the *Drosophila* LRRK and Rab7, where dLRRK localises to Rab7-positive late endosomes and lysosomes.

Xiong et al. (2012) determined that LRRK2 also interacts with ArfGAP1 *in vivo*, based on co-immunoprecipitation assays. ArfGAP1 is a GTPase activating protein (GAP) for LRRK2 that enhances GTP hydrolysis of LRRK2 and reduces its toxicity both *in vitro* and *in vivo*. GTPase activity is regulated by GAPs and guanine exchange factors (GEF). GAPs enhance hydrolysis of GTP by GTPases and GEFs promote the release of GDP allowing access of GTP to the GTPase (Barr and Lambright, 2010; Vigil et al., 2010; East and Kahn, 2011). GAPs and GEFs have some specificity for their target proteins. They proved that LRRK2 prosphorylates ArfGAP1 resulting in inhibition of the GAP activity of ArfGAP1 providing reciprocal regulation of LRRK2 and ArfGAP1.

Beilina et al. (2013) proved that LRRK2 also interacts with Rab7L1 (Rab7, member RAS oncogene family-like 1) based on protein-protein arrays with biotinylated Glutathione-S transferase (GST)-LRRK2, where LRRK2 was FLAG-tagged. Rab7L1 is localised to the trans-Golgi network, possibly in its GTP-bound form, where it is likely to recruit LRRK2 and other components to cooperatively cause TGN to be engulfed by the autophagosomes. What is interesting is that Rab7L1 has also been proposed as a high-risk loci for sporadic PD (MacLeod et al., 2013).

Martin et al. (2014) performed a LRRK2 tandem affinity purification and *in vitro* kinase screening of LRRK2-interacting phosphoproteins in order to identify candidate LRRK2 substrates and understand the connection between LRRK2 kinase activity and neurotoxicity. They demonstrated that ribosomal proteins were major LRRK2 interactors and LRRK2 kinase targets and that LRRK2 is remarkably enriched in the ribosomal subcellular fraction. The main finding was that s15 is a novel *in vivo* LRRK2 substrate that underlies PD-related phenotypes in *Drosophila* and directly links LRRK2 toxicity to altered mRNA translation. This study revealed a novel mechanism of PD pathogenesis linked to elevated LRRK2 kinase activity and aberrant protein synthesis *in vivo*.

Steger et al. (2016) made use of the power of modern phosphoproteomics in combination to genetic, biochemical and pharmacological approaches in order to establish direct *in vivo* LRRK2 substrates. From this study, Rab10 came up as interacting with LRRK2. Rab GTPases consist of ~70 family members in humans and they are involved in intracellular vesicular trafficking events (Stenmark, 2009; Rivero-Rios et al., 2015). The characteristic domain of Rab proteins is the switch II, and there is evidence that LRRK2 directly phosphorylates Rab10 at each T73 residue, which is located in that switch II domain. That region changes conformation upon nucleotide binding and regulates the interaction with multiple regulatory proteins (Pfeffer, 2005). Because of the high conservation of that T73 residue among the Rab proteins, more investigation was performed in order to test if LRRK2 can possibly phosphorylate other Rabs at the same position as well. They measured the LRRK2-mediated phorsphorylation of Rab8a, Rab1a, and Rab1b, all of which contain a Thr at the site equivalent to T73-Rab10 and all proteins were phosphorylated on the predicted LRRK2 phosphorylation site in the switch II domain.

1.14 Aims

The aim of this project was to shed new light on our understanding of the chain of events that cause nerve cells with the *LRRK2*-G2019S mutation to die. A better understanding of the biological functions of *LRRK2* and its roles in signal transduction pathways may be important for future therapeutic development for PD, and this is because the kinase pathway is an easy target for drug development. There were two main hypotheses in this study; the first one is that it is the regulation of dopamine by *LRRK2-G2019S* causing neuronal cells to die, and the second is that LRRK2 genetically interacts with Rab proteins leading to that neuronal loss. The different approaches that were deployed in order to address those hypotheses are summarized below:

1. Visual assays were performed in order to assess the visual function of *Drosophila* mutants and controls. The Steady State Visually Evoked Potential assay (SSVEP) method was utilised. In that series of experiments, DA release was manipulated by expressing Tetanus Toxin (TNT) in the dopaminergic neurons of *Drosophila*.

2. Make use of two different binary systems, including the *Gal4-UAS* and the *LexA-LexAop* binary systems in order to manipulate different genes at the same time.

3. High Performance Liquid Chromatography (HPLC) analysis in order to measure the dopamine levels in the fly brain in different genotypes, including the *hLRRK2-G2019S* mutation, the *hLRRK2* wild type and other mutants and controls.

4. Expression of different Rab transgenes in *Drosophila* both in isolation and in combination with the *G2019S* mutation in order to test for genetic interaction between the different Rabs tested and LRRK2 in vivo.

2. Materials and Methods

2.1 *Drosophila* Husbandry and Genetics

2.1.1 *Drosophila* stocks

Drosophila stocks used during this research project were purchased from Bloomington *Drosophila* Stock Centre (Indiana University, Bloomington, USA), the Vienna *Drosophila* RNAi Centre (VDRC; Institute of Molecular Biotechnology, Vienna, Austria), or were kindly donated from members of the *Drosophila* community. A detailed summary of stocks can be found in Table 2.1. All stocks, without exception were quarantined for at least 2 generations and were inspected for the presence of mites. Post-quarantine, mite free stocks were transferred to the stock rooms.

All stocks were raised at either 18 ^{o}C or 25 ^{o}C and were transferred to a fresh medium every 4 or 2 weeks, respectively. All the experimental crosses performed were raised at either 25 ^{o}C or 29 ^{o}C, giving a generation time of ~ 10-12 days (egg to adult).

Table 2.1 Stocks Used During The Course of This Investigation

Summary of all the stocks used during this work. Only primary stocks are listed on this table; double balanced stocks, stocks combining multiple genetic elements are listed below

Stock	Chromosome	Description	Source
Wild types			
Canton S (*CS*)	n/a	Wild-type, red eyes	Elliott/Sweeney Lab Stock
w^{1118} (w^{-})	n/a	Wild-type, white eyes	Elliott/Sweeney Lab Stock
$w^{apricot}$ (w^{α})	n/a	Wild-type, orange eyes	Bloomington Stock Centre 148
Balancer Stocks			
CyO/Sco	Second	Second Chromosome Balancer	Elliott/Sweeney Lab Stock
TM3/TM6b	Third	Third Chromosome Balancer	Elliott/Sweeney Lab Stock
CyO-GFP/If;TM6b/MKRS	Second & Third	Second and Third Chromosome Balancer	Elliott/Sweeney Lab Stock
CyO/If; TM6b/MKRS	Second & Third	Second and Third Chromosome Balancer	Elliott/Sweeney Lab Stock

Stock	Chromosome	Description	Source
Gal4 stocks			
Actin5c-Gal4/CyO-GFP	Second	Actin promoter; global driver	Elliott/Sweeney Lab Stock
LongGMR-Gal4/CyO-GFP	Second	Glass multimer reporter; eye specific driver	Elliott/Sweeney Lab Stock
TH-Gal4/TM3	Third	Tyrosine hydroxylase; DA neuron specific driver	Kind gift of Serge Birman via Stephen Goodwin
elav-Gal4	Third	Embryonic lethal abnormal vision; pan-neuronal specific driver	Elliott/Sweeney Lab Stock
LexAop Stocks			
LexAop-*hLRRK2*/*Sm6a*	Second	Human *hLRRK2* transgene	Generated during this study; University of Cambridge/ Fly Facility
LexAop-*hLRRK2-G2019S*/*Sm6a*	Second	Human *hLRRK2-G2019S* transgene	Generated during this study; University of Cambridge/ Fly Facility
LexAop-*hLRRK2*/*TM6c*	Third	Human *hLRRK2* transgene	Generated during this study; University of Cambridge/ Fly Facility
LexAop-*hLRRK2-G2019S*/*TM6c*	Third	Human *hLRRK2-G2019S* transgene	Generated during this study; University of Cambridge/ Fly Facility

Stock	Chromosome	Description	Source
LexA Stocks			
TH-LexA/*CyO*	Second	Tyrosine hydroxylase; DA neuron specific driver	Kind gift of Yoshi Aso, Janelia Farm (unpublished)
UAS Stocks			
UAS-*hLRRK2*	Third	Human *LRRK2* transgene	(Liu et al., 2008)
UAS-*hLRRK2-G2019S*	Third	Human *LRRK2-G2019S* mutant transgene	(Liu et al., 2008)
UAS-*hLRRK2*	Third	Human *LRRK2* transgene	(Lin et al., 2010)
UAS-*hLRRK2-G2019S*	Third	Human *LRRK2-G2019S* mutant transgene	(Lin et al., 2010)
UAS-*hLRRK2/CyO*	Second	Human *LRRK2* transgene	H. Lundbeck A/S, Denmark
UAS-*hLRRK2-G2019S/CyO*	Second	Human *LRRK2-G2019S* mutant transgene	H. Lundbeck A/S, Denmark

Stock	Chromosome	Description	Source
UAS-*hLRRK2-D1994A/CyO*	Second	Kinase-dead human *LRRK2* transgene	H. Lundbeck A/S, Denmark
UAS-*hLRRK2-I2020T*/*TM6b*	Third	Human *LRRK2-I2020T* mutant transgene	Kind gift of Katerina Venderova (Venderova et al., 2009)
UAS-*hLRRK2-R1441C*/*TM6b*	Third	Human *LRRK2-R1441C* mutant transgene	(Lin et al., 2010)
UAS-TNT/CyO	Second	Expresses the *TNTxLC* transgene	Elliott/Sweeney Lab Stock
Mutant Stocks			
$dLRRK^{e03680}$	Third	PBac{RB} P-element disruption of *dLRRK*, generating a *dLRRK* null mutant	Kind gift of Zhuohua Zhang (Wang et al., 2008)

Table 2.2 *UAS-Rab Drosophila* Stocks Used During The Course of This Investigation

Stock	Chromosome	Description	Bloomington Stock Centre Number
UAS-Rab1	Third	Expresses a YFP-tagged, wild type Rab1 protein under UAS control	24104
UAS-Rab2/TM3	Third	Expresses a YFP-tagged, wild type Rab2 protein under UAS control	23246
UAS-Rab4	Third	Expresses a YFP-tagged, wild type Rab4 protein under UAS control	9767
UAS-Rab5	First	Expresses a YFP-tagged, wild type Rab5 protein under UAS control	50788
UAS-Rab6/CyO	Second	Expresses a YFP-tagged, wild type Rab6 protein under UAS control	23251
UAS-Rab7	Third	Expresses a YFP-tagged, wild type Rab7 protein under UAS control	23270
UAS-Rab8	Second	Expresses a YFP-tagged, wild type Rab8 protein under UAS control	9782

UAS-Rab9	Third	Expresses a YFP-tagged, wild type Rab9 protein under UAS control	9784
UAS-Rab10	Second	Expresses a YFP-tagged, wild type Rab10 protein under UAS control	24097
UAS-Rab11	Second	Expresses a YFP-tagged, wild-type Rab11 protein under UAS control	50782
UAS-Rab14	Second	Expresses a YFP-tagged, wild type Rab14 protein under UAS control	9793
UAS-Rab18	Third	Expresses a YFP-tagged, wild type Rab18 protein under UAS control	9796
UAS-Rab19	Second	Expresses a YFP-tagged, wild type Rab19 protein under UAS control	24150
UAS-Rab21	Second	Expresses a YFP-tagged, wild type Rab21 protein under UAS control	23242
UAS-Rab23	Third	Expresses a YFP-tagged, wild type Rab23 protein under UAS control	9802
UAS-Rab26/CyO	Second	Expresses a YFP-tagged, wild type Rab26 protein under UAS control	23245

UAS-Rab27	Second	Expresses a YFP-tagged, wild type Rab27 protein under UAS control	9810
UAS-Rab32	Second	Expresses a YFP-tagged, wild type Rab32 protein under UAS control	23282
UAS-Rab35	Second	Expresses a YFP-tagged, wild type Rab35 protein under UAS control	9821
UAS-Rab39	Second	Expresses a YFP-tagged, wild type Rab39 protein under UAS control	9825
UAS-Rab40/TM3	Third	Expresses a YFP-tagged, wild type Rab40 protein under UAS control	9830

2.1.2 *Drosophila* Media

Stocks were maintained in 25x95 mm plastic vials (Dutcher Scientific, UK) plugged with cotton wool (Fisher Scientific, UK) containing ~7 ml standard yeast-sucrose-agar media: 25 g/l sucrose, 3.75 g/l agar, 0.125 g/l $CaCl_2$, 0.125 g/l $FeSO_4$, 0.125 g/l $MnCl_2$, 0.125 g/l NaCl, 2 g/l $KNaC_4H_4O_6$, $4H_20$; following autoclaving and cooling for 1h to ~ 45 ^oC, the antifungal agents Bavistin (1.5 mg/l in 100 % ethanol; BASF, Auckland, New Zealand) and Nipagin (0.7 mg/l in 100 % ethanol; Sigma, UK) were added. Experimental flies kept on this media were transferred to fresh vials every 3-4 days.

For the Rab set of experiments a new recipe was followed, and as before stocks were maintained in 25x95 mm plastic vials. This enriched fly food contained 120 g agar, 469.4 g cornmeal, 444.2 g yeast and 1125 g sucrose. After approximately 75 min and when the temperature was down to 70 ^oC, 81 ml of propionic acid was added and mixed with the rest of the ingredients. When the food had cooled down, 7 ml of fly food was added to the plastic vials (Fisher Scientific, UK).

When required in large numbers stocks were raised in 1/3 pint bottles on a maize based medium (119.0 g/l maize meal, 17.5 g/l yeast, 15.9 g/l agar, 103.2 g/l sucrose). Post-cooking of the primary ingredients media was cooled to 45 ^oC and the antifungal agents Nipagin (0.4 mg/l in 100% ethanol; Sigma, UK) and propionic acid (0.4% v/v; Arcos Organics, Geel, Belgium) were added. The medium was then dispensed into 1/3 pint glass bottles and the bottles bunged using Flugs® (Dutscher Scientific, UK). Bottles containing medium were autoclaved at 121^oC for approximately 20min.

To encourage egg-laying medium could be supplemented with dried yeast or yeast paste. Experimental flies were kept at the maize-based media until eclosion at which time female flies were transferred to vials containing the standard yeast-sucrose-agar medium. Experimental flies were then aged at 29 ^oC in constant darkness or with continuous flashing blue LED lights, depending on the experimental protocol.

2.1.3 *Drosophila* Anaesthesia

In order to allow the identification of the gender and the genotype, adult *Drosophila* flies were anaesthetised on a porous gas pad using continuous administration of carbon dioxide (CO_2). The constant flow of CO_2 provided immediate and maintained anaesthetisation. The anaesthetised *Drosophila* adults were then observed using a dissecting microscope (Zeiss Stemi-2000, Carl Zeiss AG, Germany). CO_2 was the principal technique used to anaesthetise flies in this research. However, cold immobilisation on dry ice was used in order to collect them for being further processed for Western blotting.

2.1.4 *Drosophila* crossing techniques

Crosses were performed by adding males to their virgin female mates. At 25 ^{o}C females that have been eclosed within the last 8 hours should reject courtship and therefore should be virgins (reviewed in Dickson, 2008). Virgin females can be identified because when they are newly eclosed they have a pale pigmentation, display a meconium that is visible through the abdominal cuticle, and they have unexpanded wings. On this basis virgin females were collected daily through completely emptying vials and isolating virgins that were then kept at 25 ^{o}C for a week time in order to confirm their virgin nature. Adult males and female virgins were then crossed in a fresh vial of medium or bottle. The F_o generation of flies was then removed after 7 days and transferred in a new vial or bottle in order to prevent over-crowding and specific selection of F_1 flies for further crosses or experiments.

2.2 Physiological analyses

2.2.1 Flash Electroretinograms (ERGs)

Unanaesthetised female flies were left to crawl up a trimmed 200 µl Gilson pipette tip and were forced to the end by blowing down the wider end. The fly was fixed with its head protruding from the tip using nail varnish. After placing the fly in the ERG apparatus, glass electrodes were pulled and filled with *Drosophila* solution (0.13 M NaCl, 4.7 mM KCl, 1.9 mM CaCl2; Heisenberg, 1971). One of the electrodes was placed on the surface of the eyes, where the recordings were made from, and the other on the mouthparts as a reference by using micromanipulators (Figure 2.1a). Once in position all flies were dark adapted for 5 min. ERGs were recorded in response to three to five stimuli (10 sec apart, 0.5 sec long) from the blue component of an LED light (Kingbright, KAF-5060PBESEEVGC, maximum emission wavelength 465 nm, Taipei, Taiwan) placed ~6 cm in from of the fly. In another set up that was used, only a single LED channel was present centered at 467 nm (Gaussian spectral profile, FWHM 34 nm) (Prizmatix FC5-LED). The input/output linearity of the LED was verified using both a photodiode and a photospectrometer (Ocean Optics USB2000). *DASYLab* software was used in order to record the ERGs and *DASYView* (Version 2.1.6) was used for the analysis of the data (*DASYLab* customised software, C. J. H. Elliott, University of York). The ERG method was only used to check that the fly gave a response, indicating proper electrical connection.

An example of the ERG output is presented in Figure 2.1b. The photoreceptor response (1 in Figure 2.1) was measured as the difference in potential between the start level and the bottom of the first decline in the trace. The off-transient response was inferred from the potential difference between the start and the minimum levels (2 in Figure 2.1). The initial rate of recovery was measured as time taken to reach half way between the start and the minimum levels (3 in Figure 2.1).

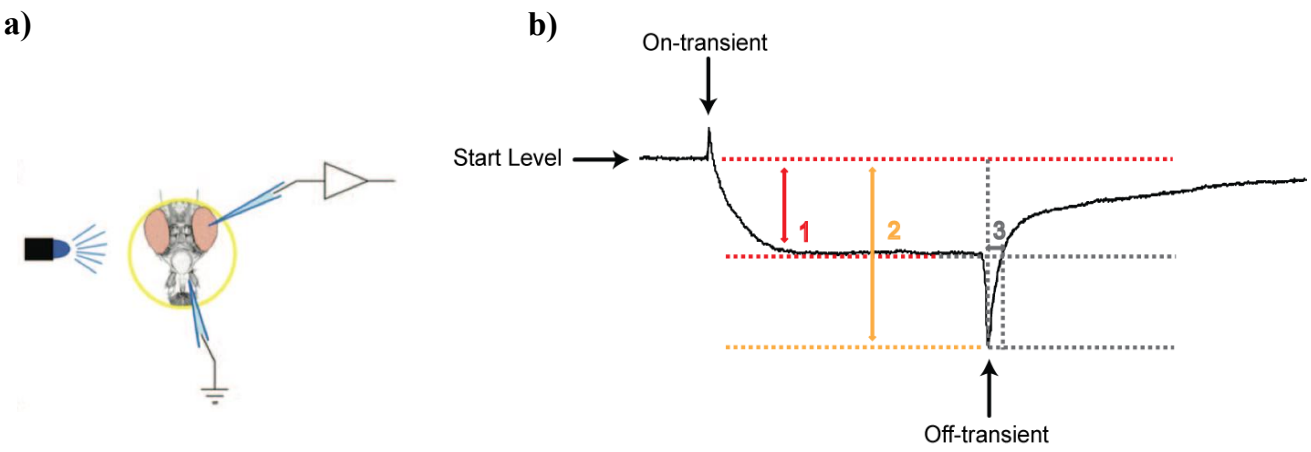

Figure 2.1: Recording the visual response of *Drosophila* using the flash ERG. a) Flies were left to climb in a shortened Gilson pipette tip and exposed to 500 ms pulse of light from the blue component of an LED light. A glass electrode filled with *Drosophila* saline was placed on the surface of the eye in order to record the response of the visual network, while a second reference electrode was placed in the mouthparts. b) The ERG consists of 4 main elements: the photoreceptor response (1), the on-transient, the off-transient and the recovery phase (3). The photoreceptor response was determined as the difference between the starting potential and the potential a third of the distance along the recording. The off-transient amplitude can be inferred from the maximum potential (2), which measures the potential difference from the starting level to the minimum level (the peak of the off-transient). The initial phase of the recovery response was calculated as time taken to reach half the distance between the off-transient peak and the start level (3) (Hindle et al., 2013).

2.2.2 Steady-State Visually Evoked Potential (SSVEP) assay

The SSVEP assay, as was first described in Afsari et al. (2014), combines features of the flash ERG with a computational approach that is based on human visual experiments, in which flickering stimulation is linked to the analysis of 'frequency-tagged' responses. Female adult flies were prepared as described in section 2.2.1 and their visual responses were verified (Figure 2.2). The fly was

illuminated by a blue light LED channel centred at a wavelength of 467 nm. The intensity of the light was controlled by a sequence generator encoded in Matlab (Version 2013a; Mathworks, Natick, MA; Source code at http://github.com/wadelab/flyCode), with the data acquisition toolbox installed. In some parts of the sequence, a single square wave was flickering about the mean illumination at a frequency of 12 Hz, was delivered. In other parts of the sequence, two square wave modulations with different frequencies were added together and delivered. One of the frequencies used was at 12 Hz and the other was at 15 Hz. The responses to 11 different contrast levels of the probe were also recorded. The contrast levels ranged from 0 to 69% contrast in equal steps.

For the SSVEP recordings the temporal contrast of the probe stimuli (F1) was swept through a range of values (0-69%) and the responses were measured both in isolation and in the presence of a 30% contrast mask at a different temporal frequency. When a mask contrast is applied at a different frequency (F2) the response to the swept input probe changes. The grey curves are used as a baseline, as they show the response when the mask is absent. The red curves show the response with the presence of a constant contrast (30%) mask as the probe contrast increases from 0% to 69%.

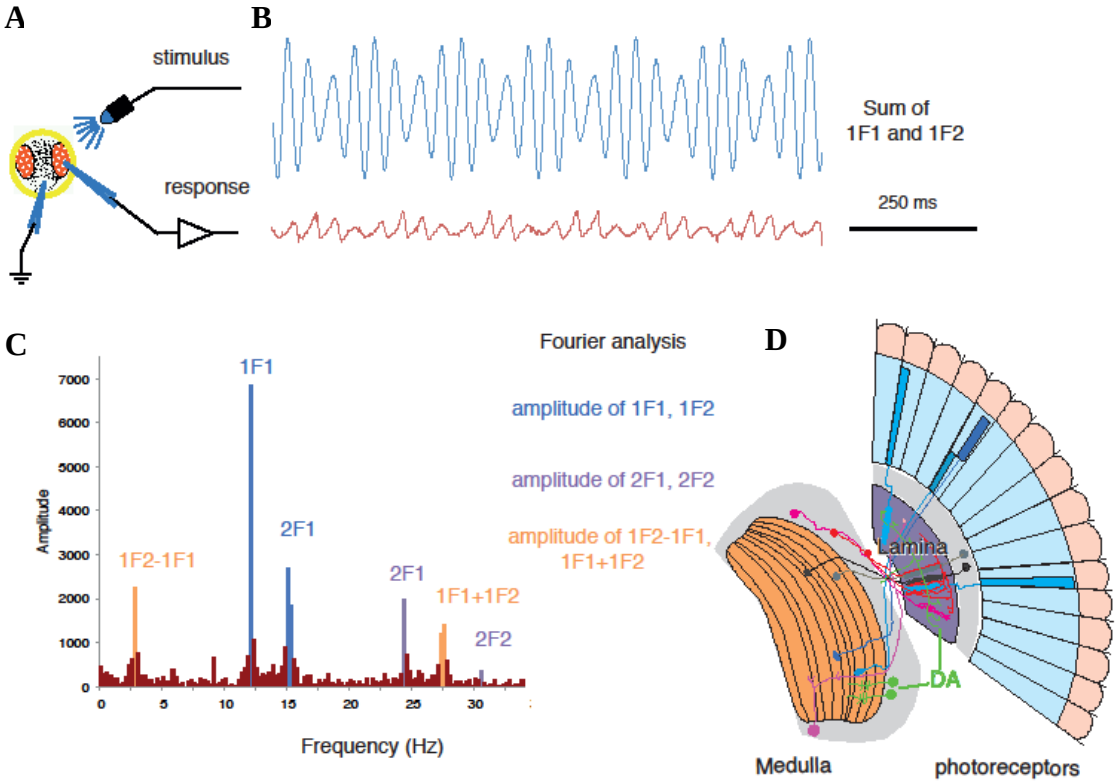
A
B
stimulus
response
Sum of
1F1 and 1F2
250 ms
C
Fourier analysis
amplitude of 1F1, 1F2
amplitude of 2F1, 2F2
amplitude of 1F2-1F1,
1F1+1F2
1F1
2F1
1F2-1F1
2F1
1F1+1F2
2F2
Amplitude
Frequency (Hz)
D
Lamina
DA
Medulla
photoreceptors

Figure 2.2: Recording and analysing the visual responses of *Drosophila* using the SSVEP method A) Flies were left to climb in a shortened Gilson pipette tip and exposed to a blue LED that is driven by a continuously flickering wave. A glass electrode filled with *Drosophila* saline was placed on the surface of the eye in order to record the response of the visual network, while a second reference electrode was placed in the mouthparts. **B**) The blue line represents the stimulus, which is the sum of two square waves of 12Hz and 15Hz known as 1F1 and 1F2, respectively. The red line represents a typical response (1 second of data from a single trial) to this stimulus from a white-eyed fly. **C)** A Fourier analysis is used to separate the response into parts depending on frequency, which is then plotted. Harmonics of the input frequencies (12 Hz and 15 Hz) are shown in the Fourier transform of the signal as blue (first harmonic) and purple (second harmonic) bars. Low order intermodulation terms (1F2-1F1 and 1F1+1F2) are shown in orange (Afsari et al., 2014). D) The SSVEP method is very sensitive, as it shows how the different components of the visual system contribute to the final signal. Different harmonics of the selected frequencies represent visual responses from the different components of the visual system.

2.3 Molecular Biology

2.3.1 Extraction of genomic DNA

Genomic DNA was extracted from single adult flies by homogenisation in 50 µl of extraction buffer (10mM Tris-Cl pH8.2, 1mM EDTA, 25mM NaCl, Proteinase K 200 µg/ml). The proteinase K should be added fresh on the day of the experiment. The homogenate was incubated at 25-37ºC (or room temperature) for 20-30 min, followed by heating to 95ºC for 1-2 min in order to inactivate the proteinase K. 1-2 µl of supernatant was used as a PCR template.

Table 2.3 Summary of the PCR Reagents

PCR Reagents	Volume (µl)
PCR master mix	10µl
Primer (Forward)	1µl
Primer (Reverse)	1µl
DNA	1µl
dH_2O	7µl
Final volume	20µl

For higher concentrations of genomic DNA, 15 adult flies of the same genotype were used using the Gentra Puregene DNA purification kit (Qiagen, UK) as per the manufacturer's instructions (Qiagen, 2010). 1-2 µl of the extracted DNA was used per PCR reaction.

2.3.2 Polymerase Chain Reaction (PCR)

PCR reactions were run using PCR mastermix (Promega, UK; 25 U/ml *Taq* DNA polymerase, *Taq* Reaction buffer, 200µM of each dNTP, 1.5mM $MgCl_2$) with 1µl of each primer and 0.5-1 mg of genomic DNA or 1-2 ng of plasmid DNA.

Reactions were run in a Techne TC512 PCR thermocycler (CamLab, UK), typically for 30 cycles. The annealing temperatures that were used were 5^oC lower than the lowest primers melting temperature (Tm) with an extension time of 1 min per kb. Standard PCR cycling conditions were: initial denaturation at 95 ^oC for 10 min; cycles of 95 ^oC for 30 sec, Tm for 60 sec, 72^oC for 5 min. Reactions were then cooled at 4 ^oC to prevent DNA decomposition. The primers used were designed using Primer3 software and synthesised by Eurogentec (U.K). A list of primers that were used during this investigation are summarized in Table 2.4.

Table 2.4. Primer sequences summary

Primers	Sequence
5’ pUAST	CTGCAACTACTGAAATCTGC
3’ pUAST	ATCTCTGTAGGTAGTTTGTCCA
5’ LexAop	GAGCGCCGGAGTATAAATAGAG
3’ LexAop	CCATTCATCAGTTCCATAGG
5’ hLRRK2 (used for sequencing)	ATCAGTTTACCGAGCAGCCT
5’ hLRRK2	TCCAGATCAACCAAGGCTCA
3’ hLRRK2	TCAAAGACCTGGGCAGAAGT
5’ DVM-5	ATTGCTGCTGGTGCCATCACGTTC
3’ DVM-6	AGCCAACACAGAAGCCCACATCAC
3’ Pry4-N	CGACACTCAGAATACTATTCC
5’ Plac1-N	CAACCTTTCCTCTCAACAAGC

2.3.3 DNA Agarose Gel Electrophoresis

Agarose gel electrophoresis was performed in order to analyse DNA products from PCR reactions or restriction enzyme digests. 0.7% and 1 % agarose gels (in TAE buffer; 40 mM Tris acetate, 1 mM EDTA, pH 8.3) were used for large and small (<1kb) DNA products, respectively. Addition of SYBR® safe (Invitrogen, UK; 10 µl/100 ml) to the gel allowed the visualisation of the DNA using a blue light transilluminator. Bromophenol blue loading dye (0.25% w/v bromophenol blue, 30 % glycerol v/v in dH_2O) was added to the DNA to assist with the loading. A 1Kb or 100bp DNA ladder (0.5 µl/lane, NEB, UK) was run alongside the DNA products in order to be able to determine the size. All gels were run at ~80 V for 30-45 min.

2.3.4 DNA purification; Gel Extraction

The DNA fragments that were further needed for cloning or sequencing were excised from electrophoresis gels, using a sharp sterile scalpel and visualisation by a blue light transilluminator box. Gel slices were transferred to 1.5 ml eppendorf tubes and processed according to the QIAquick® Gel Extraction kit (Qiagen, UK) via the manufacturer's instructions (Qiagen, 2015). The DNA concentration was determined using a NanoDrop ND-1000 spectrophotometer (Thermo Scientific, DE, USA).

2.3.5 DNA Sequencing

DNA sequencing was used in order to confirm the generation of new transgenic flies (*Lexop-hLRRK2* and *LexAop-G2019S*). Samples were submitted, in accordance with provided guidelines, for sequencing by GATC Biotech (Konstanz, Germany).

2.3.6 Restriction Endonuclease Digestion

Plasmids contain several restriction sites that are specifically recognised by restriction enzymes. These enzymes can be used in order to specifically cleave plasmids, allowing for excision and insertion of DNA fragments during sub-cloning. This approach was used to excise *hLRRK2* and *hLRRK2-G2019S* from their donor plasmids and cleave their recipient plasmid, in both cases LexAop, for their insertion. Restriction enzymes were also used to cleave plasmid DNA from transformed clones in order to check for the presence of the plasmid and the newly inserted gene by gel electrophoresis. In every case the required restriction enzymes were added to the plasmid along with the appropriate buffer with a total reaction volume of 20 µl. Reactions were incubated for 2 hrs at 37ºC followed by a 20 min incubation at 80ºC to inactivate the enzymes. All the restriction products were run on an electrophoresis gel to ensure the correct cleavage of the restriction enzymes.

2.3.7 DNA ligation

The purified DNA fragments that were previously treated with restriction enzymes were ligated together and into cleaved vector plasmids using T4 DNA ligase. Ligation reactions were typically a 3:1 (insert: vector (ng)) ratio, determined using the following formula: Insert mass (ng)= [3 x (insert length bp/ vector length bp)] x vector mass (ng). DNA concentration was ascertained using a NanoDrop ND-1000 spectrophotometer (Thermo Scientific, DE, USA). For the ligation reaction 0.2 µl of T4 ligase (Fermentas, UK) was used with 2 µl of T4 buffer (Fermentas, UK) and the DNA in a total reaction volume of 20 µl. All the reactions were incubated at 16ºC overnight followed by a 10 min inactivation of the ligase at 65ºC.

For this course of investigation the donor vector for *hLRRK2* and *hLRRK2-G2019S* transgenes that was used was the pcDNA-DEST53 (Invitrogen). The backbone size without the insert was 7767bp and the insert size was 7584 bp (Figure 2.3). Gateway cloning was used as has been described previously (Greggio et al., 2006).

The LexAop vector that was used was the pJFRC19-13XLexAop2-IVS-myr::GFP, size 9011 bp (Figure 2.4).

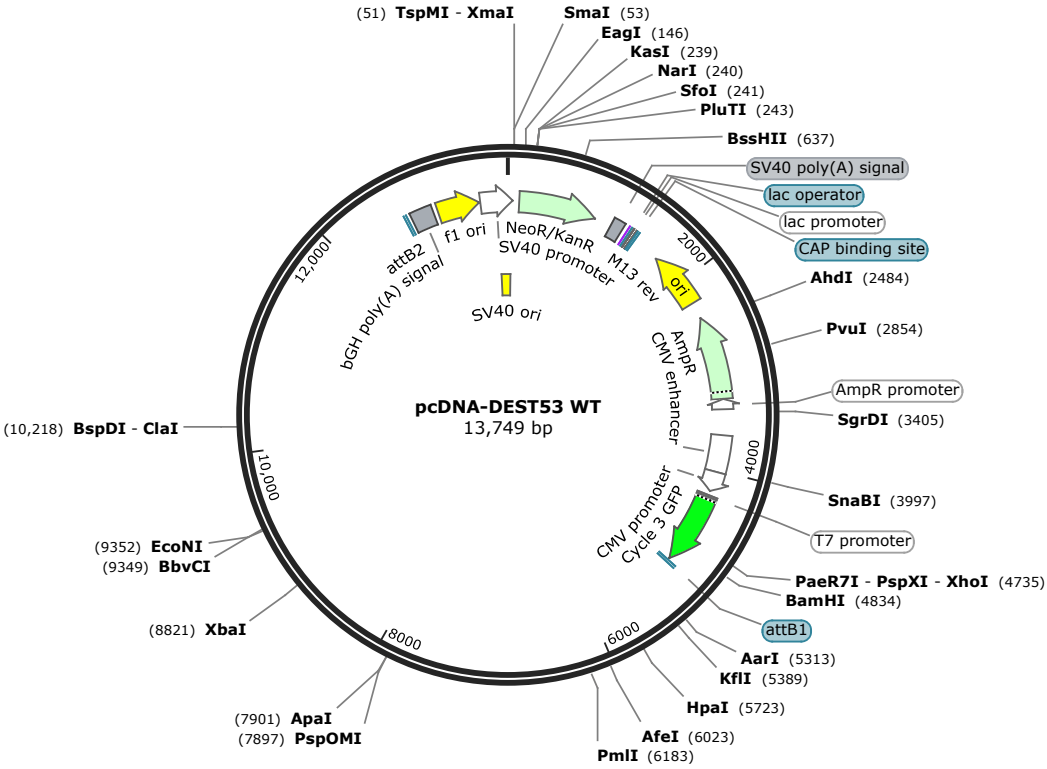

Figure 2.3 Full sequence map for pcDNA-DEST53-LRRK2-WT. This is the donor vector that was utilised containing the *LRRK2* and *LRRK2-G2019S* sequences. The backbone vector sized 7767 bp and the insert *LRRK2* gene 7584 bp. Gateway cloning was performed to create this vector with the 5' cloning site being the attR1 and the 3' being the attR2 (none of these sites was destroyed). The map was created using the SnapGene software.

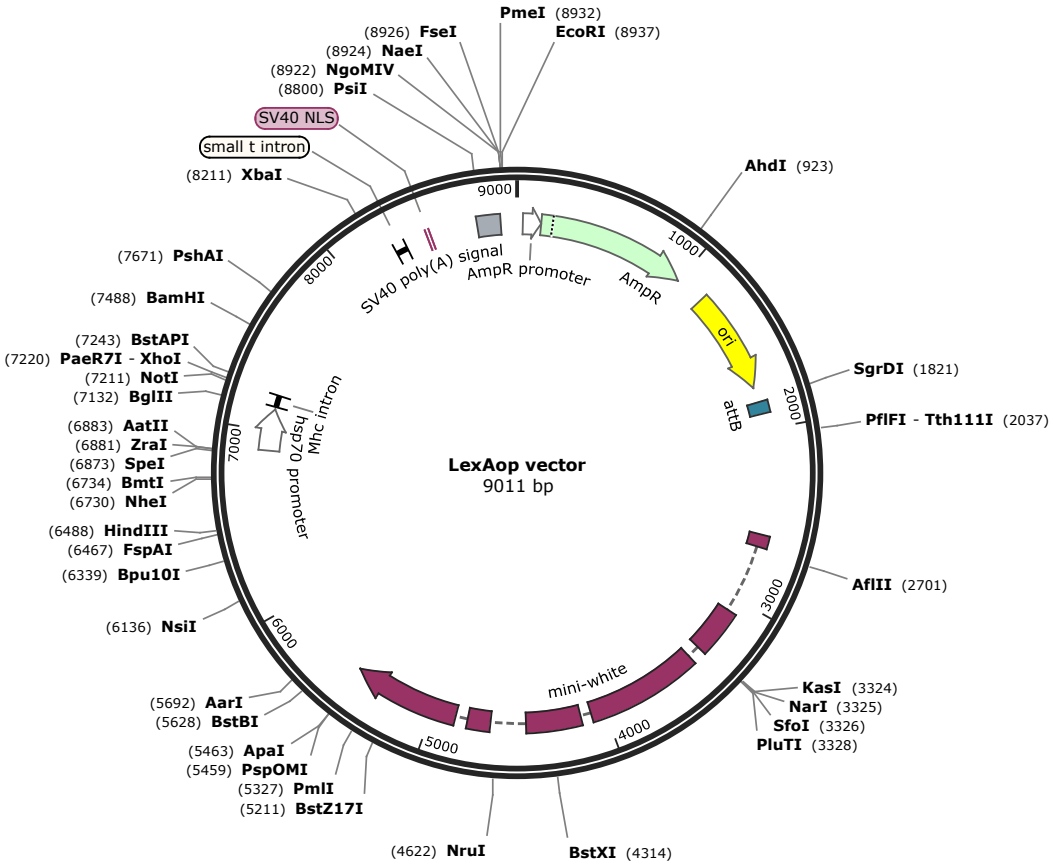

Figure 2.4 Full sequence map for pJFRC19-13XLexAop2-IVS-myr::GFP. This is the LexAop vector that was utilised in order to insert the *LRRK2* and *LRRK2-G2019S* transgenes downstream of the LexAop sequence. The vector sized 9011 bp. The map was created using the SnapGene software.

2.3.8 *E. coli* Transformation and Amplification of plasmid DNA

For the generation of new transgenic *Drosophila* lines, XL-1 Blue supercompetent *E. coli* cells (Agilent Technologies, CA, USA) were used in order to amplify plasmid DNA, as the desired antibiotic resistant was ampicillin (Amp). Transformation was achieved via heat-shock in accordance with the manufacturers instructions. The protocol was modified and was scaled to use 20 µl of cells as opposed to the recommended 100 µl. Luria broth (LB; 10 g/l tryptone, 5 g/l yeast extract, 10 g/l NaCl) was also used instead of SOC media.

For transformation of plasmid from a ligation mix 1 µl of the ligation reaction was used, as recommended. Post-transformation cells were plated on LB agar plates (20 g/l agar in LB broth) containing the appropriate antibiotic, in this investigation Ampicillin (Amp; 200 µg/ml), in accordance with the manufacturers instructions. Plates were then incubated overnight at 37^{o}C.

Individual colonies were harvested from the plates using a sterile pipette tip and transferred into a sterile 15 ml falcon tube containing 5 ml sterile LB broth and the appropriate antibiotic (Amp). Cultures were incubated at 37^{o}C overnight (12-16 h) with vigorous shaking. The transformed *E. coli* stocks can be long-term stored at -80^{o}C by adding 50 % v/v sterile glycerol. These glycerol stocks were used to streak fresh plates when required.

In order to check for the presence of the insert within transformed colonies, following the ligation process during sub-cloning, plasmid DNA should first be purified by miniprep (section 2.3.10.1) and then confirm the insert presence by restriction enzyme digestion (section 2.3.6). For minipreps 2 ml of each overnight culture was pelleted via centrifugation at 13000 g for 2 min at room temperature (RT), followed by the removal of the supernatant. That stock was stored at -20^{o}C. In order to ascertain those colonies that most likely have taken up the insert prior to miniprep, in order to reduce the number of minipreps required, colony cracking could be performed using 15 µl of the overnight culture.

2.3.9 Colony cracking

Colony cracking is a quick method in order to confirm the presence of the desired insert from colonies before carrying on to the purification of the plasmid DNA. It relies on cell lysis using alkaline conditions and identification of positive clones based on electrophoretic mobility variance between supercoiled DNA plasmids with and without the insert. The insert carrying colonies are expected to move slower on the electrophoresis gel. By using that method inserts as small as 200 bp can be detected.

20 µl of bromophenol blue loading dye was added to 1 ml of 5x cracking buffer (25 g sucrose, 5 ml 5M NaOH, 2.5 ml 10 % SDS, 40 ml ddH_2O). 5 µl of cracking buffer and bromophenol blue loading dye was added to 5 µl of resuspension buffer (50 mM Tris-HCl pH 8.0, 10 mM EDTA, 100 µg/ml RNaseA) and mixed with 15 µl of the overnight culture. That mixture was then loaded and run on an electrophoresis gel (section 2.3.3) using uncut empty plasmid as the control, with no ladder being required. Alternatively, single colonies can be patched and used directly for cracking instead of 15 µl of overnight culture. The colonies containing the insert will show different electrophoretic mobility compared to the control. The colonies that the insert has been successfully inserted can then used for purification via miniprep (section 2.3.10.1).

2.3.10 Plasmid Purification

2.3.10.1 MiniPrep Purification

For the purification of the plasmid DNA the QIAprep spin miniprep kit (Qiagen, UK) was used providing up to 20 µg of molecular biology grade plasmid DNA from *E. coli*. Frozen pellets produced by centrifugation of 2 ml of overnight cultures (section 2.3.8) were processed in accordance with the manufacturers instructions. Concentrations of the purified DNA were determined using a NanoDrop 1000 spectrophotometer (Thermo Scientific, DE, USA). The purified DNA plasmid was stored at -20^{o}C.

The plasmid DNA purified by miniprep was used in order to confirm the presence of the insert by restriction digest (section 2.3.6) followed by gel electrophoresis.

2.3.10.2 MidiPrep Purification

To provide a greater purity of plasmid DNA (up to 200 µg of transfection-grade plasmid DNA) and greater yields for microinjection of *Drosophila* embryos, plasmids were purified using the Qiagen HiSpeed Plasmid Midi kit (Qiagen, UK).

Following the confirmation of the presence of the desired insert via colony cracking, miniprep, restriction digest and gel electrophoresis, 100 µl of the appropriate overnight culture (section 2.3.8) was used to inoculate 100 ml of LB broth containing Amp (200 µg/ml). 100 ml cultures were incubated at 37ºC overnight with vigorous shaking. Alternatively, for optimal results a single colony could be picked from patched plates or a freshly streaked plate, streaked from the appropriate glycerol stock, and used to inoculate a 5 ml starter culture of LB broth containing Amp (200 µg/ml). Starter cultures were incubated at 37ºC for 8h with vigorous shaking before used to inoculate a 100 ml culture (100 µl in 100 ml) and incubated as above. Following incubation, all 100 ml from the culture were centrifuged at 6000 rpm for 15min at 4 ºC. After removal of the supernatant, the pellets were frozen before being processed for midiprep in accordance with the Qiagen HiSpeed Midi kit protocol (Qiagen, 2010).

2.3.11 Ethanol precipitation of DNA

Following midipreps, the concentration of the plasmid DNA was determined using a NanoDrop 1000 spectrophotometer (Thermo Scientific, DE, USA). For the microinjection of *Drosophila* embryos, a plasmid concentration of 0.4 µg/µl was required. To achieve this concentration the plasmid DNA obtained from midiprep was precipitated with a $1/10^{th}$ volume of sodium acetate (3M, pH 5.2) and 3 volumes of cold 100 % ethanol. That mixture was then incubated at -20 ºC overnight. Following centrifugation at 16000g for 15 min at RT the supernatant was carefully removed. 1 ml of 70 % ethanol was then added to the pellet and after the mixture was well mixed the supernatant was removed and the pellet was resuspended in the appropriate volume of nuclease-free H_2O. Concentrations of the purified DNA were determined using a NanoDrop 1000 spectrophotometer (Thermo Scientific, DE, USA). The purified DNA plasmid was stored at -20 ºC.

2.3.12 Microinjection of *Drosophila* embryos

For microinjections, the LRRK2-LexA LRRK2-G2019S-LexA constructs were sent to the University of Cambridge, Department of Genetics, Fly Facility. The phiC31 integrase system was utilised for microinjections. The phiC31 integrase is a sequence-specific recombinase that is encoded within the genome of the phiC31 bacteriophage. The phiC31 integrase mediates recombination between two 34 bp sequences known as attachment sites (att), one found within the donor plasmid (attB) and the other found within the target genome (attP). In the presence of phiC31 integrase an attB- containing donor plasmid can be unidirectionally integrated into the target genome through recombination with the attP site. The phiC31 fly stock used for microinjections during this investigation was the stock 13-20, (genotype: y w M (eGFP, vas-int, dmRFP) ZH-2A; P{CaryP}attP40) which has an attP site on the 2nd chromosome (25C6), marked with RFP and GFP to make it easier to identify those stocks in which plasmid integration was successful. Successful lines were balanced over a 2nd chromosomal balancer and the integrase was removed before being sent back from Cambridge. Moreover, another phiC31 fly stock that was used was the stock 13-106: vas-int; attp-3B, VK00033, (genotype: y w M (eGFP, vas-int, dmRFP) ZH-2A;; PBac{y[+]-attP-3B}VK00033) which has an attP site on the 3rd chromosome (2A3), marked with GFP and RFP to make it easier to identify those stocks in which plasmid integration was successful. Successful lines were balanced over a 3rd chromosomal balancer and the integrase was removed before being sent back from Cambridge.

2.4 Western Blotting

Western Blotting was performed in order to determine the expression pattern of hLRRK2, hLRRK2-G2019S for all the available lines in the lab and control flies. The method for western blotting was adapted from Abcam (2016).

2.4.1 Protein extraction

Proteins were extracted from 30 whole adult heads per genotype after 3 days incubation at 29ºC. Flies were collected in 15 ml falcon tubes and were snap frozen on dry ice. In order to separate the heads from the rest of the fly body the 15 ml falcon tubes were placed into a 50 ml falcon tube containing dry ice and vortexed 2-3 times for 30sec. The fly heads were then collected under the microscope and transferred to 1.5 ml eppendorf tubes keeping them on dry ice. In order to extract protein, one complete mini protease inhibitor cocktail tablet (cOmplete tablet, Mini EDTA-free, *EASYpack*; Roche) was dissolved in 7 ml of RIPA (Radioimmunoprecipitation assay) buffer (150mM NaCl, 1.0% IGEPAL® CA-630, 0.5% sodium deoxycholate, 0.1% SDS, 50 mM Tris, pH 8.0; Sigma, UK). 30 µl of that mix was added to tubes of 30 fly heads placed on ice. The heads were homogenized using a sterile plastic pestle followed by centrifugation at 13000g for 15 min at 4ºC. The supernatant was removed and placed in a new 1.5 ml eppendorf tube and the protein concentration was quantified using the BCA (bicinchoninic acid) assay (µg/µl).

2.4.2 Quantification of protein concentration: BCA assay

Protein quantification was performed to determine the amount of protein in each solution (µg/µl). The BCA assay is highly sensitive colorimetric assay that is not affected by chemicals in the sample. It primarily reduces Cu^{2+} to Cu^{1+} by proteins in an alkaline environment followed by highly sensitive and selective colorimetric detection of BCA/copper complex. It is water-soluble and strongly absorbs light at 561nm in a linear fashion with increasing protein concentration. Protein samples (10 µl) were added to 200 µl BCA reaction solution and the absorbance was recorded. A bovine serum albumin (BSA) standard curve was also produced by measuring the absorbance of known concentrations of BSA. The protein concentrations of the unknown samples were calculated from the BSA standard curve. Known amounts of protein sample were mixed in a 3:1 ratio with sample buffer (100 µl β-mercaptoethanol in 900 µl 4x laemmli buffer), followed by heating at 95ºC for 5min and loaded on the SDS-PAGE gel. The

protocol that was followed was in accordance to the manufacturer's guidelines (BCA Protein Assay kit, Cohesion Biosciences, UK).

The concentration determination was estimated by using bicinchoninic acid (BCA) reagent with bovine serum albumin (BSA) as a standard. A set of diluted BSA standards were added to the reagent in order to produce a coloured reaction which is in proportion to the amount of the protein. The absorbance of all the BSA standards were measured with the spectrophotometer set to 561 nm within 10 min as suggested by the manufacturer's manual.

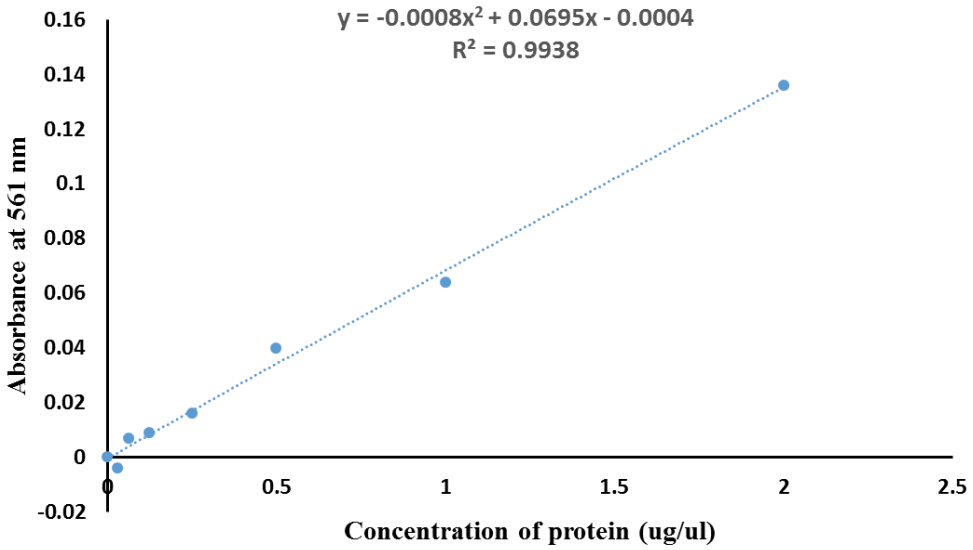

Figure 2.5 Standard curve for BSA protein. Plot of BSA protein standards vs the absorbance at λ=561nm.

Table 2.5 summarises the numeric data obtained including the absorbance at 561 nm and the protein concentration (ug/ul).

Table 2.5 Numeric report of absorbance generated by spectrophotometer

Concentration of BSA protein (ug/ul)	A (λ=561nm)
0	0
0.03125	- 0.004
0.0625	0.007
0.125	0.009
0.25	0.016
0.5	0.04
1	0.064
2	0.136

The intensity of the coloured reaction product is a direct function of the protein amount that can be determined by comparing its absorbance value to a standard curve. Using Microsoft Office Excel to plot and apply a standard curve (Figure 2.5) with the absorbance value as the dependent variable (Y-axis) and concentration as the independent variable (X-axis), resulted in the equitation $y = -0.0008x^2 + 0.0695x - 0.0004$, where solving for x determines the protein concentration of the sample. After determining the protein concentration for all of the tested samples, the concentration that was finally loaded for further analysis in the Western blot was 20ug/ul. That applies for all the different Western blots performed throughout this course of investigation.

2.4.3 Sodium Dodecyl Sulphate Polyacrylamide Gel Electrophoresis (SDS-PAGE)

Following heating to 95°C in sample buffer (100 mM Tris, pH 6.7, 15% (v/v) β-mercaptoethanol, 2% (w/v) SDS, 5% (v/v) glycerol, 0.002% (w/v) bromophenol blue), protein samples were separated on SDS-PAGE gels. The gels were composed of a 7.5 % (v/v) acrylamide resolving gel and a 4% (v/v) acrylamide stacking gel. After loading of samples and a protein ladder (7 µl Spectra™ Multicolor High Range Protein Ladder, ThermoFisher Scientific, USA), SDS-PAGE gels were run in running buffer (25 mM Tris, 192 mM Glycine, 0.1 %

SDS) at 75 V for approximately 30 min (to narrow the running front) and then increased to 150 V.

2.4.4 Protein transfer to a PVDF membrane

Following SDS-PAGE, a Mini-Trans-Blot® Cell was used in order to transfer the proteins from the SDS-PAGE gel to a PVDF membrane (Amersham Hybond 0.45 μm PVDF; GE Healthcare, UK). Foam pads, 4 pieces of Whatman® gel blot paper (0.8 mm thick; Thermo Fisher Scientific Pierce, UK) and the SDS-PAGE gel were all soaked in transfer buffer (25 mM Tris, 192 mM glycine, 20% [v/v] methanol, 0.1% [w/v] SDS). PVDF membrane was cut at the same size as the gel and then activated in 100% methanol for 1min, followed by a quick dip into the transfer buffer. Each of the soaked foam pads were placed on each side of a Mini Gel Holder Cassette, one on the negative (black) side and one on the positive (white) side. On top of the foam pads two pieces of soaked Whatman® gel blot paper were placed on each side followed by the gel on the negative side and the activated PVDF membrane on the positive side. The cassette was then closed carefully, making sure no bubbles are trapped, and was placed into the tank along with the transfer buffer and a Bio-Ice cooling unit that had been stored at -80oC. Proteins were transferred by applying 30V overnight at 4^{o}C, increasing to 60V the next morning for another 30 min.

2.4.5 Probing of PVDF membrane

Following the transfer of proteins to the PVDF membrane, then membrane was blocked for 1h in 3% (w/v) marvel milk in Tris buffered saline (TBS-T; 10 mM Tris, pH 7.6, 150 mM NaCl) supplemented with 0.1% (v/v) Tween® 20 (VWR, Pennsylvania, USA). That was followed by staining with the primary antibody in 3% (w/v) marvel milk in TBS-T after incubation at 4^{o}C overnight. Membranes were washed (5 x 3 min) in TBS-T. The appropriate species of secondary antibody (conjugated to HRP) was added in 3% (w/v) marvel milk in TBS-T for 1h at RT. Any excess secondary antibody was removed by washing the membranes (5 x 3 min) in TBS-T. All the washes and incubations were performed on a rocking platform. Membranes were then incubated in ECL

reagent (GE Healthcare, UK) for 1min. CL-XPosureTM x-ray film (Thermo Fisher Scientific Pierce, UK) was placed on the blot for 30 sec (α-hLRRK2) or 5 sec (α-myosin and β-actin). Exposed film was developed in Carestream® Kodak® autoradiography GBX Developer/Replenisher (Sigma, UK) for 1min, rinsed in dH_2O for 1 min and then fixed in Carestream® Kodak® autoradiography GBX Fixer/Replenisher (Sigma, UK) for 1 min. All the antibodies used and their concentrations are summarized in Table 2.6.

Table 2.6. Antibody dilutions used for western blotting

Antibody	Species	Concentration	Source
α -hLRRK2	Mouse monoclonal	1/1000	NeuroMab
α -hLRRK2	Rabbit polyclonal	1/3000	Novus
β -actin	Mouse	1/180000	Proteintech
α -myosin	Rat monoclonal	1/40000	Abcam
α-rabbit IgG HRP linked	Goat	1/1000	New England Biolabs
α-mouse IgG HRP linked	Horse	1/1000	New England Biolabs
α-rat IgG HRP linked	Goat	1/1000	New England Biolabs

2.5 *Drosophila* dissections

2.5.1 Dissection of *Drosophila* Retina

1 day, 7 days and 14 days post-eclosion adult flies of the correct genotype were anesthetised by CO_2 (section 2.1.3). Flies were orientated ventral side up and, using forceps the thorax was gently grasped causing an extension of legs and proboscis. While remaining hold of the body forceps, were used to grasp the proboscis in order to gently remove the head. The body was discarded and the head submerged in a drop of HL3 (hemolymph-like solution) on a sylgard dish. The eye was carefully dissected from the head. That is most easily done by teasing apart the connective tissue between the eye and the proboscis and working round gently tease the eye from the head. Eyes were transferred into a 0.5 ml eppendorf tube containing 3.7 % formaldehyde in PBS, for 40 min. Eyes were washed 3 times (5 min each time with rocking) in 0.4% PBS-T/PBT (0.4 % v/v triton X-100 in PBS). Post-washing eyes were transferred back onto a sylgard dish and, in a drop of PBS or PBT, any excess tissue removed from the eyes. Eyes were then transferred into a 0.5 % eppenforf containing 0.4 % PBS-T and incubated at 4oC, overnight, in the dark under shaking in order to remove any auto-fluorescent pigment. Following incubation eyes were washed 3 further times in PBT (5 min each time with rocking). The protocol was modified from Williamson and Hiesinger (2010), (Williamson and Hiesinger, 2010).

2.5.2 Immunohistochemical Staining of *Drosophila* Retinas

Following preparation, as was described above, *Drosophila* retinas were incubated in rhodamine conjugated phalloidin (1:100 in 0.4 % PBT) overnight, in darkness, with rocking at 4^{o}C. After incubation eyes were washed 3 times in 0.4 % PBT before being submerged in 70 % glycerol (70 % v/v in PBS) for 1-2 h to displace any air from the preparation. Eyes were mounted in Vectashield® (Vector Laboratories LTD, UK) on a standard microscope slide. Coverslips were elevated, to avoid compressing the eye, on two 22 x 22 mm coverslips fixed either side of the preparations. Coverslips were sealed in place using nail varnish.

Table 2.7 Antibody dilutions used for staining of the *Drosophila* retina

Antibody	Concentration	Source
αnti-Rab5	1:100	Abcam (ab31261)
α-spin	1:1000	Sweeney lab (Sweeney and Davis 2002)
a-POSH	1:200	Sweeney lab

2.5.3 Imaging of *Drosophila* Retina; Confocal microscopy

Following immunohistochemical staining *Drosophila* retinas were imaged using a Zeiss LSM 710 Axio Observer Z1 confocal microscope, using Zen 2009 software (Carl Zeiss AG, Germany). Single focal plane images of *Drosophila* retinas were taken using the 40x, 60x and 100x oil objectives during the course of this inverstigation. When taking confocal images for quantification of fluorescence all settings were kept the same between images.

2.5.4 Dissection of *Drosophila* brains

The legs and wings were first removed to reduce obstructions to the head. This was performed by apposing pairs of forceps against each other to break the tissue; this prevented pulling of the peripheral nervous system. Once these appendages had been removed, the proboscis was detached from the head by lifting the proboscis and severing the connections to the head. The silvery trachea and air sacs were excised and the eye and cuticle removed with a peeling action. At no point was the brain held within the forceps. The brain was severed from the cervical connective and placed in an eppendorf tube containing fresh 0.1% perchloric acid (PCA). Once collected they were kept on dry ice and stored at -80^{o}C until the day of the HPLC analysis.

2.6 High Performance Liquid Chromatography (HPLC) analysis

Dopamine and serotonin levels were measured by HPLC–EC on a LC-10AD HPLC system (Shimadzu). This set of experiments was performed at Nigel Maidment's and David Krantz's labs, at UCLA in California. To determine intracellular monoamine levels, fly heads were collected and homogenized in 50 µl perchloric acid (0.1M) and 0.1% EDTA (0.1 % wt/vol) using a sonicator (Sonifier cell disruptor, model W185D, Heat systems-Ultasonics). After a 1 min centrifugation at 13000g, the samples were filtered using Millipore cartridge and centrifuged for 10 min at 5000 rpm. The samples were collected and stored in HPLC tubes at -80°C until the day of the experiment where 5 µl of the sample were injected into the HPLC.

Samples were separated on a C18 reverse phase column (TSKgel Super ODS 3 µm particle size, 10 Å~ 2.1 mm, maintained at 33 °C, ThermoFisher Scientific) using a mobile phase (817.2 mg Sodium dodecane sulfonate, 24.613 mg Sodium acetate anhydrous, 500 ml acetonitrile, 500 ml methanol, 0.4 ml EDTA (100mM stock), 3000 ml water, pH 5.5) pumped at 0.2 mL/min (LC-10AD pump, Shimadzu). Data were collected using EzChrom software (Agilent) (Fitzmaurice et al., 2012).

2.7 Statistical analysis

All statistical analyses were carried out in IBM SPSS Statistics v22. Student's t-test was performed to test for statistical significance between two groups; univariate ANOVA followed by a Bonferroni post-hoc test was performed to test for statistical significance between multiple groups; and univariate ANOVA followed by a post-hoc Dunnett's comparison was performed when comparing genotypes to a wild-type control. Although the visual neurons are all linked in the same neural network, the responses from the photoreceptors, lamina and medulla were treated as independent events, with separate univariate ANOVAs as previously described in Afsari et al. (2014), rather than a multivariate approach. This decision was based on the idea that the visual network would use

feedback to regulate signaling in each layer of the network (Zheng et al., 2006, Tuthill et al., 2014, Hu et al., 2015). Statistical significance was defined as $p<0.05$ throughout. On graphs with 'error bars', these represent the standard error, and P values are indicated graphically: * $P < 0.05$; ** $P < 0.01$; ***$P < 0.001$.

Chapter 3

Understanding the role of Dopamine in the pathogenesis of the fly model of Parkinson's disease

3.1 Introduction

One of the main aims of this project was to shed new light on our understanding of the chain of events that cause nerve cells with the *LRRK2-G2019S* mutation to die. A better understanding of the biological functions of *LRRK2* and its relationship to dopamine metabolism and signalling may be important for future therapeutic developments in PD.

Previous studies have shown that the *LRRK2*-G2019S mutation severely reduces the visual function of the flies after 28 days (Hindle et al., 2013). The fly retina, like the human retina, has dopaminergic innervation (Crooks and Kolb, 1992), and isolated fly photoreceptors respond to dopamine application (Chyb et al., 1999). These dopaminergic neurons regulate the visual contrast response (Afsari et al., 2014; Jackson et al., 2012). The loss of these dopaminergic neurons in PD leads to deficits in neural processing in both the retina (Langheinrich et al., 2000) and visual cortex (Price et al., 1992), at least in part due to aberrant contrast response functions. The same is true of flies: using an SSVEP (Steady State Visual Evoked Potential) assay, modeled on the human scenario, it was found that knock-out of PD related genes led to aberrant electroretinograms (Afsari et al., 2014). In fact, each gene that was tested shows different deficits, so that it is possible to determine the fly genotype from the SSVEP response (West et al., 2015). The key question is how does dopamine affect the photoreceptors and the lamina neurons? This question was addressed by blocking the evoked neurotransmitter release from dopaminergic neurons in the CNS of the fly.

Visual assays in the fly provide an alternative approach to the cellular and biochemical assays. The fast generation time, fecundity of the fly and fast electroretinogram processing facilitates rapid progress, so that we are able to test large numbers of flies, and so identify even small changes in neuronal signaling. It was demonstrated that of the *LRRK2* mutations available, the pathogenic *G2019S* mutation produced the most dramatic loss of vision in old flies, and this was most pronounced when it was expressed in the dopaminergic neurons (Hindle et al., 2013). Since biochemical assays indicate that the *G2019S*

mutation increases kinase activity, two kinase inhibitors were tested, and found that both prevented (or slowed) the loss of vision (Afsari et al., 2014; West et al., 2015) suggesting the increased kinase activity is indeed the cause of neurodegeneration.

Hindle et al (2013) hypothesized that, as *G2019S* is a gain of function mutation, one of the first consequences might be neuronal hyperactivity. On testing this hypothesis, it was found that young flies expressing *LRRK2-G2019S* in their dopaminergic neurons (*TH > G2019S*) had increased visual signaling compared with those expressing the wild-type form of *LRRK2* (*TH > hLRRK2*), or controls with no LRRK2 expression (Afsari et al., 2014). This transient excitatory response may lead to sodium or calcium ion entry, extra demand for ATP from the ion exchange pumps, which the mitochondria may not be able to fulfill without generating extra oxidative stress. In this scenario, mitochondrial failure is followed by autophagy, apoptosis and other forms of cellular damage. A transient excitotoxic cascade may be present in mice too, as younger *LRRK2-G2019S* animals show hyperactivity, followed by loss of movement and cognitive deficits (Volta et al., 2015). The excitotoxic model is also supported by cell-culture data, with *LRRK2* expression in HEK293 cells leading to increased calcium influx as a result of increased calcium channel density (Bedford et al., 2016). One possible cause of increased calcium channel density is an increase in protein production, due to phosphorylation and consequent upregulation of the ribosomal s15 activity by pathogenic mutants of LRRK2 (Martin et al., 2014).

In the first part of this chapter, the effect of *LRRK2* transgenes on dopamine concentration was determined. In addition, it was tested if early hyperactivity might be linked to loss of dopamine, finding young *TH > G2019S* flies have reduced dopamine levels, and that the hyperactivity is affected by blocking dopamine release with tetanus toxin.

3.1.1 Measurement of dopamine in fly heads

As the hallmark of PD is the loss of the dopaminergic neurons in the SNpc, which has as a result the loss of dopamine in the striatal projection areas of these neurons, the first aim of these sets of experiments was the measure of dopamine concentration from fly heads by performing HPLC analysis (as described in section 2.6). The discovery of genetic causes of pathogenic PD led to the creation of genetic model organisms, with both gain of function (overexpression) and loss of function (knock-out) mouse models. Progress with these has been slow, whereas rapid progress was made using the fruit fly (*Drosophila melanogaster*). These provided excellent recapitulation of LRRK2 pathology (Hewitt and Whitworth, 2017), including locomotion defects and loss of some (but not all) clusters of dopaminergic neurons. In particular, old flies show a loss of dopaminergic neurons in the PPM and PPL clusters (Liu et al., 2008; Martin et al., 2014), and some of the PPL neurons innervate the retina (Hindle et al., 2013).

A very approachable way to measure dopamine levels has been achieved in the past, as proposed by Riemensperger et al. (2011). Using fly adult brains, they performed HPLC analysis in order to determine the absolute magnitude of reduction in adult brain. Tyrosine hydroxylase (TH) is the rate-limiting step in dopamine biosynthesis and alternative splicing of the *Drosophila* TH (DTH) produces two isoforms, DTH1 and DTH2. DTH1 is only expressed in DA neurons in the CNS while DTH2 is expressed in peripheral no nervous tissues. Moreover, inactivating mutations of the genomic TH, *pale (ple)* locus results in unpigmented cuticle and late embryonic lethality. Taking advantage of this alternative splicing, they constructed mutants, the $DTHg^{FS\pm}$, which only expresses an active TH in noneural tissues and the $DTHg^{FS+}$ that only expresses active TH in neural tissues. Homozygous *ple* mutants are rescued by this transgene to adult stage, generating *Drosophila* essentially devoid of DA in the adult brain. Brain extracts from control flies and *DTHg;ple* revealed equivalent levels of DA per brain, while $DTHg^{FS\pm}$ showed ~85% reduction in DA levels.

Several other papers were released using HPLC analysis in order to test dopamine levels in *Drosophila*. Faust et al (2009) used 20 fly heads per genotype they tested while Kayser et al (2014) used 21 fly brains per sample. On the other hand, Gonzalo-Gomez et al. (2012) used 10 fly heads in order to determine the DA levels while Calcagno et al (2013) used 5 fly heads per sample providing enough statistical power. These findings encouraged us to determine that 10 fly heads could provide enough statistical power in order to determine the DA in our *TH>G2019S* and *TH>hLRRK2* flies. Even though the amount of fly heads or fly brains used in each study varies, the only common parameter within all of them was that they used the very sensitive electrochemical detection HPLC analysis.

3.1.2 Blocking neurotransmission with Tetanus toxin

A number of approaches to block neuronal signalling are available in the fly: use of inwardly rectifying potassium channels (Nitabach et al., 2002), tetanus toxin (Sweeney et al., 1995) or *shibire* (Kitamoto, 2001; Potter et al., 2010). In the case of dopaminergic neurons, manipulations of VMAT or dopamine synthesis would also be possible, or abolition of the dopaminergic cells by expression of the pro-apototic gene *reaper* (Zhou et al., 1997). Many of these systems have disadvantages. Expression of inwardly rectifying potassium channels or *reaper* in dopaminergic neurons is lethal. While some have avoided this by using temperature sensitive GAL80, it does make the genetics more complex. Manipulations of VMAT may have consequences for other aminergic systems (octopamine, serotonin), and does not necessarily deliver the specificity required. S*hibire* can be temperature sensitive, making experiments harder to control. Thus using tetanus toxin provides the simplest way to manipulate dopaminergic neuronal activity.

Neurons communicate with their target cells by the Ca^{2+}-regulated exocytotic release of neurotransmitters that are stored in synaptic vesicles. Many proteins are implicated in the synaptic release machinery, which are located in the

synapses (Walch-Solimena et al., 1993). Several proteins are included in this machinery, known as N-ethylmaleimide-sensitive fusion proteins (NSF), α-soluble NSF attachment proteins (α-SNAP), and γ-SNAP. Specific receptor proteins in the vesicle membrane (v-SNAREs) and other proteins in the target membranes (t-SNAREs) determine the specificity of that fusion. For the neurotransmitter release, synaptobrevin (VAMP) (Trimble et al., 1988; Baumert et al., 1989), that is located in the synaptic vesicles, is considered as a v-SNARE that targets the vesicle to the plasma membrane using t-SNAREs syntaxin and SNAP-25 (Sollner et al. 1993). Several clostridial neurotoxins identify these proteins as targets; syntaxin and SNAP-25; which are the targets of synaptobrevin in the synaptic vesicle exocytosis process, making these neurotoxins potential inhibitors of neurotransmitter release. For the purpose of this investigation, Tetanus toxin (TeTx) was used in order to achieve that targeted neurotransmitter release.

TeTx belongs to the botulinal neurotoxins family (BoNT/A to G) and consists of two polypeptide chains. A heavy chain mediates neuroselective binding, internalization, intraneuronal sorting, and translocation of the light chain to the cytosol. The light chains catalytically inhibit synaptic transmission when present in the cytosol by cleaving either synaptobrevin, syntaxin, or SNAP-25 with unique selectivity at single sites (Sweeney et al., 1995). The light chain of Tetanus toxin (TeTxLC) targets the membrane protein of the synaptic vesicles, synaptobrevin in the synapse. Even though there might be more cellular targets for these toxins, for example cellubrevin that is a synaptobrevin homolog, synaptobrevin is the only detectable protein to be cleaved (McMahon et al., 1993). Sweeney et al. in 1995 expressed TeTxLC in synapses in *Drosophila*, showing that it cleaved fly synaptobrevin (n-syb), and abolished synaptic transmission at a defined neuromuscular junction (Sweeney et al., 1995).

3.1.3 Blockage of neurotransmission in dopaminergic neurons

During the course of this investigation Tetanus toxin was expressed in the dopaminergic neurons of the fly in order to block the evoked release of dopaminergic vesicles (Figure 3.1). Any potential lethality was avoided as TNT permits some spontaneous release (Sweeney et al., 1995). In addition, TNT is effective in modulating dopamine-dependent behaviours (Alekseyenko et al., 2013; Friggi-Grelin et al., 2003; Suster et al., 2003) including arousal, courtship, memory and locomotion.

This was accomplished by the driving expression of the UAS-*TNT* transgene with *TH-Gal4* that places the Gal4 under the control of the *tyrosine hydroxylase* locus; where tyrosine hydroxylase is the rate-limiting enzyme for the synthesis of dopamine. Moreover, TNT was also expressed in *TH>G2019S* and *TH>hLRRK2* flies and controls including *TH/w*$^{-}$ and *TH/w*^{apr}. Full field SSVEP stimuli was used in order to separate the responses of the photoreceptors from the lamina neurons.

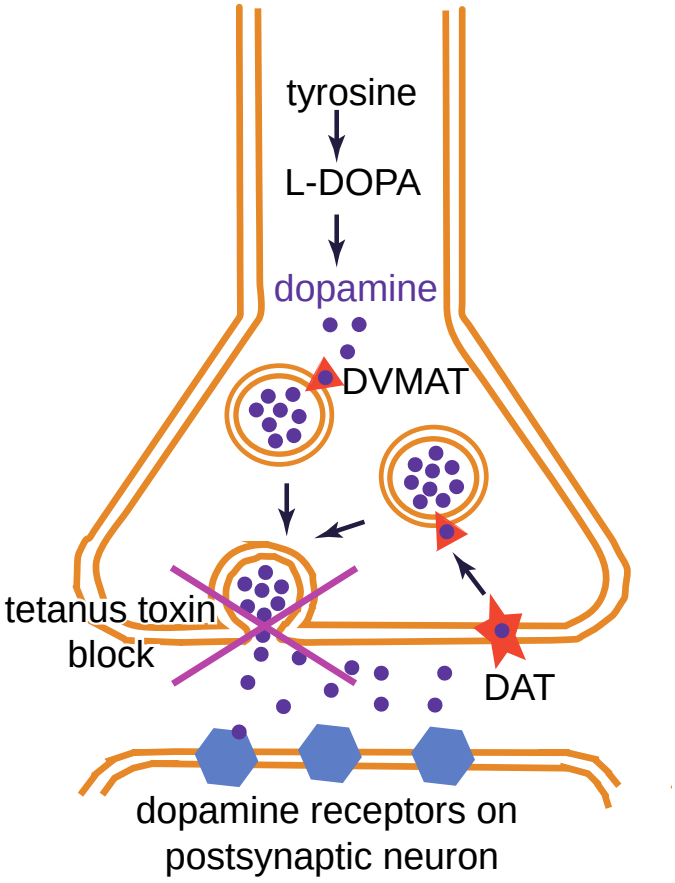

Figure 3.1 Schematic diagram of dopamine pathways in neurotransmission. Dopamine is synthesized from tyrosine by L-DOPA, and then packaged into vesicles by DVMAT (*Drosophila* Vesicular MonoAmine Transporter). Released dopamine may bind to dopaminergic receptors, and/or be taken up the dopamine transporter (DAT). Tetanus toxin blocks the release of neurotransmitter vesicles by cleaving the intrinsic synaptic membrane protein synaptobrevin.

3.2 Aims

1. Test if the *G2019S* mutation has any effect in the loss of dopamine that is present in PD compared to control flies including the wild type *hLRRK2*.

2. Test if the blockage of dopamine release by expressing TNT in the dopaminergic neurons can reverse the loss of vision present in old flies carrying the *G2019S* mutation.

3.3 Results

3.3.1 Measurement of dopamine levels

Manipulations of the fly homolog of *hLRRK2* (*dLRRK*) affect the levels of dopamine in fly heads: young *dLRRK* knockout flies have ~3x elevated dopamine, while those with extra kinase activity (expressing *dLRRK-I1915T* the homolog of the human *I2020T* mutation), have reduced dopamine content (down to about 20% of controls) (Imai et al., 2008). We therefore aimed to determine the effect of manipulating the human *LRRK2* gene in the fly.

Dopamine levels were determined by HPLC analysis of fly heads expressing a range of LRRK2 transgenes (Section 2.6). 1 day old, 7 day old and 14 day old flies were used in this set of experiments. *TH > hLRRK2* flies were used as a control, as the wild type version of the gene is being expressed. Two different mutations within the kinase domain were also tested, *TH>G2019S* and *TH >I2020T* and finally another mutation within the GTPase domain of the gene, the *TH >R1441C.* The final volume of fly heads used for this analysis was 90 in total (N=90), giving us enough statistical power in order to make our conclusions. Figure 3.2 shows the obtained dopamine levels from three different time points including the wild type *LRRK2*, and three additional mutations within this gene.

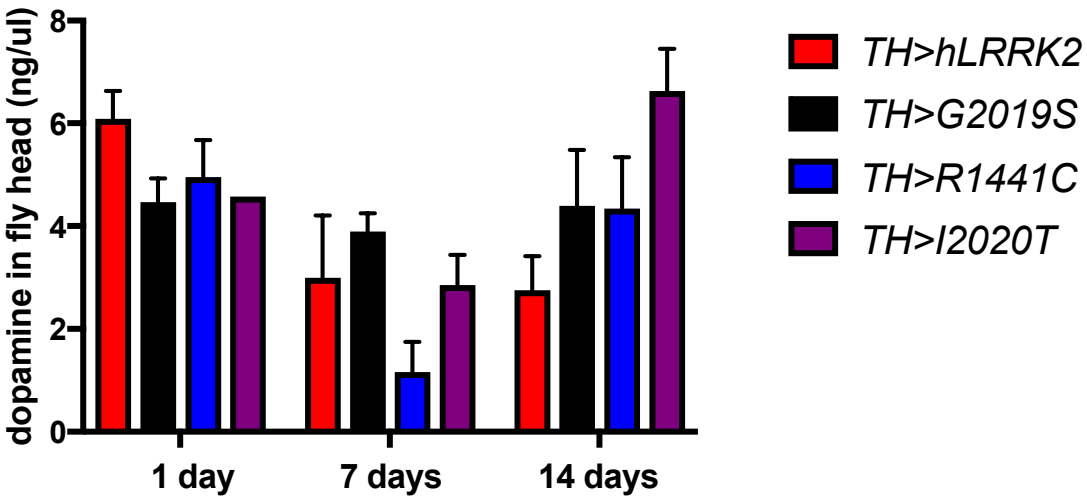

Figure 3.2 Young, but not old flies, expressing *LRRK2-G2019S* or *hLRRK2* in dopaminergic neurons show differences in dopamine concentration. 1 day, 7 days and 14 days old flies were tested in order to measure the dopamine levels. A range of LRRK2 transgenes were tested by HPLC analysis in fly heads. Apart from the wild type hLRRK2 (N= 21), G2019S (N= 22), I2020T (N=21) and R1441C (N=23) mutations were also included in the screening**.** There is a strong interaction term in the ANOVA between age and genotype (P= 0.0279), indicating that the genotypes behave differently with age. *N*= 87.

Even though the dopamine levels of the *TH > G2019S* flies were very consistent among all the different ages that were tested, it appears that the ones expressing the *TH > I2020T* mutation are not so consistent. 1 day old flies have similar DA levels to the *TH > G2019S* but after 7 days that levels drop down to wild type levels as they exhibit similar levels to the *TH >hLRRK2*. What is even more interesting is that after 14 days the DA levels go back up, similar to wild type levels of 1 day old flies. Similar pattern of DA expression is followed by the *TH >R1441C* flies. This strong interaction between genotypes and age is also statistical significant for the *TH>I2020T* and *TH>R1441C* flies (Two-way ANOVA, P=0.0279).

Of great interest were the differences of the dopamine levels between the genotypes *TH>G2019S* and *TH>hLLRK2* as shown in more detail in Figure 3.3. The concentration of dopamine was 65% higher in 1 day old *TH > hLRRK2* than in *TH > G2019S* flies. Over two weeks, the levels of dopamine remained constant in the *TH > G2019S* flies, but that in *TH > hLRRK2* flies reduced until it was about half (53%) of the *TH>G2019S* flies (Figure 3.3). Wild-type flies show a similar decline in dopamine concentration over the first 14 days of life (Imai et al., 2008). The conclusion that can be made is that reduced dopamine content could contribute to the hyperactivity of young *TH > G2019S* retina.

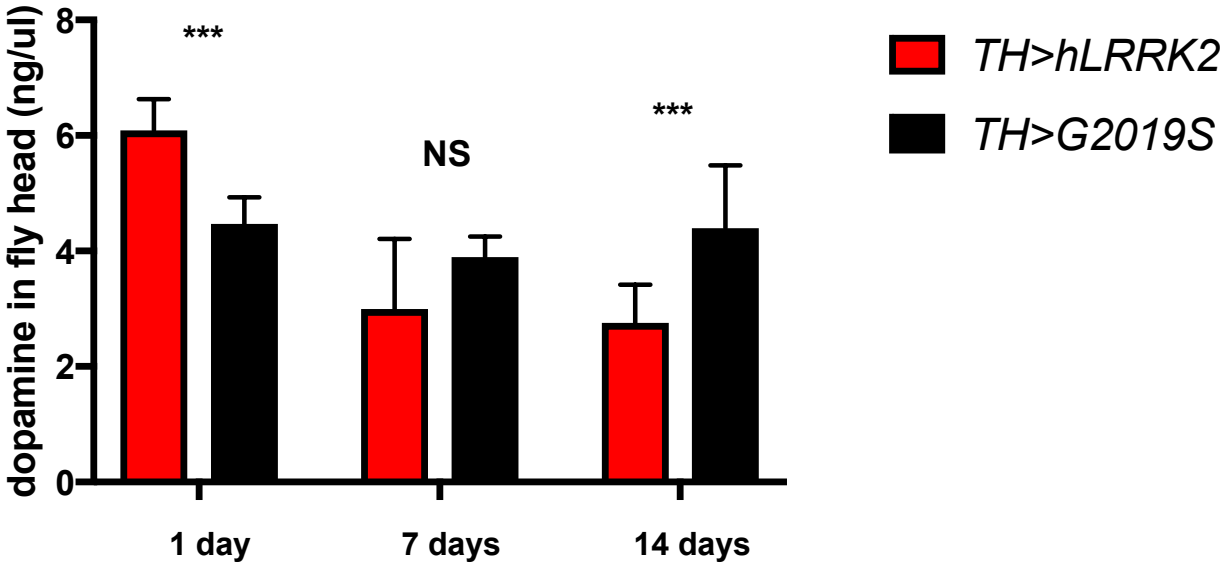

Figure 3.3 The Dopamine levels of *TH>G2019S* and *TH>hLRRK2* flies show different effects as they age. Age does not affect dopamine concentration in *TH>G2019S* flies, but *TH>hLRRK2* flies show a dramatic drop in dopamine, from a mean of 6.7 ± 0.6 to 2.6 ± 0.5. There is a strong interaction term in the ANOVA between age and genotype ($F_{2,33df}$ = 6.1, P= 0.005), indicating that the genotypes behave differently with age. *N*= 39.

3.3.2 Blockage of the neurotransmitter release in *Drosophila*

For the next set of experiments, the aim was to block synaptic transmission in the dopaminergic neurons in order to determine how blocking of dopamine release affects fly vision. The first result is that flies expressing TNT flies (with or without) *LRRK2* transgenes were found to be viable.

3.3.2.1 Flies co-expressing *TH>G2019S, TH>hLRRK2* compared to *TH/w*$^{-}$ and flies co-expressing *TH>TNT;G2019S, TH>TNT;hLRRK2* compared to *TH>TNT*

In order to address this question recordings from 1 day old, 7 day old, 14 day old and 21 day old flies were conducted, expressing *TH>G2019S* and *TH>hLRRK2* both in the presence and the absence of TNT. The summarized genotypes of flies that were crossed for this experiment are summarized in Table 3.1, with flies carrying the balancers *CyO* or *TM6B* being rejected.

Table 3.1 Summarized crossing scheme of the experimental flies

	Male	
Virgin female ***TH*-Gal4**	$\frac{TNT}{CyO};\frac{G2019S}{TM6B}$	$\frac{G2019S}{TM6B}$
	$\frac{TNT}{CyO};\frac{hLRRK2}{TM6B}$	$\frac{hLRRK2}{TM6B}$
	$\frac{TNT}{CyO}$	w^{-}

3.3.2.2 Measurement of the visual responses using the SSVEP recordings

As previously described in more detail in Chapter 2.2.2, a more sensitive assay based on the SSVEP method was developed for recording the visual response of flies (Afsari et al., 2014). This is a highly sensitive assay that allows the isolation of the responses from the photoreceptors, second-order lamina neurons and third-order medulla neurons. The fly SSVEP is designed to deliver stimuli that sweep through different contrast levels, enabling the measurement and analysis of contrast response functions. The SSVEP assay has proved sensitive enough to be able to detect abnormal visual phenotypes caused by DA expression of *hLRRK2-G2019S* in 1 day old flies (Afsari et al., 2014). Thus this assay provides a robust and stable platform to assess the visual response of flies and to determine how different genotypes respond (Afsari et al., 2014).

The typical SSVEP analysis from Matlab is shown in Figure 3.4. This demonstrates the typical contrast response function (CRF), with the responses increasing with contrast. A representative example of two different genotypes are shown here; *TH>G2019S* and *TH>TNT;G2019S*; at 1 day old and 21 day old flies. As expected after 21 days the responses decrease dramatically as part of the ageing process.

A

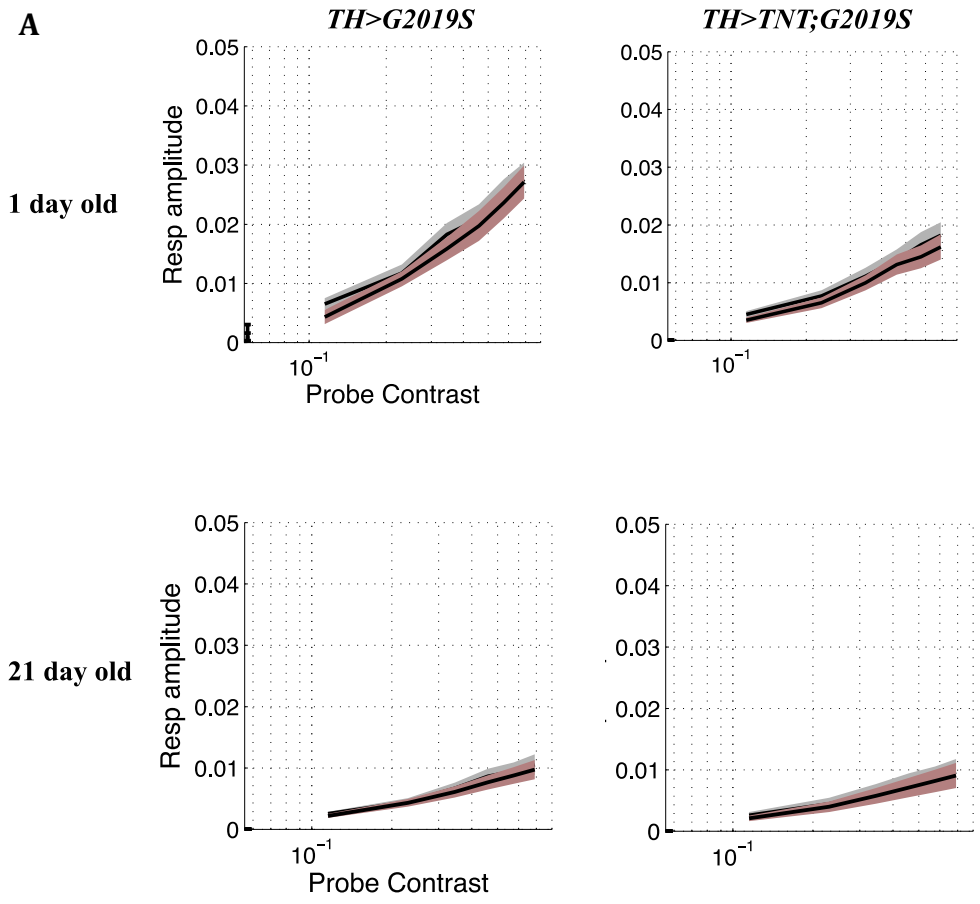
TH>G2019S
TH>TNT;G2019S
1 day old
21 day old
Resp amplitude
Probe Contrast
0.05
0.04
0.03
0.02
0.01
0
10^{-1}

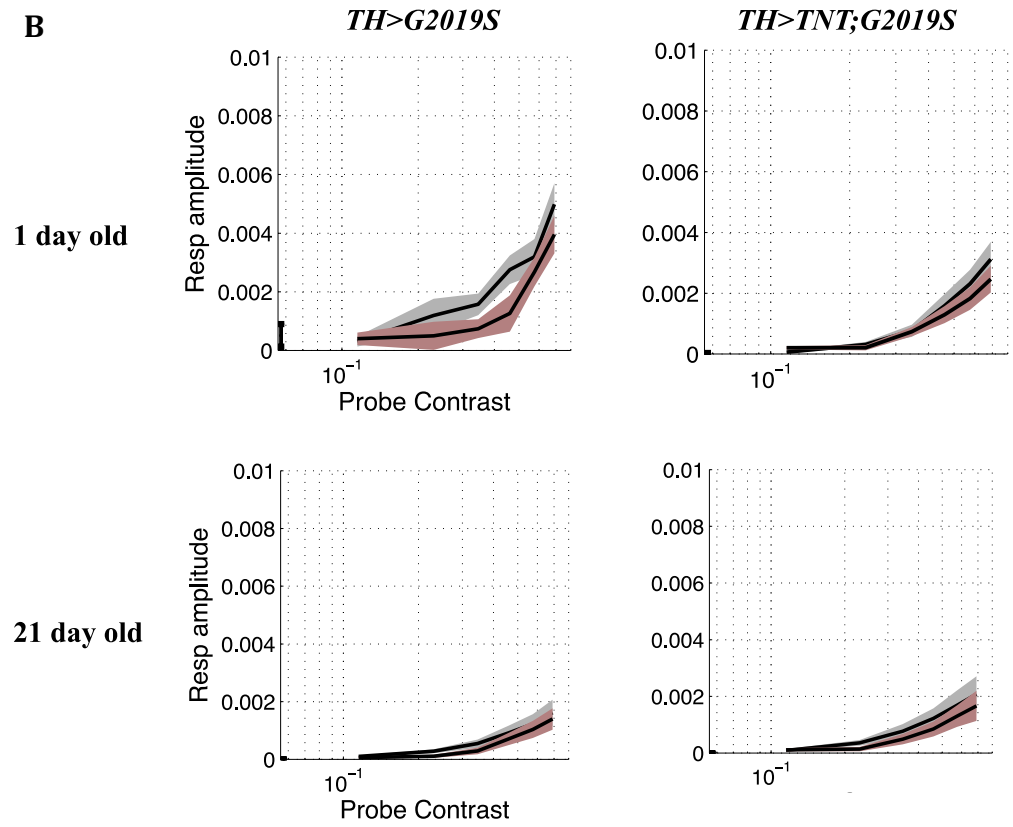

Figure 3.4 Representative example of the MatLab outcome. Photoreceptor responses (A) and lamina neuron responses (B) to swept contrast flicker with (pink) and without (grey) a 30% mask as the probe contrast is increased from 0 to 69%. 1 day old and 21 day old flies are shown here, in order to compare the responses between *TH>G2019S* and *TH>TNT;G2019S* flies (N=50).

As well as being more sensitive, the SSVEP assay generates a very large data set, with responses at a range of contrasts, with and without the mask and at a range of harmonics. Here, a simpler approach is taken, reporting the maximal response at 1F1 (photoreceptors) and 2F1 (lamina neurons) of the unmasked signal.

3.3.2.3 Effect of TNT is age dependent

The original hypothesis was that TNT expression in dopaminergic neurons might affect the release of dopamine and its expression does affect fly vision. The effect of TNT on the fly vision was tested both in the *hLRRK2* and the *G2019S* background.

The largest effect of TNT on the fly vision occurs at 7-day-old flies, where TNT increases the visual responses both from the photoreceptors and the lamina neurons. By 7 days, eye development is complete and all genotypes have their largest SSVEP 1F1 and 2F1 responses independently of the expression of TNT. Figure 3.5 shows that expressing tetanus toxin increased the maximal response of each genotype by about 45% for the photoreceptor and 55% for the lamina neurons. That was true for both *LRRK2-G2019S* and for the wild-type. At older time points (14 days and 21 days), TNT also increases the visual responses independently of the genetic background.

However, at 1-day-old flies, even though in the *TH>hLRRK2* and *TH/w-* background, the effect of TNT was the same as at 7 day old flies, a surprising result was established (Figure 3.6). 1-day-old *TH>G2019S* where TNT is expressed, the responses from both the photoreceptors and the lamina neurons are at higher levels compared to the responses in the presence of TNT.

After 14 and 21 days gradually the response is decreasing, and this is what is expected as a normal aging process. Moreover, the effect of TNT at this later time points is the same for all the different genotypes, as its expression leads to increased photoreceptor responses compared to the ones we get when it is not expressed.

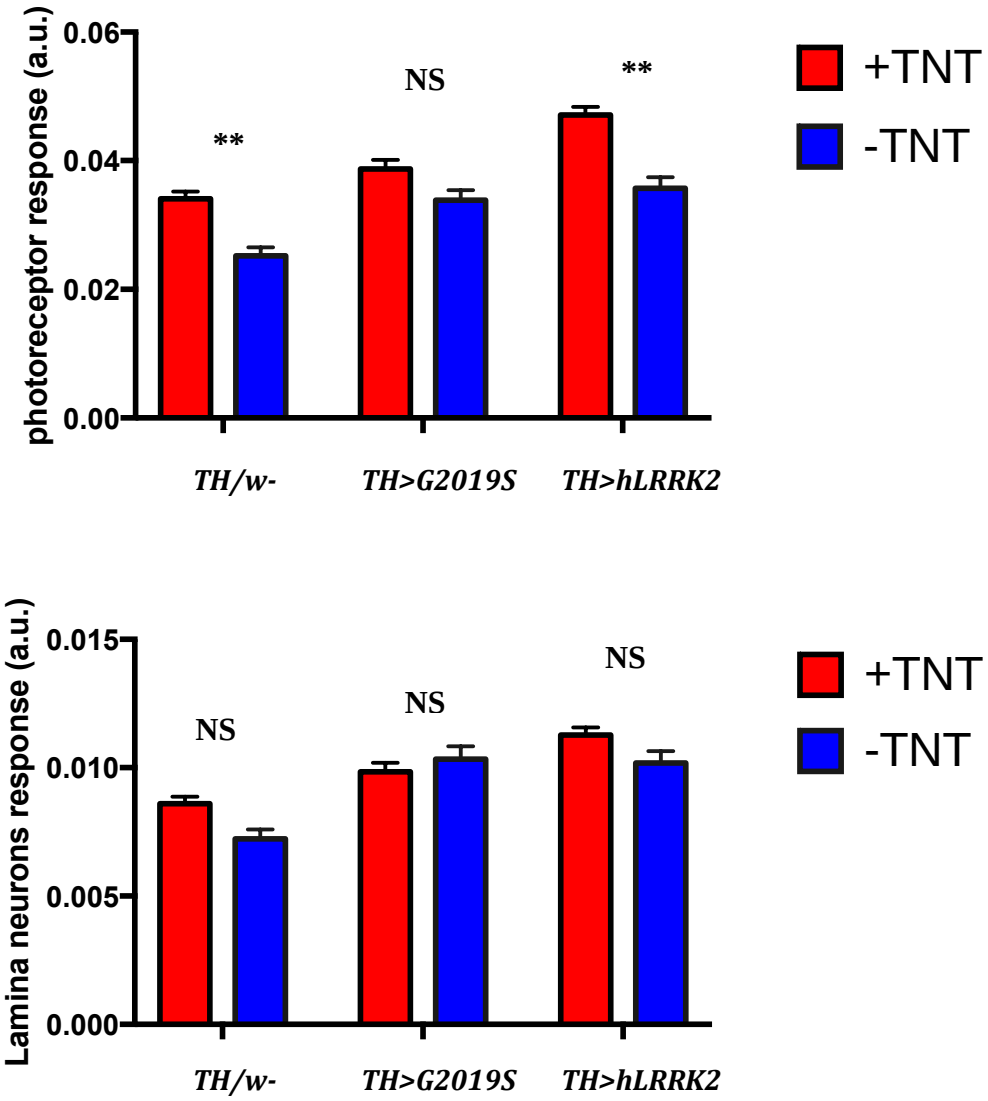

Figure 3.5 Expression of TNT in the *G2019S* background indicates a big effect in fly vision. Mean ±95%CI responses from *TH>G2019S*, *TH>hLRRK2* and *TH/w-* flies after incubation at 29ºC for 7 days with or without expressing TNT. Dopaminergic expression of tetanus toxin (TNT) has opposite effects on G2019S or control (hLRRK2, +) 7-day-old flies as indicated by the two-way ANOVA (genotype/TNT interaction $P<0.0001$ and $P<0.0001$ for photoreceptors (A) and lamina neurons (B), respectively. N = 336 - at least 11 in each sample.

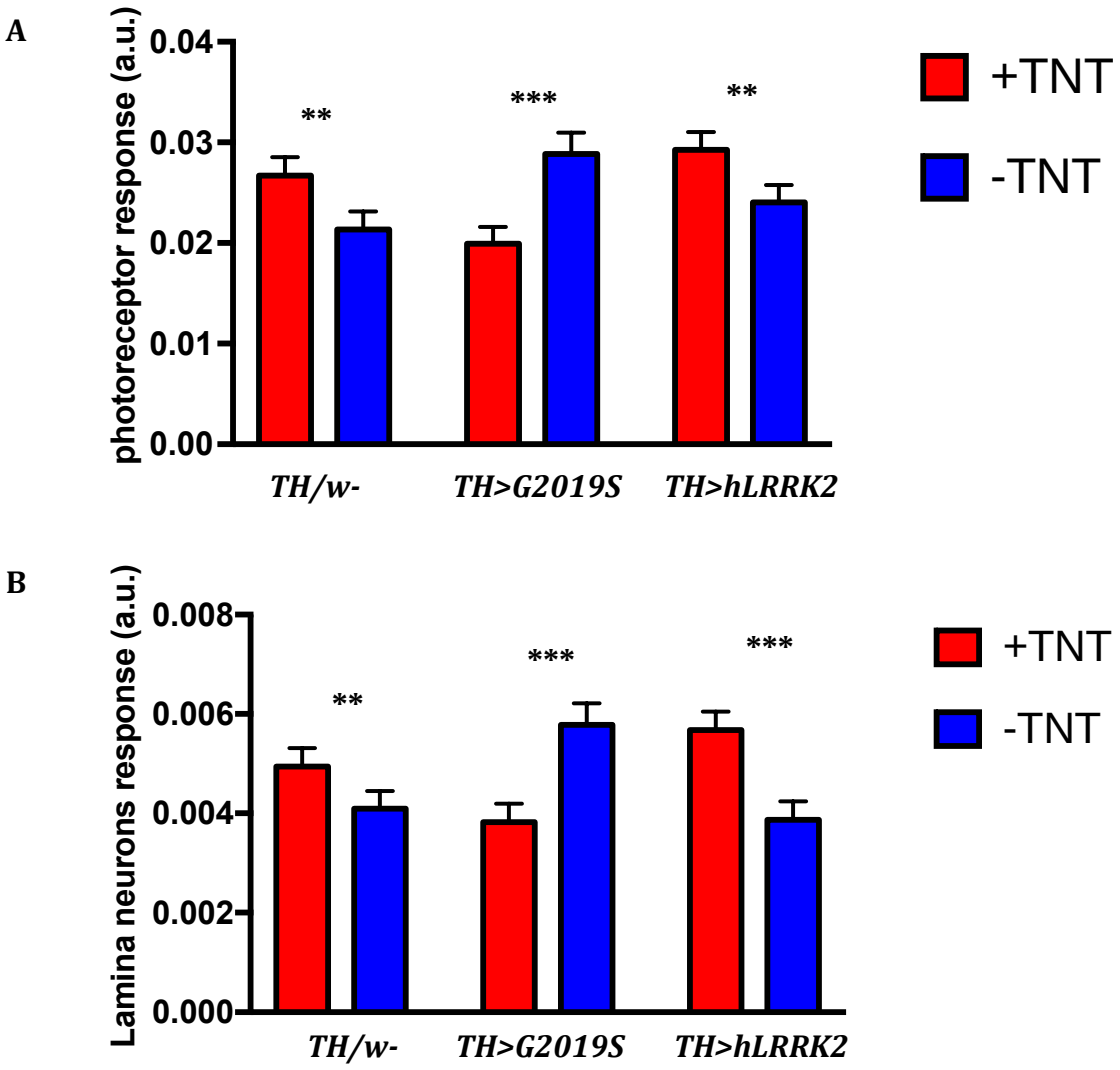

Figure 3.6 In Young flies, expression of TNT in the *G2019S* background reduces the SSVEP response, whereas in the other (control) genotypes TNT increases the response. Mean ±95%CI responses from *TH>G2019S*, *TH>hLRRK2* and *TH/w-* flies after incubation at 29^{o}C for 1 day with or without expressing TNT. Dopaminergic expression of tetanus toxin (TNT) has opposite effects on G2019S or control (hLRRK2, +) 1-day-old flies as indicated by the 2-way ANOVA (genotype/TNT interaction P = 0.027 and 0.012 for photoreceptors (A) and lamina neurons (B). N = 107 - at least 11 in each sample.

A summarized graph presenting the effect of TNT for all the different ages in the visual responses from the photoreceptors and the lamina neurons is presented in Figure 3.7.

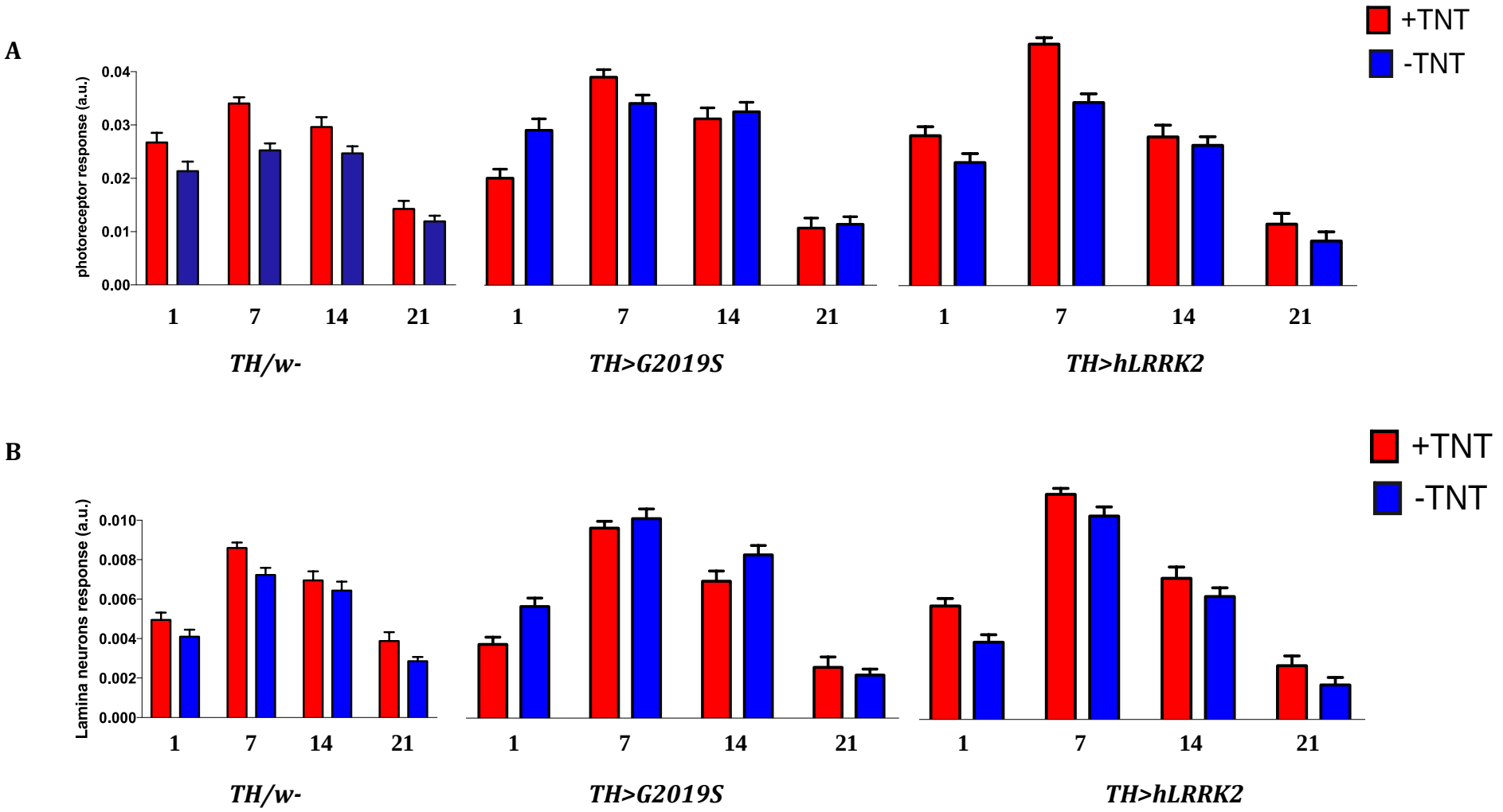
A
+TNT
-TNT
photoreceptor response (a.u.)
0.04
0.03
0.02
0.01
0.00
1
7
14
21
TH/w-
TH>G2019S
TH>hLRRK2
B
+TNT
-TNT
Lamina neurons response (a.u.)
0.010
0.008
0.006
0.004
0.002
0.000
1
7
14
21
TH/w-
TH>G2019S
TH>hLRRK2

Figure 3.7 Flies show largest visual responses at 7 days

Mean ±95%CI responses from *TH>G2019S*, *TH>hLRRK2* and *TH/w-* flies after incubation at 29ºC for 1,7,14 and 21 days with or without expressing TNT. Dopaminergic expression of tetanus toxin (TNT) has opposite effects on *G2019S* or control (*hLRRK2*, +) 1-day-old flies as indicated by the two-way ANOVA (genotype/TNT interaction P = 0.027 and 0.012 for photoreceptors (A) and lamina neurons (B). N = 107 - at least 11 in each sample. The differential effect of tetanus toxin decreases with time: by 7 days the expression of tetanus toxin in the *TH > G2019S* line has no effect, and this is also true at later time points. Over days 7-21, TNT reduced the photoreceptor response, independent of genotype (2-way ANOVA, TNT, P = 0.037, genotype/TNT interaction P = 0.12), but had no effect on the lamina neurons. N = 485 - at least 9 in each sample.

3.3.2.4 Effect of TNT depends on the genotype

The most interesting finding came from 1-day-old flies, as the expression of TNT in the *G2019S* background didn't have the same effect as in the *w-* and *hLRRK2* flies at the same age (Figure 3.6).

The early onset hyperactivity of *TH >G2019S* was confirmed (Fig. 3.6): the *TH> G2019S* response in both the photoreceptors and the lamina neurons is larger than that of *TH >hLRRK2* or *TH/+*. However, co-expressing tetanus toxin (TNT) with *G2019S* substantially reduced the SSVEP signal on day 1 (photoreceptors by 38 %; lamina neurons by 42 %). With increasing age, the difference made by TNT on *TH > G2019S* declined and disappeared by 7 days. In contrast, for the control *TH > hLRRK2* and *TH/+* flies, TNT appeared to have the opposite effect enhancing their SSVEP response. Furthermore, for all genotypes, TNT expression increased the visual response across all time points – for photoreceptors by 19 %, for lamina neurons by 10 %.

This finding suggesting the early hyperactivity in young flies expressing the G2019S mutation agrees with the data presented by Afsari et al (2013). There is an indication that TNT expression is preventing signalling between the dopaminergic neurons and the photoreceptors/lamina neurons. The hypothesis was that the flies are failing to adapt to the light due to a lack of dopamine. In young flies, there may be dopamine circulating from the cuticle, where dopamine is needed too (darken & crosslink) the cuticlar proteins.

3.3.2.5 Calculated Rmax and C50 for flies expressing TNT

The changes in visual response due to age and TNT expression could be due to an effect on the maximum sensitivity of the eye (Rmax) or to a change in contrast sensitivity (c50).

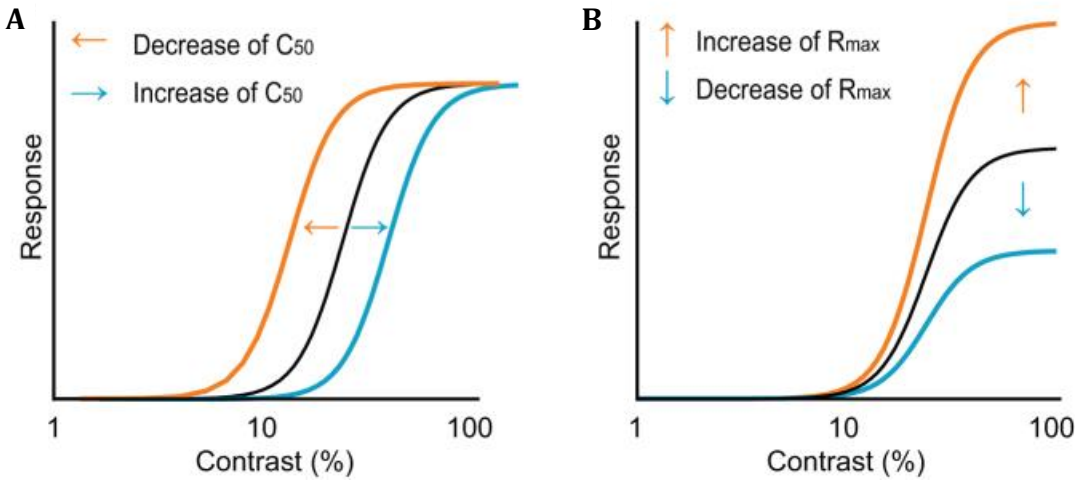

Figure 3.8 Naka-Rushton function presenting two types of gain control in the contrast-response function. (Adapted from Soma et al., 2013).

The Rmax represents the max response while C_{50} represents the semisaturation contrast. The Contrast response functions were fitted with the Naka-Rushton function (Soma et al., 2013) and the effect of age and TNT were determined.

The Rmax of the responses at the 1F1 (photoreceptors) and 2F1 (lamina neurons) are presented in Figure 3.9. The increased sensitivity of TH>G2019S flies could result from a change in either the Rmax or C_{50} parameter.

The changes in Rmax with age follow the same pattern as the raw data: flies at day 7 have a bigger Rmax than those aged 1, 14 days and 21 days. At day 7, there is no effect of *TNT* on any of the genotypes in either the photoreceptors or lamina neurons, and the same is true for days 14 and 21. However, in young flies, at 1 day old, the presence of TNT has the opposite effect for the *TH>G2019S* and *TH>hLRRK2* flies, as the absence of TNT increases the responses at significant levels.

Unlike Rmax, the C_{50} is quite consistent between the different genotypes and ages, as the effect of TNT is not statistically significant (Figure 3.9).

Calculated Rmax of the photoreceptor responses

A

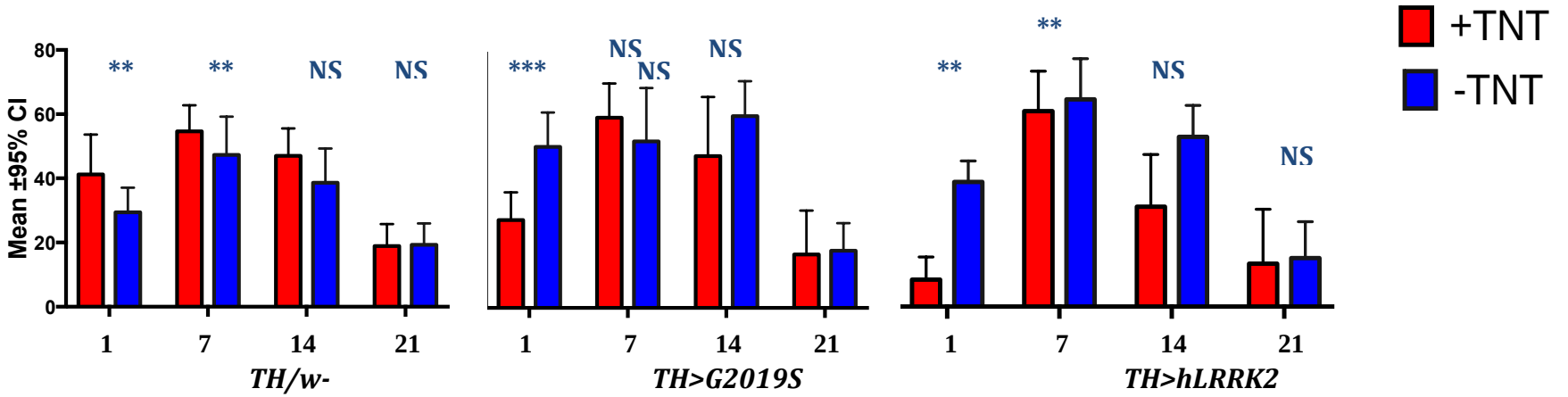

Calculated Rmax of the lamina neuron responses

B

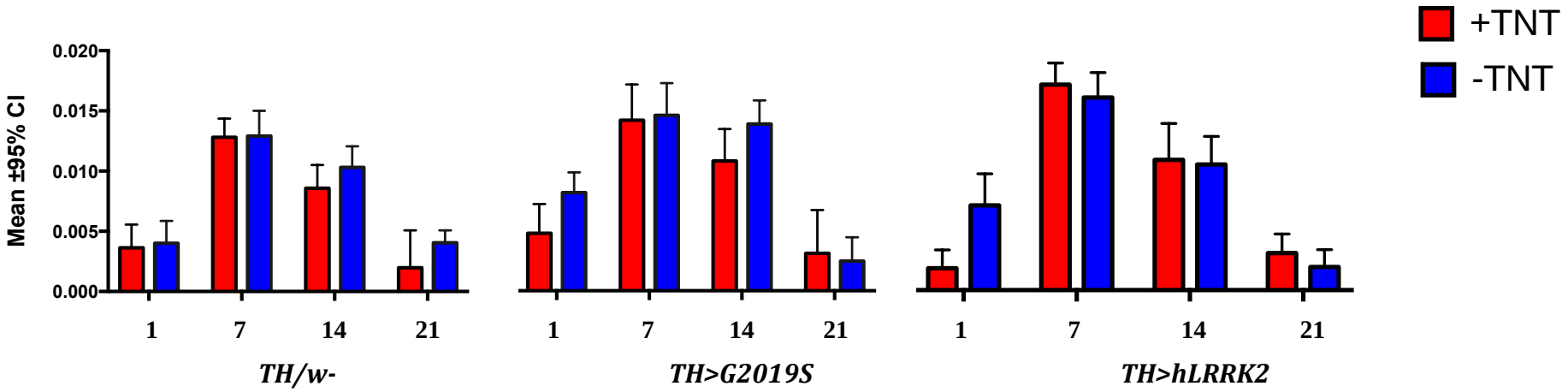

Figure 3.9 Calculated Rmax from the photoreceptors (A) and the Lamina neurons (B). Mean ±95% CI responses from *TH>G2019S*, *TH>hLRRK2* and *TH/w-* flies after incubation at 29ºC for 1, 7, 14 and 21 days with or without expressing TNT.

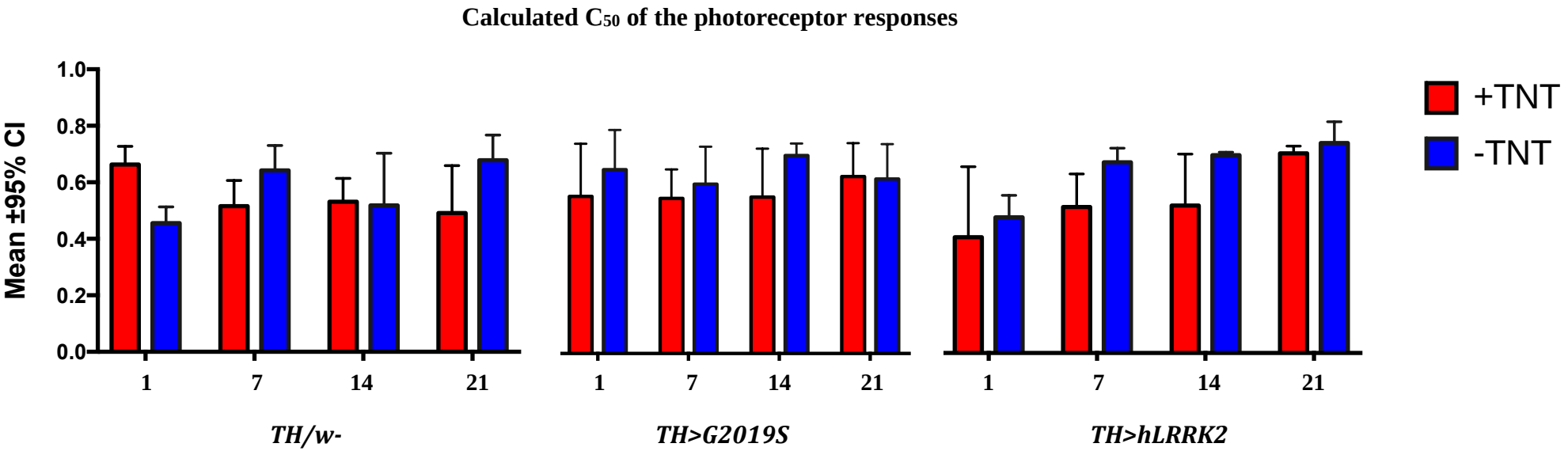

Figure 3.10 Calculated C50 from the photoreceptors. Mean ±95% CI responses from *TH>G2019S*, *TH>hLRRK2* and *TH/w-* flies after incubation at 29ºC for 1, 7, 14 and 21 days with or without expressing TNT.

3.3.2.6 Eye colour does not affect the maximal SSVEP response

A possible confounding factor is that the flies with TNT have an extra *mini-white* gene. To test if this has an effect in the SSVEP, *TH*/w^{-} with *TH*/w^{apr} at 1 and 7 days were compared as the eyes of the w^{apr} flies are similar to the *mini-white* transgenics (Fig. 3.11). No difference was found in either the photoreceptor or lamina neuron response (P>0.3, N=25). Thus the differences in visual response between *TH > G2019S* flies and the controls when neurotransmission is blocked with tetanus toxin is not likely to be due to eye colour.

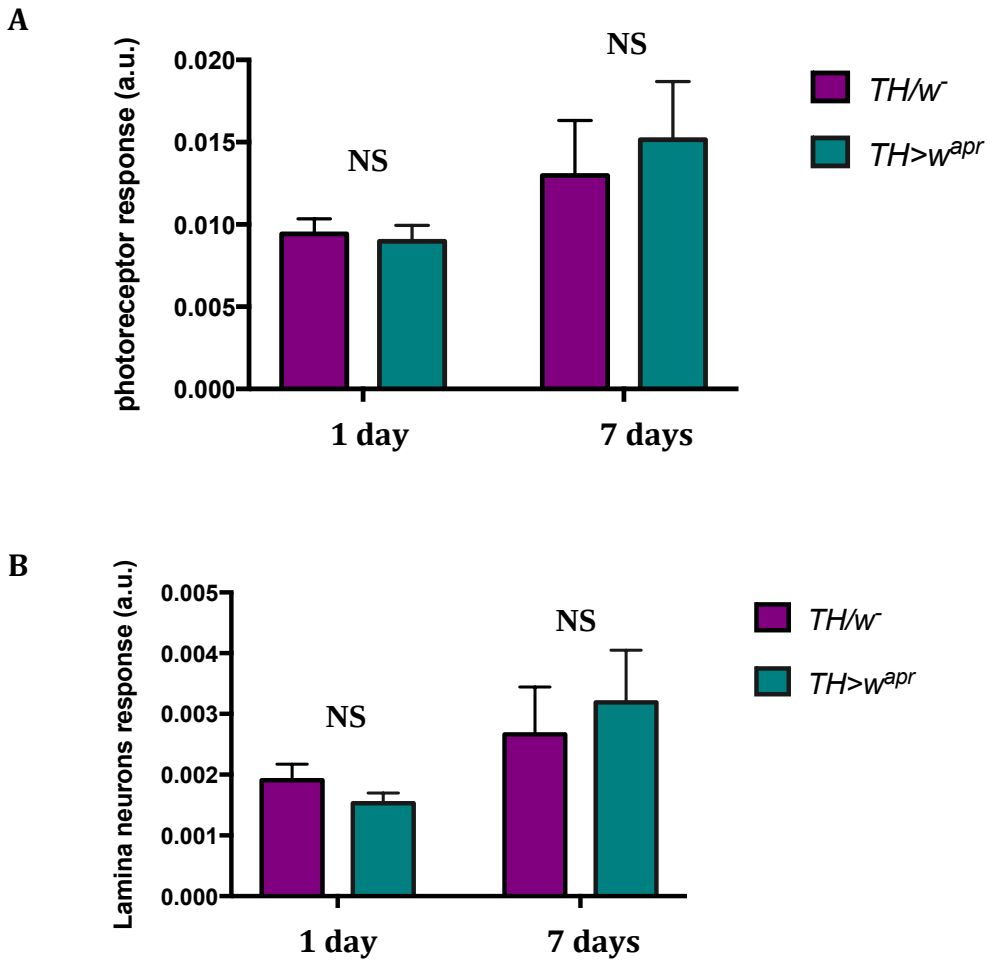

Figure 3.11 Eye pigmentation does not affect the SSVEP response. No difference is seen between *TH/w-* and *TH>w^{apr}* flies. 1 day and 7 day old flies were tested but no significant difference was seen in the visual responses of that two control flies (P>0.3, N=30). The responses from the photoreceptors (A) and the lamina neurons (B) were compared.

3.4 Discussion

3.4.1 Measurement of dopamine levels

The hallmark of PD is the loss of the melanised dopaminergic neurons in the SNpc leading to loss of dopamine in the areas where these neurons project. That has led many research labs using animal models, rodents or *Drosophila*, to have in depth investigate whether that is the case or not. Moreover, the hypothesis that was tried to be addressed in this chapter was whether this loss of dopamine is *LRRK2-G2019S* dependent or not.

The data in this chapter show that young *TH > G2019S* flies have less dopamine than the *TH>hLRRK2* and that *TNT* expression in the *G2019S* background reduces the SSVEP response, whereas in the other (control) genotypes *TH>TNT* increases the response. Old flies have similar amounts of dopamine and TNT always increases the SSVEP response.

The normal high level of dopamine in young flies is prevented by dopaminergic expression of *LRRK2-G2019S*. Isolated photoreceptors are dopamine sensitive (Chyb et al., 1999), so that less dopamine in the retina will make photoreceptor responses larger and faster. The axons of some PPL neurons terminate in the lamina (Hindle et al., 2013), making this a feasible scenario: *LRRK2-G2019S* in the PPL neurons reduces their dopamine content, leading to decreased release in the lamina, faster responses by the photoreceptors and stronger activation of the lamina neurons. This fits with the observations described by Afsari et al. (2014) of initial hyperactivity in the *TH>G2019S* flies. In older flies, the levels of dopamine are more equal, and the difference in retinal physiology is less. Although the focus was on the PPL neurons, because their axons project to the lamina, an indirect contribution from the other types of dopaminergic neurons in the optic lobes cannot be excluded (Nassel and Elekes, 1992; Nassel et al., 1988). Li et al (2010) used transgenic mice as animal models in order to measure the dopamine levels from striatum brain lysates. Two BAC transgenic strains were created expressing similar levels of wild type LRRK2 and G2019S, providing evidence of the physiological function of LRRK2 and unravel the role of the

G2019S mutation in the pathogenesis of PD. They established that wild type LRRK2 increases striatal dopamine release and enhances motor performance. On the contrary, overexpression of the most common familial PD mutation G2019S failed to provide these benefits. This decrease in the DA content was age-dependent. Moreover, the G2019S mice neither enhanced not compromised motor function in mice up to 12 months, supporting the hypothesis that LRRK2 regulates striatal DA transmission facilitating motor activity. The observed loss of DA release and content in the mutated G2019S mice surprisingly wasn't accompanied by neuronal death or nigrostriatal degeneration and motor deficits. This is surprising because the increased kinase activity of the *LRRK2-G2019S* mutation has been associated with enhanced neurotoxicity (Smith et al., 2006; West et al., 2007). This indicates that maybe the *G2019S* mutation could impair LRRK2 function without activating neuronal cell death pathways at early disease stages. And that is further supported from the fact that many G2019S carriers never develop PD symptoms.

On the other hand, as has been described in more detail in chapter 1, section 1.12, *Drosophila* PD models expressing the *G2019S* mutation consistently produce neurodegeneration (Ng et al., 2009; Liu et al., 2009; Imai et al., 2008). Taken together, that supports previous evidence that in mouse models it is very unlikely to recapitulate the full spectrum of PD symptoms.

3.4.2 Blocking of neurotransmitter release

Overall, expressing tetanus toxin increases the visual response, as would be expected if it blocked transmitter release from dopaminergic neurons. As noted earlier, tetanus toxin expression in dopaminergic neurons affects a range of fly behaviors (Alekseyenko et al., 2013; Friggi-Grelin et al., 2003; Suster et al., 2003). However, in young flies, it might be expected that tetanus toxin would have minimal effect, because they had less dopamine than the other genotypes. In fact, it appears that TNT reduces the photoreceptor and lamina neuron response of the young *TH > G2019S* flies, but increases it in the *TH > hLRRK2* and *TH/+* flies which have high dopamine. One explanation for this is that G2019S and tetanus toxin may interact to severely affect the development of the

dopaminergic projections to the retina. Fly eye development is not generally considered to be complete until the 3rd day of adult life, and disruption to dopaminergic signaling affects a number of aspects of development, including the visual response to flash electroretinograms (Neckameyer, 1996; Neckameyer and Bhatt, 2012; Neckameyer et al., 2001). A disruption to sensory startle responses in young flies with dopaminergic expression of tetanus toxin (Friggi-Grelin et al., 2003) might also be indicative of effects of tetanus toxin on development.

The evoked neurotransmitter release is abolished by TNT expression in larval motoneurons (Sweeney et al., 1995). The neuromuscular junctions are structurally normal in the presence of TNT, based on immunohistochemistry and electron microscopy. That is an indication that synaptogenesis is not affected by the expression of TNT (Broadie et al., 1995). Moreover, targeted TNT induction silences adult motor neurons (Thum et al., 2006). On the other hand, photoreceptors showed that their mature synapses are resistant to TNT (Rister and Heisenberg, 2006). On the other hand, Tabuchi et al (2000) found that expression of TNT in the photoreceptors R1-R6 would block synaptic transmission eliminating the on/off transient responses when performing ERGs. Moreover, Keller et al (2002) expressed TNT in the photoreceptors using the *GMR-Gal4* driver and concluded that TNT blocks synaptic transmission.

The only known TNT target in *Drosophila* is n-synaptobrevin (Sweeney et al., 1995). Apart from the role n-Syb has on synaptogenesis, this protein could have addition functions as it can be detected in the early pupal optic lobe (Hiesinger et al., 1999). Expression of TNT in the photoreceptors affects the columnar organization and morphology of photoreceptor terminals R7 and R8 which project in the medulla neurons (Hiesinger et al., 1999). Temporally restricted expression of n-Syb in the early pupa led to a rough eye while the structurally similar impotent TNT had no effect (Sweeney et al., 1995). These findings indicate that this rough eye genotype that was obtained could be because of the absence of n-Syb or it is the result of n-Syb cleavage products. Rister and Heisenberg (2006) showed that TNT-induced effects don't need to be developmental, as expressing the same Gal80ts tool successfully blocked adult

motor neurons (Thum et al., 2006). Furthermore, memory phenotypes were established after TNT-induction in adult central complex neurons (Liu et al., 2006). Their findings support the idea that the adult nervous system has two types of chemical synapses: TNT sensitive and TNT-resistant.

TNT was originally tested in glutamatergic motor neurons, but perhaps the release machinery for biogenic amines, including serotonin, dopamine, octopamine, tyramine, and neuropeptides may differ. However, the expression of TNT has proven aminergic neurons phenotypes (Friggi-Grelin et al., 2003). As it targets a neural-specific protein, it is expected that it should only block vesicle release in neurons. Our aim was to block the release of DA in the dopaminergic neurons, without being sure that TNT doesn't affect other co-neurotransmitters of DA at the same time.

In addition to that, previous studies have shown that expression of the *G2019S* mutation in mammalian cells, fly motoneurons and sensory cells lead to reduced neurite outgrowth (Lin et al., 2010; Lin et al., 2015; MacLeod et al., 2006). Failure of the dopaminergic axons to reach the lamina/retina might contribute (along with low dopamine production) to the early hyperactivity seen in the *TH>G2019S* visual response.

Lin et al. (2010) expressed the *G2019S* mutation in DA neurons using *Drosophila* as an animal model. This expression led to several dendritic defects, including tau mislocalisation in dendrites and tau hyper-phosphorylation leading to the accumulation of tau-positive inclusions with lysosomal characteristics. MacLeod et al (2006) first identified that overexpression the most common mutation within *LRRK2* leads to phospho-tau inclusions that display abnormal lysosomal features, undergoing apoptosis.

Tau protein is a microtubule-associated protein (MAP) that has been linked to neurodegenerative diseases, including Alzheimer disease (Hanger et al., 2009) and PD (Bancher et al., 1993). Tau protein is encoded by the *MAPT* gene, which has also been associated to Frontotemporal dementia (FTD) (Lee et al., 2001). The recent findings linking tau to PD pathogenesis and a probable interaction

with LRRK2, triggered the interest of my researchers studying this protein in more detail. Tau is mostly found in neuronal cells with its main role being maintaining the integrity of cytoskeleton by interacting with motor proteins, dynein and kinesin. Tau is also involved in axonal transport along this network (De Vos et al., 2008). Hyper-phosphorylation of tau could result in MT destabilization and impaired protein transport leading to the creation of toxic protein aggregates (Lee et al., 2001) propagating neuronal death, which is characteristic of my neurodegenerative disorders. Furthermore, tau co-localizes with α-synuclein, the protein aggregates in Lewy bodies (Ishizawa et al., 2003), implying a physiological or pathophysiological interaction.

Thus, our results coincide with previously published data, supporting our initial hypothesis even further. The early hyperactivity of young flies carrying the *G2019S* mutation was confirmed. Moreover, we can confidently conclude that the SSVEP method is more sensitive than the ERGs, as Hindle et al (2013) showed that wild type flies, *LRRK2* and *TH/+*, had no ERG changes up to 28 day old, while that is not the case with the SSVEP method. This is very encouraging, as the SSVEP method could actually have an application in humans and even to harder populations to be tested, including children.

3.5 Conclusion

Taken together the results presented in this chapter the overall conclusion that could be made is that dopaminergic signaling is defective in the *TH>G2019S* retina of young flies, and this might be a major factor in starting the neurodegenerative cascade. This could be the beginning of understanding the molecular pathway of PD that leads to the neurodegeneration of the dopaminergic neurons.

Chapter 4

Genetic interaction of LRRK2 and Rabs

4.1 Introduction

One of the main aims of this project was to shed new light on our understanding of the chain of events that cause nerve cells with the *LRRK2-G2019S* mutation to die. A better understanding of the biological functions of *LRRK2* and its roles in signal transduction pathways may be important for future therapeutic development for PD, and this is because the kinase pathway is an easy target for drug development. Many previous studies have highlighted Rab proteins as potential targets that could be phosphorylated by LRRK2, but the exact Rab has differed substantially. Since *Drosophila* has been a highly successful organism for genetic screens, we undertook a screen for *LRRK2-G2019S*↔Rab genetic interactions, using the SSVEP electroretinogram as a readout.

4.1.1 Rab proteins

Rab (Ras related in brain) proteins are small (20-25 kDa), monomeric G-proteins, constituting the largest subfamily of the Ras GTPase superfamily (Ng and Tang, 2008; Pfeffer, 2001; Stenmark, 2009; Zerial and McBride, 2001). Rab GTPases were first described in 1987 when Touchot isolated four family members from a rat brain cDNA library (Touchot et al., 1987). Later on it was established that these proteins are key regulators of membrane organisation and intracellular membrane trafficking in all eukaryotic cells (Zerial and McBride 2001; Pfeffer et al., 2007; Pfeffer et al., 1994; Stenmark et al., 2009). They are involved in many steps in membrane trafficking, including vesicle formation, vesicle movement and membrane fusion. These processes are responsible for the transfer of membrane proteins from the Golgi to the plasma membrane and recycled. Specific Rabs are physically associated with each organelle as well as their associated transport vesicles (Figure 4.1). Moreover, Table 4.1 summarizes all the needed information for each one of the Rabs, including the exact location, pathway that they are involved and the human ortholog that each one has been associated with.

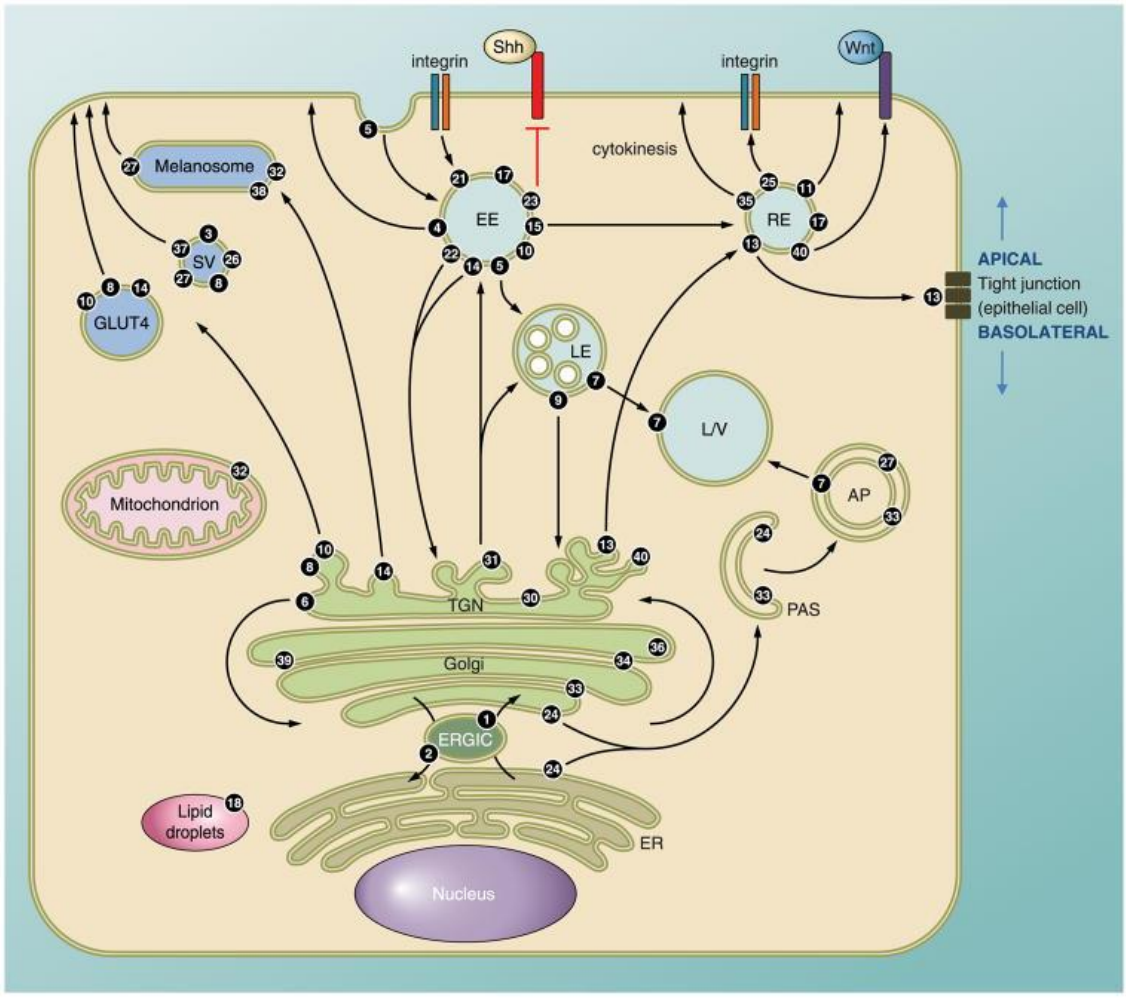

Figure 4.1 The intracellular localization of Rabs.

Each Rab has been associated to a district cellular compartment and vesicle transport pathway(s). Rab1 is located in the intermediate of the ER and Golgi regulating the traffic between those two compartments while Rab2 is involved in recycling, or retrograde traffic, from Golgi and ERGIC back to the ER. Early endocytic steps rely on Rab5, which mediates fusion of endocytic vesicles to form the early endosome. Rab7 is a marker for the lysosomal pathway, which directs traffic towards degradation, or to various recycling compartments to return factors to the plasma membrane. More specialised Rab functions include Rab18, which is located in the lipid droplets, regulating intracellular lipid storage sites. (Adapted from Hutagalung and Novick, 2011).

Table 4.1 Summary of the function of the Rab proteins and their similarity to *Drosophila* (Information taken from Ensembl and GeneCards)

Rab protein	Localization	Pathway	Fly ortholog	Similarity to the human homolog %
Rab1	Extracellular, Golgi apparatus, ER, cytosol	ER to Golgi, intra-Golgi	Rab1	84
Rab2	Extracellular, ER, Golgi, ER-Golgi intermediate compartment	ER to Golgi	Rab2	90
Rab4	Early endosome	Protein recycling, transport to plasma membrane	Rab4	75
Rab5	Early endosome, extracellular, cytosol, plasma membrane	Early endosome fusion	Rab5	73

Rab6	Golgi	Endosome to Golgi, intra-Golgi transport, Golgi to ER	Rab6	85
Rab7	Late endosomes, lysosomes, melanosomes, phagosomes	Late endosome to lysosome	Rab7	76
Rab8	Cell membrane, vesicles, extracellular	Exocytosis, TGN/RE to plasma membrane	Rab8	78
Rab9	Late endosomes, Golgi	Endosome to TGN	Rab9	50
Rab10	ER, Golgi, basolateral sorting endosomes, GLUT4 vesicles	Exocytosis, TGN/RE to plasma membrane	Rab10	80
Rab11	Golgi, ER, endosomes	TGN/RE to plasma membrane	Rab11	85

Rab14	Golgi, early endosomes, GLUT4 vesicles	TGN/RE to plasma membrane	Rab14	81
Rab18	ER, Golgi, lipid droplets	Lipid droplet formation	Rab18	55
Rab19	Golgi	Unknown	Rab-RP3	47
Rab21	Early endosome	Endosomal transport	Rab21	65
Rab23	Plasma membrane, endosome	Protein recycling/ transport to plasma membrane	Rab23	59.94
Rab26	Secretory granules	Exocytosis	Rab26	65
Rab27	Melanosomes, lysosomes	Exocytosis	Rab27	60

Rab30	ER, Golgi	Unknown	CG9100 Rab30	73 64.22
Rab32	Mitochondria, melanosomes	TGN to melanosome, mitochondrial fission	Ltd	69
Rab34	Golgi	Intra-Golgi transport, peri-Golgi positioning of lysosome	RabX5 CG7980	38 52
Rab35	PM, endosome	RE to plasma membrane	Rab35 CG9575 CG2885	68.52 66 44
Rab36	Golgi	Unknown	RabX5 CG7980	55.17 52

Rab37	Secretory granules	Exocytosis	Rab26	31
Rab39	Golgi	Unknown	Rab39	56
Rab40	Golgi, ER	Endosome/intracellular transport	Rab40	54
Rab43	ER, Golgi	ER to Golgi	Rab19	63

There are numerous Rabs associated with the endosomal traffic, and the most active site of localization is the early endosome. Most of the early endocytic steps rely on Rab5, which is located in the early endosomes, mediating fusion of endocytic vesicles to form the early endosome. Traffic can be directed towards the lysosome for degradation, which relies on action of Rab7, or to various recycling compartments to return factors to the plasma membrane. Rab4, which is also located in the early endosomes regulate fast endocytic recycling. Rab9, which is located in the late endosomes, regulates membrane traffic between late endosomes and the trans-Golgi network (TGN). Rab21 regulates transport of integrins to control cell adhesion and cytokinesis while Rab23 acts downstream to negatively regulate Sonic hedgehog (Shh) signaling during dorsoventral development of the mouse spinal cord. It potentially interacts with the transcription factors activated by the Shh pathway. Rab27 is well-studied in the melanosome transport system, which also relies on Rabs 32 and 38. Rab35 is one of the less characterised Rabs, controlling plasma membrane recycling of an essential factor in cytokinesis (Reviewed from Shi et al., 2017; Hutagalung and Novick, 2011).

Several Rab GTPases have been associated with the ER-Golgi trafficking pathway. Rab1 is located in the intermediate of the ER and Golgi, regulating this traffic pathway while Rab2 is involved in recycling, or retrograde traffic, from Golgi and the ERGIC back to the ER. Rab6 is involved in the intra-Golgi trafficking. Several other Rabs including Rab8 and Rab10 are responsible for the biosynthetic pathway from the trans-Golgi network (TGN) to the plasma membrane. Rab18 has a more specific role as it mediates the regulation of the lipid droplets, which are intracellular lipid storage sites. Rab40 acts in a signalling pathway where it recruits components of the ubiquitination machinery to regulate Wnt pathway (Reviewed from Shi et al., 2017; Hutagalung and Novick, 2011).

Many Rabs have been implicated in the vesicle recycling pathway being located in the synaptic vesicles or the glucose transporters (GLUT4). GLUT4 is found in vesicles that can use different Rabs to reach the plasma membrane. One of these Rabs is Rab8. Apart from that Rab8 also regulates the biosynthetic traffic from

the *trans*-Golgi network (TGN) to the plasma membrane. Several secretory vesicles and granules use Rab3, Rab26, Rab27 and Rab37 in order to exocytose their cargo. Rab35 that belongs to this pathway is very poor characterized. Rab26 and Rab27 localise in the synaptic vesicles regulating exocytosis to the plasma membrane (Reviewed from Shi et al., 2017; Hutagalung and Novick, 2011).

4.1.2 Rab proteins structure

Overall, Rab proteins show a typically conserved core structure that is mainly conserved among the entire Ras superfamily. That includes the presence of a 20 kDa catalytic GTPase fold composed of a six-stranded β-sheet, with five parallel strands and one anti-parallel stand, flanked by five α-helices (Figure 4.2). The structural basis of the Rab molecular switch can be defined as the portions of the Rab protein that are unique to and therefore specify the GDP and GTP-bound conformations. These elements are known as "Switch regions" (Hutagalung and Novick 2011; Pfeffer 2005). As with Ras, there are two Switch elements, termed Switch I and Switch II. These regions appear to be the only elements of the protein that change conformation upon nucleotide binding.

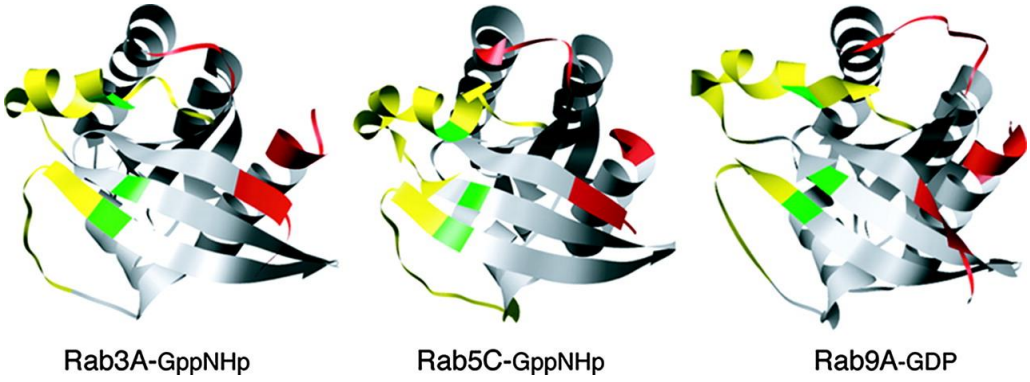

Figure 4.2 Structure of three different Rabs. In yellow are shown the Switch regions and in red are domains that correspond to the complementarity-determining regions identified in Rab3a. Green positions are the hydrophobic triad residues in which side chains have different orientation in Rab structures despite their identical sequences. (Adapted from Pfeffer 2005).

Apart from the N-terminal catalytic core Rab proteins also contain a hypervariable C-terminal domain, which was originally implicated in the localization of Rab's to specific target membranes (Chavrier et al., 1991). However, assessment of a wider range of Rabs suggests that multiple regions contribute towards the localization of the Rabs (Ali et al., 2004). For most of the Rab proteins the C-terminal domain terminates with a distinctive cysteine rich motif (CC, CCX, CCXX or CCXXX) (Leung et al., 2007; Calero et al., 2003). This motif is then recognised by RabGGT (Rab geranylgeranyl transferase) catalysing the addition of prenyl groups that is essential for membrane associate and anchoring of Rabs (Leung et al., 2007; Calero et al., 2003).

4.1.3 The function of Rab GTPases; Molecular Switches

The Rab proteins, as GTPases, function as molecular switches that alternate between two conformational states: the GTP-bound 'on' form and the GDP-bound 'off' form. Exchange of GDP with GTP is catalysed by Guanine nucleotide exchange factors (GEFs), which recognise specific residues in the switch regions and facilitate GDP release (Delprato et al., 2004). Conversion from GTP- to GDP-bound form occurs through GTP hydrolysis, which is catalysed by GTPase-activating proteins (GAPs). That cycling between GTP- and GDP-bound form is associated with significant conformational alternations in two distinct variable regions, the Switch I and Switch II (Zhu et al., 2010).

Rab proteins cycle between the cytosol and the membrane of its respective transport compartment (Figure 4.3). The nucleotide-bound state of the Rab influences its localization and activity. The newly synthesised Rabs are associated with Rab escort proteins (REP), which present the Rab to Rab geranylgeranyl transferase (RabGGT) that catalyses the addition of one or two geranylgeranyl lipid groups to the COOH terminus of the Rab (Alexandrov et al., 1994; Andres et al., 1993; Desnoyers et al., 1996). In its inactive, GDP-bound form, the Rab is inserted into its respective membrane. A GDP dissociation inhibitor (GDI) and dissociation factor (GDF) may also assist to insert the Rab in the appropriate membrane (Collins, 2003); Sivars et al., 2003). A guanine

nucleotide exchange factor (GEF) acts on the membrane where the Rab has been inserted to convert it to a GTP-bound or to its active state. Now the activated Rab interacts with effector proteins that facilitate trafficking in its respective pathway. A GTPase accelerating protein (GAP) then binds to the activated Rab inducing hydrolysis of the GTP-bound to GDP-bound converting in that way the Rab back to its inactive state (Pfeffer, 2001; Segev, 2001). The GDP-bound form of the Rab is now a substrate for GDI, which is now able to extract the Rab in its GDP-bound conformation from the membrane. The Rab is now ready to be reinserted into a membrane and begin the cycle again (Hutagalung and Novick 2011).

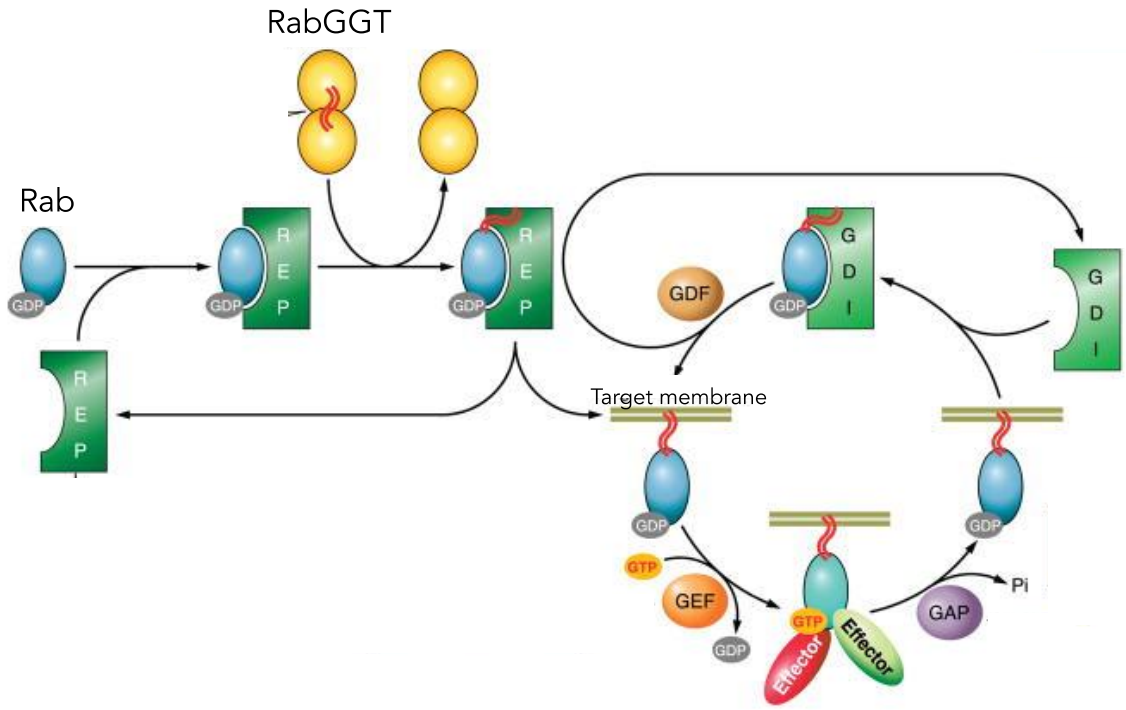

Figure 4.3 The Rab GTPase cycle.

Newly synthesized Rab proteins associate with Rab escort proteins (REP) which direct them to Rab geranylgeranyl trasnferase (RabGGT) in order to receive their prenyl tails (shown in red wavy lines). REP proteins deliver Rabs to their target membranes. Throughout that process, the Rabs are GDP-bound. A guanine nucleotide exchange factor (GEF) then catalyses exchange of GDP for GTP to activate the Rab. The GTP-bound Rab then interacts with effector proteins that mediate membrane traffic in the pathway regulated by its associated Rab. This process is followed by Rab interacting with its associated GTPase activating protein (GAP) which catalyses hydrolysis of GTP to GDP by the Rab. The Rab is then removed from the membrane by guanine nucleotide dissociation inhibitor (GDI) in preparation for the next cycle. Insertion of the Rab into its associated membrane is mediated by a GDI dissociation factor (GDF) that releases the Rab from GDI. (Adapted from Hutagalung and Novick, 2011).

Through this conformational cycling, and the specific localization of different Rabs, and the effector proteins they activate and/or recruit, Rab proteins act as multifaceted organisers (Ng and Tang, 2008; Stenmark, 2009). For that reason they convey strict regulation to both rate and specificity for almost all trafficking event occurring in the eukaryotic cells (Ng and Tang, 2008; Stenmark, 2009). These events include vesicle transport, tethering and docking to target membranes and exocytosis by interaction with cytoskeletal motor proteins, N-ethylmaleimide-sensitive factor (NSF) and soluble NSF attachment receptor (SNARE) proteins, respectively (Ng and Tang, 2008; Pfeffer, 2001; Stenmark, 2009). When in GTP-bound active state Rab proteins have been shown to activate and recruit several effector proteins including motor proteins, tethering factors, adaptor proteins, kinases and phosphatases. They also recruit and activate GEF's that proceed to activate other, downstream, Rab proteins (Knodler et al., 2010).

4.1.4 The role of Rab proteins in Disease

The physiological importance of Rab GTPases, which is expected from their central role in membrane trafficking, is reflected by the association of these proteins and their regulators or effectors with many diseases. In general, infectious, neurological and endocrinological diseases can be the result of pathogen-induced or inherited dysfunctions of Rab pathways (Stenmark 2009).

Neurons have specialized demands on membrane trafficking both during development and function indicating the importance of Rab function in the nervous system. That is highlighted by observations that mutations within *Rab* genes and their effectors and interactors cause several hereditary and neurological diseases (Chan et al., 2011). A summary of their function and their association with specific neurological and neurodegenerative diseases is listed on Table 4.2.

Table 4.2 The role of Rab proteins and their functions in Neurodegenerative Diseases (Adapted and modified from Hutagalung and Novick, 2011; Seixas et al., 2013).

Rab protein	Localization/ Function	Membrane Traffic Pathway	Association with a Disease	Reference
Rab1	ER, Golgi	ER to Golgi complex trafficking	Parkinson's disease	Cooper et al., 2006
Rab3a	Secretory vesicles, plasma membrane	Exocytosis, neurotransmitter release	Warburg Micro/Martsoft syndromes	Aligianis et al., 2005; Dalfo et al., 2004; Gitler et al., 2008
Rab4a	Early endosome	Protein recycling, transport to plasma membrane	Alzheimer's disease	Ginsberg et al., 2011 Ginsberg et al., 2010
Rab5a	Early endosome, clathrin-coated vesicles, plasma membrane	Early endosome fusion	Alzheimer's disease	Ginsrberg et al., 2011
			Parkinson's disease	Dalfo et al., 2004

Rab7	Late endosomes	Late endosome to lysosome	Alzheimer's disease	Ginsberg et al., 2011; Ginsberg et al., 2010
			Charcot-Marie-Tooth Disease Type 2B	De Luca et al., 2008; McCray et al., 2010; Verhoeven et al., 2003
			Batten disease	Agola et al., 2011; Luiro et al., 2004
Rab8	Cell membrane, vesicles	Exocytosis, TGN/RE to plasma membrane	Huntington's Disease	Del Toro et al., 2009; Hattula and Peranen, 2000
			Parkinson's Disease	Dalfo et al., 2004; Gitler et al., 2008
			Alzheimer's Disease	Kametani et al., 2004
Rab9	Late endosomes, Golgi	Endosome to TGN	Niemann Pick C	Ganley and Pfeffer, 2006
			Batten Disease	Agola et al., 2011;

				Luiro et al., 2004
Rab10	Golgi, basolateral sorting endosomes, GLUT4 vesicles	Exocytosis, TGN/RE to plasma membrane	Parkinson's disease	Steger et al., 2016
Rab11	Golgi, ER, early endosomes	TGN/RE to plasma membrane	Huntington's Disease	Li et al., 2009b; Li et al., 2009c
			Batten disease	Agola et al., 2011; Luiro et al., 2004
			Charcot-Marie-Tooth Disease Type 4C	Roberts et al., 2010
Rab23	PM, endosome	Protein recycling/ transport to plasma membrane	Carpenter Syndrome	Eggenschwiler et al., 2001; Jenkins et al., 2007
Rab27	Melanosomes	Exocytosis	Griscelli syndrome	Meschede et al., 2008

4.1.5 Interaction between LRRK2 and Rabs

As LRRK2 is a multi-domain protein with the presence of many protein-protein binding domains, it has been proposed that this protein acts as a scaffold for several other proteins. Many different LRRK2 substrates have been identified including FADD [Fas-associated protein with death domain, (Ho et al., 2009)], heat shock protein 90 [Hsp90, (Wang et al., 2008)], the dishevelled family members [DVL1-3, (Sancho et al., 2009)] and others (Dachsel et al., 2007).

More recent studies identified several Rab GTPases as LRRK2 substrates, initiating a whole new era of investigation in PD genetics. Most of these approaches focused on *in vitro* experiments or to cellular systems using overexpressed kinase (Jaleel et al., 2007; Kumar et al., 2010; Ohta et al., 2011; Kawakami et al., 2012; Bailey et al., 2013; Martin et al., 2014; Qing et al., 2009; Chen et al., 2012; Gloeckner et al., 2009; Imai et al., 2008; Gillardon, 2009; Kanao et al., 2010; Matta et al., 2012; Xiong et al., 2012; Yun et al., 2013; Yun et al.,2015; Krumova et al., 2015). The first Rab identified as LRRK2 substrate was Rab7L1 (MacLeod et al., 2013). Since then Rab8a, Rab1 and Rab3a have been also linked contributing to the pathogenesis of PD, by functionally interplaying with known PD factors (Cooper, 2006; Gitler et al., 2008). The different Rabs that have been identified interacting with LRRK2 are listed on Table 4.3. Additionally, Rabs have been linked to other genetic forms of PD (e.g. α-synuclein) (Gitler et al., 2008; Stefanis, 2012; Shi et al., 2017). Even though the interaction between LRRK2 and several Rab GTPases has been confirmed, it is not clear yet if LRRK2 directly or indirectly modulates Rabs at the molecular level and by which mechanism. *In vitro* experiments indicated that LRRK2 directly phosphorylates Thr but not Ser sites in Rab isoforms (Jaleel et al., 2007; Martin et al., 2014; Nichols et al., 2009), although the major characterised *in vivo* LRRK2 autophosphorylation site is a Ser residue (Ser1291) (Sheng et al., 2012). Investigating the functional role of LRRK2-mediated Rab phosphorylation, it was established that LRRK2 is an important regulator of Rab homeostasis which is very likely contributing to PD development (Steger et al., 2016). PD-associated LRRK2 mutations could shift the membrane-cytosol balance of Rabs towards the membrane compartment, leading to the accumulation of inactive

Rabs in the membranes. The T73 residue, that is located in the Switch II domain, is characteristic of the Rab GTPase proteins. This domain changes conformation upon nucleotide binding and regulates the interaction with multiple regulatory proteins (Pfeffer, 2005). Sequence alignment of that residue revealed its high evolutionary conservation among more than 40 human Rabs, which is an indication of a strong functional relevance.

Table 4.3 Summary of that Rab proteins that have been identified interacting with LRRK2

Rab interacting with hLRRK2	Function of Rab	Reference
Rab3	Exocytosis through synaptic vesicles	Islam et al., 2016
Rab5b	Key regulator of endocytic vesicular transport from PM to endosomes	Shin et al., 2008
Rab7	Late endosomal/lysosomal pathway	Dodson et al., 2012
Rab8	Exocytosis, TGN/RE to plasma membrane	Steger et al., 2016 Kim et al., 2017
Rab10	Exocytosis, TGN/RE to plasma membrane	Steger et al., 2016 Ito et al., 2016
Rab29 (Rab7L1)	Trans-Golgi network	Beilina et al., 2014 MacLeod et al., 2013
Rab32	TGN network/ transport of key enzymes in melanogenesis	Waschbusch et al., 2014

4.1.6 *Drosophila* as an animal model for Rabs

Drosophila is considered an ideal model for the investigation of Rab GTPases in the nervous system. There are ~33 *Rab* or *Rab*-related genes in the fly genome of which at least six do not have a clear vertebrate ortholog (Chan et al., 2011). Twenty-three *rab* genes have direct orthologs in human that are at least 50% identical at the protein level. Therefore, Rab proteins in *Drosophila* exhibit high evolution conservation and low redundancy compared to over 70 *Rab* genes in humans (Colicelli, 2004). Clear orthologs exist that serve as gold standard markers for many intracellular compartments across species, as different Rab proteins are found to be associated with distinct subcellular membrane compartments. For instance, Rab1 acts as a marker for the endoplasmic reticulum, Rab5 for the early endosomes, Rab6 for Golgi, Rab7 for late endosomes and Rab11 for recycling endosome. Apart from the fact that there are fewer Rab proteins in *Drosophila* compared to vertebrates, *Drosophila* genetics will be useful in identifying interacting genes and proteins. Moreover, most developmental signalling pathways are also evolutionally conserved from *Drosophila* to humans and are easily studied in the fly. Studying and characterization of Rab functions in flies will improve our understanding of the normal cellular functions of Rab proteins and the molecular nature of Rab-induced diseases.

Zhang et al (2007), taking into account all the benefits obtained by using *Drosophila* as an animal model, isolated cDNA clones representing 31 out of the 33 *Rab* genes. They generated transgenic flies that can be stimulated, under UAS-control, to produce yellow fluorescent protein (YFP)-tagged wild-type, dominant negative and constitutively active forms of each of the 31 *Drosophila* Rab proteins. A few years later, a '*Rab*-Gal4 kit' was created making *Gal4* lines for each *Rab* gene, which provided further details on the comparative analysis of the cellular and subcellular expression of all Rab GTPases (Jin et al., 2012; Chan et al., 2011). Most recently, a '*Rab*-knockout kit' was provided, showing that removal of any Rab was not lethal (Dunst et al., 2015).

4.2 Aims

1. Test for genetic interaction between LRRK2 and Rabs *in vivo*, by dopaminergic expression of different *Rab* transgenes in *Drosophila* both in isolation and in combination with the *G2019S* mutation.

2. Take advantage of the evolutionary conservation using *Drosophila* as an animal model in order to test in which subcellular compartment *LRRK2-G2019S* mutation could be involved.

4.3 Results

4.3.1 Expression of different UAS-Rab constructs in the dopaminergic neurons

More than 1000 flies were recorded in this genetic screen, including 21 different Rabs and 3 different controls. One of the aims of this study was to test if it is a specific cellular pathway that can be implicated in the interaction between LRRK2 and Rabs. As every Rab is associated with a different cellular compartment, Rabs were grouped according to their subcellular localization. As described in more details in section 2.1.1, *TH-Gal4;G2019S* or *TH-Gal4* flies were crossed to *UAS-Rab* flies and the SSVEP (Steady State Visual Evoked Potential) of the F1 generation was tested at 1 and 7 days old.

In this course of investigation three controls were deployed including *TH>G2019S, TH>hLRRK2* and *TH/w-*. For all the recorded Rabs that were tested here, the visual response is represented as a percentage (%) of that recorded from *TH/w-* and *TH::G2019S/w-* flies at 1 and 7 days old. Figure 4.4 shows the raw data from the controls that utilised during this set of experiment.

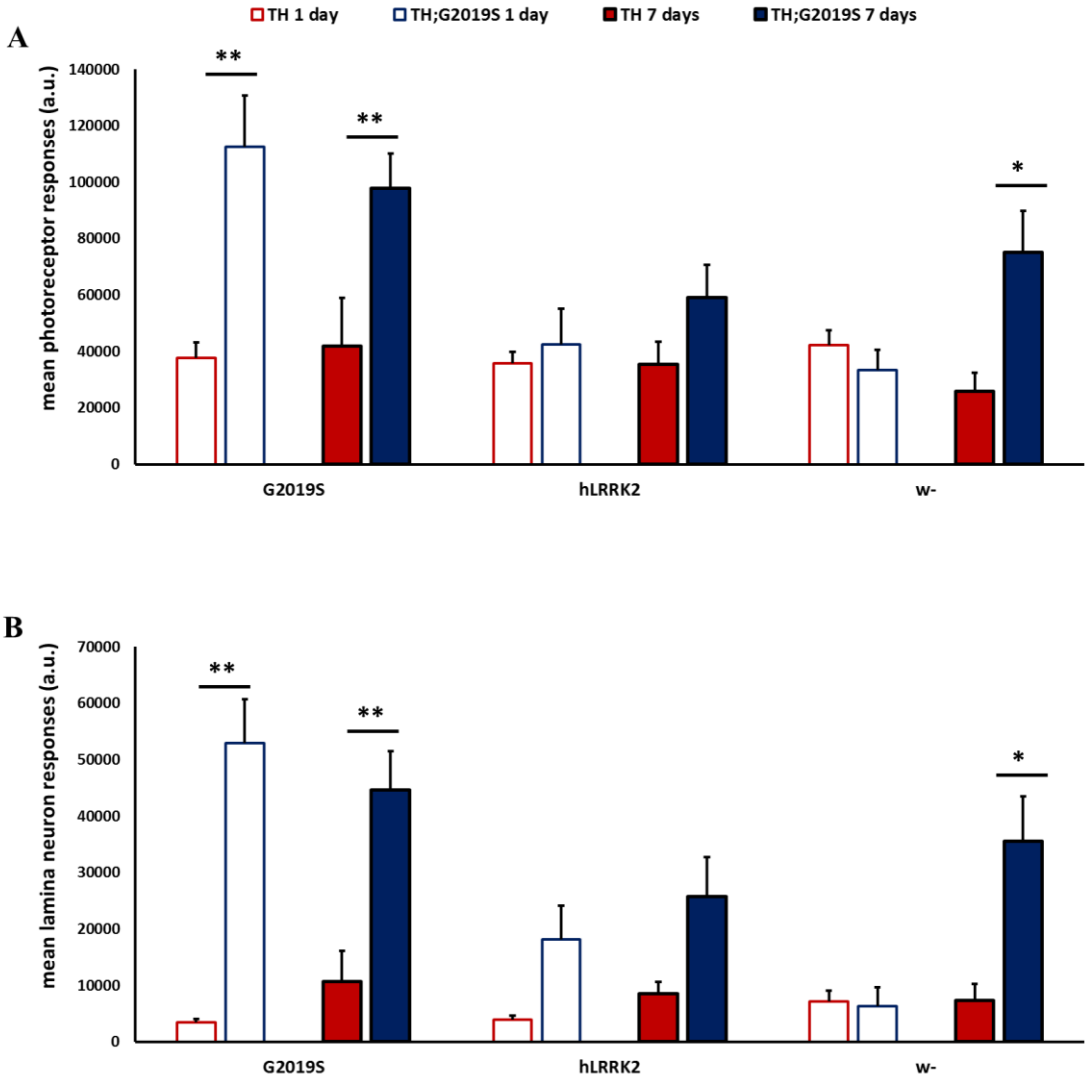

Figure 4.4 Presentation of the deployed controls in this genetic screen. The mean responses ±SE from the photoreceptors (A) and the lamina neurons (B) are presented. *TH>G2019S*, *TH>hLRRK2* and *TH/w-* flies were tested both in the presence and the absence of the *G2019S* mutation. Each fly line was tested at 1 day and 7 days, after being crossed to *TH-Gal4* or *TH::G2019S-Gal4*. N=123. For all the different groups two-way ANOVA was performed, when * P<0.05, ** P<0.01 and when *** P<0.001.

The criteria by which the *Rab↔G2019S* interaction was determined was increased (P<0.05) 1F1 and 2F1 responses in the presence of the *G2019S* mutation at 1 or 7 days compared with the expression of the Rab alone. In addition, responses to expression of a *Rab* that increased the photoreceptors responses above control levels in the absence of the *G2019S* mutation are reported.

4.3.1.1 Rabs involved in the endo-lysosomal pathway

The available Rab fly stocks that were associated with the endo-lysosomal pathway including *Rab4, Rab5, Rab7, Rab9, Rab21, Rab23, Rab27* and *Rab35* were tested. All the *UAS-Rabs* were expressed in the dopaminergic neurons using the *TH-Gal4* driver and the visual responses were obtained using the SSVEP assay as described in section 2.2.2.

The eight different *UAS-Rabs* were recorded in both the presence and the absence of the *G2019S* mutation. From the SSVEP recording, the visual responses from the photoreceptors and the lamina neurons were obtained as shown in Figure 4.5 (A and B, respectively).

From this genetic screen, it was established that there is an interaction between *LRRK2-G2019S* and *Rab5* and *LRRK2-G2019S* and *Rab9*, as the presence of the *G2019S* mutation has a big effect on the vision of flies expressing these Rabs. The photoreceptor responses are massively increased compared to the absence of the *Rab* transgene and compared to the control levels as well. At 1 day and 7 days there is 100% increase in the photoreceptor response in the *TH::G2019S>Rab5* compared with *TH>Rab5* (P=0.04 and 0.025, respectively), establishing a strong interaction. Additionally, the lamina neurons show a similar effect: *TH::G2019S>Rab5* is 35% bigger on day 1 and 50% on day 7 compared with *TH>Rab5* (P=0.03, P=0.0091, respectively); (Figure 4.5; B).

Rab5 is not the only Rab in the endo-lysosomal pathway to show an interaction with *G2019S*: Rab9 also shows some interaction. At 7 days, there is a 250% increase in the responses from the photoreceptors in the *TH::G2019S>Rab9*

compared with *TH>Rab9* (P=0.001) (Figure 5.5; A). This interaction is also confirmed from the responses from the lamina neurons as there is a 50% increase at 7 days (P=0.03) (Figure 4.5; B).

The rest of the tested Rabs show responses similar to the control levels irrespectively of the presence of the *G2019S* mutation.

In a cluster analysis, the percentage change in visual response due to expression of an endo-lysosomal Rab was plotted against the combined effect (expression of *Rab* and *G2019S* (Figure 4.5: C- 1 day; D- 7 days). Most of the Rabs are in a cluster, and *Rab5* is a clear outlier on day 1, but both *Rab5* and *Rab9* are outliers on day 7.

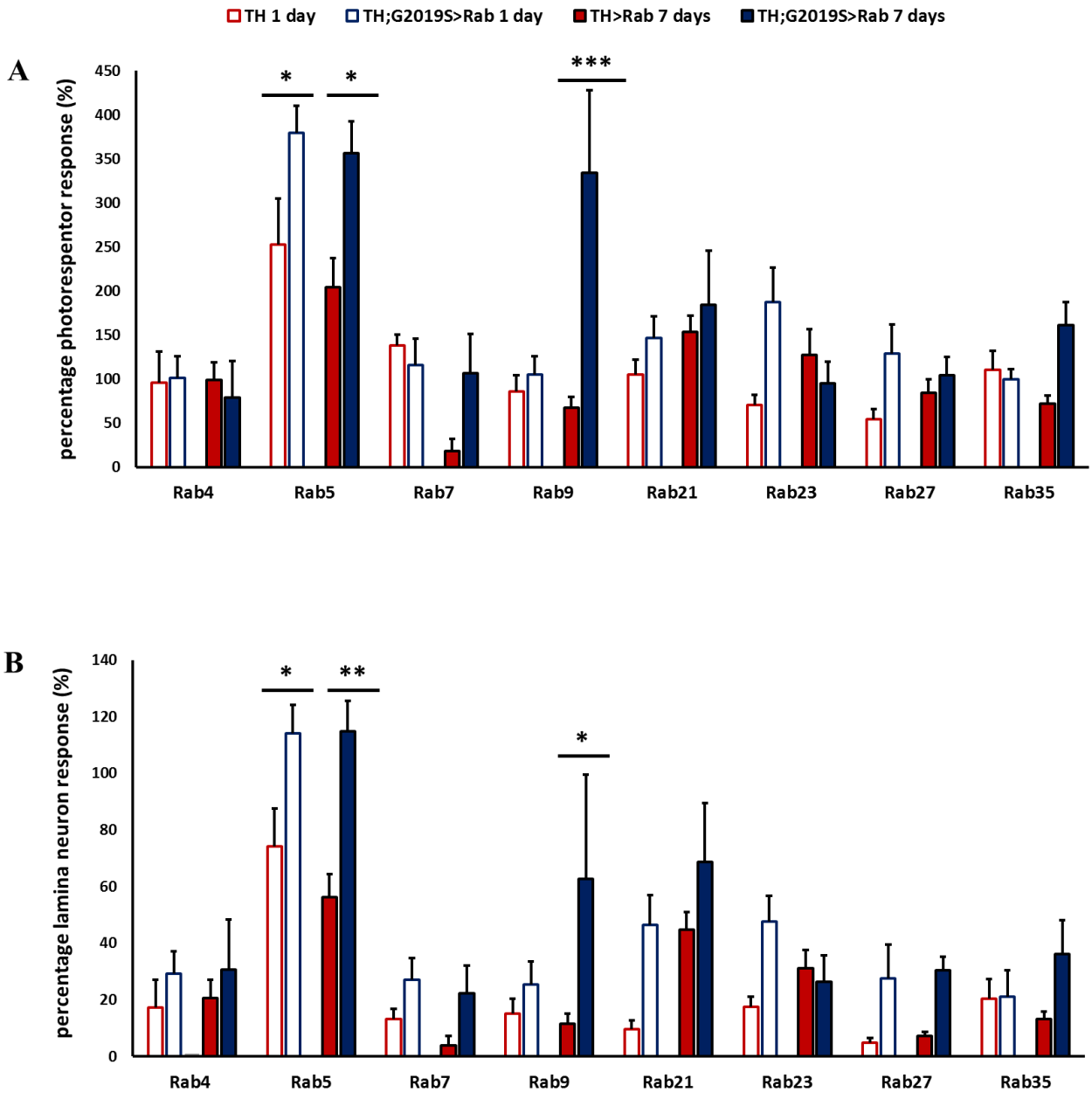
A
TH 1 day
TH;G2019S>Rab 1 day
TH>Rab 7 days
TH;G2019S>Rab 7 days
percentage photorespentor response (%)
450
400
350
300
250
200
150
100
50
0
*
*
***
Rab4
Rab5
Rab7
Rab9
Rab21
Rab23
Rab27
Rab35
B
percentage lamina neuron response (%)
140
120
100
80
60
40
20
0
*
**
*
Rab4
Rab5
Rab7
Rab9
Rab21
Rab23
Rab27
Rab35

C

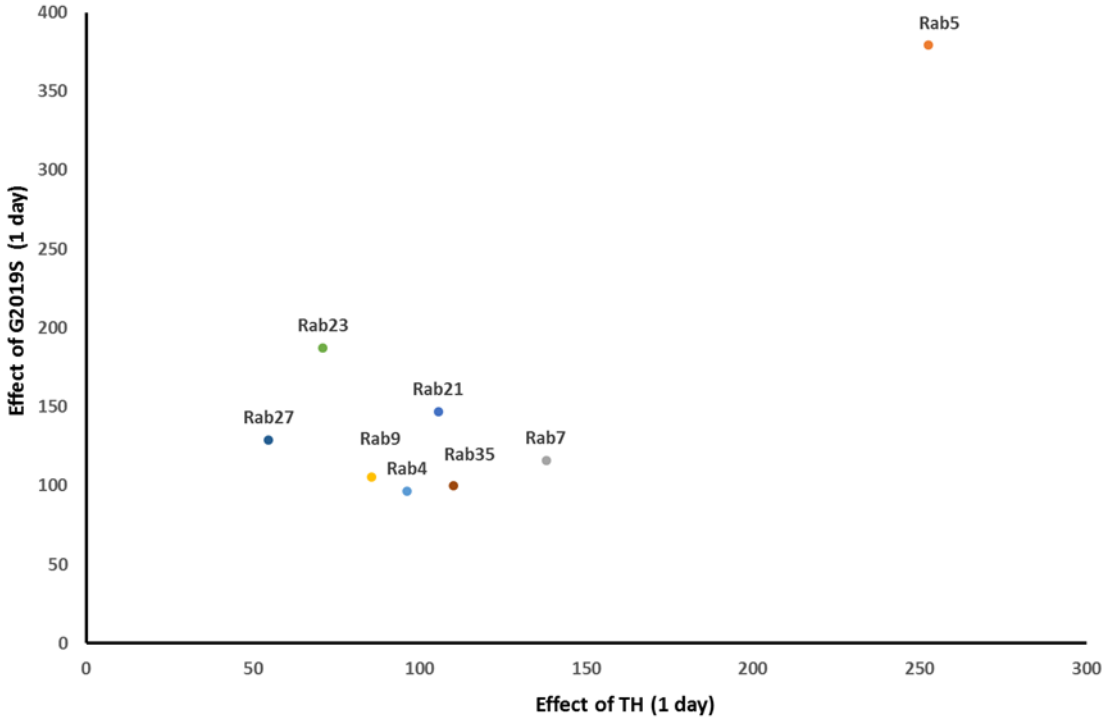
Effect of G2019S (1 day)
Effect of TH (1 day)
Rab5
Rab23
Rab21
Rab27
Rab9
Rab7
Rab35
Rab4
0
50
100
150
200
250
300
350
400

D

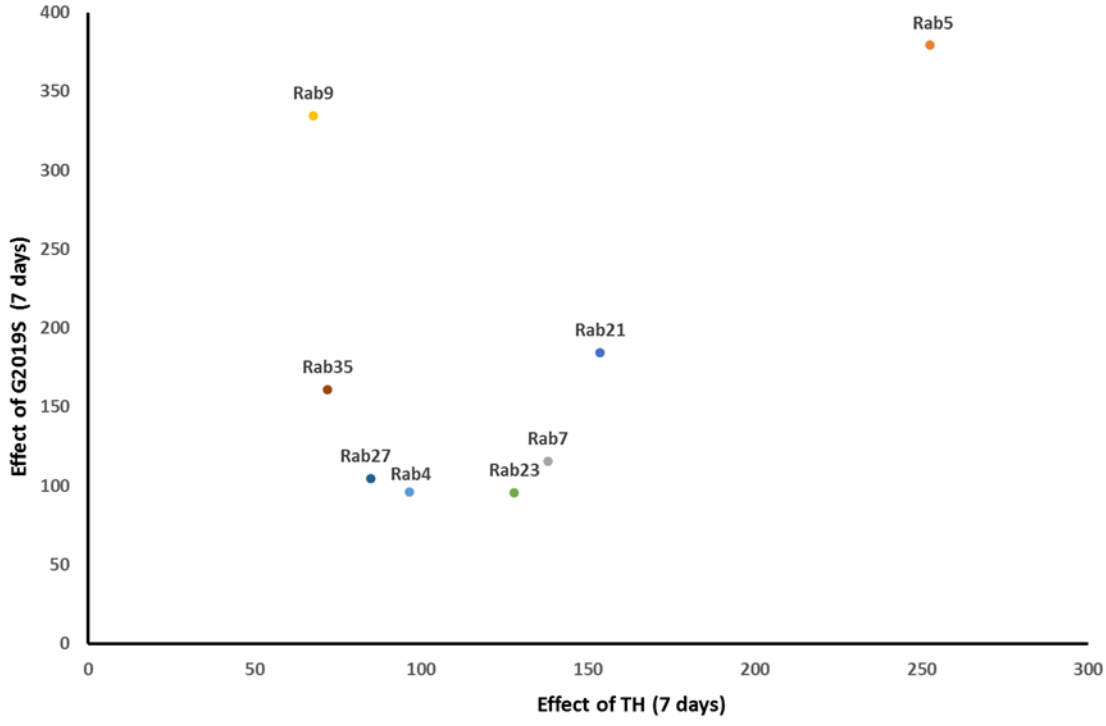
Effect of G2019S (7 days)
Effect of TH (7 days)
Rab5
Rab9
Rab21
Rab35
Rab7
Rab27
Rab4
Rab23
0
50
100
150
200
250
300
350
400

Figure 4.5 Rab5 and Rab9 interact with *hLRRK2.*

From the endosomal/lysosomal Rabs, *Rab5* has a much bigger response than any other Rab, or control flies. Additionally, it shows a strong interaction with *G2019S*. *Rab9* also indicates a strong interaction with the *G2019S*, as at 7-day-old flies the presence of the *G2019S* mutation increases the visual responses. The percentage (%) visual responses from the photoreceptors (A) and the lamina neurons (B) are shown, with the 100% being the baseline as represents the mean responses from the control flies *TH/w-.* (C) This graph confirms a strong interaction between *G2019S* and *Rab5* at 1 day, as its presence dramatically increases the visual response compared to the other Rabs. (D) This graph confirms a strong interaction between *G2019S* and *Rab9* at 7 days, as its presence dramatically increases the visual response compared to the other Rabs. Each fly line was tested at 1 day and 7 days, after being crossed to *TH-Gal4* or *TH-Gal4;G2019S.* (N=416). For all the different groups two-way ANOVA was performed, when * $P<0.05$, ** $P<0.01$ and when *** $P<0.001$.

4.3.1.2 Rabs involved in Golgi and the Endoplasmic reticulum

The available Rab fly stocks that were associated with the Golgi/Endoplasmic reticulum pathway include *Rab1, Rab2, Rab6, Rab8, Rab10, Rab18, Rab19, Rab30* and *Rab40*, were tested.

The visual responses from the photoreceptors and the lamina neurons are shown in Figure 4.6 (A and B, respectively).

From the genetic screening, the most marked interactions are between *LRRK2-G2019S* and *Rab10* and *Rab18*. In both cases, the visual responses are massively increased compared to the absence of the *G2019S* transgene and compared to the control levels as well, on both 1 day and 7 days.

For Rab10, there is a 70% increase in the photoreceptor responses at 1 day in the *TH::G2019S>Rab10* compared to *TH>Rab10* (P=0.03), establishing a strong interaction. Moreover, at 7 days, there is a 170% increase in the responses from the photoreceptors in the *TH::G2019S>Rab10* background (P=0.01) (Figure 4.6; A). This interaction is also confirmed from the responses from the lamina neurons, as there is a 40% and 70% increase in the lamina neuron responses at 1 day and 7 days respectively (P=0.05, P=0.021) (Figure 5.6; B).

The second Golgi/Endoplasmic reticulum *Rab* that shows a strong interaction with *G2019S* is Rab18. For *Rab18* there is an 80% increase in the photoreceptor responses in the *TH::G2019S>Rab18* compared to *TH>Rab18* at 1 day (P=0.018) while there is a 100% increase at 7 days (P=0.03). In addition, there is a 40% increase in the responses from the lamina neurons at 7 days (P=0.01). That increase in the photoreceptor and lamina neuron responses establishes a strong interaction to *LRRK2-G2019S* according to our criteria, even though there was no increase in the lamina neurons at day 1.

While *Rab10* and *Rab18* gave the most consistent interaction over the timepoints tested, one more *Rab, Rab40*, indicate an interaction to the *G2019S* at some timepoints. At 1 day, photoreceptor responses in the *TH::G2019S>Rab40* compared to *TH>Rab40* increased by 150% (P=0.05), while the responses are in general increased, independently of the presence of the mutation. In addition, the responses from the lamina neurons show a 30% increase at 1 day (P=0.05), confirming the interaction.

Rab1 and *Rab19* on the other hand, do not show an interaction to the *G2019S* mutation but to the dopaminergic expression, as their expression increased the photoreceptor responses compared to the control *TH/w-* and *TH;G2019S/w-* averages. For Rab1 the photoreceptor responses increase by 200% compared to the baseline of the control *TH/w-* flies, irrespectively of the presence of the *G2019S* mutation (P=0.02). For Rab19 there was a 180% increase in the photoreceptor responses compared to the baseline of the control *TH/w-* flies, irrespectively of the presence of the *G2019S* mutation (P=0.04).

The rest of the tested Rabs show responses similar to the control levels irrespectively of the presence of the presence of the *G2019S* mutation.

Using a similar cluster analysis, the percentage change in visual responses due to expression of Golgi-Endoplasmic reticulum Rabs was plotted against the combined effect (expression of Rab and *G2019S*) (Figure 4.6, C-1 day and D- 7 days). Most of the Rabs cluster while Rab10 and Rab18 are clear outliers at 7 days.

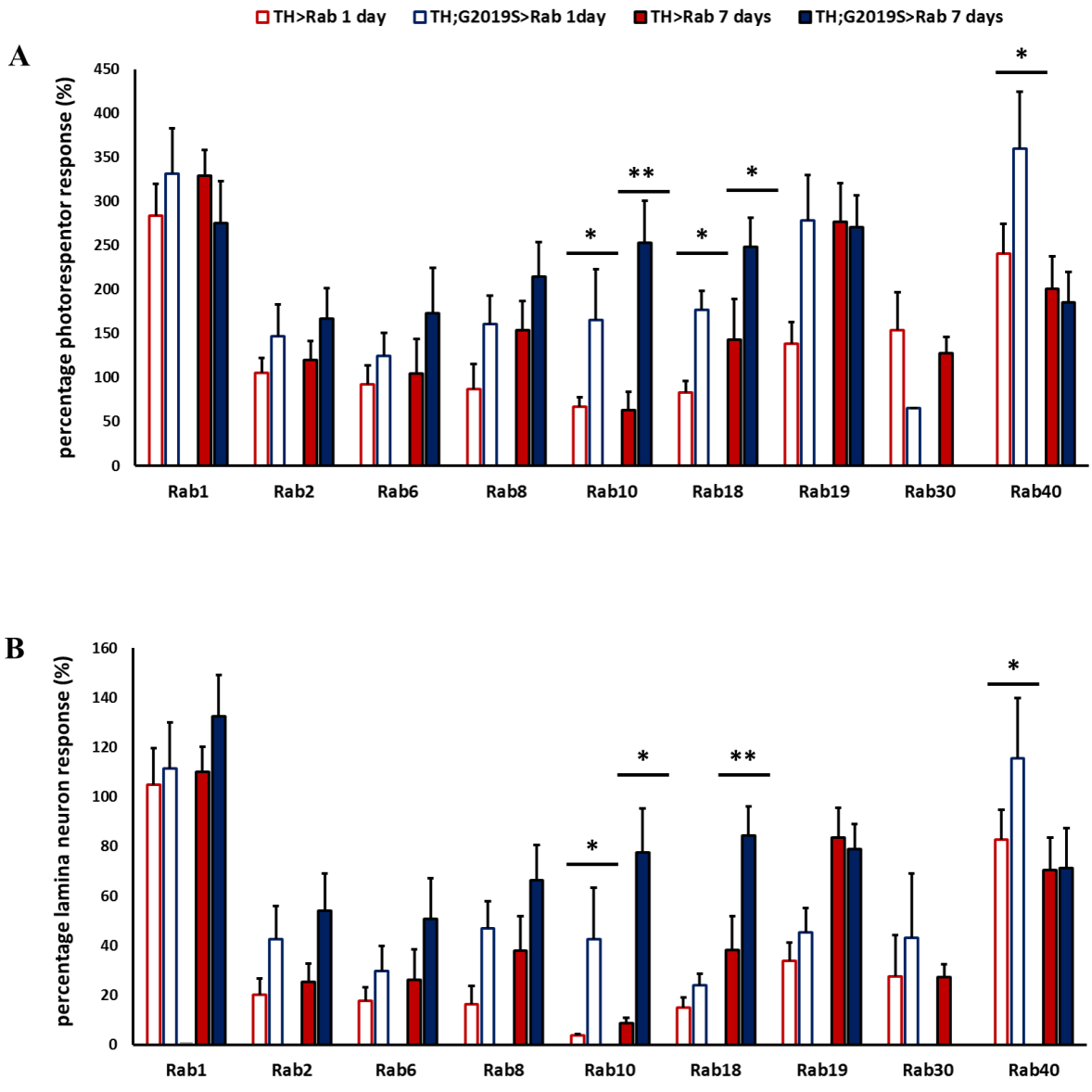

C

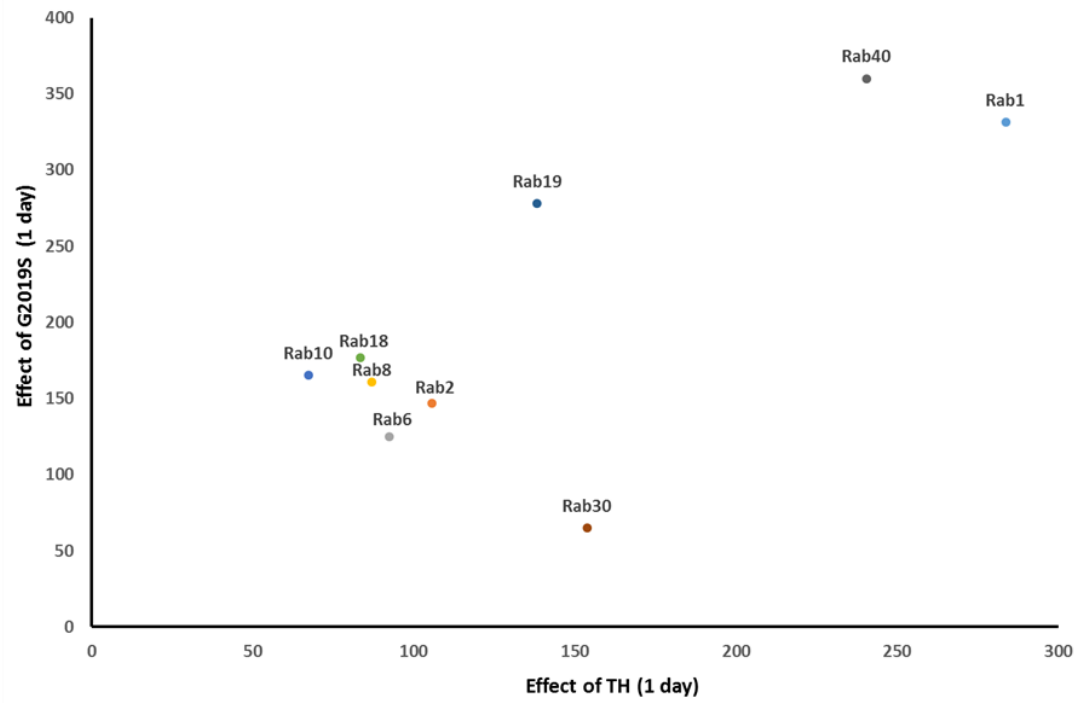
Effect of G2019S (1 day)
Effect of TH (1 day)
Rab40
Rab1
Rab19
Rab10
Rab18
Rab8
Rab2
Rab6
Rab30
0
50
100
150
200
250
300
350
400

D

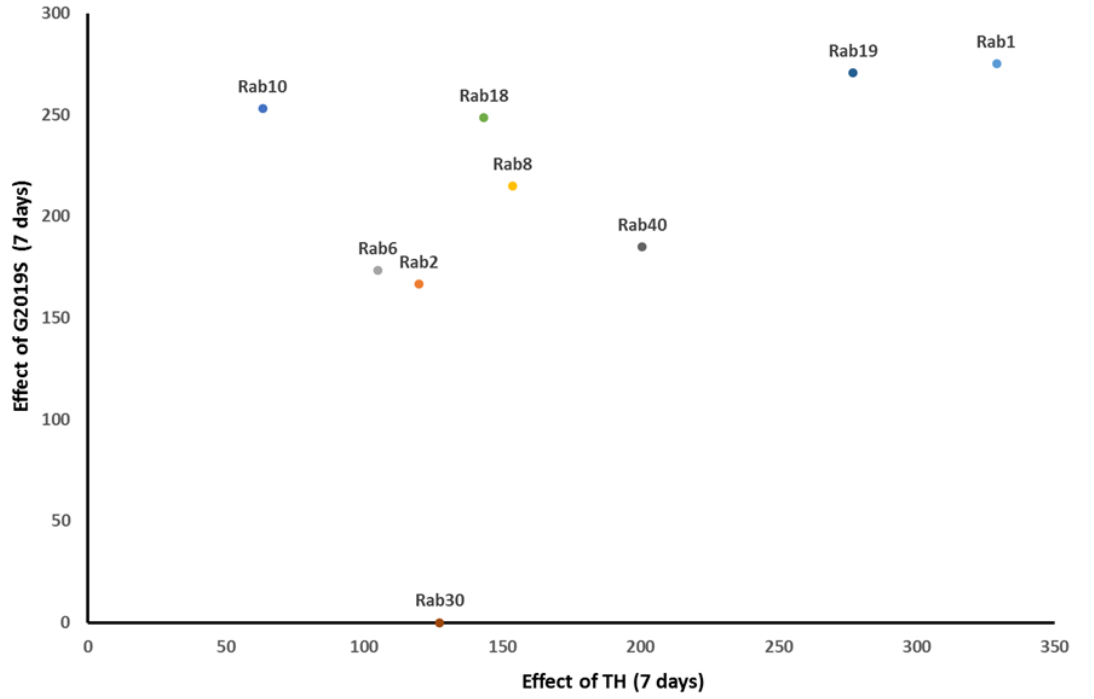
Effect of G2019S (7 days)
Effect of TH (7 days)
Rab19
Rab1
Rab10
Rab18
Rab8
Rab40
Rab6
Rab2
Rab30
0
50
100
150
200
250
300
350

Figure 4.6 Rab1, Rab10, Rab18, Rab19 and Rab40 interact with *hLRRK2*. From the ER-Golgi Rabs, Rab1, Rab10, Rab18, Rab19 and Rab40 have much bigger responses than any other Rab, or control flies. Additionally they show a strong interaction with *G2019S*. The percentage (%) visual responses from the photoreceptors (A) and the lamina neurons (B) are shown, with the 100% being the baseline as represents the mean responses from the control flies *TH/w-.* (C) This graph confirms the strong interaction between *G2019S-Rab1*, *G2019S-Rab19* and *G2019S-Rab40*, at day 1, as its presence dramatically increases the visual response compared to the other Rabs. (D) This graph confirms a strong interaction between *G2019S-Rab10* and G2019S-*Rab18* at 7 days, as its presence dramatically increases the visual response compared to the other Rabs. Each fly line was tested at 1 day and 7 days, after being crossed to *TH-Gal4* or *TH::G2019S-Gal4*. N=465.

4.3.1.3 Rabs involved in vesicle recycling

The available Rab fly stocks that were associated with the secretory pathway including *Rab3*, *Rab8*, *Rab27* and *Rab35*, were tested. All the *UAS-Rabs* were expressed in the dopaminergic neurons using the *TH-Gal4* driver and the visual responses were obtained using the SSVEP assay giving responses from the photoreceptors and the lamina neurons were obtained as shown in Figure 4.7 (A and B, respectively).

From the genetic screening, it was established that in this group there is an interaction between *LRRK2-G2019S* and *Rab3,* as the presence of the *G2019S* mutation has a big effect in the fly vision. The visual responses are massively increased compared to the absence of the mutation and compared to the control levels as well. At 7 days there is a 300% increase in the photoreceptor responses in the *TH::G2019S>Rab3* compared to *TH>Rab3* (P=0.027), and a 150% increase in the lamina neuron responses (P=0.05) establishing a strong interaction (Figure 4.7; A). Moreover, compared to the baseline, which

represents the mean responses from the *TH/w-* control flies, there was a 400% increase in the photoreceptor responses.

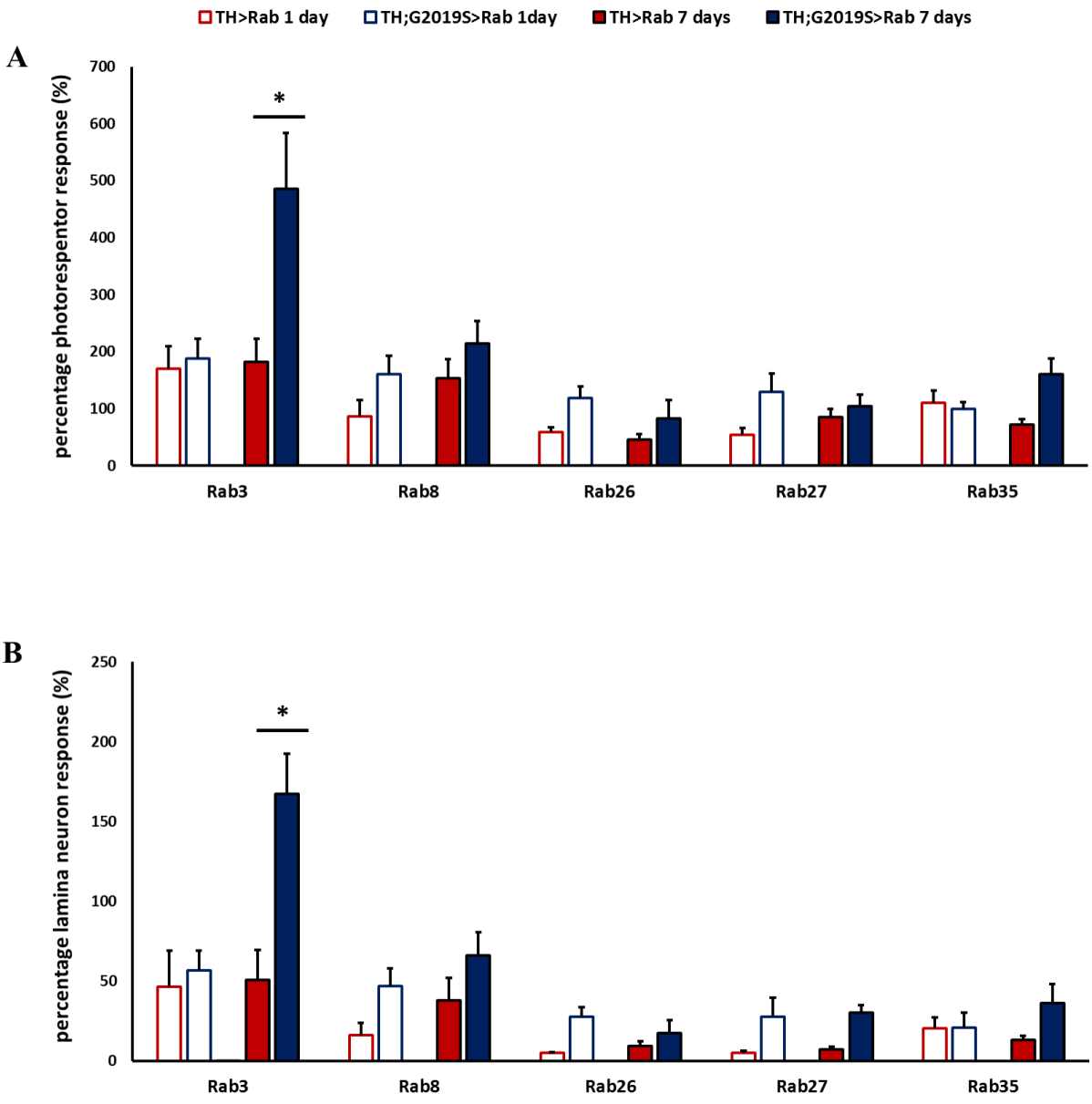

Figure 5.7 *Rab3* interacts with *hLRRK2*.

From the vesicle recycling Rabs, *Rab3* seems to have an effect on fly vision in the presence of the *G2019S* mutation, indicating an interaction. The percentage (%) visual responses from the photoreceptors (A) and the lamina neurons (B) are shown, with the 100% being the baseline as represents the mean responses from the control flies *TH/w-.* Each fly line was tested at 1 day and 7 days, after being crossed to *TH-Gal4* or *TH::G2019S-Gal4.* N=253.

4.3.1.4 Rabs involved in mitochondria

The available Rab fly stocks that were associated with the mitochondria, including *Rab27* and *Rab32*, were tested. All the *UAS-Rabs* were expressed in the dopaminergic neurons using the *TH-Gal4* driver and the visual responses were obtained using the SSVEP assay as described in section 2.2.2.

The two different *UAS-Rabs* were recorded in both the presence and the absence of the *G2019S* mutation. From the SSVEP recording, the visual responses from the photoreceptors and the lamina neurons were obtained as shown in Figure 4.8 (A and B, respectively).

From the genetic screening, it was established that there is no interaction between *LRRK2-G2019S* and any of these two *Rabs,* as the presence of the *G2019S* transgene did not have any effect in the fly vision. Moreover, compared to the baseline, which represents the mean responses from the *TH/w-* control flies, there was not much of increase in the photoreceptor or the lamina neurons responses (Figure 4.8; A and B).

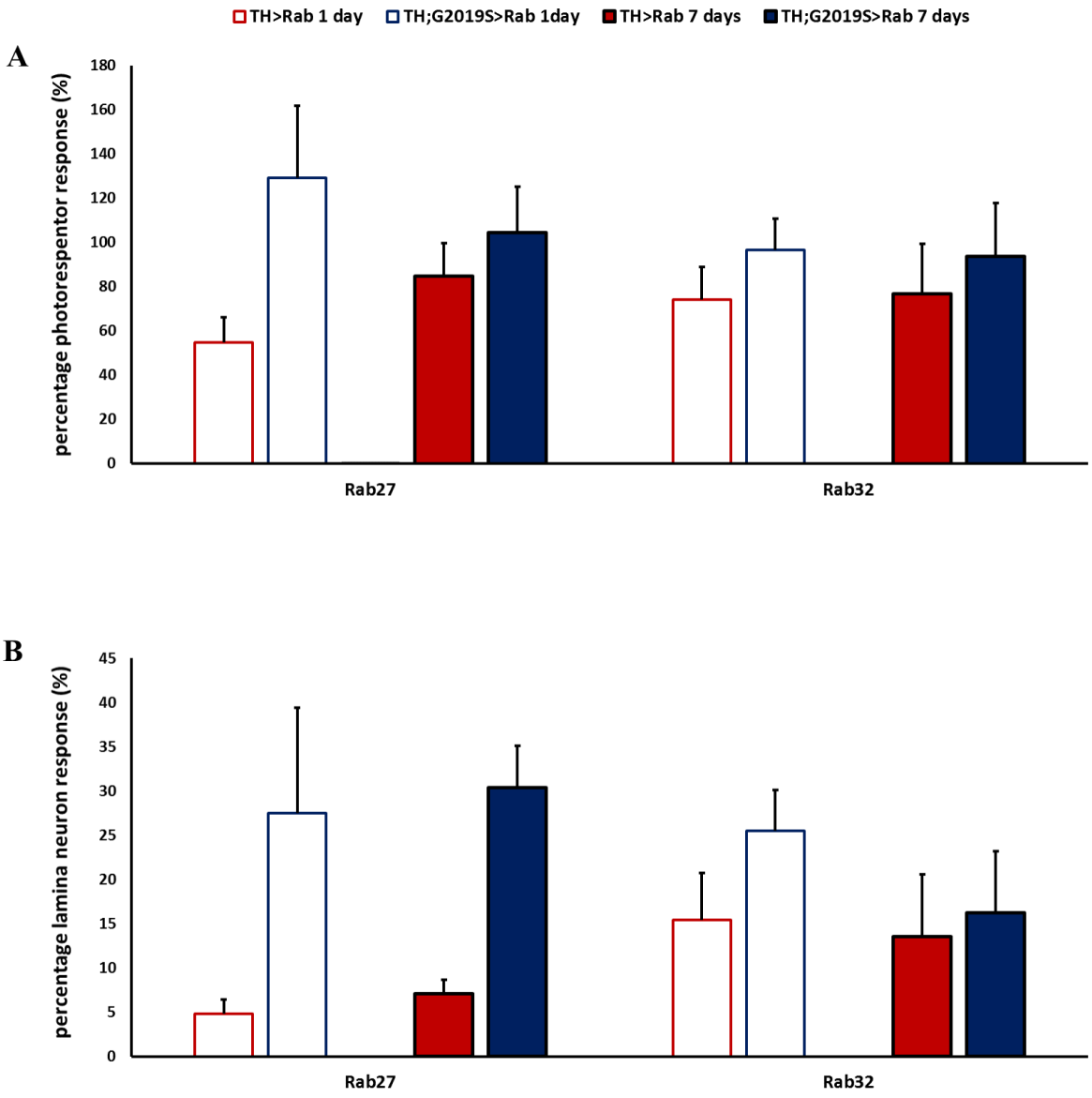

Figure 4.8 None of the *Rabs* involved in the mitochondria indicate a possible interaction to *LRRK2*. Two Rabs involved in the mitochondria were tested, Rab27 and Rab32. The percentage (%) visual responses from the photoreceptors (A) and the lamina neurons (B) are shown, with the 100% being the baseline as represents the mean responses from the control flies *TH/w-.* Each fly line was tested at 1 day and 7 days, after being crossed to *TH-Gal4* or *TH::G2019S-Gal4.* N=194 (N>10 per genotype and age).

Table 4.4 summarizes the identified Rab proteins that regulate the phenotype of LRRK2 mutants based on the set criteria. In addition, two Rabs show no genetic interaction with LRRK2 but a strong association with the dopaminergic neurons.

Table 4.4 Summary of Rab effects on the visual system

Rab	Pathway	Effect of dopaminergic Rab expression at				Interaction with *G2019S* at			
		ph – day 1	Ln – day 1	ph – day 7	Ln – day 7	ph – day 1	Ln – day 1	ph – day 7	Ln – day 7
1	ER-Golgi	x	x	x	x				
3	Synaptic vesicles							X	X
5	Endo-lysosomal					X	X	X	X
9	Endo-lysosomal							X	X
10	ER-Golgi					X	X	X	X
18	ER-Golgi					X	X	X	X
19	ER-Golgi	x	x	x	x				
40	ER-Golgi	x	x	x	x	x	x		

ph: photoreceptors, Ln: Lamina neurons

Thus, in summary, even though the *Rabs* identified as *LRRK2* interactors belong to all of the subcellular pathways, five out of eight (62.5%) are associated with the ER-Golgi trafficking pathway, suggesting a stronger interaction with LRRK2.

4.4 Does the kinase domain cause these increased visual responses?

The screen of *Rab* lines shows that dopaminergic expression of some lines had a big impact on the fly visual system. In particular, *Rab3*, *Rab5*, *Rab9*, *Rab10*, *Rab18* and *Rab40* showed a strong positive interaction with *LRRK2-G2019S*, based on the criteria set on this study. As noted in section 1.3, LRRK2 is a multidomain protein with both kinase and GTPase functions. In order to test the initial hypothesis that it really is the kinase domain of the LRRK2 protein that interacts with several Rab proteins, it was decided to express a *LRRK2* transgene containing a substitution in the GTPase domain of the protein: *R1441C* (Figure 1.1). As both TH-Gal4 and the UAS-R1441C are on the 3rd chromosome, they were recombined. This permitted co-expression in the dopaminergic neurons and subsequent visual assays. If it really is the kinase domain that plays a vital role in the interaction between *LRRK2* and *Rabs* then the expected visual responses would be similar to the levels obtained from expressing just a Rab in the dopaminergic neurons.

From the eight identified *Rabs* interacting with *LRRK2-G2019S* or the dopaminergic neurons in this genetic screening, three were chosen in order to test this hypothesis. *Rab1* was chosen because of the increased visual responses independently of the presence of the *G2019S* mutation, while *Rab10* and *Rab18* were chosen because of the big effect that *G2019S* had in the responses compared to the ones that it was absent from. Flies expressing *TH::R1441C* with and without *Rab1* or *Rab5* or *Rab18* were tested and the mean photoreceptor and lamina neuron responses are shown in Figure 4.9.

As presented in Figure 4.9 for all of the three different *Rabs*, the expression of the *R1441C* mutation decreases the visual responses to wild type levels, when the Rabs are expressing in the dopaminergic neurons without the presence of any other factor. Taken together, the increased visual responses obtained from the expression of the *G2019S* mutation and the reduced responses in the *R1441C* background establishes that it really is the kinase domain playing a vital role in

the *LRRK2-G2019S-Rabs* interaction. That applies both for the photoreceptor and the lamina neuron responses.

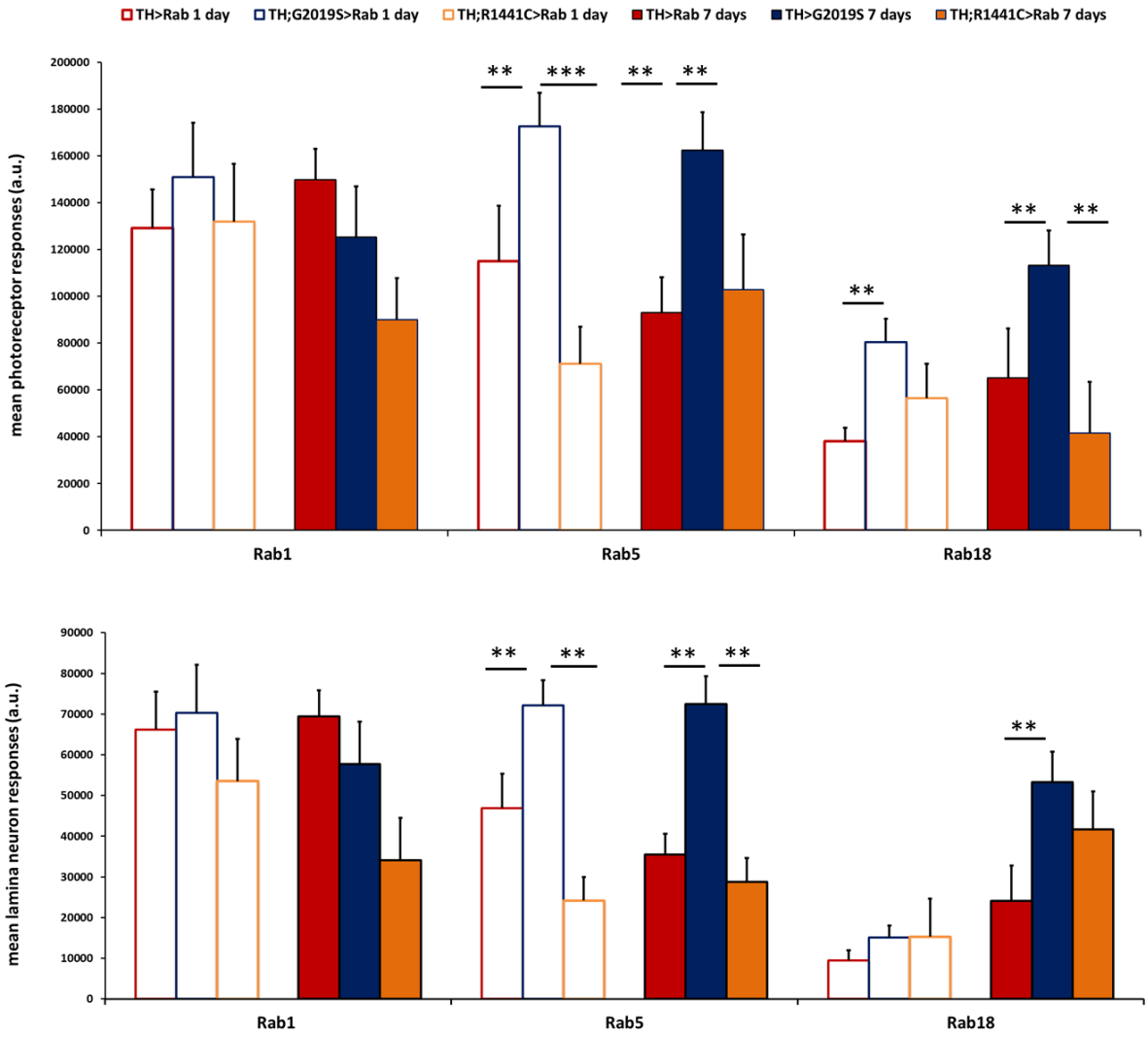

Figure 4.9 Co-expression of the *R1441C* mutation with *Rabs* reduces the visual responses to wild type levels. The mean responses ±SE from the photoreceptors (A) and the lamina neurons (B) are shown. Three *Rabs* were tested in this set of experiments, *Rab1* (N=71), *Rab5* (N=70) and *Rab18* (N=65). The presence of the *R1441C* mutation decreases the visual responses down to wild type levels, when only the Rabs are expressed in the dopaminergic neurons. That's an indication that it really is the kinase domain that plays a vital role in the *LRRK2-Rabs* interaction. Each fly line was tested at 1 day and 7 days, after being crossed to *TH-Gal4* or *TH::G2019S-Gal4.* N=206.

For all the different Rabs that were expressed, two-way ANOVA was performed followed a Bonferroni post-hoc test, and from that analysis it was determined than none of the tested *TH>Rab* were statistically significant to the *TH;R1441C>Rab*. That is an indication that the expression of the *R1441C* mutation in the dopaminergic neurons does not have an effect on the fly vision. On the other hand, the expression of the *G2019S* mutation does affect the visual responses, as in the *Rab18* background at 1 day old and 7 day old flies its expression leads to increased visual responses (P=0.014, P=0.013, respectively). In the *Rab5* background, the expression of the *R1441C* mutation has a similar effect, as there in no statistically significant difference to the *TH>Rab5* flies (P=0.3 at 1 day and P=0.9 at 7 days), while there is a significant difference in the *G2019S* background (P=0.001 at 1 day and P=0.03). On the other hand, there is statistically significant difference between the *TH>Rab5* and *TH;G2019S>Rab5* (P=0.032). The same pattern is followed in the responses from the lamina neurons as well, confirming the hypothesis that the interaction between *LRRK2* and different *Rabs* depends on the kinase domain of the gene.

4.5 Does LRRK2 prefer Threonine to Serine?

The first hypothesis that was addressed in this study was whether or not all of the identified *Rabs* interacting with *LRRK2-G2019S* were part of the same subcellular pathway or not. Apart from that, *in vitro* it is suggested that LRRK2 protein shows a preference of phosphorylating Thr over Ser in the Rab sequence,at the position corresponding to T73 in Rab10 (Steger et al., 2016). This hypothesis can now be tested *in vivo*. Table 4.5 summarizes the identified *Rabs* linked to *LRRK2-G2019S* according to that criteria.

Table 4.5 *In vivo* analysis of LRRK2 phosphorylation preference

T73-Rab10 residue	Rabs showing an interaction	Rabs not showing an interaction
Serine	Rab5 Rab9	Rab2 Rab4 Rab6 Rab7 Rab21 Rab23 Rab26 Rab27
Threonine	Rab3 Rab10 Rab18 Rab40	Rab1 Rab19 Rab30 Rab35

Taken together these results, there is an indication that LRRK2 protein indeed prefers Thr over Ser, as four out the six identified Rabs contain a Thr residue at this position. That means that 67% of the identified *Rabs* interacting with the *G2019S* have a Thr in this vital residue for the function of Rab proteins, confirming the hypothesis that LRRK2 protein has a preference for Thr residues. On the other hand, most of the Rabs that were not identified as LRRK2 interactors have a Ser at this conserved residue, indicating that Thr plays a vital role in the *LRRK2-Rab* interaction.

4.6 Are eye deformities induced by the *G2019S/Rab5* combination?

The co-expression of the *G2019S* and *Rab5* in the dopaminergic neurons leads to increased visual responses, indicating an interaction between the two proteins. The mechanism under which the two proteins could interact was not clear and for

that reason eye screening was performed in order to test if the presence of the *G2019S* mutation could lead to any eye phenotype.

4.6.1 External Morphology: Eye screening

For eye screening 1 day and 7 day old flies co-expressing *hLRRK2* or *G2019S* in the *Rab5* background in the fly eye using the *GMR-Gal4* driver were examined. The *GMR-Gal4* driver was chosen as it is regularly used in screens for eye deformities (Freeman, 1996). For each genotype 100 flies were tested (Figure 4.10).

Co-expression of *LRRK2* or *LRRK2-G2019S* in the *Rab5* background did not induce any eye phenotype, as in both cases the external surface of the eye was similar to control *LRRK2* and *G2019S* flies.

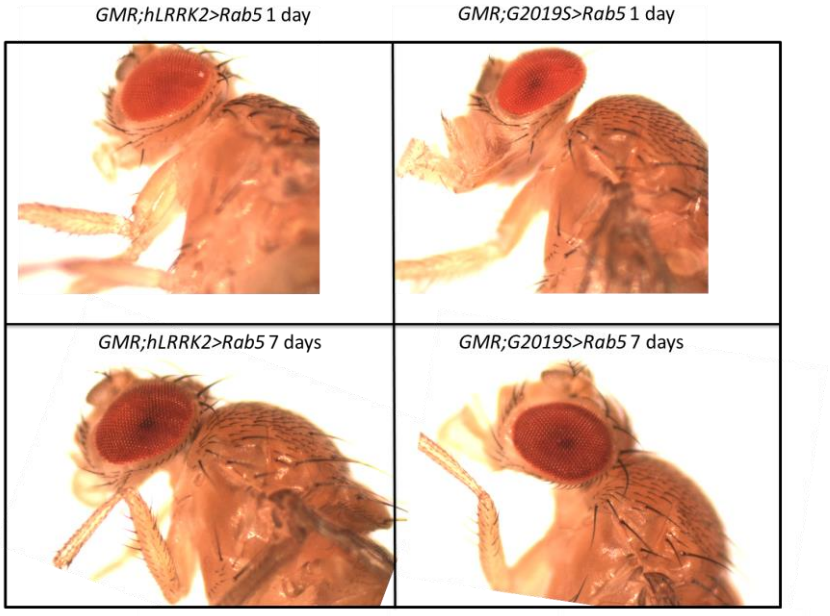

Figure 4.10 The presence of the *G2019S* does not induce an eye phenotype. Expression of *hLRRK2* and *G2019S* in the fly eye, under the control of the eye specific driver *GMR-Gal4*, does not induce any district phenotype, as the wild type *hLRRK2* and the *G2019S* flies present normal eye phenotypes (n=100 per genotype). Flies at 1 and 7 days old were tested after incubation in the dark at 29 ^{0}C.

4.6.2 Internal morphology: Staining of *Drosophila* retinas

Since the visual responses increased in the *G2019S/Rab5* background, but the external morphology was not affected, the next step was to examine the internal anatomy of the eye, using endosomal markers. 1 day and 7 day old flies were tested after incubation in the dark at 29 ^{o}C, and dissection of the *Drosophila* retinas followed (section 2.5.1).

From that analysis it can be determined that there is no difference between the *TH>G2019S* and *TH>hLRRK2* flies, indicating that the enlarged endosomes seen are not dependent on the genotype but probably on the genetic background of the flies that have an extra *mini-white* gene. That theory is also supported from the fact that the *TH/w-* flies do not show these enlarged endosomes.

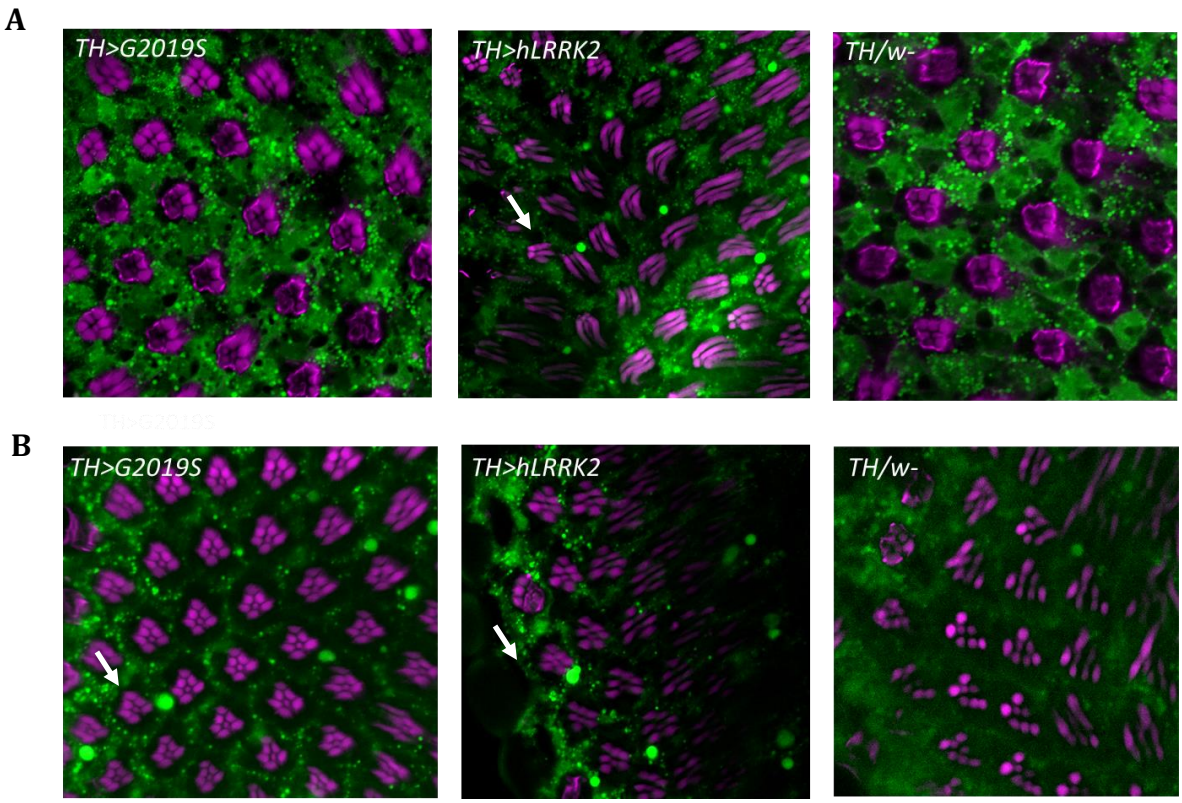

Figure 4.11 Enlarged endosomes present in the *hLRRK2* and *G2019S* retinas. Confocal images show enlarged endosomes (as pointed by the white arrows) for the *hLRRK2* and *G2019S* flies in contrast to the *w-* background flies. The fly retinas were stained with an anti-Rab5 antibody (green) as an early endosome marker and an anti-actin antibody (magenta) that stains the photoreceptors. The data shown 1 day old (A) and 7 day old (B) retinas after incubation at 29ºC in the dark. N=60 (10 retinas per genotype).

4.7 *Rab7* and its interaction with *LRRK2*

Based on the findings from MacLeod et al. (2013) and Beilina et al. (2014), proposing that LRRK2 protein interacts with Rab7L1, the fly homolog *Lightoid* (*ltd*) (Hermann et al., 2005) and as *Rab7L1* is risk factor for PD , independently of any other factor, triggered the interest for further investigation. Furthermore, *ltd* is a known *Rab32* homolog (Ma et al., 2004). Dodson et al (2012; 2014) on the other hand, proposed that *LRRK2* interacted with *Rab7*, rather than *Rab32/ltd*. Even though neither *Rab7* nor *Rab32* were identified interactors from my overexpression genetic screen, it was decided to test the effect of RNAi mediated knockdown of these genes. The RNAi lines aimed to silence *Rab7* or *ltd* in order to test if these proteins contribute to the visual responses. If *Rab7* and *ltd* really interact with the *G2019S* mutation, the expression of the RNAi lines would bring the visual responses down to control levels, as this interaction wouldn't be functional anymore.

As described previously, flies were tested at 1 day and 7 days both in the presence and the absence of the *G2019S* mutation. *UAS-Rab7*, *UAS-Rab7*^{RNAi}, *UAS-ltd* and *UAS-ltd*^{RNAi} were expressed in the dopaminergic neurons under the control of the *TH-Gal4* driver and the *TH::G2019S-Gal4* recombinant. The visual responses that were obtained both from the photoreceptors and the lamina neurons are presented in Figure 4.12.

Expression of the RNAi lines both in the *Rab7* and *ltd* background increased the photoreceptor and the lamina neuron responses, compared to the *TH>Rab7* and *TH>ltd* responses. Although, the presence of the *G2019S* mutation didn't have a big effect on the visual responses.

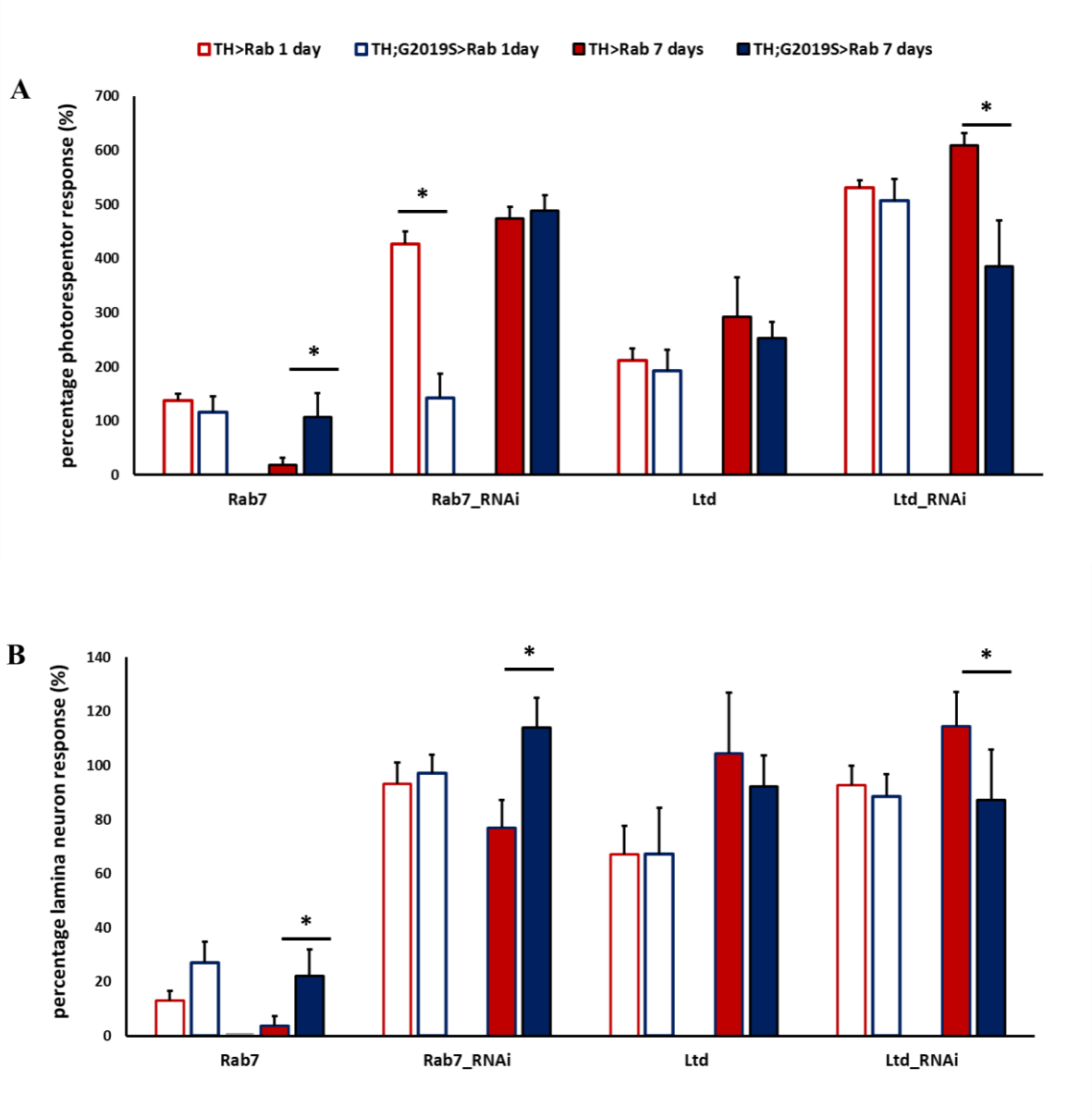

Figure 4.12 Expression of RNAi increased the visual responses.
The mean responses ±SE from the photoreceptors (A) and the lamina neurons (B) are being presented. Each fly line was tested at 1 day and 7 days, after being crossed to *TH-Gal4* or *TH::G2019S-Gal4*. Total number of flies tested N=286.

4.8 Discussion

In this course of investigation, where a genetic screening was performed in order to identify *LRRK2* substrates *in vivo*, Rab3, Rab5, Rab9, Rab10, Rab18 and Rab40 were identified as *LRRK2* interactors in the dopaminergic neurons. Whenever *G2019S* was added in the genetic background, the responses for theses Rabs increased both from the photoreceptors and the lamina neurons. *Rab1* and *Rab19* showed increased visual responses that were obtained independently of the presence of the *G2019S* mutation, compared to the control *TH/w-* flies.

Furthermore, the preference of *LRRK2* to threonine residues was confirmed, as six out of the eight identified Rabs interacting to *LRRK2-G2019S* had a Thr residue in their conserved T73-Rab10 equivalent site. In addition, five out of the eight identified Rabs are associated with the ER-Golgi trafficking pathway, shedding new light on the function of the LRRK2 protein.

In addition, expression of RNAi lines for *Rab7* and *ltd* showed increased visual responses both from the photoreceptors and the lamina neuros independently of the presence of the *G2019S* mutation, indicating that there is no interaction between LRRK2 and those two tested Rabs.

The insertion site for all the *UAS-Rab* stocks that were used in this study were not the same, as for most of them the landing site of the transgenes was random. That could cause questions on whether or not the eye colour of the different stocks could contribute differently in the obtained visual responses. Although, as it was described in Chapter 3, section 3.3.3.5, the eye colour is not a confounding factor, indicating that this increase in the visual responses is real and not because of the eye colour.

Figure 4.13 summarizes the expression pattern of the Rabs in the visual system of *Drosophila* as was described by Jin et al. (2012) and whether they have been linked to LRRK2 protein from previous studies or not. In addition, the findings from this course of investigation are summarised.

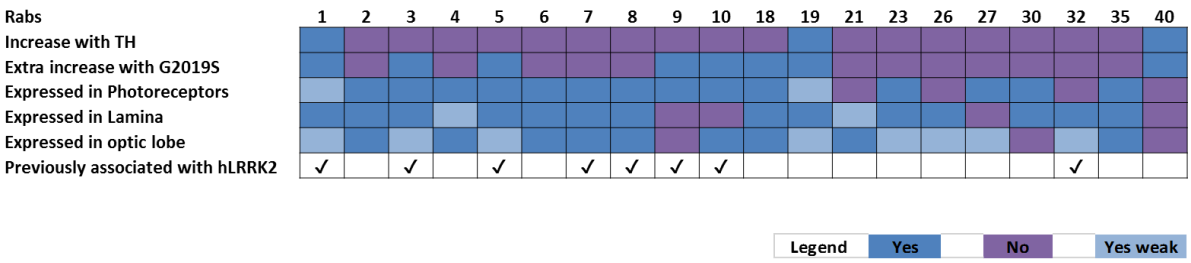

Figure 4.13 Expression pattern of Rabs in the *Drosophila* visual system related to the visual physiology shown by the SSVEP assay.

4.8.1 Rabs involved in the endo-lysosomal pathway

The findings from this course of investigation confirm the *LRRK2-G2019S-Rab5* and *LRRK2-G2019S-Rab9* interaction, as in the genetic screening that was performed Rab5 and Rab9 are two of the Rabs that support this interaction. In the presence of the *G2019S* the visual responses both from the photoreceptors and the lamina neurons are higher compared to ones in the absence of the mutation. In addition, as far as the X73 residue is concerned, both Rab5 and Rab9 contain a Ser in this catalytic region of the switch II domain, which is surprising taking into account LRRK2 preference on Thr residues.

This is the first time that *Rab5* and *Rab9* are confirmed as *LRRK2* interactors *in vivo*. This builds on similar data from previous studies on *in vitro* models, making more powerful the findings from this study.

Rab5 is by far the best-characterised endosomal Rab protein, which localises mainly to the sorting endosome (as shown in Figure 5.1), but it is also present on the plasma membrane and on endocytic vesicles. It has been proposed that the active form of Rab5 promotes endosome fusion by recruiting cytosolic components of the fusion apparatus (Woodman, 2000). Rab5, co-operating with LRRK2, contributes to the pathogenesis of PD by regulating the endocytosis of synaptic vesicles, proving for the first time that LRRK2 has a functional role in

the regulation of synaptic vesicles endocytosis. The reduced rate of endocytosis may cause defects in synaptic transmission in the long run, especially during intense neuronal activity, where the vesicle replenishment from the endosomal compartments is crucial for effective neurotransmitter secretion (Shin et al., 2008).

Heo et al. (2010) showed two years later that *LRRK2*, and more specifically *LRRK2-G2019S*, is a more critical factor than Rab5 in regulating neurite outgrowth even though they both functionally coordinate regulation of neurite outgrowth (Hen et al., 2010). Several studies proposed that increased kinase activity in mutant forms appears to induce decrease of neurite length and branching, formation of inclusion bodies, and/or neuronal toxicity (Gloeckner et al., 2006; Greggio et al., 2006; Smith et al., 2005; MacLeod et al., 2006; Smith et al., 2006; West et al., 2007). The active form of Rab5 negatively regulates neurite outgrowth (Liu et al., 2007). However, the conclusion that was made was that the regulation of the neurite outgrowth via LRRK2 and Rab5 is not effected independently, but through a shared mechanism (Heo et al., 2010).

On the other hand, *Rab9* is less well characterised. Using *Drosophila* as an animal model, and more specifically *dLRRK*, was proved that it co-localises with Rab7 in the late endosomes and lysosomes. *dLRRK* loss of function mutants display abnormalities in the endosomes and *dLRRK* can negatively regulate Rab-7 dependent perinuclear localisation of lysosome (Dodson et al., 2012). In contrast, a gain of function mutation within *dLRRK* that is equivalent to *G2019S* in *LRRK2*, promotes Rab7-dependent perinuclear positioning of lysosomes. Accumulation of autophagosomes and the presence of enlarged lysosomes and endosomes were also observed in *dLRRK* loss of function mutants (Dodson et al., 2014). This phenotype was rescued by the over-expression of *Rab9*, which promotes recycling of the endosomes to the TGN via the retromer, possibly due to a direct interaction (Dodson et al., 2014).

4.8.2 Rabs involved in Golgi and the Endoplasmic reticulum

The findings from this course of investigation establish an interaction between *LRRK2-G2019S* and *Rab10*, *Rab18* and *Rab40*. In the presence of the *G2019S* the visual responses both from the photoreceptors and the lamina neurons are higher compared to ones in the absence of the mutation. In addition, as far as the X73 (where X is Thr or Ser) residue is concerned, all the identified *Rabs* contain a Thr in this catalytic region of the switch II domain, confirming the preference of *LRRK2* to Thr. Furthermore, *Rab1* and *Rab19*, even though they do not show an interaction with *G2019S*, an association with the dopaminergic neurons is shown, as the visual responses were increased compared to the control levels independently of the *G2019S* presence.

This is the first time that these *Rabs* are confirmed as *LRRK2* interactors *in vivo*. Although, previous studies based on *in vitro* models, have identified *Rab10* as *LRRK2* interactor, emphasising the findings from this study.

Rab10 is a well characterised GTPase protein that regulates the intracellular vesicular transport. It is located in the TGN regulating its traffic to the synaptic vesicles. The T73 residue of Rab10 is located in the Switch II domain, which is characteristic of the Rab GTPase proteins. This domain changes conformation upon nucleotide binding and regulates the interaction with multiple regulatory proteins (Pfeffer, 2005). Steger et al (2016) showed that the interaction between *LRRK2* and *Rab10* is direct, as both the wild type and the *G2019S*, but neither kinase inactive *D1994A* mutant nor small molecule-inhibited *LRRK2*, effectively phosphorylated Rab10 (Steger et al., 2016). In this study was also confirmed the preference of LRRK2 for Thr compared to Ser residues (Nichols et al., 2009), as all the Rabs family members containing Thr sites in the switch II region (Rab1b, Rab8a and Rab10) were effectively phosphorylated compared to the Rabs containing a Ser in the equivalent position (Rab5b, Rab7a, Rab7L1, Rab12 and Rab39b), which were phosphorylated to a drastically lower extent.

Rab18 has been linked to lipid droplet formation (Martin et al., 2005; Ozeki et al., 2005), ER–Golgi trafficking (Dejgaard et al., 2008), and the regulation of secretory granules (Vazquez-Martinez et al., 2007) and peroxisomes (Gronemeyer et al., 2013), and may be exploited during hepatitis C infection (Salloum et al., 2013). However, no clear molecular function or site of action has been defined for Rab18 (Gerondopoulos et al., 2014). Not many effectors of Rab18 have been identified, the only human disease that it has been associated to is Warburg Micro syndrome, a developmental disorder with brain abnormalities (Bem et al. 2011). However, an affinity chromatography screen reported that *dLRRK*, the *Drosophila* ortholog of human *LRRK2*, is a GTP-specific interactor to Rab18 (Gillingham et al., 2014). This is the only previous link between *Rab18* and PD.

Rab1 is located at the endoplasmic reticulum (ER) exit sites and the pre-Golgi intermediate compartment (IC) mediating ER–Golgi trafficking (Stenmark 2009). Rab1 has been linked to PD by interacting with α-synuclein, rescuing the toxicity induced by aberrant α-synuclein. α-synuclein accumulation could lead to the collapse of the ER-Golgi trafficking during the process of tethering or docking (Shi et al., 2017). Winslow et al. (2010) determined that overexpression of α-synuclein impairs macro-autophagy, with the proposed interaction between Rab1 and *SNCA* being in the early steps in autophagy during the synthesis of auto-phagosomes. Even though no interaction has been identified between *LRRK2* and *Rab1*, impairment of *Rab1* contributes to the pathogenesis of PD through the *SNCA* gene, which has been identified contributing to sporadic PD. However, Steger et al. (2016) based on a phospho-proteomics analysis, proved that LRRK2 protein phosphorylates Rab1a, but it is not determined if this interaction is direct or indirect. This could shed new light in our understanding of the molecular pathways causing the neuron cells to die in PD.

4.8.3 Rabs involved in vesicle recycling

The findings from this course of investigation determined the interaction between *LRRK2-G2019S* and *Rab3*. In the presence of the *G2019S* the visual responses both from the photoreceptors and the lamina neurons are higher compared to ones in the absence of the mutation. Moreover, the preference of LRRK2 protein in Thr was confirmed, as Rab3 contains a Thr at the T73-Rab10 equivalent site (T86).

This is the first time that *Rab3* is confirmed as interacting with *LRRK2 in vivo*. However, previous *in vitro* work has identified *Rab3* as a *LRRK2* interactor, increasing the interest of this study.

Rab3 localises in the synaptic vesicles regulating the traffic to the plasma membrane playing an important role in exocytosis and neurotransmitter release. Rab3 has been confirmed interacting with both *SNCA* and *LRRK2* contributing to PD (Chen et al., 2013; Steger et al., 2016). Rab3 co-localizes with α-synuclein and regulates its distribution. On the other hand, it has been determined that *Rab3* is a substrate of LRRK2-mediated phosphorylation (Steger et al., 2016). Overexpression of Rab3a protein induces α-synuclein cytotoxicity in cellular and animal models of PD (Cooper et al., 2006; Gitler et al., 2008).

4.8.4 Rabs involved in mitochondria

From this course of investigation, none of the tested Rabs (*Rab27* and *Rab32*) were confirmed as *LRRK2* interactors.

However, *Rab32* has been identified as a *LRRK2* interactor from *in vitro* studies. It is a well characterised Rab that is located in the mitochondria (Bui et al., 2010) and the melanosomes (Wasmeier et al., 2006; Park et al., 2007) mediating the fission of mitochondria and the trafficking from TGN to the melanosomes playing a key role in melanogenesis. Waschbusch et al. (2014) confirmed that Rab32 binds to the amino-terminal region of LRRK2. Moreover, they found co-

localisation of LRRK2 and Rab32 wild type at transport vesicles and recycling endosomes, suggesting a role of Rab32 in the late endosomal trafficking of LRRK2. Besides that, the exact role of Rab32 in PD pathogenesis is still unclear. However, it is a promising target for further functional analyses. In flies, Rab32 is mainly localised in the pigment cells surrounding the photoreceptors, so may be too far away from the dopaminergic neurons to influence the SSVEP assay. Possibly, utilising another pigment cell *Gal4* line would show an interaction between Rab32 and LRRK2.

4.8.5 Examination of the *Drosophila* compound eye

During this study, examination of the external and internal of the *Drosophila* compound eye was performed. External examination of the fly eye in the Rab5 background did not induce any district phenotype. On the other hand, staining of *Drosophila* retinas with endosomal markers established enlarged endosomes both in the *LRRK2* and *G2019S* background. In *w-* control flies these enlarged endosomes were not present independently of the age that the retinas were examined. That indicates an interaction between *LRRK2* and *Rab5* in the endo-lysosomal trafficking pathway, paving the way for a more clear understanding on the molecular pathway that these two proteins interact contributing to the pathogenesis of PD.

Previous studies have tried to address the role of *LRRK2* in the compound *Drosophila* eye. Chuang et al. (2014) established that *LRRK2* could rescue neuronal apoptosis that was induced by expression of death genes, *grim, hid* and *reaper* in the fly visual system. On the other hand, expression of the PD-linked mutations R1441C and G2019S did not suppress the grim-induced apoptosis, resulting in reduced eye size phenotype. These findings highlight a pro-survival role of *LRRK2* that is mediated through activation of the Akt signalling pathway. A role that is compromised in the presence of the *R1441C* or the *G2019S* mutations (Chuang et al., 2014).

Hindle et al. (2013) established a decline in vision after 28 days in the *TH>G2019S* background. Their follow up on that discovery was whether this

loss of vision is accompanied by anatomical phenotypes and neurodegeneration or not. *TH>G2019S* flies at the age of 28 days in contrast to *TH>LRRK2* and *TH/w-* flies, showed strong neurodegeneration in the internal structure of the retina, which was disorganised while the visual lobes (lamina and medulla) had frequent vacuoles. Furthermore, *TH>G2019S* flies showed increased autophagy and apoptosis in the photoreceptors in 21 day old flies. In addition, the mitochondria in the photoreceptors became swollen and broken. Even though there was an established neurodegeneration in the internal structure of the *TH>G2019S* flies, the exterior surface was normal. This discovery coincides with the findings observed in this study, as there was no district eye phenotype in the *TH::G2019S>Rab5* flies, while enlarged endosomes were shown in the *Drosophila* retina.

Venderova et al. (2009) also examined the role of *LRRK2* in contributing to eye defects. Their first examination after incubation of the flies at RT did not induce any eye phenotype independently of genotype. The next step was to examine flies at 29^{O}C, as it is known that *GMR* can induce defects at 29^{o}C. Examination of *LRRK2* and *LRRK2* mutants under the optic microscope showed significantly more black lesions compared to controls. They next analysed the eyes using scanning electron microscopy (SEM), which only confirmed that *LRRK2* and *LRRK2* mutants caused large defects, including glossy, rough and sometimes collapsing surface of the eye, disorganised interommatidial bristles and irregular lens shape. Finally, examination of the ommatidial structure on sections showed that the regular trapezoidal arrangement of the photoreceptor cells was disrupted, accompanied by the presence of large holes that altered the architecture of the ommatidial array (Venderona et al., 2009). The presence of large holes is characteristic in many fly models of neurodegenerative diseases (Marsh et al., 2000).

4.9 Conclusion

Taken together, this chapter provides new insights into *LRRK2* function, which is still very unclear even though it is under thorough investigating for the last few years. Six new interactors of *LRRK2* have been identified in this *in vivo* analysis, indicating a role in dopaminergic neurons. These are *Rab3*, *Rab5*, *Rab9*, *Rab10*, *Rab18* and *Rab40*. In addition, two Rabs, Rab1 and Rab19, were identified interacting with the dopaminergic neurons. From these, *Rab18* has not been reported previously.

The increase in the visual responses in the *G2019S* background, might indicate failure of the photoreceptors to adapt in light, with dopamine playing a very important role, as it has been proposed that in the *G2019S* flies the levels of dopamine are reduced compared to the wild type (Harnois et al., 1990). That is based on the fact that dopamine is a very important neurotransmitter playing a significant role in the light adaptation. The question that now remains, is how the interaction of *hLRRK2* and *Rabs*, might affect this role of dopamine on the light adaptation.

Chapter 5

Generation of novel *LRRK2* transgenic flies in a second binary system and their protein expression

5.1 Introduction

In order to have a better understanding of the function of *hLRRK2* and how the *G2019S* mutation contributes to the pathogenesis of PD, it would be beneficial to be able to manipulate LRRK2 and a second protein simultaneously. In other words, the creation of new transgenic flies carrying an alternative binary expression system would give us the opportunity to express different transgenes under different drivers simultaneously. This chapter describes the generation of novel *LRRK2* transgenics for one such system, the LexA-*LexAop*. Their success was validated by Western blotting, comparing the protein production with existing *Gal4-UAS* transgenics.

5.1.1 Creation of new transgenic flies

5.1.1.1 LexA-*LexAop* binary system

The *Gal4-UAS* system is considered the workhorse of *Drosophila* genetics, and only few papers have been published that are not using it as their primary system. As described in more detail in section 1.10.2 the *Gal4-UAS* system consists of two components. The yeast GAL4 transcriptional activator, which determines the expression pattern under which the gene downstream of the UAS promoter is going to be expressed (Brand et al., 1993). The *Gal4-UAS* binary system is the most extensively used binary system in *Drosophila*, with thousands of Gal4 drivers being available which determine various expression patterns during development (Brand and Perrimon, 1993). Because of this extensive use of this binary system, several tools have been established that control the expression or the activity of the Gal4 driver (Duffy, 2002). These tools include the yeast repressor Gal80 that efficiently represses Gal4 (Lee and Luo, 1999; Del Valle Rodriguez et al., 2013); a temperature sensitive Gal80 mutant (Gal80ts) which allows temporal control (McGuire et al., 2003) and also the yeast Flp/FRT recombinase system to render the Gal4 system inducible in an irreversible manner (Nellen et al., 1996; Pignoni and Zipursky, 1997). Despite the fact that this system is so powerful, there are a number of sophisticated experiments that can't be performed by using this system alone. Two independent binary transcriptional systems could permit the targeted expression of distinct

transgenes in different patterns in the same organism, facilitating various studies in the *Drosophila* nervous system (Lai and Lee, 2006).

These conditions spawned the generation of a second independent binary system for *Drosophila*, the *LexA-LexAop*, which is extensively used in yeast two-hybrid assays. LexA binds to and activates the LexA operator (LexAop) (Lai et al., 2006). LexA is a 202 amino acid protein consisting of a DNA-binding domain from a bacterial transcription factor and a dimerization domain that binds as a dimer with varying affinities to single or multiple copies of gene-specific LexA (Figure 5.1). DNA-binding motifs (LexAop) found upstream of its target genes (Little and Mount 1982; Butala et al., 2008).

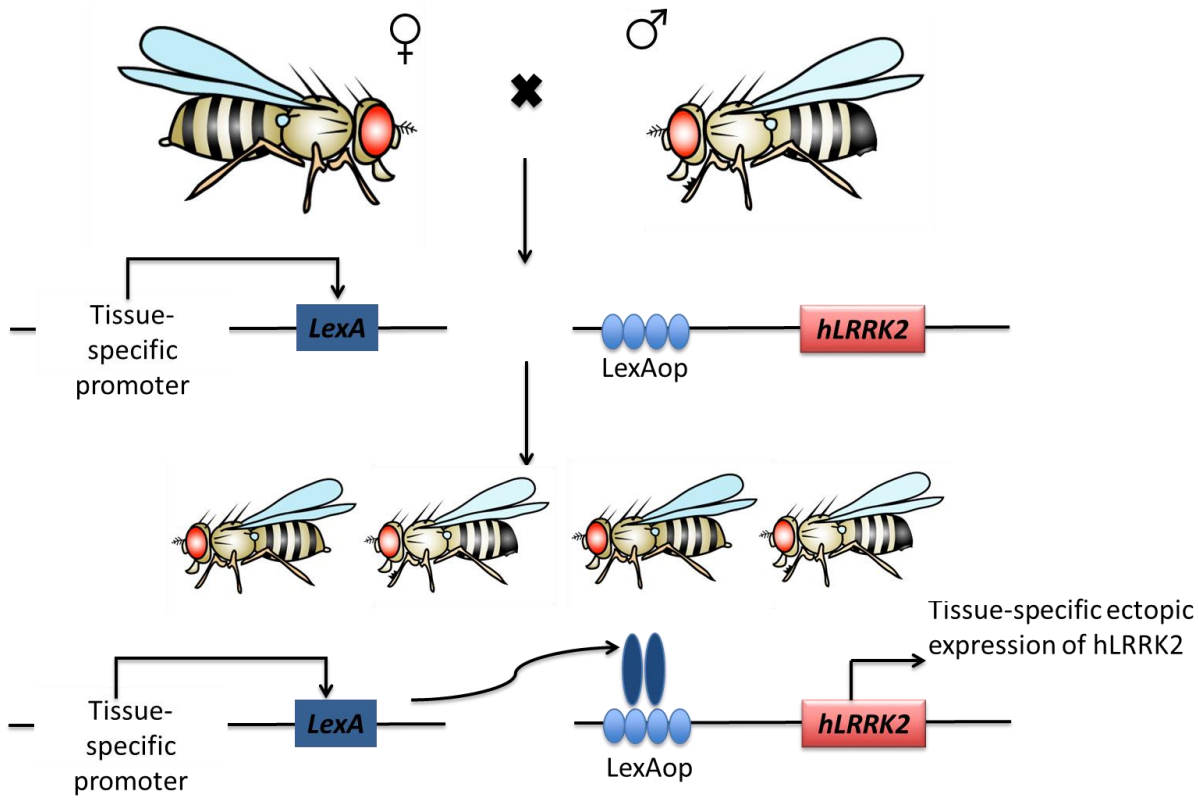

Figure 5.1 The LexA-LexAop binary system.
In order to achieve this cell or tissue specific expression of a gene of interest a fly line that expresses LexA under the control of a tissue specific promoter is crossed to a second line that the gene of interest has been inserted downstream of the LexAop, which is the binding site of LexA. Once these two components are together in a mating scheme, progeny will be generated in which that gene of interest is only expressed in that cell or tissue specific pattern. Fly images generated using the Genotype Builder from Roote and Prokop (2013).

The *TH-LexA* stock was already available in the lab (Chris Elliott's lab stock) and the *LRRK2* plasmids (Invitrogen, California, USA) were a kind gift from Gareth Evans, University of York. The LexAop plasmids were bought from Addgene (Addgene, Cambridge, Massachusetts, USA). Therefore, sub-cloning was performed in order to create a vector containing LexAop-*hLRRK2* or LexAop-*hLRRK2-G2019S*.

5.2 Aims

1. To generate new transgenic flies in order to be able to have an alternative binary system apart from the *Gal4-UAS*.

2. To determine protein expression of all the available UAS and LexAop stocks available in the lab in order to compare protein expression levels between hLRRK2 and G2019S.

5.3 Results

5.3.1 Pathway for the generation of new transgenic flies

The first step was to confirm that the donor vector with the insert was the one of our interest, containing the genes that we were expecting. Restriction digestion

was performed followed by agarose electrophoresis. The restriction enzymes used were BamHI and ApaI in order to confirm that it was the expected size (Figure 5.2). BamHI was chosen as it only cuts at one site the backbone vector and ApaI was chosen as it only cuts within the *hLRRK2* sequence at one site. In that way it was confirmed that *hLRRK2* and *hLRRK2-G2019S* were really present in the backbone vector.

As before, for the LexAop vector restriction digestion was performed in order to confirm that it really was the expected vector. For that reason NheI and PmeI enzymes were used (Figure 5.2). For each one of these restriction enzymes there was one recognition site within the plasmid sequence.

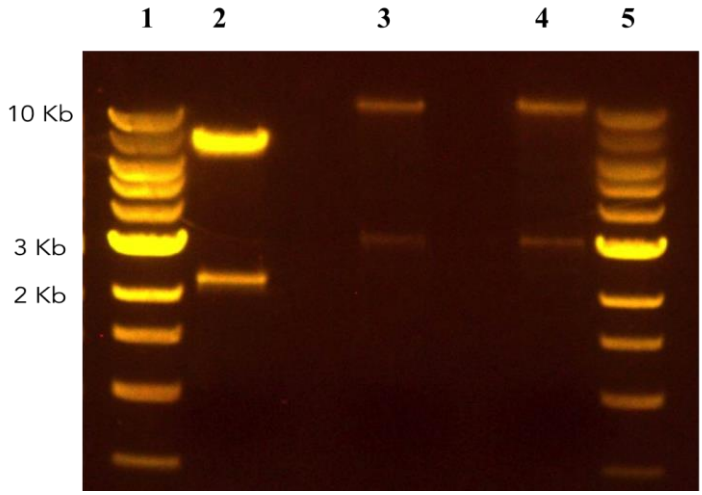

Figure 5.2 Restriction digest of hLRRK2 and LexAop vectors show the expected bands. For the *hLRRK2* and *hLRRK2-G2019S* vectors BamHI and ApaI restriction enzymes were used and the expected size bands were obtained; 11Kb and 3Kb (3 and 4). For the LexAop vector NheI and PmeI restriction enzymes were used and the expected size bands were obtained; 7Kb and 2.2Kb (2). In that way it was confirmed that both vectors were the ones of our interest. 1Kb DNA ladder (NEB) was used in order to confirm the size of all the DNA bands (1 and 5).

After DNA gel extraction, DNA samples were also sent for sequencing and the presence of the *hLRRK2* sequence was confirmed using primers within exon 1 of *hLRRK2* (Figure 5.3).

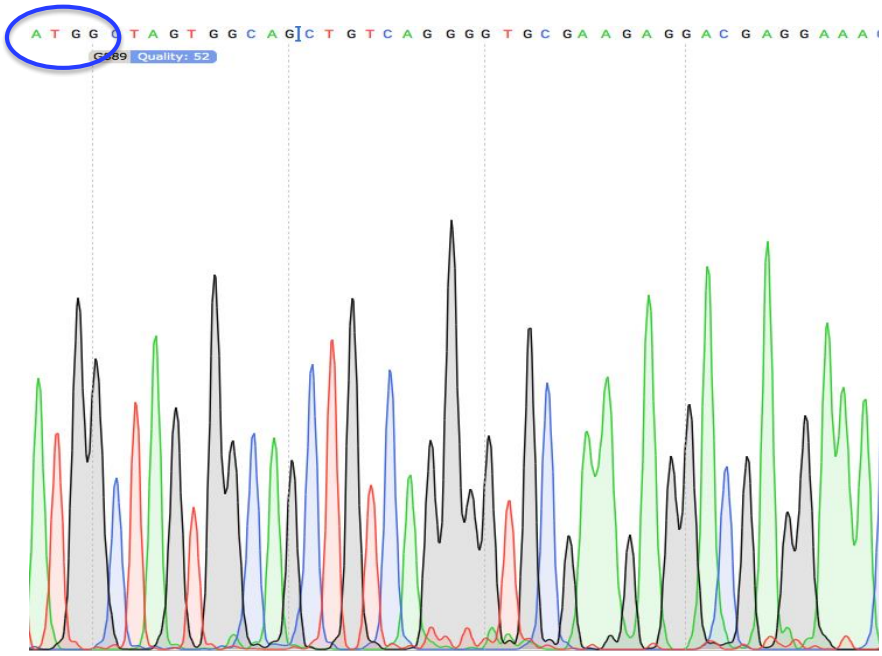

Figure 5.3. Sequencing confirmed the presence of the *hLRRK2* transgene within our donor vector. Sanger sequencing of the *hLRRK2* vector using primers within the exon 1 of our gene of interest in order to confirm its presence. The highlighted ATG codon is the starting codon of the *LRRK2* transgene.

5.3.2 Ligation of the *hLRRK2* transgene into the *LexAop* vector

The next step was the ligation of the cut insert and the cut host vector in order to insert *hLRRK2* and *hLRRK2-G2019S* downstream of the LexAop sequence. To achieve that the *hLRRK2* vector was digested with BamHI and EagI as these enzymes cut around the *hLRRK2* gene but not within the *hLRRK2* sequence. From that digestion two bands were expected, one was 9 Kb, which contained *hLRRK2* and one 4.7 Kb which contained the rest of the plasmid (Figure 5.4). Moreover, restriction digestion of the LexAop vector was performed with NotI and BglII (Figure 5.4) so compatible ends in the same orientation to the insert

were being created in order the cut insert to be able to be ligated between these endings. The expected size DNA bands from this digestion were 9 Kb and 79 bp. The recognition sites of the enzymes used in the process of ligation are summarized in table 5.1.

Table 5.1 Recognition sites of the enzymes used

Enzyme (For the *hLRRK2* vector)	Ligated to (For the LexAop vector)
BamHI	BglII
5’ G/GATCC 3’	5’ A/GATCT 3’
EagI	NotI
5’ C/GGCCG 3’	5’ G/CGGCCGC 3’

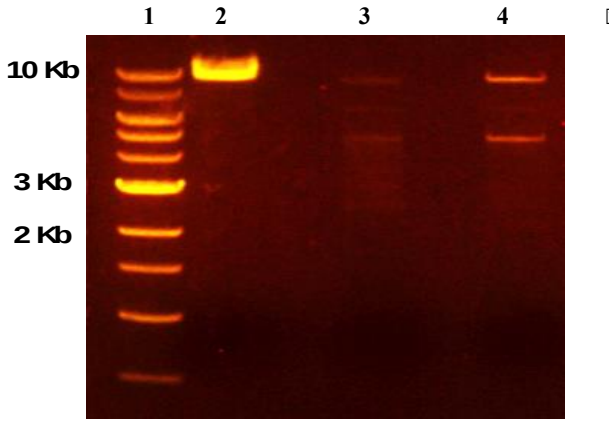

Figure 5.4 Steps for the ligation of *hLRRK2* downstream the *LexAop* sequence. Restriction digest of both the host vector and the donor vector in order to get compatible ends to proceed with the ligation. The hLRRK2 vector was cut with BamHI and EagI (3) and the hLRRK2-G2019S vector was also cut with BamHI and Eagl (4). The LexAop vector was cut with NotI and BglII (2). 1Kb DNA ladder (NEB) was used in order to confirm the size of all the DNA bands (1).

Ligation was followed by transformation and colony cracking to test if there were any successfully ligated samples. In colony cracking single colonies run next to the uncut host vector and any colonies that are heavier than the uncut, so they run slower, was an indication that the insert had been ligated successfully. A summary diagram of the procedure that was followed is shown in Figure 5.5.

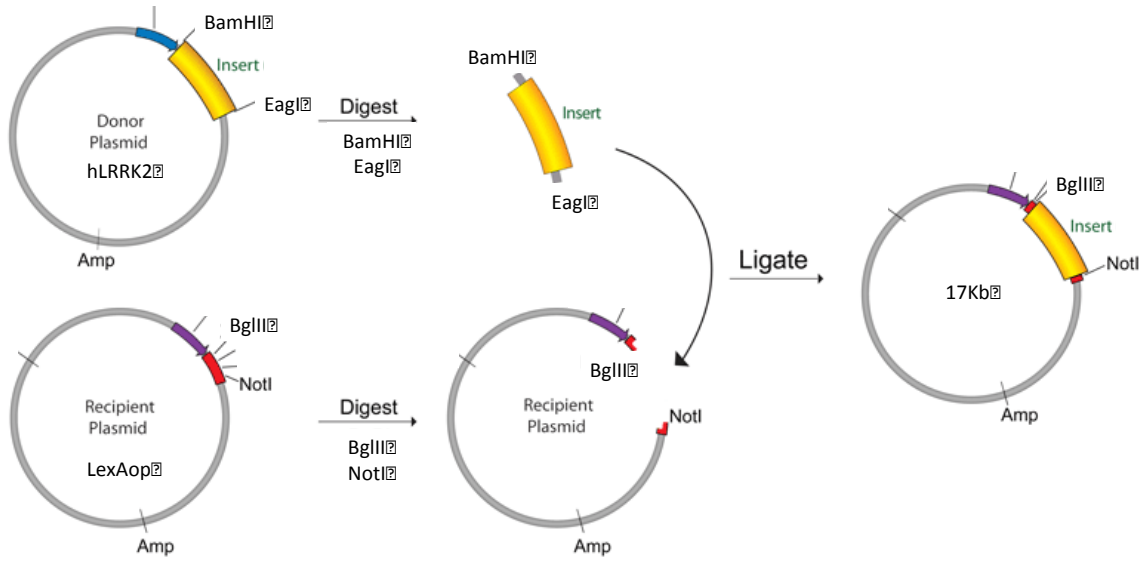

Figure 5.5 Summary diagram of the restriction digest protocol.
This protocol was followed in order to successfully ligate the insert that was containing the *hLRRK2* or the *hLRRK2-G2019S* downstream the LexAop sequence.

In order to confirm that the ligation was really successful restriction digest was performed using enzymes that recognise either *hLRRK2* or the LexAop vector. Xbal was used from which two DNA bands were expected sized 11.8 Kb and 6 Kb and SacI from which three DNA bands were expected sized 9.7 Kb, 4.38 Kb and 3.3 Kb (Figure 5.6).

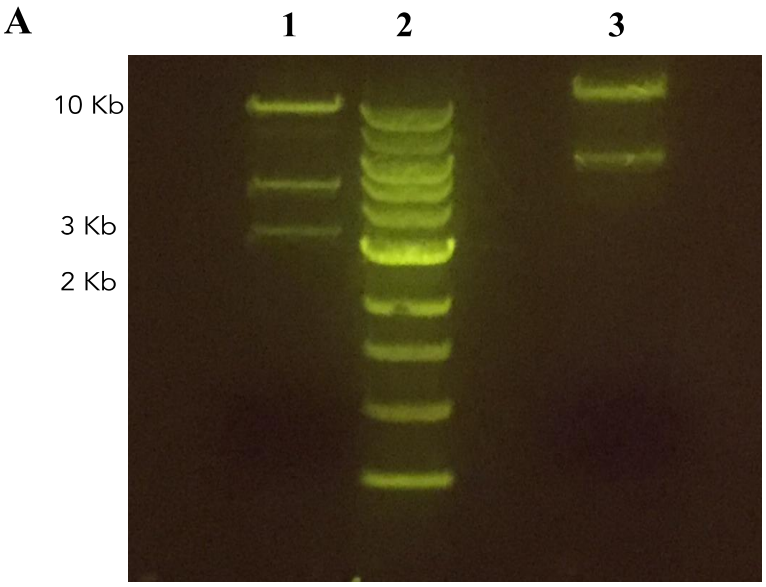
A
1
2
3
10 Kb
3 Kb
2 Kb

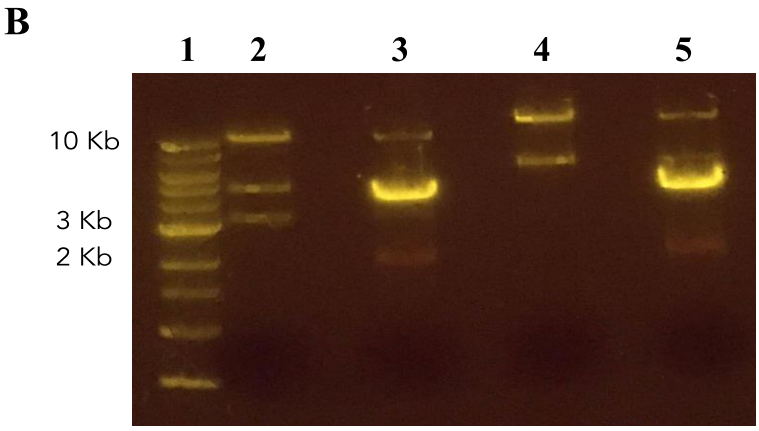
B
1
2
3
4
5
10 Kb
3 Kb
2 Kb

Figure 5.6 Restriction digestion of the successfully ligated candidates.

A) Restriction digestion of the *LexAop-hLRRK2* plasmid in order to confirm that the ligation was being successful. That was confirmed by digesting with SacI, which has three recognition sites within the newly created plasmid. As expected three DNA bands were obtained (1) sized 9.7 Kb, 4.38 Kb and 3.3 Kb. From the digestion with Xbal, which has two recognition sites within the newly created plasmid, also revealed the expected DNA bands (3) sized 11.8 Kb and 6 Kb confirming that the *hLRRK2* transgene has been successfully inserted downstream of the LexAop sequence. 1Kb DNA ladder (NEB) was used in order to confirm the size of all the DNA bands (2). B) Restriction digestion of the *LexAop-G2019S* plasmid in order to confirm that the ligation was being successful. That was confirmed by digesting with SacI, which has three recognition sites within the newly created plasmid. As expected three DNA bands were obtained (2) sized 9.7 Kb, 4.38 Kb and 3.3 Kb. As a comparison, an unsuccessfully ligated DNA was also digested with SacI (3), which revealed four DNA bands that were not of the expected size. From the digestion with Xbal, which has two recognition sites within the newly created plasmid, revealed the expected DNA bands (4) sized 11.8 Kb and 6 Kb confirming that the *hLRRK2* transgene has been successfully inserted downstream of the LexAop sequence. The unsuccessfully ligated *LexAop-G2019S* was also digested with Xbal confirming that the *hLRRK2* transgene wasn't inserted, as 4 DNA were obtained which were not of the expected size (5). 1Kb DNA ladder (NEB) was used in order to confirm the size of all the DNA bands (1).

The plasmid DNA of all the successfully ligated samples that were obtained were sent for microinjection of fly embryos (as described in section 2.3.12) in order to create flies of the desired genotype (Fly facility, Department of Genetics, University of Cambridge).

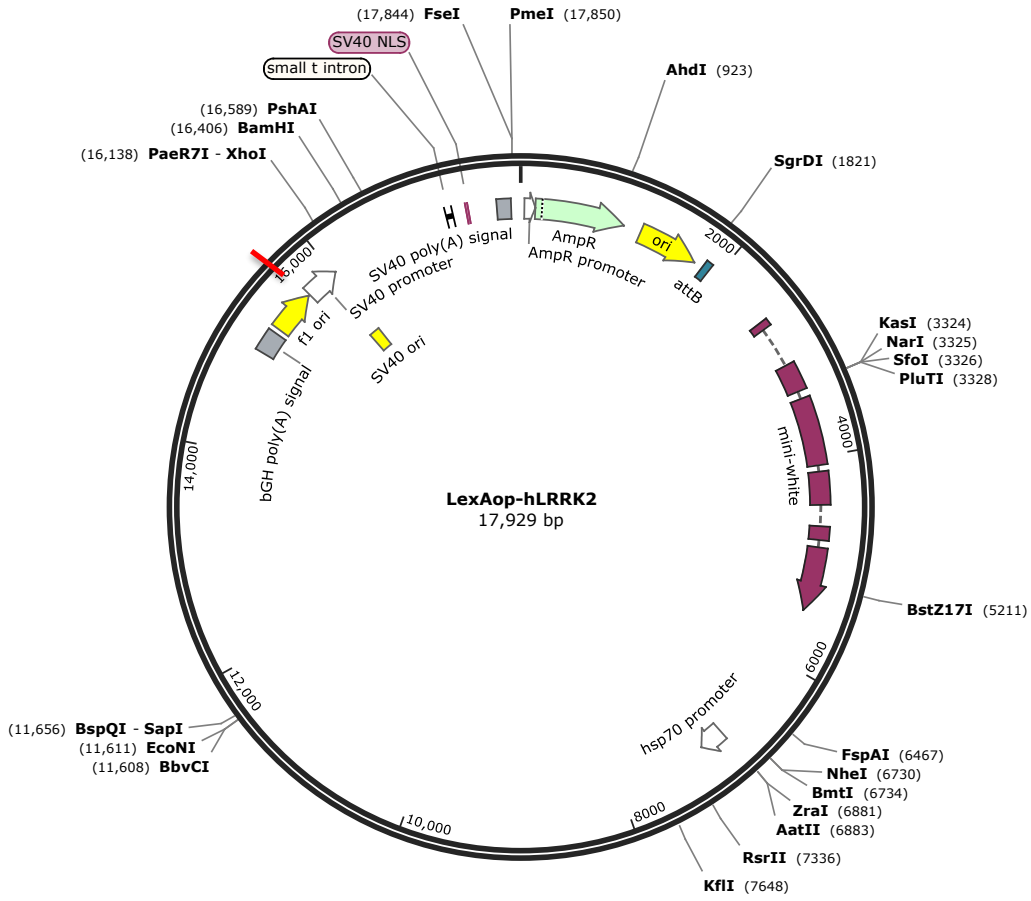

Figure 5.7 Full sequence map for the LexAop-hLRRK2 created vector. This is the final LexAop-*hLRRK2* vector that was created in order to insert the *LRRK2* transgene downstream the LexAop sequence, sized 17929 bp. The map was created using the SnapGene software.

5.3.3 DNA Sequencing of the new transgenic flies

In order to confirm the presence of the *hLRRK2* and *hLRRK2-G2019S* genes downstream from the LexAop sequence, DNA was extracted from single flies followed by PCR using primers within the kinase domain of the gene (Figure 5.8 and Figure 5.9).

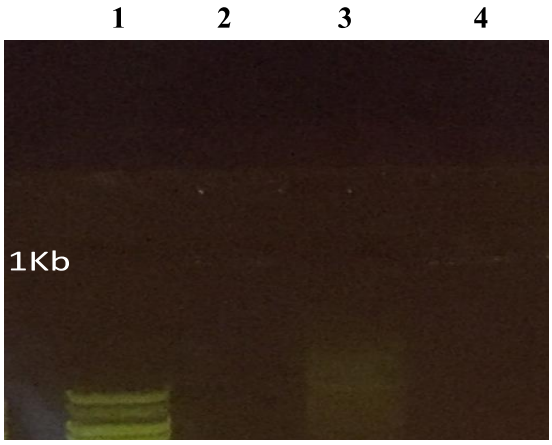

Figure 5.8 Confirmation of the presence of the *hLRRK2-G2019S* gene in the new transgenic flies. PCR was performed using primers within the kinase domain of the *hLRRK2* gene, after DNA extraction from the LexAop-*G2019S* flies. The expected sized band was obtained at ~ 1Kb (2). As a positive control the plasmid DNA from the LexAop-G2019S vector was also tested (3) while a negative control was included containing DNA extracted from TH flies where no bands were seen (4). 1Kb DNA ladder (NEB) was used in order to confirm the size of all the DNA bands (1).

Figure 5.9 Confirmation of the presence of the *hLRRK2* gene in the new transgenic flies. PCR was performed using primers within the kinase domain of the *hLRRK2* gene, after DNA extraction from the LexAop-*hLRRK2* flies. The expected sized band was obtained at ~ 1Kb. Each lane represents a single hLRRK2 fly. 1Kb DNA ladder (NEB) was used in order to confirm the size of all the DNA bands.

The PCR confirmed the presence of the *hLRRK2* gene in both stocks, *LexAop-hLRRK2* and *LexAop-hLRRK2-G2019S*. The next step was to confirm that the *G2019S* mutation was present in the *LexAop-G2019S* stock, but not in *LexAop-hLRRK2*. DNA samples were sent for sequencing at GATC Company, which indeed confirmed the presence of the G>A mutation (Figure 5.10).

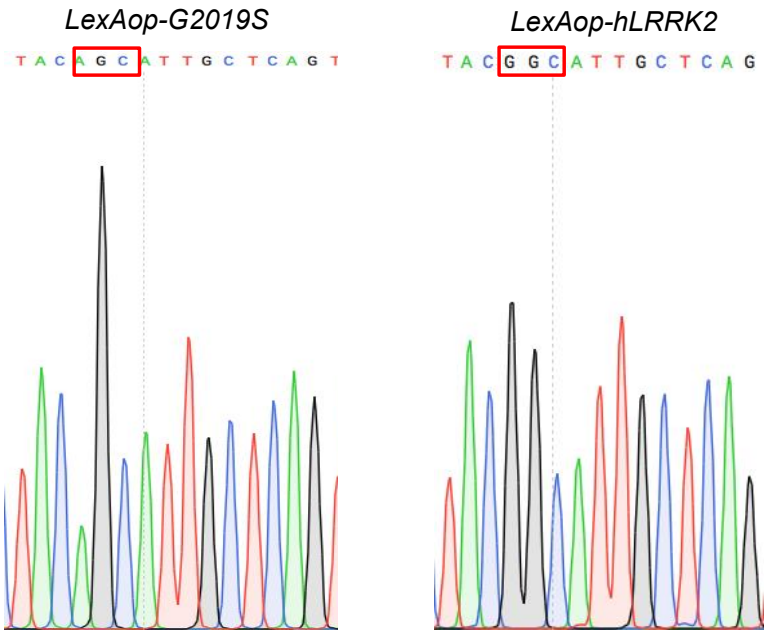

Figure 5.10 Confirmation of the presence of the G>A mutation. DNA sequencing of the LexAop-*hLRRK2* and LexAop-*G2019S* stocks. Within the kinase domain where the mutation lies, in the LexAop-*hLRRK2* flies the codon is GGC (Glysine, G), while in the LexAop-*G2019S* the AGC codon (Serine,S).

5.4 Protein expression of hLRRK2 and hLRRK2-G2019S

In order to be able to compare the protein expression of the newly created *LexAop-hLRRK2* and *LexAop-G2019S* flies that were created to the UAS lines, Western blots were performed to all the different *hLRRK2* and G2019S lines available in the lab. Three independently generated *TH-Gal4>hLRRK2* and *TH-Gal4>G2019S* lines (Lin et al., 2010, Liu et al., 2008, Lundbeck, unpublished) were examined. The Liu et al. (2008) fly stocks were also FLAG tagged. In summary, 30 female fly heads were collected after 3 days of incubation at 29ºC, and after homogenisation with RIPA (Radioimmunoprecipitation assay) buffer, in order to extract the protein from the fly heads, BCA (bicinchoninic acid assay) protein assay was performed, in order to determine the total concentration of protein in the solution (ug/ul) (Full details on section 2.4).

5.4.1 Protein expression levels after expression of *LRRK2* and *G2019S* in the fly eye

To begin with, the protein expression levels of hLRRK2 in comparison to G2019S were tested by expressing the *UAS-hLRRK2*, *UAS-G2019S* or *UAS-I2020T* in the eye under the *GMR-Gal4* control. The *GMR-Gal4* driver was chosen as it is the most widely used driver for targeting expression in the developing eye. A *CS/w*$^{-}$ cross (such flies will contain dLRRK protein) and *dLLRK*^{e03680} flies (knock-out of the *dLRRK* gene, expressing no dLRRK protein), were used as controls in order to confirm if the dLRRK protein is recognised by the human hLRRK2 antibody.

Figure 5.11 shows the staining achieved with the Novus anti-hLRRK2 rabbit polyclonal antibody, while Figure 5.12 shows staining from the same protein samples with the NeuroMab anti-hLRRK2 mouse monoclonal antibody. Two different gels were run at the same time.

Both antibodies suggest that hLRRK2 is expressed in higher levels compared to the G2019S, when the *hLRRK2* transgene is expressed in the eye. Moreover, it is worth mentioning that G2019S and I2020T proteins, which are both mutations within the kinase domain of the *hLRRK2* gene, are expressed at similar levels in the eye.

Even though both antibodies recognise the C-terminus of the LRRK2 protein, the anti-LRRK2 rabbit polyclonal (Novus), also gave some non-specific bands, at around ~250 KDa, as well as the expected band at 286 KDa. On the other hand, the mouse monoclonal antibody (NeuroMab), was more specific giving only the expected band at ~286 KDa. For that reason, it was determined that for the following up experiments, only the NeuroMab antibody would be used.

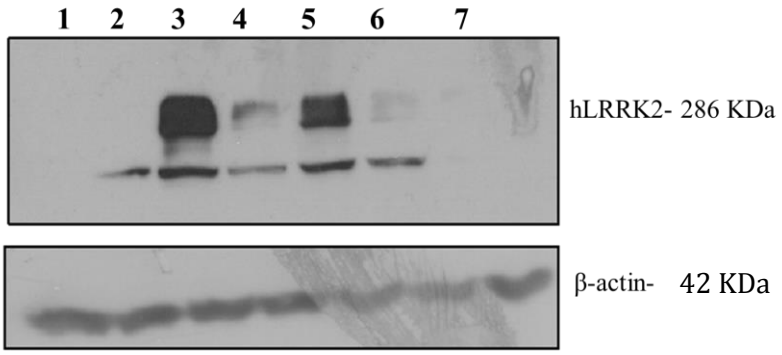

Figure 5.11 hLRRK2 is expressed at higher level than G2019S.

Western blot showing protein levels in head lysates from flies with eye expression of *CS/w-* (1*), dLRRK*^{e03680} (2), *UAS-hLRRK2* (3), *UAS-G2019S* (4), *UAS-hLRRK2 II* (sample 2) (5), *UAS-G2019S II* (sample 2) (6) and *UAS-I2020T* (7). Probing with anti-hLRRK2 rabbit polyclonal antibody (Novus) reveals the expected bands at 286 KDa. β-actin was used as the loading control. For both of the different UAS stocks of *hLRRK2* and *G2019S* that were tested, expression levels of hLRRK2 are much higher compared to the G2019S. The *hLRRK2* and *G2019S* flies were the Liu (2008) lines, with the two samples derived from stocks maintained by different members of the lab.

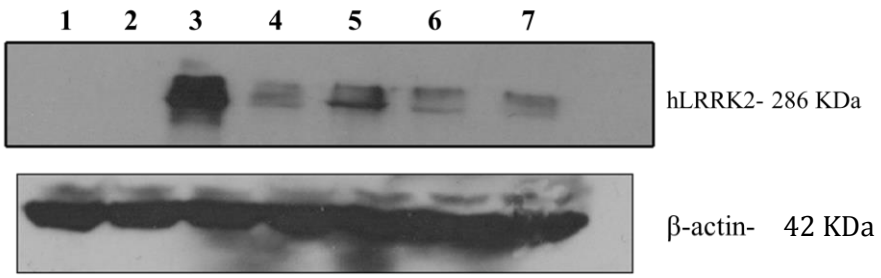

Figure 5.12 A second antibody confirms that hLRRK2 is expressed much more than the G2019S. Western blot showing protein levels in head lysates from flies with eye expression of *CS/w-* (1), *dLRRK;e03680* (2), *UAS-hLRRK2* (3), *UAS-G2019S* (4), *UAS-hLRRK2 II* (sample 2) (5), *UAS-G2019S II* (sample 2) (6) and *UAS-I2020T* (7). Probing with anti-hLRRK2 mouse monclonal antibody (NeuroMab) reveals the expected bands at 286 KDa. β-actin was used as the loading control. For both of the different UAS stocks of *hLRRK2* and *G2019S* that were tested, expression levels of hLRRK2 are much higher compared to the G2019S. The *hLRRK2* and *G2019S* flies were the Liu et al. (2008) lines, with the two samples derived from stocks maintained by different members of the lab.

5.4.2 Protein expression levels of LRRK2 and G2019S in the dopaminergic neurons

In the next round of assays, it was decided to perform a BCA assay before Western blotting, in order to determine the protein concentration of each sample and to ensure equal loading between samples (Section 2.4.2). This time all the different UAS stocks were expressed in the dopaminergic neurons under the control of the *TH-Gal4* driver.

5.4.2.1 Protein expression levels of LRRK2 and G2019S after the BCA analysis

For this set of experiments, four different pairs of *UAS-hLRRK2* and *UAS-G2019S* were tested while *TH/dLRRK*^{e03680} was used as a control, which is a cross between the *TH-Gal4* and the knock-out of the *Drosophila LRRK2* (Figure 5.13;A). The fly stocks that were tested included the UAS- *hLRRK2* 2008 and UAS-*G2019S 2008* (Liu et al., 2008), three stocks of each were analysed like previously, which are labelled as *TH> hLRRK2 2008*, *TH> hLRRK2 II* 2008, *TH> hLRRK2 III* 2008, *TH>G2019S* 2008, *TH>G2019S II* 2008 and *TH>G2019S III* 2008. Moreover, the FLAG tagged stocks were also used (Lin et al., 2010), labelled as TH> *hLRRK2* 2010 and *TH>G2019S* 2010. In addition, the newly created *UAS* fly stocks for *hLRRK2* and *G2019S* were tested (Lundbeck) which are inserted at the same site, unlike the Liu et al. (2008) and Lin et al. (2010) where the insertion site is unknown (Figure 4.13; B & C). In the last set of these experiments, two additional mutations within the *LRRK2* gene were also tested, *R1441C* (which lies within the GTP domain of the LRRK2 protein) and *G2019S-K1906M* (a kinase-dead LRRK2). The controls that were used included *CS/w-* flies and a cross between *TH-Gal4* and the *Drosophila* knock-out (*TH/e03680)*. In order to establish that there is no undriven expression of the *UAS- hLRRK2* and *UAS-G2019S* stocks, *hLRRK2/w-* and *G2019S/w-* genotypes were also included (Figure 5.13;D). As before, 3-day-old fly heads were collected and the protein was extracted (Section 2.4.1).

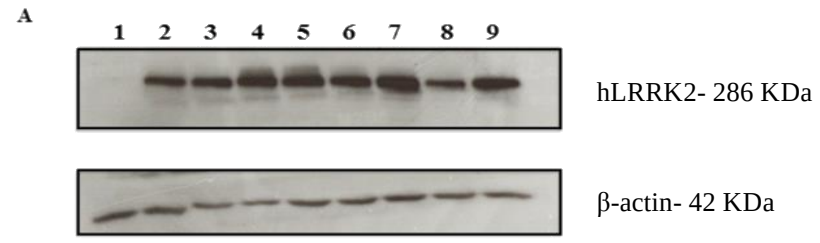
A
1 2 3 4 5 6 7 8 9
hLRRK2- 286 KDa
β-actin- 42 KDa

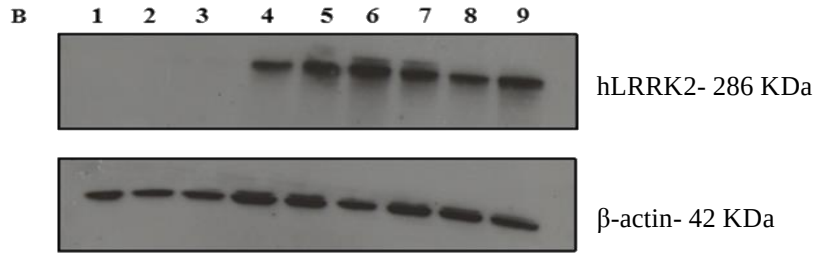
B
1 2 3 4 5 6 7 8 9
hLRRK2- 286 KDa
β-actin- 42 KDa

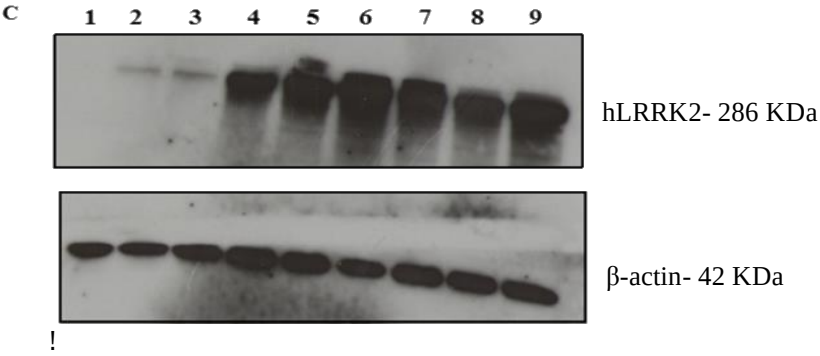
C
1 2 3 4 5 6 7 8 9
hLRRK2- 286 KDa
β-actin- 42 KDa

!

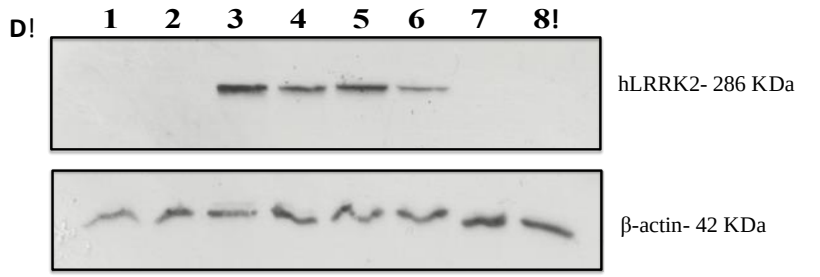
D!
1 2 3 4 5 6 7 8!
hLRRK2- 286 KDa
β-actin- 42 KDa

Figure 5.13 hLRRK2 higher expression levels are confirmed.

Western blot showing protein levels in head lysates from flies. Probing with anti-hLRRK2 mouse monclonal antibody (NeuroMab) reveals the expected bands at 286 KDa. β-actin was used as the loading control. (A) *TH/dLRRK*^{e03680} (1), *UAS-G2019S II* 2008 (2), *UAS-hLRRK2 II* (3), *UAS-G2019S* 2010 (4), *UAS-hLRRK2* 2010 (5), *UAS-G2019S* 2008 (6), *UAS-hLRRK2* 2008 (7), *UAS-G2019S* III 2008 (8) and *UAS-hLRRK2* III 2008 (9). (B and C) *TH/dLRRK*^{e03680} (1), *UAS-G2019S* Lundbeck (2), *UAS-hLRRK2* Lundbeck (3), *UAS-G2019S II* 2008 (4), *UAS-hLRRK2 II* (5), *UAS-G2019S* 2010 (6), *UAS-hLRRK2* 2010 (7), *UAS-G2019S* III 2008 (8) and *UAS-hLRRK2* III 2008 (9). (D) *TH/dLRRK*^{e03680} (1), *CS/w-* (2), *UAS-hLRRK2* III 2008 (3) and *UAS- G2019S* III 2008 (4), *UAS-G2019S-K1906M* (5), *UAS-R1441C* (6), *hLRRK2/w-* (7) and *G2019S/w-* (8). For all the different lines that were tested (Lin, 2010; Liu, 2008 and Lundbeck, unpublished) hLRRK2 is expressed in higher levels compared to G2019S. hLRRK2 is also expressed in higher levels compared to the additional mutations within the *LRRK2* gene that were tested. Moreover, *hLRRK2/w-* and *G2019S/w-* do not show any bands, proving that there is no undriven expression.

As before, expression of *hLRRK2* and *G2019S* in the dopaminergic neurons indicated that LRRK2 protein is expressed in higher levels compared to the G2019S (Figure 5.13; A, B, C). That applies for all the different UAS stocks that were used (Lin et al., 2010; Liu et al., 2008; Lundbeck, unpublished). The Lundbeck likes, which were created expressing the *hLRRK2* and *G2019S* transgenes at specific landing sites, are expressed in lower levels compared to the other UAS stocks, in which the landing site of the transgenes is unknown (Figure 5.13; B and C). In the last panel of Figure 4.16, different mutations within the *hLRRK2* gene were expressed, and it is indicated that the kinase-dead form of LRRK2 protein is expressed at similar levels to the G2019S, while the R1441C form of the hLRRK2 protein, which is a mutation within the GTPase domain, is expressed in lower levels. The undriven expression of hLRRK2 and G2019S

shows that the *hLRRK2* and the *G2019S* transgenes are not expressed in the absence of the *TH-Gal4* driver.

5.5 Expression levels of hLRRK2 and hLRRK2-G2019S in the newly created LexAop transgenic flies

The next step was to perform a Western blot in order to compare the Lundbeck lines to the newly made *LexAop-hLRRK2* and *LexAop-G2019S* lines, in which the insertion site of the transgenes is like the Lundbeck oneson the 2nd chromosome or else on the 3rd chromosome (Section 2.3.12). For the expression of the transgenes in the dopaminergic neurons the *TH-Gal4* and *TH-LexA* drivers were utilised.

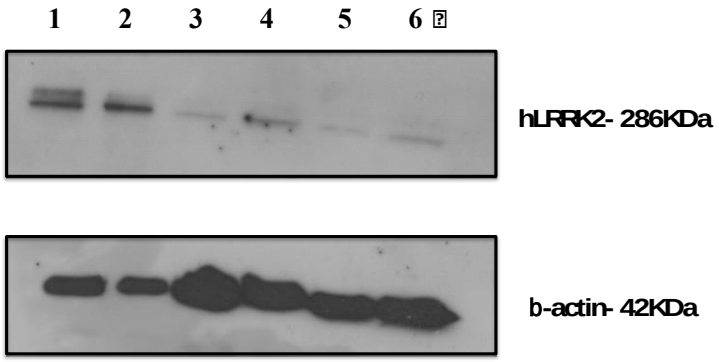

Figure 5.14 The LexAop lines are expressed in lower levels compared to the UAS ones. Western blot showing protein levels in head lysates from flies with DA expression of *UAS-hLRRK2* (1), *UAS-G2019S* (2), *LexAop-hLRRK2* inserted on the thrid chromosome (3), *LexAop-G2019S* inserted on the third chromosome (4), *LexAop-hLRRK2* inserted on the second chromosome (5) and *LexAop-G2019S* inserted on the second chromosome (6). β-actin was used as the loading control. Probing with anti-hLRRK2 reveals the expected bands at 286 KDa. Expression of the UAS lines are at higher levels compared to the LexAop ones, while the protein expression between the hLRRK2 and G2019S seems to be at similar levels for the LexA lines.

From this protein analysis, it can be concluded that the newly created *LexA-LexAop* lines are expressed in lower levels compared to the UAS. The Lundbeck lines were chosen because among all the available UAS lines available, they are expressed in the lower levels, so they could be comparable to the newly created lines. For the LexAop lines, hLRRK2 and G2019S proteins are expressing in similar levels, irrespective of the landing site. On the other hand, the *UAS-hLRRK2* is expressed at higher levels compared to the *UAS-G2019S*.

5.6 Discussion

Having created new transgenic flies including *LexAop-hLRRK2* and *LexAop-G2019S* will be a big advantage, allowing us to express at the same time two different transgenes under different expression pattern in the same animal. Validation by Western blotting shows that the LRRK2 protein is expressed at higher levels than the G2019S for all the available UAS lines. Protein analysis of the newly created LexAop lines didn't dispose any differences between LRRK2 and G2019S, although these lines are expressed at much lower levels than the UAS ones.

Hindle et al. (2013) performed Western blots in order to compare the expression pattern of hLRRK2 and hLRRK2-G2019S. Their interpretation was that the expression of hLRRK2 was at a comparable level to G2019S (Hindle et al., 2013). Re-examination of their blot suggests that in fact hLRRK2 is expressed in greater levels than the G2019S. This finding is similar to the results obtained from this investigation as it is suggested that for all the available lines tested hLRRK2 is expressed in greater levels compared to G2019S. This was shown both with expression in the eye (*GMR-Gal4*) and in the dopaminergic neurons (*TH-Gal4*). The independent insertions by Liu et al. (2008) and Lin et al. (2010) also both show this effect. In addition, comparing LRRK2 to I2020T, proposes that LRRK2 is again expressed at higher levels compared to I2020T, which is expressed at similar levels to G2019S. The fact that both of these mutations lie within the kinase domain of the gene is an indication that this decrease in the protein expression could be a common kinase effect.

Venderova et al. (2009) generated new *LRRK2* and *LRRK2* mutant lines and in order to confirm the expression of these transgenes they performed Western blotting by driving the expression in the eye using the *GMR-Gal4* driver. From the data they presented, it can be concluded that LRRK2 is expressed in higher levels compared to the I2020T mutated protein. Even though they didn't include the *G2019S* mutation in their analysis, their data our consistent with the results presented in this thesis, as I2020T mutant protein is also expressed in lower levels compared to the wild type. As both mutations, *I2020T* and *G2019S*, lie within the kinase domain of the protein is an indication that the kinase activity of the protein should play a role in this difference in the expression pattern observed.

In previous stocks that were tested, the transgenes were inserted in unknown sites, while the Lundbeck lines were all inserted on the 2nd chromosome, where they have the attP site, which is the same landing site as the newly created LexAop lines. In the Lundbeck lines the *TH>G2019S* was expressed in lower levels than *TH> hLRRK2*, just like the other UAS lines. Even though it was expected that the LexAop lines would show similar protein production, *TH>G2019S* and *TH> hLRRK2* were expressed in similar levels in these lines.

That poses the question, why is the level of protein consistently lower in the *G2019S* background? West et al. (2005) suggested that LRRK2 may be broken down by the proteasome, so it is possible that differences exist in the rate at which LRRK2 is degraded. One possibility is that the rate of breakdown of LRRK2 is determined by its phosphorylation level, with G2019S and I2020T being more phosphorylated than the wild type LRRK2. Ding et al. (2017) showed that manipulating the F-box protein Fbx118 affected the rate of breakdown of LRRK2, with increases in Fbx118 ubiquinating LRRK2 and targeting it for proteasomal degradation. Phosphorylated LRRK2 wild-type was degraded faster than unphosphorylated protein in these HEK293 cells. On the other hand, Lobbestael et al. (2016) concluded that de-phosphorylation of LRRK2 induced degradation of the LRRK2 protein in SH-SY5Y cells. These differences that were established from different research groups could reflect the

cell types that were utilised during their investigation. The present data shown in this thesis on the other hand, are based on an *in vivo* studying of the dopaminergic neurons of the fly, which probably is a better representation of what is actually happening at the molecular level.

Sharma et al. (2011) used post-mortem frozen tissue from controls and idiopathic PD (IPD) patients and G2019S positive PD cases and performed protein expression analysis. They determined that LRRK2 protein was ubiquitously present in the cytoplasm of neurons for all the studied groups. This cytoplasmic expression of LRRK2 was often accompanied by extension to the apical dendrites. No significant differences were obtained in the LRRK2 immunoreactivity between controls, IPD and G2019S positive PD cases. On the other hand, prominent differences in the intensity of LRRK2 staining were observed in different regions. The CNS of the fly would also be like this, where different transgenes are present in different regions or degradation of the accumulated proteins is taking place in different regions. Moreover, regions that are known to be vulnerable to α-synuclein pathology in IPD presented extensive variability in LRRK2 immunoreactivity. It was established that in the nigrostriatal dopamine system neurons the weakest LRRK2 immunoreactivity was recorded, irrespective of the disease status. Moreover, they discovered that LRRK2 is present in the halo of a small proportion of LBs. The inconsistence of LRRK2 presence in brainstem LBs and its absence in cortical LBs, indicates that LRRK2 in not an obligate component of LBs. Other studies have confirmed that LRRK2 phosphorylates α-synuclein *in vitro* (Qing et al., 2009), even though a physical interaction between them hasn't been confirmed. The key question that arises is if LRRK2 functions upstream of α-synuclein in the PD pathway as a signalling molecule triggering α-synuclein aggregation.

Taken together, this study establishes that LRRK2 protein is expressed in higher levels than the G2019S mutated one in all the available UAS lines tested. On the other hand, the newly created LexAop lines do not follow this pattern, as no difference was observed between LRRK2 and G2019S. Taking into account the much lower expression levels of the LexAop lines in comparison to the UAS ones, one explanation could be that the protein expression levels are so much

lower that Western blotting is not a sensitive enough assay to detect any differences between these lines. In addition, if the breaking down of LRRK2 by the proteasome plays any role in the observed expression differences, one reasonable explanation could be that this degradation process is only activated after higher levels of proteins are expressed in the cells. The low levels of LRRK2 and G2019S proteins in the LexAop lines could prevent this process to start, explaining the similar levels of protein expression obtained from these lines.

5.7 Conclusion

Taken together the results presented in this chapter the overall conclusion that could be made is that hLRRK2 is massively expressed compared to the G2019S mutated version of the gene. This could be the beginning of understanding the molecular pathway of PD that leads to the neurodegeneration of the dopaminergic neurons.

6. Discussion and Future Research

6.1 Introduction

The overall aim of this course of investigation was to advance our knowledge on how *LRRK2* contributes to the pathogenesis of PD using *Drosophila* as an animal model. The purpose was to shew new light on the molecular pathway and the physiological progression, leading to neurodegeneration and more specifically what role the *G2019S* mutation has on this process. The key role of *LRRK2* as a kinase could pave the way for new drug discoveries in the future, as the kinase pathway has always been an easy target for drug development. In order to achieve that, the following primary questions were investigated:

1. Determine if manipulating dopamine release from the synaptic vesicles leads to visual defects in adult flies.

2. Establish if the dopamine levels are affected in the *LRRK2-G2019S* mutated flies causing neuronal death.

3. Test the hypothesis that Rab proteins are *in vivo* substrates of LRRK2.

This final chapter reviews the outcome of these questions, providing a comprehensive, succinct overview of the key data generated from this investigation. It also looks to pose further questions and areas for further investigation.

6.2 *LRRK2* and dopamine relation

DA is a very important neurotransmitter in the brain and retina of both insects and mammals. Even though the pathophysiology of the DAergic loss in PD remains unclear, it seems that DA may play a role in this process. Cytosolic DA and its metabolites conjugate to PD-related proteins and generally increase oxidative stress. One of the proposed protein candidates interacting with

dopamine is LRRK2. As has been described in more detail in Chapter 1, section 1.3, *LRRK2* is the most common cause of PD, being responsible for ~10% of all the familial PD cases. More specifically the *G2019S* mutation, which lies within the kinase domain of the protein, is the most common genetic cause of PD being responsible for 2-40% of all the PD cases depending on the population under study (Houlden and Singleton, 2012). The key hypothesis in this thesis was that it is the interaction between dopamine and *LRRK2-G2019S* leading to the neurodegeneration observed in PD.

Taking advantage of the *Drosophila* visual system, which has been a great and approachable *in vivo* model to study neurodegeneration, the relation between dopamine and *LRRK2* was tested. The photoreceptors project into the lamina where they ramify, possibly contacting the terminals of the photoreceptors. The medulla also contains many dopaminergic neurons that could interact with the terminals of the lamina neurons.

The findings from this thesis, both HPLC assay and TNT manipulation, confirm the interaction between *LRRK2-G2019S* and dopamine. Measurement of dopamine levels from flies with the *G2019S* mutation determined that young flies carrying the mutation have reduced levels of dopamine compared to the normal high levels observed in the wild type *LRRK2* flies. This supports the idea of the early onset excitotoxicity pathway, as having less dopamine in the retina would make the photoreceptor responses faster and larger. As described by Chyb et al. (1999) dopamine slows the response of individual photoreceptors forcing the visual system to respond faster. The less dopamine observed in the *G2019S* flies could lead to decreased release in the lamina leading to faster responses by the photoreceptors and stronger activation of the lamina neurons. This discovery could explain how the excitotoxic pathway starts. Older flies, 7 day and 14 day old, that have similar dopamine levels, do not exhibit any significant differences in their visual responses when TNT is expressed, and the retinal physiology is also similar. This implies a hyperactivity in the *G2019S* retina confirming the initial hypothesis of an early onset hyperactivity in these flies. As a follow up analysis, blockage of dopamine release and synaptic signalling was performed by expressing tetanus toxin in the dopaminergic neurons. It appears that expression

of TNT reduces the photoreceptor and lamina neuron responses in young *TH>G2019S* flies, but increases in the *TH>LRRK2* and *TH/w-* flies. It would be expected that expression of TNT would increase the visual responses if it blocked transmitter release from dopaminergic neurons. The effect TNT has on the *G2019S* flies is not surprising as they have less dopamine at this stage compared to *LRRK2* and *w-* flies.

My findings also support the data of Afsari et al. (2014) that young flies expressing the *G2019S* mutation had increased visual signalling compared to the wild types. This excitotoxicity response could lead to extra ATP demand from the ion exchange pumps, contributing to mitochondrial failure that might not be able to fulfil without the generation of extra oxidative stress. That would only lead to mitochondrial defects followed by increased apoptosis and autophagy. That coincides with the enlarged endosomes that were observed in *TH>G2019S* and *TH>hLRRK2* young flies in this thesis. Another independent study by Imai et al. (2008) showed that manipulations of the *Drosophila* homolog of *LRRK2* (*dLRRK)* also affect the levels of dopamine in fly heads. They determined that young *dLRRK* knock-out flies have elevated DA levels, while those that were expressing a mutation leading to increased kinase activity, *I1915T*, which is the homolog of the human *I2020T*, had reduced dopamine levels compared to the controls.

This early onset hyperactivity observed in young *TH>G2019S* could be only the first step towards the neurodegeneration, which is the hallmark of PD. The findings from this study support the theory that young *TH>G2019S* flies have defective dopaminergic signalling in their retina, and that could be a vital factor in starting the neurodegeneration cascade.

Taking into account the strong clinical association between *LRRK2-G2019S* and PD, the research interest focused on how the *G2019S* mutation affects the survival of the SNpc DA neurons *in vivo*. The initial hypothesis was that cells carrying the *G2019S* mutation have no robust transgene overexpression. Liu et al. (2015) overexpressed the wild type *LRRK2* and the *LRRK2-G2019S* selectively in mouse mid brain DA neurons utilising the tetracycline-dependent

binary expression system. In the *LRRK2-G2019S* model, a 6-fold increase in the LRRK2 protein expression was detected compared to the non-transgenic controls. Moreover, the dopamine levels were measured, and the *G2019S* mice were characterised by a significant reduction in dopamine content and release. That finding triggered the interest of researchers to proteins that are responsible for dopamine synthesis, transport and degradation, including dopamine vesicular monoamine transporters (*VMAT*), dopamine transporters (*DAT*) and aldehyde dehydrogenase 1 (*ALDH1A1*). Their findings support the hypothesis that the *LRRK2-G2019S* mutation supresses DA transmission by down-regulating key DA genes (Liu et al., 2015).

As described in Chapter 3, section 3.3.1, my findings agree with the ones previously published (Li et al., 2010; Lin et al., 2010; Lin et al., 2015). Using *Drosophila* heads, the flies carrying the *LRRK2-G2019S* mutation exhibit reduced dopamine levels in young age compared to the controls. That only confirms the interaction between *LRRK2* and dopamine, triggering our interest for further investigation.

6.3 LRRK2 and dopamine vesicular monoamine transporters (DVMATs)

While tetanus toxin has provided a good way to manipulate transmitter release from dopaminergic neurons, it would be good to support this with a second experimental manipulation. One way to achieve this might be to exploit the tools available with the transporters responsible for the DA take up from the extracellular space (*DAT*) and the package of DA into the synaptic vesicles-the vesicular monoamine transporters (*DVMAT*) (Krantz, 2006).

Since DA is synthesized in the cytoplasm, *VMATs* are responsible in all the aminergic neurons to transport the neurotransmitter out of the cytoplasm and into the lumen of synaptic vesicles. Inside these vesicles, the oxidation-prone dopamine is stable because of the acidic pH inside there. That prevents oxidative stress in the cytosol and the accumulation of the toxic by-products of the dopamine metabolism (Lawal et al., 2010; Meiser et al., 2013). The *VMAT*

transportation of DA from the cytoplasm into the synaptic vesicles is considered as neuroprotective. Invertebrates like *Drosophila melanogaster* contain a single *VMAT* gene providing a genetically tractable model to study the effects of *VMAT* on neurodegenerative processes (Lawal et al., 2010; Romero-Calderón et al., 2008).

The effects of increasing and blocking the vesicular transport could be examined in both the *G2019S* and *hLRRK2* background, in order to test for improvement or suppression of the visual function. The transport of DA into the synaptic vesicles could be blocked by manipulating two *dVMAT* loss of function alleles: $DVMAT^{P}$ and $DVMAT^{\Delta 14}$ (Lawal et al., 2010; Romero-Calderón et al., 2008). More recently (2014), two more loss of function mutations were created, the $DVMAT^{\Delta 3}$ and $DVMAT^{Y600A}$. The $DVMAT^{\Delta 3}$ is a deletion of the terminal 23 amino-acids of the *Drosophila VMAT*. This deletion disrupts known and predicted endocytosis signals proposed to be required for both de novo trafficking and recycling to synaptic vesicles following exocytosis at the synapse. The $DVMAT^{Y600A}$ is an alanine substitution mutant that disrupts a tyrosine-based sorting motif (Y600A) (Grygoruk et al., 2014). Moreover, overexpression of the wild type $DVMAT^{A}$ transgene could be used as a control, testing what effect the manipulation of DA packaging would have in visual function.

6.4 Utilising new binary expression systems in *Drosophila*

One of the greatest challenges in *Drosophila* genetics is the fact that using one binary expression system makes it very challenging to perform multiple tasks independently at the same time. For example, the use of the *Gal4-UAS* system alone, does not allow the expression of different transgenes in different cell types in the same animal. Having another binary transcriptional system would provide solutions to that limitation. Using two independent binary systems could allow the targeted expression of distinct transgenes under different expression patterns in the same animal. In addition, a complementary binary system in conjunction with *Gal4-UAS* has been very useful for mosaic analysis (Lai and Lee, 2006), GFP reconstruction across synaptic partners (Feinberg et al., 2008; Gordon and

Scott, 2009), and intersectional strategies for refining gene expression patterns (Shang et al., 2008).

Lai and Lee (2006) for the first time used two independent binary expression systems, providing insights in the *Drosophila* nervous system, by introducing the *LexA-LexAop* system. The transgenes of interest were put under the control of a basal promoter containing eight LexA binding sights (*LexAop*). Fusing LexA with VP16 or GAD, they obtained both GAL80-insensitive and GAL80-suppressible transcriptional factors that can efficiently drive the expression of LexAop-controlled transgenes *in vivo*. Different LexA drivers were used demonstrating how combining *Gal4* and *LexA* systems facilitate the dissection of the cellular and molecular networks in the *Drosophila* CNS. Since then many fly geneticists have started using dual binary expression systems (Yagi et al., 2010; Pfeiffer et al., 2010).

The creation of the new transgenic lines in this study will give us the opportunity to express at the same animal under different expression patterns the wild type *LRRK2* and the *G2019S*. That could shed new light on our understanding on how *LRRK2* functions and how the *G2019S* mutation could affect different cell types and regions of the *Drosophila* CNS. In addition, an interesting question that could be addressed would be how the simultaneous expression of *LRRK2* and *G2019S* affects the fly visual system. Moreover, the confirmed interaction between dopamine and *G2019S* can be further investigated by manipulating the DA receptors postsynaptically using the *Gal4-UAS* system while at the same time *LRRK2* or *G2019S* is expressed in the dopaminergic neurons of the fly using the *LexA-LexAop* system. There are many different ways that the newly created transgenic flies could be utilised in order to investigate the role of *G2019S* mutation in the pathogenesis of PD.

6.5 LRRK2 and Rab proteins interaction

Even though it has been more than 15 years that the role of *LRRK2* in the pathogenesis of PD was confirmed, it's actual function and localisation in the cell hasn't been established yet. The presence of all that different protein-protein interactions domains within the gene is an indication that this protein acts as a scaffold for several other proteins. Moreover, having two enzymatic domains within the gene contributes to its importance as a therapeutic target, as kinases has always been at the front for new drug discoveries. For that reasons *LRRK2* seems as very promising target that is targeted for new therapeutic interventions.

The other proteins that LRRK2 could phosphorylate and interact with has been of great interest for the last few years. This course of investigation focused on a genetic screening aiming to identify new LRRK2 substrates, and more specifically which of the Rab GTPase proteins interact with LRRK2 *in vivo*. Many Rab proteins have been identified interacting with LRRK2, with the first one being Rab7L1, which is itself a risk factor for PD (Dodson et al., 2002; MacLeod et al., 2013; Beilina et al., 2014). Rab5b has also been identified to physically interact with LRRK2, based on *in vitro* studies, which has a vital role in the early endosomal pathway (Shin et al., 2008; Yun et al., 2015). This interaction indicates that LRRK2 is present in the early endosomes, broadening our knowledge on the LRRK2 localisation, which has been so blurred so far. Moreover, Steger et al. (2016) identified Rab10, Rab1b and Rab8a as LRRK2 interactors, placing LRRK2 in the endoplasmic reticulum and Golgi trafficking to the synaptic vesicles. Within this sub-cellular trafficking pathway, Rab32 has also been identified as a LRRK2-mediated phosphorylation. In addition, Rab7, which is regulating the endo-lysosomal pathway has been identified, linking LRRK2 to the lysosomes.

Most of these Rabs have a confirmed role in the pathogenesis of PD; Rab1 (Cooper et al., 2006), Rab5a (Dalfo et al., 2004), Rab8a (Dalfo et al., 2004; Gitler et al., 2008), Rab3a (Dalfo et al., 2004; Gitler et al., 2008) and Rab10 (Steger et al., 2016). Among the other Rabs, several have been identified to

contribute to other neurodegeneration diseases. The identification of all these different Rab proteins pave the way for a new era of investigation, as LRRK2 focus now has shifted to vesicle trafficking and its role on that among with the other theories on its role in mitochondrial dysfunction, protein misfolding and aggregation and impaired autophagy-lysosome system.

From this thesis, six different Rabs were identified as LRRK2 interactors based on the *in vivo* analysis that was performed. Among the 21 *Rabs* that were screened, *Rab3, Rab5, Rab9, Rab10, Rab18* and *Rab40* were confirmed as *LRRK2* substrates. In addition, two *Rabs* were identified interacting with the dopaminergic neurons in the fly visual system including *Rab1* and *Rab19*. These *Rabs* regulate both the endo-lysosomal pathway and the Endoplasmic Reticulum-Golgi trafficking to the synaptic vesicles. That means that *LRRK2* plays a key role in both of the sub-cellular signaling pathways, confirming the original theory that *LRRK2* is really implicated in many different pathways.
Rab1 is located in the intermediate of ER-Golgi, regulating their traffic. Even though Rab1 has been identified as a LRRK2 interactor, its actual role in the pathogenesis of PD has not been very clear. On the other hand, Cooper et al. (2006) confirmed that the interaction of Rab1 and α-synuclein leads to PD, as Rab1 rescues the toxicity that is caused by the accumulation of α-synuclein. That aggregation of α-synuclein is cytotoxic, disrupting the ER-Golgi trafficking and they proved that overexpression of Rab1 protected the dopaminergic neuron loss induced by α-synuclein.

Rab3 is located in the synaptic vesicles, regulating their traffic to the plasma membrane and having a vital role in the exocytosis. Same as Rab1, it has been confirmed that LRRK2 phosphorylates this Rab protein, but its actual connection to the pathogenesis of PD has not been established. On the other hand, it was proved that α-synuclein co-localizes with Rab3a in the presynaptic membranes forming a complex with the actual role of Rab3 being regulating the α-synuclein distribution. Their results suggest that the membrane bound GTP-Rab3a stabilizes α-synuclein on the synaptic vesicles preventing the accumulation of this protein, indicating a protective role over the pathogenesis of PD (Chen et al., 2013).

As previously described, Rab5 is a key regulator of the early endosomal pathway and previous studies have linked it to both *SNCA* and *LRRK2*. Shin et al. (2008) determined the role of LRRK2 in the regulation of synaptic vesicles endocytosis by interacting with Rab5a. That sheds new insight on LRRK2 function, and helps us have a better understanding on the molecular pathway leading to the generation of PD.

Rab10 was only recently identified as a substrate of LRRK2-mediated phosphorylation (Steger et al., 2016; Ito et al., 2016) implicating this small Rab GTPase in the pathogenesis of PD. That places LRRK2 is the exocytosis pathway and its localization in the TNG-ER and synaptic vesicles, confirming previous studies that had already linked LRRK2 to these pathways.

The extensive genetic toolbox of *Drosophila* provides us with the appropriate tools to further investigate gene functions by performing knockout experiments. That tools give us the opportunity to test the role of Rab proteins by following loss of function strategies. One approach generating mutations and deletions within the *Drosophila* genome is the transposon-mediated mutagenesis. Utilising P-elements has many advantages, as more than two-thirds of all P-element insertions occur within 400 bp of transcription start-sites (Bellen et al., 2004; Spradling et al., 1999). Moreover, it is predicted that more than 80% of the *Drosophila* genes can be tagged and mutated with P-elements (Bellen et al., 2004). On the other hand, one disadvantage of P-elements is their insertional preference. One-third of all P-element insertions are not found in hot or medium-hotspots (which are defined as genes that ‘attract’ numerous P-element insertions).

Another approach for the inhibition of gene function that is widely used nowadays is by RNAi lines, enabling systematic surveys of gene function by reverse genetics. In that way, the function of almost every predicted gene can be disrupted and the obtained phenotype is assessed (Dietzl et al., 2007). This method is successfully used in *Drosophila* (Boutros et al., 2004) and mammalian cells (Berns et al., 2004; Paddison et al., 2004) in culture, enlightening our

knowledge on many basic cellular processes. In *Drosophila* the expression of RNAi is cell autonomous and it can be triggered by the expression of a long double stranded 'hairpin' RNA from a transgene that contains a gene fragment cloned as an inverted repeat. By utilizing the *Gal4-UAS* binary expression system, RNAi transgenes can trigger the inactivation of the gene of interest in any desired cell type and during any stage of the animal's lifespan.

In overall, these results indicate that Rabs could be regarded as novel biomarkers or therapeutic targets in order to halt or at least slow down the progression of PD. In addition, discovery of other interactors for LRRK2 could be crucial for a better understanding of physiological functions of LRRK2 and pathogenic mechanisms of PD as well as for development of novel therapeutic treatments. For further investigation, RNAi, dominant-negative and constantly active Rab lines of the identified Rab interactors could be used in order to determine the resulting phenotypic consequences occurring through their manipulation.

6.6 LRRK2 and its effect on the neuronal outgrowth

Expressing the *LRRK2-G2019S* in hiPSCs cell lines from PD patients determined that the differentiation of DA neurons is happening but it displays morphological defects compared to the controls. After 1, 3 and 5 days of neuronal differentiation, the *G2019S* mutated cells have a more complex neuritic arborisation and also shorter total neurite length at day 5 in contrast to the controls (Borgs et al., 2016). Those results are similar to previous cell culture experiments at older time points, which also showed reduced neuritic length that is the hallmark of PD (Gillardon et al., 2009; MacLeod et al., 2006).

MacLeod et al. (2006) established the role of *LRRK2* in neuronal outgrowth. Overexpression of the *LRRK2-G2019S* mutation led to a reduction in neuron process length and complexity and the accumulation of tau-positive inclusions with lysosomal characteristics ultimately leading to increased apoptosis and autophagy. On the other hand, suppression of *LRRK2* by using shRNAs led to the opposite phenotype showing increased neurite process length and complexity.

Zou et al. (2015) using C. *elegans* and *Drosophila* as animal models showed that *Rab10* is also required for the growth and branching of higher-order dendrites in PVD neurons. Loss of function mutations of *Rab10* led to severe dendrite arborisation defects in the proximal region of PVD neurons. Those findings were consistent with Taylor et al (2015) who established that *Rab10* mutants led to dramatic dendritic morphogenesis defects in the PVD neurons. These discoveries suggest a role of *Rab10* in branch outgrowth and in the regulation of the distribution of branching activity along the dendrite. The confirmed interaction between *Rab10* and *LRRK2-G2019S* while both genes play vital role in neuronal outgrowth could shed new light on our understanding of the molecular pathway leading to the loss of the dopaminergic neurons in PD.

The implication of autophagy in the maintenance of neurite length has been associated with the neuropathology of PD (Sanchez-Danes et al., 2012; Menzies et al., 2011; Yang and Mao, 2010). Borgs et al. (2006) detected the induction of autophagy at 7 days of differentiation in cells expressing the *G2019S* mutation contributing to neurite length defects with increased branching complexity at early developmental stages. At later developmental stages, DA neurons differentiated from PD hiPSCs display decreased branching complexity indicating a cellular pathotoxicity that could result from increased oxidative stress and impaired autophagy that contributes to the vulnerability of the DAergic neurons.

That agrees with my hypothesis of early hyperactivity of the *G2019S* flies proposing elevated ATP demand and ROS production, which contributes at later stages to the degeneration of DA neurons. Hindle et al. (2013) provided evidence that expressing the *G2019S* mutation in flies increased autophagy and apoptosis in the outer part of the photoreceptors in old flies (22 day old flies) while 28 day old flies exhibited dilated mitochondria in the photoreceptors. These data suggest an increase in the energy demand contributing to neurodegeneration. All these studies contribute to the in depth understanding of the pathophysiology underlying the *LRRK2* mutations contributing to neurodegeneration.

6.7 Conclusion

Throughout this thesis, biochemical assays and SSVEPs have been utilised to record the visual responses of flies carrying the *G2019S* mutation. Together, these approaches have provided us with a rapid assay of the role that the *G2019S* mutation has in the pathogenesis of PD. Using *Drosophila* visual system as an animal model gave us the opportunity to investigate the role of LRRK2 and in that way we could begin to understand the role that LRRK2 plays within the human visual system. Applying the same SSVEP approach in humans carrying this common mutation will enable us to confirm if the findings that we have seen in flies directly relates to LRRK2-linked PD in humans. In this thesis the findings from Afsari et al. (2014) were confirmed, where young *TH>G2019S* flies have abnormal SSVEPs, providing us the opportunity to apply SSVEP in humans in order to identify people who might be at risk of developing PD before even they manifest any symptoms.

The key results and conclusions of this study are summarised as follows:

1. The *TH>G2019S* young flies exhibit an early hyperactivity that could be the first step towards neurodegeneration. 1 day old *G2019S* flies display elevated visual responses compared to *LRRK2* and other controls.

2. Expression of TNT in conjunction with *G2019S*, only confirmed the early excitotoxicity pathway, as in young flies co-expression of *G2019S* and TNT reduced the visual responses in contrast to *LRRK2* and *w-* flies.

3. Detection of dopamine levels from fly heads revealed reduced DA levels in young *G2019S* flies compared to the normal higher DA levels in controls.

4. The generation of the new transgenic flies expressing *LRRK2* and *G2019S* under the control of LexA, will pave the way for the design of a

whole new era of experiments, where two different transgenes will be expressed in the same animal by combining the *Gal4-UAS* and LexA-*LexAop* binary systems.

5. The *LRRK2* and *Rab* GTPases genetic screening that was performed, provided for the first time an *in vivo* analysis, identifying new *LRRK2* substrates. From that screening six Rab proteins were linked to the *G2019S* mutation, including *Rab3*, *Rab5*, *Rab9*, *Rab10*, *Rab18*, and *Rab40*, while *Rab1* and *Rab19* were linked to dopaminergic neurotransmission. That discovery provides new insights into the *LRRK2* function, broadening our knowledge on the underlying molecular pathway contributing to the pathogenesis of PD.

Abbreviations:

α-Syn	Alpha-Synuclein
AADC	**A**romatic **a**mino acid **dec**arboxylase
AC	**A**denylyl **c**yclase
AD	**A**utosomal **d**ominant
ADHD	**A**ttention **d**eficit **h**yperactivity **d**isorder
ALS	**A**myotrophic **L**ateral **S**clerosis
ANK	**Ank**yrin-like repeat
ANOVA	**An**alysis **o**f **Va**riance
AR	**A**utosomal **r**ecessive
BH4	Tetrahydrobiopterin
cAMP	**C**yclic 3,5 **a**denine-**m**ono**p**hosphate
COMT	**C**atechol-**o**-**m**ethyl-**t**ransferase
COR	**C**-terminal **o**f **R**OC
CNS	**C**entral **n**ervous **s**ystem
CyO	**C**url**y** of **O**ster
DA	**D**op**a**mine
DBS	**D**eep **b**rain **s**timulation
ddH_20	Double distilled water
dH_2O	Distilled water
DVMAT	**D**opamine **v**esicular **m**onoamine **t**ransporter
E	Epinephrine
EDTA	**E**thylene**d**iamine**t**etraacetic **a**cid
EMS	**E**thyl **m**ethane**s**ulphonate
EOPD	**E**arly **o**nset **P**arkinson's **d**isease
EtOH	Ethanol
ER	**E**ndoplasmic **r**eticulum
FTD	**F**rontotemporal **d**ementia

GAP	**G**TPase **a**ctivating **p**rotein
GDP	**G**uanosine-5'-**di**p**p**hosphate
GEF	**G**uanine **e**xchange **f**actor
GPCRs	**G**-**p**rotien **c**oupled **r**eceptors
GMR	**G**lass **M**ultimer **R**eporter
GST	**G**lutathione-**S t**ransferase
GTP	**G**uanosine-5'-**t**ri**p**hosphate
GTPCH	**GTP c**yclo**h**ydrolase
GWAS	**G**enome **w**ide **a**ssociation **s**tudies
HD	**H**untington **d**isease
IPD	**I**diopathic **P**arkinson's **d**isease
KD	**K**inase **d**ead
LB	**L**uria **B**roth
L-DOPA	Levodopa
LexAop	LexA operator
LOPD	**L**ate **o**nset **P**arkinon's **d**isease
LRR	**L**eucine-**r**ich **r**epeats
LRRK2	**L**eucine-**r**ich **r**epeat **K**inase **2**
MAO	**M**ono**a**mine **o**xidase
MAPK	**M**itogen-**A**ctivated **P**rotein **K**inase
MAPT	**M**icrotubule **A**ssociated **P**rotein **T**au
mRNA	**m**essenger RNA
Mi	**M**edulla **i**ntrinsic
MS	**M**ultiple **S**clerosis
NE	**N**or**e**phinephrine
NMJ	**N**euro**m**uscular **J**unction
nSyb	**n**euronal Synaptobrevin
PBS	**P**hosphate **B**uffered **S**aline

PBS-T	**P**hosphate **B**uffered **S**aline with detergent **T**ween 20
PCR	**P**olymerase **C**hain **R**eaction
PD	**P**arkinson's **d**isease
PIGD	**P**ostural **i**mbalance and **g**ait **d**isorder
PKA	Protein Kinase dependent of cAMP
Rab	**Ra**s related in **B**rain
RabGGT	**Rab G**eranyl **G**eranyl **T**ransferase
REM	**R**apid-**e**ye **m**ovement
REP	**R**ab **E**scort **P**rotein
Rh1	**Rh**odopsin **1**
RNAi	**RNA i**nterference
ROC	**R**as **o**f **c**omplex proteins
ROS	**R**eactive **O**xygen **S**pecies
RT	**R**oom **T**emperature
SDS	**S**odium **D**odecyl **S**ulphate
SEM	**S**tandard **E**rror of **M**ean
siRNA	**s**mall **i**nterferring **RNA**
SNARE	**S**oluble **N**-ethylmaleimide-sensitive factor attachment protein **Re**ceptor
SNCA	α-synuclein
SNpc	**S**ubstantia **n**igra **p**ars **c**ompacta
TH	**T**yrosine **h**ydroxylase
TGN	**T**rans-**G**olgi **n**etwork
T_m	**m**elting **T**emperature
Tris-HCl	**Tris** (hydroxymethyl) aminomethane hydrochloride
TNT	**T**etanus **T**oxin
TS	**T**ourette **S**yndrome
UAS	**U**pstream **A**ctivator **S**equence

VMAT	**V**esicular **m**onoamine **t**ransporter
WD40	Beta-transducin repeat
WT	**W**ild**t**ype

References

ABCAM. 2016. General western blot protocol (Online). Available: http://www.abcam.com/protocols/general-western-blot-protocol [Accessed 15 May 2016].

Abeliovich, A., Schmitz, Y., Farinas, I., Choi-Lundberg, D., Ho, W.H., Castillo, P.E., Shinsky, N., Verdugo, J.M., Armanini, M., Ryan, A., Hynes, M., Phillips, H., Sulzer, D., Rosenthal, A. (2000). Mice lacking alpha-synuclein display functional deficits in the nigrostriatal dopamine system. *Neuron*, 25:239–252.

Adams, MD., Celniker, SE., Holt, RA., Evans, CA., Gocayne, JD., Amanatides, PG., Scherer, SE., Li, PW., Hoskins, RA., Galle, RF., George, RA., Lewis, SE., Richards, S., Ashburner, M., Henderson, SN., Sutton, GG., Wortman, JR., Yandell, MD., Zhang, Q., Chen, LX., Brandon, RC., Rogers, YH., Blazej, RG., Champe, M., Pfeiffer, BD., Wan, KH., Doyle, C., Baxter, EG., Helt, G., Nelson, CR., Gabor, GL., Abril, JF., Agbayani, A., An, HJ., Andrews-Pfannkoch, C., Baldwin, D., Ballew, RM., Basu, A., Baxendale, J., Bayraktaroglu, L., Beasley, EM., Beeson, KY., Benos, PV., Berman, P., Bhandari, D., Bolshakov, S., Borkova, D., Botchan, MR., Bouck, J., Brokstein, P., Brottier, P., Burtis, KC., Busam, DA., Butler, H., Cadieu, E., Center, A., Chandra, I., Cherry, JM., Cawley, S., Dahlke, C., Davenport, LB., Davies, P., de Pablos, B., Delcher, A., Deng, Z., Mays, AD., Dew, I., Dietz, SM., Dodson, K., Doup, LE., Downes, M., Dugan-Rocha, S., Dunkov, BC., Dunn, P., Durbin, KJ., Evangelista, CC., Ferraz, C., Ferriera, S., Fleischmann, W., Fosler, C., Gabrielian, AE., Garg, NS., Gelbart, WM., Glasser, K., Glodek, A., Gong, F., Gorrell, JH., Gu, Z., Guan, P., Harris, M., Harris, NL., Harvey, D., Heiman, TJ., Hernandez, JR., Houck, J., Hostin, D., Houston, KA., Howland, TJ., Wei, MH., Ibegwam, C., Jalali, M., Kalush, F., Karpen, GH., Ke, Z., Kennison, JA., Ketchum, KA., Kimmel, BE., Kodira, CD., Kraft, C., Kravitz, S., Kulp, D., Lai, Z., Lasko, P., Lei, Y., Levitsky, AA., Li, J., Li, Z., Liang, Y., Lin, X., Liu, X., Mattei, B., McIntosh, TC., McLeod, MP., McPherson, D., Merkulov, G., Milshina, NV., Mobarry, C., Morris, J., Moshrefi, A., Mount, SM., Moy, M., Murphy, B., Murphy, L., Muzny, DM., Nelson, DL., Nelson, DR., Nelson, KA., Nixon, K., Nusskern, DR., Pacleb, JM., Palazzolo, M., Pittman, GS., Pan, S., Pollard, J., Puri, V., Reese, MG., Reinert, K., Remington, K., Saunders, RD., Scheeler, F., Shen, H., Shue, BC., Sidén-Kiamos, I., Simpson, M., Skupski, MP., Smith, T., Spier, E., Spradling, AC., Stapleton, M., Strong, R., Sun, E., Svirskas, R., Tector, C., Turner, R., Venter, E., Wang, AH., Wang, X., Wang, ZY., Wassarman, DA., Weinstock, GM., Weissenbach, J., Williams, SM., Woodage, T., Worley, KC., Wu, D., Yang, S., Yao, QA., Ye, J., Yeh, RF., Zaveri, JS., Zhan, M., Zhang, G., Zhao, Q., Zheng, L.,

Zheng, XH., Zhong, FN., Zhong, W., Zhou, X., Zhu, S., Zhu, X., Smith, HO., Gibbs, RA., Myers, EW., Rubin, GM., Venter, JC. (2000). The genome sequence of Drosophila melanogaster. *Science*, 287:2185–2195.

Adams, M. D., Sekelsky, J. J. (2002). From sequence to phenotype: reverse genetics in Drosophila melanogaster. *Nat Rev Genet*, 3:189-98.

Afsari, F., Christensen, K., Smith, G., Hentzer, M., Nippe, O., Elliott, C., Wade, A. (2014). Abnormal nisual gain control in a Parkinson's disease model. *Hum Mol Genet,* 23(17): 4465-4478.

Agola, J.O., Jim, P.A., Ward, H.H., Basuray, S., and Wandinger-Ness, A. (2011). Rab GTPases as regulators of endocytosis, targets of disease and therapeutic opportunities. *Clin Genet,* 80:305-318.

Alegre-Abarrategui, J., Christian, H., Lufino, MM., Mutihac, R., Venda, LL., Ansorge, O., Wade-Martins, R. (2009). LRRK2 regulates autophagic activity and localizes to specific membrane microdomains in a novel human genomic reporter cellular model. *Hum Mol Genet,* 18(21):4022-4034.

Alekseyenko, O.V., Chan, Y., Li, R., Kravitz, E.A. (2013). Single dopaminergic neurons that modulate aggression in *Drosophila*. *PNAS*, 110(15): 6151-6156.

Alexandrov, K., Horiuchi, H., Steele-Mortimer, O., Seabra, M., Zerial, M. (1994). Rab escort protein-1 is a multifunctional protein that accompanies newly prenylated rab proteins to their target membranes. *EMBO J*, 13:5262–5273.

Ali, B.R., Wasmeier, C., Lamoreux, L., Strom, M., and Seabra, M.C. (2004). Multiple regions contribute to membrane targeting of Rab GTPases. *J Cell Sci*, 117:6401-6412.

Aligianis, I., Johnson, C., Gissen, P., Chen, D., Hampshire, D., Hoffmann, K., Maina, E., Morgan, N., Tee, L., Morton, J., Ainsworth, J., Horn, D., Rosser, E., Cole, T., Stolte-Dijkstra, I., Fieggen, K., Clayton-Smith, J., Mégarbané, A., Shield, J., Newbury-Ecob, R., Dobyns, W., Graham, JJ., Kjaer, K., Warburg, M., Bond, J., Trembath, R., Harris, L., Takai, Y., Mundlos, S., Tannahill, D., Woods, C., Maher, E. (2005). Mutations of the catalytic subunit of RAB3GAP cause Warburg Micro syndrome. *Nat Genet*, 37:221–223.

Alnemri, ES. (2007). HtrA2 and Parkinson's disease: think PINK? *Nat Cell Biol*, 9(11):1227-1229.

Alter, S.P., Lenzi, GM., Bernstein, AI., Miller, GW. (2013). Vesicular integrity in Parkinson's disease. *Curr Neurol Neurosci Rep,* 13:362.

Andalib, S., Vafaee, M.S., Gjedde, A. (2014). Parkinson's disease and mitochondrial gene variations: A review, *J Neurol Sci*, 346(1-2):11-19.

Andres, D., Seabra, M., Brown, M., Armstrong, S., Smeland, T., Cremers, F., Goldstein, J. (1993). cDNA cloning of component A of Rab geranylgeranyl transferase and demonstration of its role as a Rab escort protein. *Cell*, 73:1091–1099.

Archibald, N.K., Clarke, M.P., Mosimann, U.P., Burn, D.J. (2009). The retina in Parkinson's disease. *Brain,* 132: 1128–1145.

Archibald, NK., Clarke, MP., Mosimann, UP., Burn, D. (2011). Visual Symptoms in Parkinson's Disease and Parkinson's Disease Dementia. *Mov Disord*, 26:2387-2395.

Ashburner, M., Golic, K., Hawley, S. *Drosophila* (2004). A Laboratory Handbook. New Jersey: Cold Spring Harbor Laboratory Press; 2004.

Bailey, RM., Covy, JP., Melrose, HL., Rousseau, L., Watkinson, R., Knight, J., Miles, S., Farrer, MJ., Dickson, DW., Giasson, BI., Lewis, J. (2013). LRRK2 phosphorylates novel tau epitopes and promotes tauopathy. *Acta Neuropathol*, 126(6):809-827.

Bancher, C., Braak, H., Fischer, P., Jellinger, K.A. (1993). Neuropathological staging of Alzheimer lesions and intellectual status in Alzheimer's and Parkinson's disease patients. *Neurosci Lett,* 162:179–82.

Bang, S., Hyun, S., Hong, S.T., Kang, J., Jeong, K., Park, J., Choe, J., Chung J., (2011). Dopamine Signalling in Mushroom bodies regulates temperature-preference behaviour in *Drosophila*. *PLoS genet,* 7(3): e1001346.

Bardien, S., Lesage, S., Brice, A., Carr, J. (2011). Genetic characteristics of leucine-rich repeat kinase 2 (LRRK2) associated Parkinson's disease. *Parkinsonism Relat Disord,* 17:501–508.

Barr, F., Lambright, DG. (2010). Rab GEFs and GAPs. *Curr Opin Cell Biol*, 22(4):461-470.

Bassett, AR., Tibbit, C., Ponting, CP., Liu, JL. (2013). Highly Efficient Targeted Mutagenesis of *Drosophila* with the CRISPR/Cas9 System. *Cell Reports*, 4(1): 220–228.

Baumert, M., Maycox, PR., Navone, F., De Camilli, P., Jahn, R.(1989). Synaptobrevin: an integral membrane protein of 18,000 daltons present in small synaptic vesicles of rat brain. *EMBO J*, (2):379-84.

Bedford, C., Sears, C., Perez-Carrion, M., Piccoli, G., Condliffe, SB. (2016). LRRK2 Regulates Voltage-Gated Calcium Channel Function. *Front Mol Neurosci*, 9:35.

Beilina, A., Rudenko, IN., Kaganovich, A., Civiero, L., Chau, H., Kalia, SK., Kalia, LV., Lobbestael, E., Chia, R., Ndukwe, K., Ding, J., Nalls, MA.; International Parkinson's Disease Genomics Consortium; North American Brain Expression Consortium, Olszewski, M., Hauser, DN., Kumaran, R., Lozano, AM., Baekelandt, V., Greene, LE., Taymans, JM., Greggio, E., Cookson, MR. (2014). Unbiased screen for interactors of leucine-rich repeat kinase 2 supports a common pathway for sporadic and familial Parkinson disease. *Proc Natl Acad Sci USA*, 111(7):2626-2631.

Bem, D., Yoshimura, S., Nunes-Bastos, R., Bond, FC., Kurian, MA., Rahman, F., Handley, MT., Hadzhiev, Y., Masood, I., Straatman-Iwanowska, AA., Cullinane, AR., McNeill, A., Pasha, SS., Kirby, GA., Foster, K., Ahmed, Z., Morton, JE., Williams, D., Graham, JM., Dobyns, WB., Burglen, L., Ainsworth, JR., Gissen, P., Müller, F., Maher, ER., Barr, FA., Aligianis, IA. (2011). Loss-of-function mutations in RAB18 cause Warburg micro syndrome. *Am J Hum Genet*, 88:499–507.

Ben-Jonathan, N. (1985). Dopamine: a prolactin-inhibiting hormone. *Endocr Rev,* 6(4):564-589.

Bellen, H.J., Levis, R.W., Liao, G., He, Y., Carlson, J.W., Tsang, G., Evans-Holm, M., Hiesinger, R., Schulze, K.L., Rubin, G.M., Hoskins, R.A., and Spradling, A.C. (2004). The BDGP gene disruption project: single transposon insertions associated with 40% of *Drosophila* genes. *Genetics*, 167:761–781.

Berger, Z., Smith, KA., Lavoie, MJ. (2010). Membrane localization of LRRK2 is associated with increased formation of the highly active LRRK2 dimer and changes in its phosphorylation. *Biochem,* 49(26):5511-5523.

Berns, K., Hijmans, E.M., Mullenders, J., Brummelkamp, T.R., Velds, A., Heimerikx, M., Kerkhoven, R.M., Madiredjo, M., Nijkamp, W., Weigelt, B., Agami, R., Ge, W., Cavet, G., Linsley, P.S., Beijersbergen, R.L., Bernards, R. (2004). A large-scale RNAi screen in human cells identifies new components of the p53 pathway. *Nature*, 428: 431–437.

Biskup. S., Moore, DJ., Celsi, F., Higashi, S., West, AB., Andrabi, SA., Kurkinen, K., Yu, SW., Savitt, JM., Waldvogel, HJ., Faull, RL., Emson, PC., Torp, R., Ottersen, OP., Dawson, TM., Dawson, VL. (2006). Localization of LRRK2 to membranous and vesicular structures in mammalian brain. *Ann Neurol,* 60(5):557-569.

Blascko, H. (1939). The specific action of L-dopa decarboxylase. *J Physiol*, 96 (50): 50-51.

Blaschko, H. (1942). The activity of l(-)-dopa decarboxylase. *J Physiol*, 101 (3):337–349.

Borgs, L., Peyre, E., Alix, P., Hanon, K., Grobarczyk, B., Godin, J.D., Purnelle, A., Krusy, N., Maquet, P., Lefebvre, P., Seutin, V., Malgrange, B., and Nguyen, L. (2016). Dopaminergic neurons differentiating from LRRK2 G2019S induced pluripotent stem cells show early neuritic branching defects. *Sci Rep,* 6:33377.

Borst, A. (2014). Fly visual course control: behaviour, algorithms and circuits. *Nature Rev Neurosci,* 15:590-599.

Bonifati, V., Rizzu, P., van Baren, MJ., Schaap, O., Breedveld, GJ., Krieger, E., Dekker, MC., Squitieri, F., Ibanez, P., Joosse, M., van Dongen, JW., Vanacore, N., van Swieten, JC., Brice, A., Meco, G., van Duijn, CM., Oostra, BA., Heutink, P. (2003). Mutations in the DJ-1 gene associated with autosomal recessive early-onset parkinsonism. *Science*, 299(5604):256-259.

Bonini, NM., Fortini, ME. (2003). Human neurodegenerative disease modeling using Drosophila. *Annu Rev Neurosci*, 26:627–659.

Boutros, M., Kiger, A.A., Armknecht, S., Kerr, K., Hild, M., Koch, B., Haas, S.A., Paro, R., Perrimon, N., Heidelberg Fly Array Consortium. (2004). Genome-wide RNAi analysis of growth and viability in *Drosophila* cells. *Science,* 303:832–835.

Bowen, FP., Hoehn, MM., Yahr, MD. (1972). Parkinsonism: alterations in spatial orientation as determined by a route-walking test. *Neuropsychologia*, 10: 355–61.

Braak, H., Del Tredici, K., Rub, U., de Vos, R.A., Jansen-Steur, E.N., Braak, E. (2003). Staging of brain pathology related to sporadic Parkinson's disease. *Neurobiol Aging,* 24:197–211.

Brand, A.H., and Perrimon, N. (1993). Targeted gene expression as a means of altering cell fates and generating dominant phenotypes. *Development*, 118:401-415.

Broadie, K., Prokop, A., Bellen, H.J., O'Kane, C.J., Schulze, K.L.,Sweeney, S.T. (1995). Syntaxin and synaptobrevin function downstream of vesicle docking in *Drosophila*. *Neuron*, 15:663–673.

Brouns, SJ., Jore, MM., Lundgren, M., Westra, ER., Slijkhuis, RJ., Snijders, AP., Dicjman, MJ., Makarova, KS., Koonin, EV, Van der Ooost, J. (2008). Small CRISPR RNAs guide antiviral defense in prokaryotes. *Science,* 321(5891):960- 964.

Bui, M., Gilady, S.Y., Fitzsimmons, R.E., Benson, M.D., Lynes, E.M., Gesson, K., Alto, N.M., Strack, S., Scott, J.D., Simmen, T. (2010). Rab32 modulates apoptosis onset and mitochondria-associated membrane (MAM) properties. *J Biol Chem,* 285(41):31590-602.

Burman, J.L, Yu, S., Poole, A.C., Decal, R.B., Pallanck, L. (2012). Analysis of neural subtypes reveals selective mitochondrial dysfunction in dopaminergic neurons from parkin mutants. *PNAS,* 109(26): 10438-10443.

Cajal, S.R.S.D. (1915). Contribucion al conocimiento de los centros nerviosos de los insectos. *Trab Lab Inv Biol,* 13:1-68.

Cajal, S.R., and Sanchez, D. (1915). Contribucion al conocimiento de los centros nerviosos del los insectos. *Trab Lab Invest Biol,* 13:1–167.

Calabresi, P., Picconi, B., Tozzi, A., Di Filippo, M. (2007). Dopamine-mediated regulation of corticostriatal synaptic plasticity. *Trends Neurosci,* 30(5):211-219.

Calcagno, B., Eyles, D., van Alphen, B., van Swinderen, B. (2013). Transient activation of dopaminergic neurons during development modulates visual responsiveness, locomotion and brain activity in a dopamine ontogeny model of schizophrenia. *Transl Psychiatry,* 2:e2026

Calero, M., Chen, C.Z., Zhu, W., Winand, N., Havas, K.A., Gilbert, P.M., Burd, C.G., Collins, R.N. (2003). Dual prenylation is required for Rab protein localization and function. *Mol Biol Cell,* 14:1852-1867.

Campos-Ortega, JA., Hartenstein, V. (1997). The Embryonic Development of Drosophila Melanogaster. *Berlin and Heidelberg: Springer Verlag;* 1997.

Carlsson, A. (2003). Nobel Lectures. In A Half-Century of Neurotransmitter Research: Impact on Neurology and Psychiatry. Edited by Jörnvall H. Singapore: World Scientific Publishing Co.; 2003:303.

Carney, DS., Davies, BA., Horazdovsky, BF. (2006). Vps9 domain-containing proteins: activators of Rab5 GTPases from yeast to neurons. *Trends Cell Biol*, 16(1):27-35.

Cauchi, RJ. and Van den Heuvel, M. (2006). The fly as a model for neurodegenerative diseases: is it worth the jump*? Neurodegener Dis*, 3(6):338-356.

Chan, CC., Scoggin, S., Wang, D., Cherry, S., Dembo, T., Greenberg, B., Jin, EJ.,
Kuey, C., Lopez, A., Mehta, SQ., Perkins, TJ., Brankatschk, M., Rothenfluh, A., Buszczak, M., Hiesinger, PR. (2011). Systematic discovery of Rab GTPases with synaptic functions in *Drosophila*. *Curr Biol*, 21(20):1704-15.

Chan, C.S., Gertler, T.S., Surmeier, D.J., (2009). Calcium homeostasis, selective vulnerability and Parkinson's disease. *Trends Neurosci*, 32(5): 249–56.

Chaudhuri, KR., Healy, DG., Schapira, AHV. (2006). Non-motor symptoms of Parkinson's disease: diagnosis and management. *Lancet Neurol*, 5: 235–245.

Chaudhuri, KR., Schapira, A.HV., (2009). Non-motor symptoms of Parkinson's disease: Dopaminergic pathophysiology and treatment. *Lancet Neurol*, 8(5) 464-474.

Chavrier, P., Gorvel, J.P., Stelzer, E., Simons, K., Gruenberg, J., Zerial, M. (1991). Hypervariable C-terminal domain of rab proteins acts as a targeting signal. *Nature*, 353:769-772.

Chen, CY., Weng, YH., Chien, KY., Lin, KJ., Yeh, TH., Cheng, YP., Lu, CS., Wang, HL. (2012) (G2019S) LRRK2 activates MKK4-JNK pathway and causes degeneration of SN dopaminergic neurons in a transgenic mouse model of PD. *Cell Death Differ*, 19(10):1623-33.

Chen, RH., Wislet-Gendebien, S., Samuel, F., Visanji, NP., Zhang, G., Marsilio, D., Langman, T., Fraser, PE., Tandon, A. (2013). α-Synuclein membrane association is regulated by the Rab3a recycling machinery and presynaptic activity. *J Biol Chem*, 288(11):7438-7449.

Chuang, C.L., Lu, Y.N., Wang, H.C., and Chang, H.Y. (2014). Genetic dissection reveals that Akt is the critical kinase downstream of LRRK2 to

phosphorylate and inhibit FOXO1, and promotes neuron survival. *Hum Mol Genet,* 23 (21): 5649–5658.

Chung, J.M., Spencer, A.N., Gahm. K.H. (1989). Dopamine in tissues of the hydrozoan jellyfish *Polyorchis penicillatus* as revealed by HPLC and GC-MS. *J Comp Physiol B,* 159:173-181.

Chyb, S., Raghu, P., Hardie, RC. (1999). Polyunsaturated fatty acids activate the Drosophila light-sensitive channels TRP and TRPL. *Nature,* 397(6716):255-259.

Cottrell, GA. (1967). Occurrence of dopamine and noradrenaline in the nervous tissue of some invertebrate species. *Br J Pharmacol Chemother,* 29: 63–69.

Colicelli, J. (2004). Human RAS superfamily proteins and related GTPases. *Sci STKE,* (250):RE13.

Collins, R. (2003). "Getting it on"–GDI displacement and small GTPase membrane recruitment. *Mol Cell,* 12:1064–1066.

Cookson, MR., Xiromerisiou, G., Singleton, A. (2005). How genetics research in Parkinson's disease is enhancing understanding of the common idiopathic forms of the disease. *Curr Opin Neurol,* 18:706–711.

Cookson, M.R., Hardy, J., Lewis, P.A., (2008). Genetic Neuropathology of Parkinson's Disease. *Int J Clin Exp Pathol,* 1(3): 217–231.

Cookson, M.R. (2010). The role of leucine-rich repeat kinase 2 (LRRK2) in Parkinson's disease. *Neurosci,* 11:791- 797.

Cooper, AA., Gitler, AD., Cashikar, A., Haynes, CM., Hill, KJ., Bhullar, B., Liu, K., Xu, K., Strathearn, KE., Liu, F., Cao, S., Caldwell, KA., Caldwell, GA., Marsischky, G., Kolodner, RD., Labaer, J., Rochet, JC., Bonini, NM., Lindquist, S. (2006). Alpha-synuclein blocks ER-Golgi traffic and Rab1 rescues neuron loss in Parkinson's models. *Science,* 313(5785):324-328.

Cong, L., Ran, FA., Cox, D., Lin, S., Barretto, R., Habib, N., Hsu, PD., Wu, X., Jiang, W., Marraffini, LA., Zhang, F. (2013). Multiplex genome engineering using CRISPR/Cas systems. *Science,* 339(6121):819-823.

Crooks, J., Kolb, H. (1992). Localization of GABA, glycine, glutamate and tyrosine hydroxylase in the human retina. *J Compar Neurol,* 315:287-302.

Coulom, H., Birman, S. (2004). Chronic exposure to rotenone models sporadic Parkinson's disease in Drosophila melanogaster. *J Neurosci*, 24(48):10993-10998.

Dächsel, JC1., Taylor, JP., Mok, SS., Ross, OA., Hinkle, KM., Bailey, RM., Hines, JH., Szutu, J., Madden, B., Petrucelli, L., Farrer, MJ. (2007). Identification of potential protein interactors of Lrrk2. *Parkinsonism Relat Disord*, 13(7):382-385.

Dachsel, JC., Farrer, MJ. (2010). LRRK2 and Parkinson disease. *Arch Neurol*, 67(5):542-547.

Dahlem1, TJ., Hoshijima1, K., Jurynec1, MJ., Gunther1, D., Starker, CG., Locke1, AS., Weis1, AM. , Voytas, DF., Grunwald1, DJ. (2012). Simple Methods for Generating and Detecting LocusSpecific Mutations Induced with TALENs in the Zebrafish Genome. *PLOS Genetics*, 8(8): e1002861.

Dahmann, C. (2008). *Drosophila*: Methods and Protocols. New York: Humana Press; 2008.

Dalfó, E., Gómez-Isla, T., Rosa, J., Nieto Bodelón, M., Cuadrado Tejedor, M., Barrachina, M., Ambrosio, S., Ferrer, I. (2004). Abnormal alpha-synuclein interactions with Rab proteins in alpha-synuclein A30P transgenic mice. *J Neuropathol Exp Neurol*, 63:302–313.

Davie, C.A. (2008). A review of Parkinson's disease. *Br Med Bull*, 86: 109-127.

Dejgaard, SY., Murshid, A., Erman, A., Kizilay, O., Verbich, D., Lodge, R., Dejgaard, K., Ly-Hartig, TB., Pepperkok, R., Simpson, JC., Presley. JF. (2008). Rab18 and Rab43 have key roles in ER-Golgi trafficking. *J Cell Sci*, 121(16):2768-81.

De Luca, A., Progida, C., Spinosa, M.R., Alifano, P., and Bucci, C. (2008). Characterization of the Rab7K157N mutant protein associated with Charcot-Marie-Tooth type 2B. *Biochem Biophys Res Commun*, 372:283-287.

De Vos, K.J., Grierson, A.J., Ackerley, S., Miller, C.C. (2008) Role of axonal transport in neurodegenerative diseases. *Annu Rev Neurosci*, 31:151–173.

Del Toro, D., Alberch, J., Lazaro-Dieguez, F., Martin-Ibanez, R., Xifro, X., Egea, G., and Canals, J.M. (2009). Mutant huntingtin impairs post-Golgi trafficking to lysosomes by delocalizing optineurin/Rab8 complex from the Golgi apparatus. *Mol Biol Cell*, 20:1478-1492.

Delprato, A., Merithew, E. and Lambright, DG. (2004). Structure, exchange determinants, and family-wide rab specificity of the tandem helical bundle and Vps9 domains of Rabex-5. *Cell*, 118(5):607-617.

Desnoyers, L., Anant, J., Seabra, M. (1996), Geranylgeranylation of Rab proteins. *Biochem Soc Trans*, 24:699–703.

Dickson, BJ. (2008). Wired for sex: the neurobiology of Drosophila mating decisions. *Science*, 322(5903):904-909.

Dietzl, G., Chen, D., Schnorrer, F., Su, K.C., Barinova, Y., Fellner, M., Gasser, B.,
Kinsey, K., Oppel, S., Scheiblauer, S., Couto, A., Marra, V., Keleman, K., Dickson, BJ. (2007). A genome-wide transgenic RNAi library for conditional gene inactivation in Drosophila. *Nature*, 448:151-156.

Di Fonzo, A., Tassorelli, C., De Mari, M., Chien, HF., Ferreira, J., Rohé, CF., Riboldazzi, G., Antonini, A., Albani, G., Mauro, A., Marconi, R., Abbruzzese, G., Lopiano, L., Fincati, E., Guidi, M., Marini, P., Stocchi, F., Onofrj, M., Toni, V., Tinazzi, M., Fabbrini, G., Lamberti, P., Vanacore, N., Meco, G., Leitner, P., Uitti, RJ., Wszolek, ZK., Gasser, T., Simons, EJ., Breedveld, GJ., Goldwurm, S., Pezzoli, G., Sampaio, C., Barbosa, E., Martignoni, E., Oostra, BA., Bonifati, V., Italian Parkinson's Genetics Network.; (2006). Comprehensive analysis of the LRRK2 gene in sixty families with Parkinson's disease. *Eur J Hum Genet*, 14(3):322-331.

Di Fonzo, A., Chien, HF., Socal, M., Giraudo, S., Tassorelli, C., Iliceto, G., Fabbrini, G., Marconi, R., Fincati, E., Abbruzzese, G., Marini, P., Squitieri, F., Horstink, MW., Montagna, P., Libera, AD., Stocchi, F., Goldwurm, S., Ferreira, JJ., Meco, G., Martignoni, E., Lopiano, L., Jardim, LB., Oostra, BA., Barbos,a ER.; Italian Parkinson Genetics Network, Bonifati, V. (2007). ATP13A2 missense mutations in juvenile parkinsonism and young onset Parkinson disease. *Neurol*, 68(19):1557-1562.

Diamond, A., Jankovic, J.. (2005). The effect of deep brain stimulation on quality of life in movement disorders. *J Neurol Neurosurg Psychiatry*,76:1188–93.

Ding, X., Barodia, S.K., Ma, L., Goldberg, M.S. (2017). Fbxl18 targets LRRK2 for proteasomal degradation and attenuates cell toxicity. *Neurobiol Dis*, 98:122-136.

Dodson, MW., Zhang, T., Jiang, C., Chen, S., Guo, M. (2012). Roles of the Drosophila LRRK2 homolog in Rab7-dependent lysosomal positioning. *Hum Mol Genet*, 21(6):1350-1363.

Dodson, M.W., Leung, L.K., Lone, M., Lizzio, M.A., Guo, M. (2014). Novel ethyl methanesulfonate (EMS)-induced null alleles of the Drosophila homolog of LRRK2 reveal a crucial role in endolysosomal functions and autophagy *in vivo*. *Dis Model Mech*, 7:1351–1363.

Dorsey, E.R., Constantinescu, R., Thompson, JP., Biglan, KM., Holloway, RG., Kieburtz, K., Marshall, FJ., Ravina, BM., Schifitto, G., Siderowf, A., Tanner, CM. (2007), Projected number of people with Parkinson disease in the most populous nations, 2005 through 2030. *Neurol*, 68:384-386.

Driscoll, M., Gerstbrein, B. (2003). Dying for a cause: invertebrate genetics takes on human neurodegeneration. *Nat Rev Genet*, 4(3):181-194.

Duffy, JB. (2002). GAL4 system in Drosophila: A fly geneticist's Swiss army knife. *Genesis*, 34:1–15.

Dunst, S., Kazimiers, T., von Zadow, F., Jambor, H., Sagner, A., Brankatschk, B., Mahmoud, A., Spannl, S., Tomancak, P., Eaton, S., and Marko Brankatschk, M. (2015). Endogenously Tagged Rab Proteins: A Resource to Study Membrane Trafficking in *Drosophila*. *Dev Cell*, 33(3): 351–365.

Duty, S., Jenner, P. (2011). Animal models of Parkinson's disease: a source of novel treatments and clues to the cause of the disease. *Br J Pharmacol, 164(4):* 1357-1391.

East, MP., Kahn, RA. (2011). Models for the functions of Arf GAPs. *Semin Cell Dev Biol*, 22(1):3-9.

Eggenschwiler, J.T., Espinoza, E., and Anderson, K.V. (2001). Rab23 is an essential negative regulator of the mouse Sonic hedgehog signalling pathway. *Nature*, 412:194-198.

Eisenhofer, G., Aneman, A., Friberg, P., Hooper, D., Fandriks, L., Lonroth, H., Hunyady, B., Mezey, E. (1997). Substantial production of dopamine in the human gastrointestinal tract. *J Clin Endocrinol Metab*, 82(11): 3864-3871.

Fahn, S. (2000). The spectrum of levodopa-induced dyskinesias. *Ann Neurol*, 47:2–11.

Faust, K., Gehrke, S., Yang, Y., Yang, L., Beal, M., Lu, B. (2009). Neuroprotective effects of compounds with antioxidant and anti-

inflammatory properties in a Drosophila model of Parkinson's disease. *BMC Neurosci*, 10:109.

Feany, MB., Bender, WW. (2000). A Drosophila model of Parkinson's disease. *Nature*, 404(6776):394-398.

Feinberg, E. H., Vanhoven, M. K., Bendesky, A., Wang, G., Fetter, R. D. et al., (2008). GFP reconstitution across synaptic partners (GRASP) defines cell contacts and synapses in living nervous systems. *Neuron*, 57: 353–363.

Felten, D. L., Shetty, A. N. (2010). Netter's Atlas of Neuroscience. 2Edn. Philapdelphia: Saunders; Elsevier, 438.

Fenelon, G., Mahieux, F., Huon, R., Ziegler, M. (2000). Hallucinations in Parkinson's disease: prevalence, phenomenology and risk factors. *Brain*, 123(4): 733–45.

Freeman, M. (1996) Reiterative use of the EGF receptor triggers differentiation of all cell types in the *Drosophila* eye. *Cell*, 87:651–660.

Friggi-Grelin, F., Coulom, H., Meller, M., Gomez, D., Hirsh, J., Birman, S. (2003). Targeted gene expression in Drosophila dopaminergic cells using regulatory sequences from tyrosine hydroxylase. *J Neurobiol*, 54(4):618-27.

Fischbach, K.F. and Dittrich, A.P.M. (1989). The optic lobe of *Drosophila melanogaster*. A Golgi analysis of wildtype structure. *Cell Tissue Res*, 258:441–475.

Fitzmaurice, AG., Rhodese, SL., Lullad, A., Murphyf, NP., Lamf, HA., O'Donnellg, KC., Barnhilld, L., Casidah, JE., Cockburni, M., Sagastig, A., Stahla, MC., Maidmentf, NT., Ritzd, B., Bronsteina, JM. (2012). Aldehyde dehydrogenase inhibition as a pathogenic mechanism in Parkinson disease. *PNAS*, 110(2):636-641.

Funayama, M., Hasegawa, K., Kowa, H., Saito, M., Tsuji, S., Obata, F. (2002). A new locus for Parkinson's disease (PARK8) maps to chromosome 12p11.2-q13.1. *Ann Neurol*, 51(3):296-301.

Funayama, M., Hasegawa, K., Ohta, E., Kawashima, N., Komiyama, M., Kowa, H., Tsuji, S., Obata, F. (2005). A *LRRK2* Mutation as a cause for the Parkinsonism in the Original *PARK8* Family. *Ann Neurol*, 57: 918-921.

Gaig, C., Ezquerra, M., Marti, M.J., Munoz, E., Valldeoriola, F., Tolosa, E., (2006). LRRK2 Mutations in Spanish Patients with Parkinson Disease. *Arch Neurol*, 63:377-382.

Gaig, C., Martí, MJ., Ezquerra, M., Rey, MJ., Cardozo, A., Tolosa, E. (2006). G2019S LRRK2 mutation causing Parkinson's disease without Lewy bodies. J *Neurol Neurosurg Psychiatry*, 78:626-628.

Gandhi, P., Chen, SG., Wilson-Delfosse, AL. (2009). Leucine-Rich Repeat Kinase 2 (LRRK2): A Key Player in the Pathogenesis of Parkinson's Disease. *J Neurosci Res*, 87(6):1283-1295.

Ganley, I.G., and Pfeffer, S.R. (2006). Cholesterol accumulation sequesters Rab9 and disrupts late endosome function in NPC1-deficient cells. *J Biol Chem*, 281: 17890-17899.

Gasiunas, G., Barrangou, R., Horvath, P., Siksnys, V. (2012). Cas9–crRNA ribonucleoprotein complex mediates specific DNA cleavage for adaptive immunity in bacteria. *PNAS*, e2579-2586.

Gehrke, S., Imai, Y., Sokol, N., Lu, B. (2010). Pathogenic LRRK2 negatively regulates microRNA-mediated translational repression. *Nature*, 466(7306):637-641.

Gerondopoulos, A., Bastos, RN., Yoshimura, S, Anderson, R., Carpanini, S., Aligianis, I., Handley, MT., Barr, FA. (2014). Rab18 and a Rab18 GEF complex are required for normal ER structure. *J Cell Biol*, 205(5):707-720.

Giasson, B., Van Deerlin, V.M. (2008). Mutations in *LRRK2* as a cause of Parkinson's Disease. *Neurosignals*, 16: 99-105.

Gilks, WP1., Abou-Sleiman, PM., Gandhi, S., Jain, S., Singleton, A., Lees, AJ., Shaw, K., Bhatia, KP., Bonifati, V., Quinn, NP., Lynch, J., Healy, DG., Holton, JL., Revesz, T., Wood, NW.. (2005). A common LRRK2 mutation in idiopathic Parkinson's disease. *Lancet*, 365(9457):415-6.

Gillardon, F. (2009). Leucine-rich repeat kinase 2 phosphorylates brain tubulin-beta isoforms and modulates microtubule stability--a point of convergence in parkinsonian neurodegeneration? *J Neurochem*, 110(5):1514-1522.

Gillingham, A.K., Sinka, R., Torres, I.L., Lilley, K.S., Munro, S. (2014). Toward a Comprehensive Map of the Effectors of Rab GTPases. *Dev Cell*, 31(3): 358–373.

Ginsberg, S.D., Mufson, E.J., Alldred, M.J., Counts, S.E., Wuu, J., Nixon, R.A., Che, S. (2011). Upregulation of select rab GTPases in cholinergic basal forebrain neurons in mild cognitive impairment and Alzheimer's disease. *J Chem Neuroanat*, 42:102-110.

Ginsberg, S.D., Mufson, E.J., Counts, S.E., Wuu, J., Alldred, M.J., Nixon, R.A., Che, S. (2010). Regional selectivity of rab5 and rab7 protein upregulation in mild cognitive impairment and Alzheimer's disease. *J Alzheimers Dis*, 22:631-639.

Gitler, A., Bevis, B., Shorter, J., Strathearn, K., Hamamichi, S., Su, L., Caldwell, K., Caldwell, G., Rochet, J., McCaffery, J., Barlowe, C., Lindquist, S. (2008). The Parkinson's disease protein alpha-synuclein disrupts cellular Rab homeostasis. *Proc Natl Acad Sci USA,* 105:145–150.

Gloeckner, CJ., Kinki, N., Schumacher, A., Braun, RJ., O'Neill, E., Meitinger, T., Kolch, W. Prokisch, H., Ueffing, M. (2006). The Parkinson disease causing LRRK2 mutation I2020T is associated with increased kinase activity. *Hum Mol Genet,* 15(2):223-232.

Gloeckner, CJ., Schumacher, A., Boldt, K., Ueffing, M. (2009). The Parkinson disease-associated protein kinase LRRK2 exhibits MAPKKK activity and phosphorylates MKK3/6 and MKK4/7, in *vitro*. *J Neurochem*, 109(4):959-68.

Gloeckner, CJ., Boldt, K., Von Zweydorf, F., Helm, S., Wiesent, L., Sarioglu, H., Ueffing, M. (2010). Phosphopeptide analysis reveals two discrete clusters of phosphorylation in the N-terminus and the Roc domain of the Parkinson-disease associated protein kinase LRRK2. *J Proteome Res*, 9(4):1738-1745.

Gordon, M. D., and Scott, K. (2009). Motor control in a *Drosophila* taste circuit. *Neuron,* 61: 373–384.

Gonzalo-Gomez, A., Turiegano, E., Leon, Y., Molina, I., Torroja, L., Canal, I. (2012). Ih current is necessary to maintain normal dopamine fluctuations and sleep consolidation in *Drosophila. PLoS ONE,* 7(5): e36477.

Gratz, SJ., Wildonger, J., Harrison, MM., O'Connor-Giles, K. (2013). CRISPR/Cas9-mediated genome engineering and the promise of designer flies on demand. *Fly*, 7(4): 249–255.

Greenspan, RJ. Fly Pushing (2004). The Theory and Practice of Drosophila Genetics. New Jersey: Cold Spring Harbor Laboratory Press; 2004.

Greggio, E., Jain, S., Kingsbury, A., Bandopadhyay, R., Lewis, P., Kaganovich, A., van der Brug, MP., Beilina, A., Blackinton, J., Thomas, KJ., Ahmad, R., Miller, DW., Kesavapany, S., Singleton, A., Lees, A., Harvey, RJ., Harvey, K., Cookson, MR. (2006). Kinase activity is required for the toxic effects of mutant LRRK2/ dardarin. *Neurobiol Dis,* 23:329–341.

Greggio, E., Zambrano, I., Kaganovich, A., Beilina, A., Taymans, JM., Daniels, V., Lewis, P., Jain, S., Ding, J., Syed, A., Thomas, KJ., Baekelandt, V., Cookson, MR. (2008). The Parkinson disease-associated leucine-rich repeat kinase 2 (LRRK2) is a dimer that undergoes intramolecular autophosphorylation. *J Biol Chem,* 283:16906–16914.

Greggio, E., Tymans, J. M., Zhen, E. Y., Ryder, J., Vancraenenbroeck, R., Beilina, A., Sun, P., Deng, J., Jaffe, H., Baekelandt, V., Merchant, K. & Cookson, M. R. (2009). The Parkinson's disease kinase LRRK2 autophosphorylates its GTPase domain at multiple sites. *Biochem Biophys Res Commun*, 389: 449-54.

Greggio, E., Cookson, M.R. (2009). Leucine-rich repeat kinase 2 (LRRK2) and Parkinson's disease: three questions. *ASN Neuro,* 1(1): 13-24.

Gronemeyer, T., Wiese, S., Grinhagens, S., Schollenberger, L., Satyagraha, A., Huber, LA., Meyer, HE., Warscheid, B., Just, WW. (2013). Localization of Rab proteins to peroxisomes: a proteomics and immunofluorescence study. *FEBS Lett*, 587(4):328-38.

Gronenberg, W., Milde, J.J. and Strausfeld, N.J. (1995). Oculomotor control in calliphorid flies: organization of descending neurons to neck motor-neurons responding to visual-stimuli. *J Comp Neurol*, 361:267–284.

Grygoruk, A., Chen, A., Martin, CA., Lawal, HO., Fei, H., Gutierrez, G., Biedermann, T., Najibi, R., Hadi, R., Chouhan, AK., Murphy, NP., Schweizer, FE., Macleod, GT., Maidment, NT., Krantz, DE. (2014). The redistribution of Drosophila Vesicular Monoamine transporter mutants from synaptic vesicles to large dense-core vesicles impairs amine-dependent behaviors. *J. Neurosci*, 34(20): 6924-6937.

Guo, L., Wang, W. and Chen, S.G., (2006). Leucine-rich repeat kinase 2: relevance to Parkinson's disease. I*nt J Biochem Cell Biol,* 38(9): 1469–75.

Guo, L., Gandhi, PN., Wang, W., Petersen, RB., Wilson-Delfosse, AL., Chen, SG. (2007). The Parkinson's disease-associated protein, leucine-rich repeat kinase 2 (LRRK2), is an authentic GTPase that stimulates kinase activity. *Exp Cell Res,* 313:3658–3670.

Hammond, S.M., Caudy, A.A., Hannon, G.J. (2001). Post-transcriptional gene silencing by double-stranded RNA. *Nat Rev Genet,* 2:110-119.

Hanger, D.P., Anderton, B.H., Noble, W. (2009) Tau phosphorylation: the therapeutic challenge for neurodegenerative disease. *Trends Mol Med*, 15:112–119.

Hardie, R.C. (1989). A histamine-activated chloride channel involved in neurotransmission at a photoreceptor synapse. *Nature*, 339:704–706.

Hardie, S., Hirsh, J. (2006). An improved method for the seperation and detection of biogenic amines in adult *Drosophila* brain extracts by high performance liquid chromatography. *J Neurosci Methods,* 153: 243-249.

Harnois, C., Di, PT. (1990). Decreased dopamine in the retinas of patients with Parkinson's disease. *Invest Ophthalmol Vis Sci,* 31: 2473–5.

Hasegawa, K., Kowa, H. (1997). Autosomal dominant familial Parkinson disease:older onset of age, and good response to levodopa therapy. *Eur Neurol,* 38(1):39–43.

Hasegawa, K., Stoessl, AJ., Yokoyama, T., Kowa, H., Wszolek, ZK., Yagishita, S. (2008). Familial Parkinsonism: study of original Sagamihara PARK8 (I2020T) kindred with variable clinicopathologic outcomes. *Parkinsonism Relat Disord,* 15(4):300-306.

Hatano, T., Kubo, S., Imai, S., Maeda, M., Ishikawa, K., Mizuno, Y., Hattori, N. (2007). Leucine-rich repeat kinase 2 associates with lipid rafts. *Hum Mol Genet,* 16(6):678-690.

Hattula, K., Peranen, J. (2000). FIP-2, a coiled-coil protein, links Huntingtin to Rab8 and modulates cellular morphogenesis. *Curr Biol,* 10:1603-1606.

Haywood, AF., Staveley, BE. (2004). Parkin counteracts symptoms in a Drosophila model of Parkinson's disease. *BMC Neurosci,* 5:14.

Haywood, AF., Staveley, BE. (2006). Mutant alpha-synuclein-induced degeneration is reduced by parkin in a fly model of Parkinson's disease. *Genome,* 49(5):505-510.

Heisenberg, M. (1997). Genetic approaches to neuroethology. *Bioessays,* 19:1065–1073.

Hely, MA., Reid, WG., Adena, MA., Halliday, GM., Morris, JG. (2008). The Sydney multicenter study of Parkinson's disease: the inevitability of dementia at 20 years. *Mov Disord,* 23: 837–44.

Heo, HY1., Kim, KS., Seol, W. (2010). Coordinate Regulation of Neurite Outgrowth by LRRK2 and Its Interactor, Rab5. *Exp Neurobiol,* 19(2):97-105.

Hermann, G.J., Schroeder, L.K., Hieb, C.A., Kershner, A.M., Rabbitts, B.M., Fonarev, P., Grant, B.D., Priess, J.R. (2005). Genetic analysis of lysosomal trafficking in Caenorhabditis elegans. *Mol Biol Cell*, 16:3273–3288.

Hewitt, VL., Whitworth, AJ. (2017). Mechanisms of Parkinson's Disease: Lessons from *Drosophila*. *Curr Top Dev Biol*, 121:173-200.

Hiesinger, P.R., Reiter, C., Schau, H., Fischbach, K.F. (1999). Neuropil pattern formation and regulation of cell adhesion molecules in Drosophila optic lobe development depend on synaptobrevin. *J Neurosci*, 19:7548–7556.

Higashi, S., Moore, DJ., Yamamoto, R., Minegishi, M., Sato, K., Togo, T., Katsuse, O., Uchikado, H., Furukawa, Y., Hino, H., Kosaka, K., Emson, PC., Wada, K., Dawson, VL., Dawson, TM., Arai, H., Iseki, E. (2009). Abnormal localization of leucine-rich repeat kinase 2 to the endosomal-lysosomal compartment in lewy body disease. *J Neuropathol Exp Neurol*, 68(9):994-1005.

Hindle, S., Afsari, F., Stark, M., Middleton, C.A., Evans, G.J.O., Sweeney, S.T., Elliott, C.J.H., (2013). Dopaminergic expression of the Parkinsonian gene *LRRK2-G2019S* leads to non-autonomous visual neurodegeneration, accelerated by increased neural demands of energy. *Hum Mol Genet*, 22(11): 2129-2140.

Hirth, F. (2010). Drosophila melanogaster in the Study of Human Neurodegeneration. *CNS Neurol Disord Drug Targets*, 9(4):504-523.

Hisahara, S., Shimohama, S. (2011). Dopamine receptors and Parkinson's diease. *Int J Med Chem*, 2011: 1-16.

Ho, CC., Rideout, HJ., Ribe, E., Troy, CM., Dauer, WT. (2009). The Parkinson disease protein leucine-rich repeat kinase 2 transduces death signals via Fas-associated protein with death domain and caspase-8 in a cellular model of neurodegeneration. *J Neurosci*, 29(4):1011-1016.

Hornykiewicz, O. (2002). Dopamine miracle: from brain homogenate to dopamine replacement. *Mov Disord*, 17(3):501-508.

Houlden, H., Singleton, AB. (2012). The genetics and neuropathology of Parkinson's disease. *Acta Neuropathol*, 124(3):325-338.

Hu, W., Wang, T., Wang, X., Han, J. (2015). Ih channels control feedback regulation from amacrine cells to photoreceptors. *PLoS Biol*, 13:e1002115.

Hulihan, M.M., , Ishihara-Paul, L., Kachergus, J., Warren, L., Amouri, R., Elango, R., Prinjha, RK., Upmanyu, R., Kefi, M., Zouari, M., Sassi, SB., Yahmed, SB., El Euch-Fayeche, G., Matthews, PM., Middleton, LT., Gibson, RA., Hentati, F., Farrer, MJ. (2008). LRRK2 Gly2019Ser penetrance in Arab–Berber patients from Tunisia: a case-control genetic study. *Lancet Neurol,* 7(7):591-594.

Hutagalung, AH., Novick, PJ. (2011). Role of Rab GTPases in membrane traffic and cell physiology. *Physiol Rev,* 91(1):119-149.

Imai, Y., Gehrke, S., Wang, H., Takahashi, R., Hasegawa, K., Oota, E., Lu, B. (2008). Phosphorylation of 4E-BP by LRRK2 affects the maintenance of dopaminergic neurons in Drosophila. *EMBO J,* 27: 2432-2443.

Inamdar, A.A., Hossain, MM., Bernstein, AI., Miller, GW., Richardson, JR., Bennett, JW. (2013). Fungal-derived semiochemical 1-octen-3-ol disrupts dopamine packaging and causes neurodegeneration. *PNAS,* 110(48):19561-19566.

Ishizawa, T., Mattila, P., Davies, P.,Wang, D., Dickson, D.W. (2003) Colocalization of tau and alphasynuclein epitopes in Lewy bodies. *J Neuropathol Exp Neurol,* 62:389–397.

Islam, MS., Nolte, H., Jacob, W., Ziegler, AB., Pütz, S., Grosjean, Y., Szczepanowska, K., Trifunovic, A., Braun, T., Heumann, H., Heumann, R., Hovemann, B., Moore, DJ., Krüger, M. (2016). Human R1441C LRRK2 regulates the synaptic vesicle proteome and phosphoproteome in a *Drosophila* model of Parkinson's disease. *Hum Mol Genet,* 25(24):5365-5382.

Ito, G., Katsemonova, K., Tonelli, F., Lis, P., Baptista, MA., Shpiro, N., Duddy, G., Wilson, S., Ho, PW., Ho, SL., Reith, AD., Alessi, DR. (2010). Phos-tag analysis of Rab10 phosphorylation by LRRK2: a powerful assay for assessing kinase function and inhibitors. *Biochem J,* 473(17):2671-85.

Jackson, DM., Westlind-Danielsson, A. (1994). Dopamine receptors: molecular biology, biochemistry and behavioural aspects. *Pharmacol Ther,* 64(2):291-370.

Jackson1, CR., Ruan, GX., Aseem, F., Abey, J., Gamble, K., Stanwood, G., Palmiter, RD., Iuvone, M., McMahon, DG. (2012). Retinal Dopamine Mediates Multiple Dimensions of Light Adapted Vision. *J Neurosci,* 32(27): 9359–9368.

Jaleel, M., Nichols, RJ., Deak, M., Campbell, DG., Gillardon, F., Knebel, A., Alessi, DR. (2007). LRRK2 phosphorylates moesin at threonine-558: characterization of how Parkinson's disease mutants affect kinase activity. *Biochem J,* 405(2):307-317.

Jankovic, J. (2000). Parkinson's disease therapy: Tailoring choices for early and late disease, young and old patients. *Clin Neuropharmacol*, 23:252–61.

Jankovic, J. (2002). Levodopa strengths and weaknesses. *Neurology*, 58: 19–32.

Jankovic, J. (2005). Motor fluctuations and dyskinesias in Parkinson's disease. *Mov Disord,* 20(11): 11-16.

Jankovic, J. (2008). Parkinson's disease: clinical features and diagnosis. *J Neurol Neurosurg Phychiatry*, 79(4):368-376.

Jankovic, J., Aguillar, LG. (2008). Current approaches to the treatment of Parkinson's disease. *Neuropsychiatr Dis Treat,* 4(4):743-757.

Jenkins, D., Seelow, D., Jehee, F.S., Perlyn, C.A., Alonso, L.G., Bueno, D.F., Donnai,
D., Josifova, D., Mathijssen, I.M., Morton, J.E., Orstavik, KH., Sweeney, E., Wall, SA., Marsh, JL., Nurnberg, P., Passos-Bueno, MR., Wilkie, AO. (2007). RAB23 mutations in Carpenter syndrome imply an unexpected role for hedgehog signaling in cranial-suture development and obesity. *Am J Hum Genet,* 80:1162-1170.

Jin, EJ., Chan, CC., Agi, E., Cherry, S., Hanacik, E., Buszczak, M., Hiesinger, PR.
(2012).Similarities of Drosophila rab GTPases based on expression profiling : co-mpletion and analysis of the rab-Gal4 kit. *PLoS One,* 7(7):e40912.

Jinek, M., Chylinski, K., Fonfara, I., Hauer, M., Doudna, JA., Charpentier, E. (2012). A programmable dual-RNA-guided DNA endonuclease in adaptive bacterial immunity. *Science,* 337(6096):816-821.

Jinsmaa, Y., Florang, VR., Rees, JN., Mexas, LM., Eckert, LL., Allen, EM., Anderson, DG., Doorn, JA. (2011). Dopamine-derived biological reactive intermediates and protein modifications: Implications for Parkinson's disease. *Chem Biol Interact,* 192:118–121.

Johnston, D.S. (2002). The art and design of genetic screens: *Drosophila* melanogaster. *Nature Genet,* 3:176-188.

Johnson, MA., Kuo, YM., Westaway, SK., Parker, SM., Ching, KH., Gitschier, J., Hayflick, SJ. (2004). Mitochondrial localization of human PANK2 and hypotheses of secondary iron accumulation in pantothenate kinase-associated neurodegeneration. *Ann N Y Acad Sci,* 1012:282-298.

Juarez Olguin, H., Calderon Guzman, D., Hernadez Garcia, E., Barragan Mejia, G. (2015). The Role of Dopamine and Its Dysfunction as a Consequence of Oxidative Stress. *Oxid Med Cell Longev,* 2016:9730467.

Kametani, F., Usami, M., Tanaka, K., Kume, H., and Mori, H. (2004). Mutant presenilin (A260V) affects Rab8 in PC12D cell. *Neurochem Int,* 44:313-320.

Kanao, T., Venderova, K., Park, DS., Unterman, T., Lu, B., Imai, Y. (2010). Activation of FoxO by LRRK2 induces expression of proapoptotic proteins and alters survival of postmitotic dopaminergic neuron in Drosophila. *Hum Mol Genet,* 19(19):3747-3758.

Kawakami, F., Yabata, T., Ohta, E., Maekawa, T., Shimada, N., Suzuki, M., Maruyama, H., Ichikawa, T., Obata, F. (2012). LRRK2 phosphorylates tubulin-associated tau but not the free molecule: LRRK2-mediatedregulation of the tau tubulin association and neurite outgrowth. *PLoS One,* 7(1):e30834.

Kay, DM., Kramer, P., Higgins, D., Zabetian, CP., Payami, H.. (2005). Escaping Parkinson's disease: a neurologically healthy octogenarian with the LRRK2 G2019S mutation. *Mov Disord,* 20:1077–1078.

Kayser, M.S., Yue, Z., Sehgal, A. (2014). A critical period of sleep for development of courtship circuitry and behavior in *Drosophila* (2014) *Science,* 344: 269-274.

Keller, A., Sweeney, S.T., Zars, T., O'Kane, C.J., Heisenberg, M. (2002). Targeted expression of tetanus neurotoxin inter-feres with behavioral responses to sensory input in Drosophila. *J Neurobiol,* 50:221–233.

Khan, NL, , Jain, S., Lynch, JM., Pavese, N., Abou-Sleiman, P., Holton, JL., Healy, DG., Gilks, WP., Sweeney, MG., Ganguly, M., Gibbons, V., Gandhi, S., Vaughan, J., Eunson, LH., Katzenschlager, R., Gayton, J., Lennox, G., Revesz, T., Nicholl, D., Bhatia, KP., Quinn, N., Brooks, D., Lees, AJ., Davis, MB., Piccini, P., Singleton, AB., Wood, NW. (2005). Mutations in the gene LRRK2 encoding dardarin (PARK8) cause familial Parkinson's disease: clinical, pathological, olfactory and functional imaging and genetic data. *Brain,* 128: 2786–2796.

Kolb, H., Linberg, KA., Fisher, SK. (1992). Neurons of the human retina: A Golgi study. *J Compar Neurol,* 318(2):147-187.

Kondo, K., Obitsu, S., Teshima, R. (2011). alpha-Synuclein aggregation and transmission are enhanced by leucine-rich repeat kinase 2 in human neuroblastoma SH-SY5Y cells. *Biol Pharm Bull,* 34:1078–1083.

Kim, MJ., Deng, HX., Wong, YC., Siddique, T., Krainc, D. (2017). The Parkinson's disease-linked protein TMEM230 is required for Rab8a-mediated secretory vesicle trafficking and retromer trafficking. *Hum Mol Genet,* 26(4):729-741.

Kingsbury, A.E., Bandopadhyay, R., Silveira-Moriyama, L., Ayling, H., Kallis, C., Sterlacci, W., Maeir, H., Poewe, W., Lees, A.J. (2010). Brain stem pathology in Parkinson's disease: an evaluation of the Braak staging model. *Mov Disord,* 25:2508–2515.

Kitada, T., Asakawa, S., Hattori, N., Matsumine, H., Yamamura, Y., Minoshima, S., Yokochi, M., Mizuno, Y., Shimizu, N. (1998). Mutations in the parkin gene cause autosomal recessive juvenile parkinsonism. *Nature,* 392(6676):605-608.

Kitamoto, T. (2001).Conditional modification of behavior in Drosophila by targeted expression of a temperature-sensitive shibire allele in defined neurons. *J Neurobiol,* 47(2):81-92.

Knödler, A., Feng, S., Zhang, J., Zhang, X., Das, A., Peränen, J., Guo. W. (2010). Coordination of Rab8 and Rab11 in primary ciliogenesis. *Proc Natl Acad Sci USA,* 107(14):6346-51.

Krantz DE. (2006) Vesicular monogamy? *Neuron,* 49(1):1-2.

Krumova, P., Reyniers, L., Meyer, M., Lobbestael, E., Stauffer, D., Gerrits, B., Muller, L., Hoving, S., Kaupmann, K., Voshol, J., Fabbro, D., Bauer, A., Rovelli, G., Taymans, J-M., Bouwmeester, T., Baekelandt, V. (2015). Chemical genetic approach identifies microtubule affinity-regulating kinase 1 as a leucine-rich repeat kinase 2 substrate. *FASEB J,* 29:2980–2992.

Kumar, A., Greggio, E., Beilina, A., Kaganovich, A., Chan, D., Taymans, JM., Wolozin, B., Cookson, MR. (2010). The Parkinson's disease associated LRRK2 exhibits weaker in vitro phosphorylation of 4E-BP compared to autophosphorylation. *PLoS One,* 5(1):e8730.

Kumar, S., Chen, D., Sehgal, A. (2012). Dopamine acts through Cryptochrome to promote acute arousal in *Drosophila Genes Develop,* 26: 1224-1234.

Lai, SL., Lee, T. (2006). Genetic mosaic with dual binary transcriptional systems in Drosophila. *Nat Neurosci,* 9(5):703-709.

Langheinrich, T., Tebartz van Elst, L., Lagrèze, WA., Bach, M., Lücking, CH., Greenlee, MW. (2000). Visual contrast response functions in Parkinson's disease: evidence from electroretinograms, visually evoked potentials and psychophysics. *Clin Neurophysiol,* 111(1):66-74.

Latourelle JC et al., (2008) The Gly2019Ser mutation in LRRK2 is not fully penetrant in familial Parkinson's disease: the GenePD study. *BMC Med,* 6:32.

Laughlin, S.B., Howard, J. and Blakeslee, B. (1987). Synaptic limitations to contrast coding in the retina of the blowfly *Calliphora*. *Proc R Soc Lond B,* 231:437–467.

Lawal, H.O., Chang, H., Terrell, A., Brooks, E.S., Pulido, D., Simon, A.F., Krantz, D.E., (2010). The *Drosophila* vesicular monoamine transporter reduces pesticide-induced loss of dopaminergic neurons. *Neurol Dis,* 40:102-112.

Lee, SB., Kim, W., Lee, S., Chung, J. (2007). Loss of LRRK2/PARK8 induces degeneration of dopaminergic neurons in *Drosophila*. *Biochem Biophys Res Commun,* 358(2):534-539.

Lee, T., Luo, L. (1999). Mosaic analysis with a repressible cell marker for studies of gene function in neuronal morphogenesis. *Neuron,* 22:451–461.

Lee, V.M., Goedert, M., Trojanowski, J.Q. (2001) Neurodegenerative tauopathies. *Annu Rev Neurosci,* 24:1121–1159.

Lesage, S., Dürr, A., Tazir, M., Lohmann, E., Leutenegger, AL., Janin, S., Pollak, P., Brice, A.; French Parkinson's Disease Genetics Study Group. (2007). LRRK2 G2019S as a cause of Parkinson's disease in North African Arabs. *N Engl J Med,* 354(4):422-423.

Leung, K.F., Baron, R., Ali, B.R., Magee, A.I., and Seabra, M.C. (2007). Rab GTPases containing a CAAX motif are processed post-geranylgeranylation by proteolysis and methylation. *J Biol Chem,* 282:1487-1497.

Lewis, EB., Bacher, F. (1968). Method of feeding ethyl methane sulfonate (EMS) to Drosophila males. *Drosoph Inf Serv,* 43:192.

Lobbestael, E., Civiero, L., De Wit , T., Taymans, J.M., Greggio, E.,, Baekelandt, V. (2016) Pharmacological LRRK2 kinase inhibition induces

LRRK2 protein destabilization and proteasomal degradation. *Sci Rep*, 6:33897.

Li, X., Sapp, E., Chase, K., Comer-Tierney, L.A., Masso, N., Alexander, J., Reeves, P., Kegel, K.B., Valencia, A., Esteves, M., Aronin, N., Difiglia, M. (2009a). Disruption of Rab11 activity in a knock-in mouse model of Huntington's disease. *Neurobiol Dis*, 36: 374-383.

Li, X., Standley, C., Sapp, E., Valencia, A., Qin, Z.H., Kegel, K.B., Yoder, J., Comer-
Tierney, L.A., Esteves, M., Chase, K., Alexander, J., Masso, N., Sobin, L., Bellve, K., Tuft, R., Lifshitz, L., Fogarty, K., Aronin, N., DiFiglia M. (2009b). Mutant huntingtin impairs vesicle formation from recycling endosomes by interfering with Rab11 activity. *Mol Cell Bio*, 29:6106-6116.

Li, X., Patel, J.C., Wang, J., Avshalumov, M.V., Nicholson, C., Buxbaum, J.D., Elder, G.A., Rice, M.E., Yue, Z. (2010) Enhanced striatal dopamine transmission and motor performance with LRRK2 overexpression in mice is eliminated by familial Parkinson's disease mutation G2019S. *J Neurosci*, 30(5):1788-1797.

Lin, X., Parasiadou, L., Gu, XL., Wang, L., Shim, H., Sun, L., Xie, C., Long, CX., Yang, WJ., Ding, J., Chen, ZZ., Gallant, PE., Tao-Cheng, JH., Rudow, G., Troncoso, JC., Liu, Z., Li, Z., Cai, H. (2009). Leucine-rich repeat kinase 2 regulates the progression of neuropathology induced by Parkinson's-disease-related mutant alpha-synuclein. *Neuron*, 64(6):807-827.

Lin, C., Tsai, P., Wu, R., Chien, C. (2010). LRRK2 G2019S Mutation Induces Dendrite Degeneration through Mislocalization and Phosphorylation of Tau by Recruiting Autoactivated GSK3β. *J Neurosci*, 30(39):13138-13149.

Lin, CH., Li, H., Lee, YN., Cheng, YJ., Wu, RM., Chien, CT. (2015). Lrrk regulates the dynamic profile of dendritic Golgi outposts through the golgin Lava lamp. *J Cell Biol*, 210(3):471-83.

Linazasoro, G., Van Blercom, N., Lasa, A. (2003). Unilateral subthalamic deep brain stimulation in advanced Parkinson's disease. *Mov Disord*, 18:713–716.

Liu, Z., Wang, X., Yu, Y., Wang, T., Jiang, H., Ren, Q., Jiao, Y., Sawa, A., Moran, T., Ross, C., Montell, C., Smith, W. (2008). A *Drosophila* model for LRRK2-linked parkinsonism. *Proc Natl Acad Sci USA*, 150(7):2693-2698.

Liu, Z., Galemmo, RA., Fraser, KB., Moehle, MS., Sen, S., Volpicelli-Dale, LA., DeLucas, LJ., Ross, LJ., Valiyaveettil, J., Moukha-Chafiq, O., Pathak, AK., Ananthan, S., Kezar, H., White, EL., Gupta, V., Maddry, JA., Suto, MJ., West, AB. (2014). Unique Functional and Structural Properties of the LRRK2 Protein ATP-binding Pocket. *J Biol Chem*, 289(47):32937-32951.

Liu G, Sgobio C, Gu X, Sun L, Lin X, Yu J, Parisiadou L, Xie C, Sastry N, Ding J, Lohr KM, Miller GW, Mateo Y, Lovinger DM, Cai H. (2015) Selective expression of Parkinson's disease-related Leucine-rich repeat kinase 2 G2019S missense mutation in midbrain dopaminergic neurons impairs dopamine release and dopaminergic gene expression. *Hum Mol Genet*, 24(18):5299-312.

Lu, B., Vogel, H. (2009). *Drosophila* models of neurodegenerative diseases. *Annu Rev Pathol*, 4:315-342.

Luiro, K., Yliannala, K., Ahtiainen, L., Maunu, H., Jarvela, I., Kyttala, A., Jalanko, A. (2004). Interconnections of CLN3, Hook1 and Rab proteins link Batten disease to defects in the endocytic pathway. *Hum Mol Genet*, 13:3017-3027.

Luzón-Toro, B1., Rubio de la Torre, E., Delgado, A., Pérez-Tur, J., Hilfiker, S. (2007). Mechanistic insight into the dominant mode of the Parkinson's disease-associated G2019S LRRK2 mutation. *Hum Mol Genet*, 16(17):2031-9.

Ma, J., Plesken, H., Treisman, J.E., Edelman-Novemsky, I., Ren, M. (2004). Lightoid and Claret: a rab GTPase and its putative guanine nucleotide exchange factor in biogenesis of *Drosophila* eye pigment granules. *Proc Natl Acad Sci USA*, 101: 11652–11657.

MacLeod, DA., Rhinn, H., Kuwahara, T., Zolin, A., Di Paolo, G., McCabe, BD., Marder, KS., Honig, LS., Clark, LN., Small, SA., Abeliovick, A. (2013). RAB7L1 interacts with LRRK2 to modify intraneuronal protein sorting and Parkinson's disease risk. *Neuron*, 77(3):425-439.

MacLeod, D., Dowman, J., Hammond, R., Leete, T., Inoue, K., Abeliovich, A. (2006). The familial Parkinsonism gene LRRK2 regulates neurite process morphology. *Neuron*, 52(4):587-93.

MacLeod, D., Dowman, J., Hammond, R., Leete, T., Inoue, K., Abeliovich, A. (2006). The familial Parkinsonism gene LRRK2 regulates neurite process morphology. *Neuron*, 52(4):587-593.

Mali, P., Yang, L., Esvelt, KM., Aach, J., Guell, M., DiCarlo, JE., Norville, JE., Church, GM. (2013). RNA-guided human genome engineering via Cas9. *Science,* 339(6121):823-826.

Margulies, C., Tully, T., Dubnau, J. (2005). Deconstructing memory in *Drosophila*. *Curr Biol,* 15:R700–R713.

Mariani, AP. (1990). Amacrine cells of the rhesus monkey retina. *J Comp Neurol,* 301(3):382-400.

Mariani, AP. (1991). Synaptic organization of type 2 catecholamine amacrine cells in
the rhesus monkey retina. *J Neurocytol,* 20(4):332-342.

Marsh, J.L., Walker, H., Theisen, H., Zhu, Y.Z., Fielder, T., Purcell, J. and Thompson, L.M. (2000). Expanded polyglutamine peptides alone are intrinsically cytotoxic and cause neurodegeneration in Drosophila. *Hum Mol Genet,* 9:13–25.

Marti-Masso, JF., Ruiz-Martinez, J., Bolano, MJ., Ruiz, I,. Gorostidi, A., Moreno, F., Ferrer, I., Lopez de Munain, A. (2009). Neuropathology of Parkinson's disease with the R1441G mutation in LRRK2. Mov *Disord,* 24:1998–2001.

Martin, S., Driessen, K., Nixon, SJ., Zerial, M., Parton, RG. (2005). Regulated localization of Rab18 to lipid droplets: effects of lipolytic stimulation and inhibition of lipid droplet catabolism. *J Biol Chem,* 280(51):42325-35.

Martin, I., Kim, JW., Dawson, VL., Dawson, TM. (2014). LRRK2 pathobiology in Parkinson's disease. *J Neurochem,* 131(5):554-565.

Martin, I., Kim, JW., Lee, BD., Kang, HC., Xu, JC., Jia, H., Stankowski, J., Kim, MS., Zhong, J., Kumar, M., Andrabi, SA., Xiong, Y., Dickson, DW., Wszolek, ZK., Pandey, A., Dawson, TM., Dawson, VL. (2014). Ribosomal protein s15 phosphorylation mediates LRRK2 neurodegeneration in Parkinson's disease. *Cell,* 157(2):472-85.

Mata, IF., Wedemeyer, WJ., Farrer, MJ., Taylor, JP., Gallo, KA. (2006). LRRK2 in Parkinson's disease: protein domains and functional insights. *TRENDS Neurosci,* 29(5):286-293.

Matta, S., Van Kolen, K., da Cunha, R., van den Bogaart, G., Mandemakers, W., Miskiewicz, K., De Bock, PJ., Morais, VA., Vilain, S., Haddad, D., Delbroek, L., Swerts, J., Chávez-Gutiérrez, L., Esposito, G., Daneels, G., Karran, E., Holt, M., Gevaert, K., Moechars, DW., De Strooper, B.,

Verstreken, P. (2012). LRRK2 controls an EndoA phosphorylation cycle in synaptic endocytosis. *Neuron*, 75(6):1008-21.

McArdle, B., Hofmann, A. (2008). Coronin structure and implications. *Subcell Biochem*, 48:56–71.

McCray, B.A., Skordalakes, E., and Taylor, J.P. (2010). Disease mutations in Rab7 result in unregulated nucleotide exchange and inappropriate activation. *Hum Mol Genet*, 19:1033-1047.

McGuire, SE., Le, PT., Osborn, AJ., Matsumoto, K., Davis, RL. (2003). Spatiotemporal rescue of memory dysfunction in *Drosophila*. *Science*, 302:1765–1768.

McGuire, SE., Deshazer, M., Davis, RL. (2005). Thirty years of olfactory learning and memory research in Drosophila melanogaster. Prog. *Neurobiol*, 76:328–347.

McGurk, L., Berson, A., Bonini, NM. (2015). Drosophila as an In Vivo Model for Human Neurodegenerative Disease. *Genetics*, 201(2):377-402.

McMahon, HT., Ushkaryov, YA., Edelmann, L., Link, E., Binz, T,. Niemann, H., Jahn, R., Südhof, TC. (1993). Cellubrevin is a ubiquitous tetanus-toxin substrate homologous to a putative synaptic vesicle fusion protein. *Nature*, 364(6435):346-349.

Meinertzhagen, I.A. and O'Neil, S.D. (1991). Synaptic organization of columnar elements in the lamina of the wild type in *Drosophila melanogaster*. *J Comp Neurol*, 305: 232–263.

Meiser, J., Weindl, D., Hiller, K. (2013). Complexity of dopamine metabolism. *Cell Commun Signal*, 11:34.

Ménasché, G., Pastural, E., Feldmann, J., Certain, S., Ersoy, F., Dupuis, S., Wulffraat, N., Bianchi, D., Fischer, A., Le Deist, F., de Saint Basile, G. (2000). Mutations in RAB27A cause Griscelli syndrome associated with haemophagocytic syndrome. *Nat Genet*, 25(2):173-6.

Meschede, I.P., Santos, T.O., Izidoro-Toledo, T.C., Gurgel-Gianetti, J., Espreafico, E.M. (2008). Griscelli syndrome-type 2 in twin siblings: case report and update on RAB27A human mutations and gene structure. *Braz J Med Biol Res*, 41(10):839-48.

Menzies, F. M., Moreau, K. and Rubinsztein, D. C. (2011). Protein misfolding disorders and macroautophagy. *Curr Opin Cell Biol*, 23:190–197.

Migheli, R., Del Giudice, MG., Spissu, Y., Sanna, G., Xiong, Y., Dawson, TM., Dawson, VL., Galioto, M., Rocchitta, G., Biosa, A., Serra, PA., Carri, MT., Crosio, C., Iaccarino, C. (2013). LRRK2 Affects Vesicle Trafficking, Neurotransmitter Extracellular Level and Membrane Receptor Localization. *PloS one,* 8 (10): e77198.

Mitra T, Naidu Y, Martinez-Martin P, et al. (2008) The non declaration of non motor symptoms of Parkinson's disease to healthcare professionals. An international survey using the NMSQuest. 6th International Congress on Mental Dysfunctions and other Non-motor Features in Parkinson's disease and Related Disorders. Dresden October, *Park Related Disorders,* P0II: 161.

Monastirioti, M. (1999). Biogenic amine systems in the fruit fly Drosophila melanogaster. *Microsc Res Tech,* 45(2):106-121.

Morgan, TH. (1910). Sex limited inheritance in *Drosophila*. *Science,* 32:120-122.

Mu, L., Ito, K., Bacon, J.P. and Strausfeld, N.J. (2012). Optic glomeruli and their inputs in *Drosophila* share an organizational ground pattern with the antennal lobes. *J Neurosci,* 32:6061–6071.

Muqit, MM., Feany, MB. (2002). Modelling neurodegenerative diseases in *Drosophila*: a fruitful approach? *Nat Rev Neurosci,* 3(3):237-243.

Naidu, Y., Chaudhuri, KR. (2008). Early Parkinson's disease and non motor issues. *J Neurol,* 255:33-38.

Nassel, DR., Ohlsson, LG., Cantera, R. (1988). Metamorphosis of identified neurons innervating thoracic neurohemal organs in the blowfly: Transformation of cholecystokininlike immunoreactive neurons. *J Compar Neurol,* 267(3):343-356.

Nassel, DR., Elekes, K. (1992). Aminergic neurons in the brain of blowflies and *Drosophila*: dopamine- and tyrosine hydroxylase-immunoreactive neurons and their relationship with putative histaminergic neurons. *Cell Tissue Res,* 267(1):147-167.

Neckameyer, WS. (1996). Multiple roles for dopamine in Drosophila development. *Dev Biol,* 176(2):209-19.

Neckameyer, W., O'Donnell, J., Huang, Z., Stark, W. (2001). Dopamine and sensory tissue development in Drosophila melanogaster. *Develop Neurobiol,* 47(4):280-294.

Neckameyer, WS., Bhatt, P. (2012). Neurotrophic actions of dopamine on the development of a serotonergic feeding circuit in Drosophila melanogaster. *BMC Neurosci,* 13:26.

Nellen, D., Burke, R., Struhl,G., Basler, K. (1996). Direct and long-range action of a
DPP morphogen gradient. *Cell,* 85:357–368.

Ng, CH., Mok, SZ., Koh, C., Ouyang, X., Fivaz, ML., Tan, EK., Dawson, VL., Dawson, TM., Yu, F., Lim, KL. (2009). Parkin protects against LRRK2 G2019S mutant-induced dopaminergic neurodegeneration in Drosophila. *J Neurosci,* 29(36):11257-11262.

Ng, E.L., Tang, B.L. (2008). Rab GTPases and their roles in brain neurons and glia. *Brain Res Rev,* 58:236-246.

Nguyen-Legros, J. (1988). Functional neuroarchitecture of the retina: hypothesis on the dysfunction of retinal dopaminergic circuitry in Parkinson's disease. *Surg Radiol Anat,* 10:137–44.

Nichols, CD. (2006). *Drosophila melanogaster* neurobiology, neuropharmacology, and how the fly can inform central nervous system drug discovery. *Pharmacol Ther,* 112:677–700.

Nichols, RJ., Dzamko, N., Hutti, JE., Cantley, LC., Deak, M., Moran, J., Bamborough, P., Reith, AD,, Alessi, DR. (2009). Substrate specificity and inhibitors of LRRK2, a protein kinase mutated in parkinson's disease. *Biochem J,* 424:47–60.

Nitabach, MN., Blau, J., Holmes, TC. (2002). Electrical silencing of Drosophila pacemaker neurons stops the free-running circadian clock. *Cell,* 109(4):485-95.

Obeso, JA., Rodriguez-Oroz, MC., Goetz, CG., Marin, C., Kordower, JH., Rodriguez, M., Hirsch, EC., Farrer, M., Schapira, AH., Halliday, G. (2010). Missing pieces in the Parkinson's disease puzzle. *Nat Med,* 16: 653-661.

Ohta, E., Kawakami, F., Kubo, M., Obata, F. (2011). LRRK2 directly phosphorylates Akt1 as a possible physiological substrate: Impairment of the kinase activity by Parkinson's disease-associated mutations. *FEBS Lett,* 585: 2165–2170.

O'Kane, C.J., Gehring, W.J. (1987). Detection in situ of genomic regulatory elements in Drosophila. *Proc Natl Acad Sci USA,* 84:9123-9127.

Ozeki, S., Cheng, J., Tauchi-Sato, K., Hatano, N., Taniguchi, H., Fujimoto, T. (2005). Rab18 localizes to lipid droplets and induces their close apposition to the endoplasmic reticulum-derived membrane. *J Cell Sci*, 118(12):2601-11.

Paddison, P. J., Silva, J.M., Conklin, D.S., Schlabach, M., Li, M., Aruleba, S., Balija, V., O'Shaughnessy, A., Gnoj, L., Scobie, K., Chang, K., Westbrook, T., Cleary, M., Sachidanandam, R., McCombie, W.R., Elledge, S.J., Hannon, G.J. (2004). A resource for large-scale RNA-interference-based screens in mammals. *Nature,* 428: 427–431.

Paisán-Ruiz, C., Jain, S., Evans, EW., Gilks, WP., Simón, J., van der Brug, M., López de Munain, A., Aparicio, S., Gil, AM., Khan, N., Johnson, J., Martinez, JR., Nicholl, D., Carrera, IM., Pena, AS., de Silva, R., Lees, A., Martí-Massó, JF., Pérez-Tur, J., Wood, NW., Singleton, AB. (2004). Cloning of the gene containing mutations that cause PARK8-linked Parkinson's disease. *Neuron,* 44(4):595-600.

Paisán-Ruiz, C., Guevara, R., Federoff, M., Hanagasi, H., Sina, F., Elahi, E., Schneider, SA., Schwingenschuh, P., Bajaj, N., Emre, M., Singleton, AB., Hardy, J., Bhatia, KP., Brandner, S., Lees, AJ., Houlden, H. (2010). Early-onset L-dopa-responsive parkinsonism with pyramidal signs due to ATP13A2, PLA2G6, FBXO7 and spatacsin mutations. *Mov Disord*, 25(12):1791-1800.

Paisán-Ruiz, C., Lewis, P., Singleton, A.B., (2013). *LRRK2*: Cause, Risk, and Mechanism. *J Parkinsons Dis,* 3(2): 85–103.

Pandey, U.B., Nichols, C.D., (2011). Human Disease Models in *Drosophila* melanogaster and the Role of the Fly in Therapeutic Drug Discovery. *Pharmacol Rev,* 63(2): 411–436.

Papkovskaia, TD., Chau, KY., Inesta-Vaquera, F., Papkovsky, DB., Healy, DG., Nishio, K., Staddon, J., Duchen, MR., Hardy, J., Schapira, AH., Cooper, JM. (2012). G2019S leucine-rich repeat kinase 2 causes uncoupling protein-mediated mitochondrial depolarization. *Hum Mol Genet*, 21(19):4201-4213.

Parasiadou, L., Xie, C., Cho, HJ., Lin, X., Gu, XL., Long, CX., Lobbestael, E., Baekelandt, V., Taymans, JM., Sun, L., Cai, H. (2009). Phosphorylation of ezrin/radixin/moesin proteins by LRRK2 promotes the rearrangement of actin

Park, M., Serpinskaya, A.S., Papalopulu, N., Gelfand, V.I. (2007). Rab32 regulates melanosome transport in Xenopus melanophores by protein kinase a recruitment. *Cur Biol,* 17(23):2030-2034.

Pfeffer, SR. (1994). Rab GTPases: master regulators of membrane trafficking. *Curr Opin Cell Biol,* 6(4):522-526.

Pfeffer, S.R. (2001). Rab GTPases: specifying and deciphering organelle identity and function. *Trends Cell Biol*, 11:487-491.

Pfeffer, SR. (2005). Structural clues to Rab GTPase functional diversity. *J Biol Chem,* 280(16):15485-15488.

Pfeffer, SR. (2007). Unsolved mysteries in membrane traffic. *Annu Rev Biochem,* 76:629-645.

Pfeiffer, B.D., Ngo, T.T., Hibbard, K.L., Murphy, C., Jenett, A., Truman, J.W. and Rubin G.M. (2010) Refinement of tools for targeted gene expression in *Drosophila*. *Genetics,* 186(2):735-55.

Pickrell, AM., Youle, RJ. (2015). The roles of PINK1, parkin, and mitochondrial fidelity in Parkinson's disease. *Neuron,* 85(2):257-273.

Pignoni, F., Zipursky, SL. (1997). Induction of Drosophila eye development by decapentaplegic. *Development,* 124:271–278.

Piper, MDQ., Skorupa, D., Partridge, L. (2005). Diet, metabolism and lifespan in Drosophila. *Exp Gerontol*, 40(11): 857–862.

Pletcher, SD., Libert, S., Skorupa, D. (2005). Flies and their golden apples: the effect of dietary restriction on *Drosophila* aging and age-dependent gene expression. *Ageing Res Rev,* 4:451–480.

Plowey, E.D., Cherra, S.J., Liu, Y.J., Chu, C.T. (2008). Role of autophagy in G2019S-LRRK2-associated neurite shortening in differentiated SH-SY5Y cells. *J Neurochem*, 105(3):1048-56.

Polymeropoulos, MH., Higgins, JJ., Golbe, LI., Johnson, WG., Ide, SE., Di Iorio, G., Sanges, G., Stenroos, ES., Pho, LT., Schaffer, AA., Lazzarini, AM., Nussbaum, RL., Duvoisin, RC. (1996). Mapping of a gene for Parkinson's disease to chromosome 4q21-q23. *Science,* 274(5290):1197-1199.

Polymeropoulos MH et al., (1997) Mutation in the a-Synuclein Gene Identified in Families with Parkinson's Disease. *Science,* 276:2045-2047.

Potter, CJ., Tasic, B., Russler, EV., Liang, L., Luo, L. (2010). The Q system: a repressible binary system for transgene expression, lineage tracing, and mosaic analysis. *Cell,* 141(3):536-48.

Price, MJ., Feldman, RG., Adelberg, D., Kayne, H. (1992). Abnormalities in color vision and contrast sensitivity in Parkinson's disease. *Neurol,* 42:887–90.

QIAGEN. 2010. QIAprep Spin Miniprep Kit [Online]. Available: https://www.qiagen.com/gb/ [Accessed 15 May 2016].

QIAGEN. 2015. (EN) - QIAquick Gel Extraction Kit [Online]. Available:https://www.qiagen.com/gb/ [Accessed 15 May 2016].

Qing, H., Wong, W., McGeer, EG., McGeer, PL. (2009). Lrrk2 phosphorylates alpha synuclein at serine 129: Parkinson disease implications. *Biochem Biophys Res Commun,* 387(1):149-52.

Qing, H., Zhang, Y., Deng, Y., McGeer, E.G., McGeer, P.L. (2009). Lrrk2 interaction with alpha-synuclein in diffuse Lewy body disease. *Biochem Biophys Res Commun,* 390:1229–1234.

Rangel-Barajas, C., Malik, M., Vangveravong, S., Mach, RH., Luedtke, RR. (2014). Pharmacological modulation of abnormal involuntary DOI-induced head twitch response in male DBA/2J mice: I. Effects of D2/D3 and D2 dopamine receptor selective compounds. *Neuropharmacol,* 83:18-27.

Rangel-Barajas, C., Coronel, I., Florán, B. (2015). Dopamine Receptors and Neurodegeneration. *Aging Dis*, 6:349–368.

Ray, S., Liu, M. (2012). Current understanding of LRRK2 in Parkinson's disease: biochemical and structural features and inhibitor design. *Future Med Chem*, 4(13): 1701-1713.

Reiter, LT., Potocki, L., Chien, S., Gribskov, M., Bier, E. (2001). A systematic analysis of human disease-associated gene sequences in *Drosophila* melanogaster. *Genome Res*, 11:1114–1125.

Riemensperger, T., Isabel, G., Coulom, H., Neuser, K., Seugnet, L., Kume, K., Iché-Torres, M., Cassar, M., Strauss, R., Preat, T., Hirsh, J., Birman, S. (2011). Behavioural consequences of dopamine deficiency in the *Drosophila* central nervous system. *PNAS*, 108(2): 834-839.

Rister, J. and Heisenberg, M. (2006) Distinct functions of neuronal synaptobrevin in developing and mature fly photoreceptors. *J Neurobiol*, 66(12):1271-1284.

Rivero-Rios, P., Gomez-Suaga, P., Fernandez, B., Madero-Perez, J., Schwab, AJ., Ebert, AD., Hilfiker, S. (2015). Alterations in late endocytic trafficking

related to the pathobiology of LRRK2-linked Parkinson's disease. *Biochem Soc Trans*, 43(3):390-395.

Roberts, R.C., Peden, A.A., Buss, F., Bright, N.A., Latouche, M., Reilly, M.M., Kendrick-Jones, J., Luzio, J.P. (2010). Mistargeting of SH3TC2 away from the recycling endosome causes Charcot-Marie-Tooth disease type 4C. *Hum Mol Genet*, 19:1009-1018.

Rodriguez, A., Didiano, D., Desplan, C. (2012). Power tools for gene expression and clonal analysis in Drosophila. *Nature methods*, 9(1):47-55.

Rodriguez, M., Morales, I., Rodriguez-Sabate, C., Sanchez, A., Castro, R., Brito, J. M., Sabate, M. (2014). The degeneration and replacement of dopamine cells in Parkinson's disease: the role of aging. *Front Neuroanat*, 8 (80):1-7.

Romero-Calderón, R., Uhlenbrock, G., Borycz, J., Simon, AF., Grygoruk, A., Yee, SK., Shyer, A., Ackerson, LC., Maidment, NT., Meinertzhagen, IA., Hovemann, BT., Krantz, DE. (2008). A glial variant of the vesicular monoamine transporter is required to store histamine in the *Drosophila* visual system. *PLoS genetics*, 4(11): e1000245.

Roote, J., Prokop, A. (2013). How to design a genetic mating scheme: a basic training package for *Drosophila* genetics. *G3* 3:353-358.

Ross, OA., Toft, M., Whittle, AJ., Johnson, JL., Papapetropoulos, S., Mash, DC., Litvan, I., Gordon, MF., Wszolek, ZK., Farrer, MJ., Dickson, DW. (2006). LRRK2 and Lewy body disease. *Ann Neurol*, 59(2):388-393.

Rubin, G., Spradling, A. (1982). Genetic transformation of Drosophila with transposable element vectors. *Science*, 218: 348-353.

Rubin, GM., Yandel,l MD., Wortman, JR., Gabor Miklos, GL., Nelson, CR., Hariharan, IK., Fortini, ME., Li, PW., Apweiler, R., Fleischmann, W., Cherry, JM., Henikoff, S., Skupski, MP., Misra, S., Ashburner, M., Birney, E., Boguski, MS., Brody, T., Brokstein, P., Celniker, SE., Chervitz, SA., Coates, D., Cravchik, A., Gabrielian, A., Galle, RF., Gelbart, WM., George, RA., Goldstein, LS., Gong, F., Guan, P., Harris, NL., Hay, BA., Hoskins, RA., Li, J., Li, Z., Hynes, RO., Jones, SJ., Kuehl, PM., Lemaitre, B., Littleton, JT., Morrison, DK., Mungall, C., O'Farrell, PH., Pickeral, OK., Shue, C., Vosshall, LB., Zhang, J., Zhao, Q., Zheng, XH., Lewis, S. (2000). Comparative genomics of the eukaryotes. *Science*, 287:2204–2215.

Rudenko, I.N., Cookson, M. (2014). Heterogeneity of Leucine-Rich Repeat Kinase 2 Mutations: Genetics, Mechanisms and Therapeutic Implications. *Neurotherapheutics*, 11(4):738-750.

Sakaguchi-Nakashima, A., Meir, JY., Jin, Y., Matsumoto, K., Hisamoto, N. (2007). LRK-1, a C. elegans PARK8-related kinase, regulates axonal-dendritic polarity of SV proteins. *Curr Biol,* 17(7):592-598.

Salloum, S., Wang, H., Ferguson, C., Parton, RG., Tai, AW. (2013). Rab18 binds to hepatitis C virus NS5A and promotes interaction between sit es of viral replication and lipid droplets. *PLoS Pathog,* 9(8):e1003513.

Sanchez-Danes, A., Richaud-Patin, Y., Carballo-Carbajal, I., Jiménez-Delgado, S., Caig, C., Mora, S., Di Guglielmo, C., Ezquerra, M., Patel, B., Giralt, A., Canals, J.M., Memo, M., Alberch, J., López-Barneo, J., Vila, M., Cuervo, A.M., Tolosa, E., Consiglio, A., Raya, A. (2012). Disease-specific phenotypes in dopamine neurons from human iPS-based models of genetic and sporadic Parkinson's disease. *EMBO Mol Med,* 4:380–395.

Sancho, RM1., Law, BM., Harvey, K. (2009). Mutations in the LRRK2 Roc-COR tandem domain link Parkinson's disease to Wnt signalling pathways. *Hum Mol Genet,* 18(20):3955-3968.

Sanes, J.R., Zipursky, S.L., (2010). Design principles of insect and vertebrate visual systems. *Neuron,* 66(1): 15–36.

Sang Kang, T., Jackson, GR. (2005). *Drosophila* models of neurodegenerative disease. *NeuroRx,* 2:438-446.

Sand, TK., Chang, HY., Lawless, GM., Ratnapaekhi, A., Mee, L., Ackerson, LC., Maidment, NT., Krantz, DE., Jackson, GR. (2007). A Drosophila model of mutant human parkin-induced toxicity demonstrates selective loss of dopaminergic neurons and dependence on cellular dopamine. *J Neurosci,* 27(5):981-992.

Schulte, C., Gasser, T, (2011). Genetic basis of Parkinson's disease: inheritance, penetrance, and expression. A*ppl Clin Genet,* 4: 67–80.

Schmalfuss, H., Heider, A. (1931). Tyramin und Oxytyramin, blutdrucksteigernde Schwarzvorstufen des Besenginsters Sarothamnus scoparius WIMM. *Biochem Zeitschr,* 236: 226–230.

Segev, N. (2001). Ypt/rab GTPases: regulators of protein trafficking. *Sci STKE*. 2001:RE11.

Seixas, E., Barros, M., Seabra, MC., Barral, DC. (2013). Rab and Arf proteins in genetic diseases. *Traffic,* 14(8):871-85.

Seugnet, L., Galvin, JE., Suzuki, Y., Gottschalk, L., Shaw, PJ. (2009). Persistent Short-Term Memory Defects Following Sleep Deprivation in a *Drosophila* Model of Parkinson Disease. *Sleep*, 32(8):984-992.

Shang, Y., Griffith, L. C. and Rosbash, M. (2008). Light-arousal and circadian photoreception circuits intersect at the large PDF cells of the Drosophila brain. *Proc Natl Acad Sci USA*, 105:19587–19594.

Sharma, S., Bandopadhyay, R., Lashley, T., Renton, A.E., Kingsbury, A.E., Kumaran, R., Kallis, C., Vilariño-Güell, C., O'Sullivan, S.S., Lees, A.J., Revesz, T., Wood, N.W., Holton, J.L. (2011). LRRK2 expression in idiopathic and G2019S positive Parkinson's disease subjects: a morphological and quantitative study. *Neuropathol Appl Neurobiol*, 37(7):777-790.

Sheng, Z., Zhang, S., Bustos, D., Kleinheinz, T., Le Pichon, CE., Dominguez, SL., Solanoy, HO., Drummond, J., Zhang, X., Ding, X., Cai, F., Song, Q., Li, X., Yue, Z., van der Brug, MP., Burdick, DJ., Gunzner-Toste, J., Chen, H., Liu, X., Estrada, AA., Sweeney, ZK., Scearce-Levie, K., Moffat, JG., Kirkpatrick, DS., Zhu, H. (2012). Ser1292 autophosphorylation is an indicator of LRRK2 kinase activity and contributes to the cellular effects of PD mutations. *Sci Transl Med*, 4:164ra161.

Shi, MM., Shi, C., Xu, Y. (2017). Rab GTPases: The Key Players in the Molecular Pathway of Parkinson's Disease. *Front Cell Neurosci*, 11: 81.

Shin, N., Jeong, H., Kwon, J., Heo, HY., Kwon, JJ., Yun, HJ., Kim, CH., Han, BS., Tong, Y., Shen, J., Hatano, T., Hattori, N., Kim, KS., Chang, S., Seol, W. (2008). LRRK2 regulates synaptic vesicle endocytosis. *Exp Cell Res*, 314(10):2055-2065.

Shojaee, S., Sina, F., Banihosseini, SS., Kazemi, MH., Kalhor, R., Shahidi, GA., Fakhrai-Rad, H., Ronaghi, M., Elahi, E. (2008). Genome-wide linkage analysis of a Parkinsonian-pyramidal syndrome pedigree by 500 K SNP arrays. *Am J Hum Genet*, 82(6):1375-1384.

Singleton, AB., Farrer, M., Johnson, J., Singleton, A., Hague, S., Kachergus, J., Hulihan, M., Peuralinna, T., Dutra, A., Nussbaum, R., Lincoln, S., Crawley, A., Hanson, M., Maraganore, D., Adler, C., Cookson, MR., Muenter, M., Baptista, M., Miller, D., Blancato, J., Hardy, J., Gwinn-Hardy, K. (2003). alpha-Synuclein locus triplication causes Parkinson's disease. *Science*, 302(5646):841.

Sivars, U., Aivazian, D., Pfeffer, S. (2003). Yip3 catalyses the dissociation of endosomal Rab-GDI complexes. *Nature*, 425:856–859.

Smith, WW., Pei, Z., Jiang, H., Moore, DJ., Liang, Y., West, AB., Dawson, VL., Dawson, TM., Ross, CA. (2005). Leucine-rich repeat kinase 2 (LRRK2) interacts with parkin, and mutant LRRK2 induces neuronal degeneration. *Proc Natl Acad Sci USA,* 102(51):18676-18681.

Smith, WW., Pei, Z., Jiang, H., Dawson, VL., Dawson, TM., Ross, CA. (2006). Kinase activity of mutant LRRK2 mediates neuronal toxicity. *Nat Neurosci,* 9:1231–1233.

Söllner, T., Whiteheart, SW., Brunner, M., Erdjument-Bromage, H., Geromanos, S., Tempst, P., Rothman, JE. (1993). SNAP receptors implicated in vesicle targeting and fusion. *Nature,* 362(6418):318-24.

Soma, S., Shimegi, S., Suematsu, N., Sato, H. (2013). Cholinergic modulation of response gain in the rat primary visual cortex. *Sci Rep,* 3:1138.

Spillantini, MG., Crowther, RA., Jakes, R., Hasegawa, M., Goedert, M. (1998). alpha-Synuclein in filamentous inclusions of Lewy bodies from Parkinson's disease and dementia with lewy bodies. *Proc Natl Acad Sci USA,* 95(11):6469-6473.

Spradling, A. C., Stern, D., Beaton, A., Rhem, E.J., Laverty, T., Mozden, N., Misra, S., and Rubin, G.G. (1999). The Berkeley Drosophila Genome Project gene disruption project: single P-element insertions mutating 25% of vital *Drosophila* genes. *Genetics,* 153:135–177.

St Johnston, D. (2002). The art and design of genetic screens: Drosophila melanogaster. *Nature Rev Genet,* 3:176-188.

Steger, M., Tonelli, F., Ito, G., Davies, P., Trost, M., Vetter, M., Wachter, S., Lorentzen, E., Duddy, G., Wilson, S., Baptista, MA., Fiske, BK., Fell, MJ., Morrow, JA., Reith, AD., Alessi, DR., Mann, M. (2016). Phosphoproteomics reveals that Parkinson's disease kinase LRRK2 regulates a subset of Rab GTPases. *eLIFE,* 5:e12813.

Steganis, L. (2012). α-Synuclein in Parkinson's Disease. *Cold Spring Harb Perspect Med*, 2(2): a009399.

Stenmark, H. (2009). Rab GTPases as coordinators of vesicle traffic. *Nat Rev Mol Cell Biol,* 10(8):513-525.

Stern, MB. (2004). Dopamine agonists modify the course of Parkinson disease. *Arch Neurol,* 61:1969–71.

Strausfeld, N.J. *Atlas of an Insect Brain* (Springer,1976).

Strausfeld, N.J. and Bassemir, U.K. (1985). Lobula plate and ocellar interneurons converge onto a cluster of descending neurons leading to neck and leg motor neuropil in *Calliphora erythrocephala*. *Cell Tissue Res*, 240:617–640.

Strausfeld, N.J. and Seyan, H.S. (1985). Convergence of visual, haltere and prosternal inputs at neck motor neurons of *Calliphora erythrocephala*. *Cell Tissue Res*, 240:601–615.

Suster, ML., Martin, JR., Sung, C., Robinow, S. (2003). Targeted expression of tetanus toxin reveals sets of neurons involved in larval locomotion in *Drosoph J Neurobiol*, 55(2):233-46.

Sweeney, S.T, Broadie, K., Keane, J., Neimann, H., O'Kane, C.J. (1995). Targeted expression of tetanus toxin light chain in *Drosophila* specifically eliminates synaptic transmission and causes behavioral defects. *Neuron,* 14 (2): 341–51.

Sweeney, ST., Davis, GW. (2002). Unrestricted synaptic growth in spinster-a late endosomal protein implicated in TGF-beta-mediated synaptic growth regulation. *Neuron,* 36(3):403-416.

Tabuchi, K., Sawamoto, K., Suzuki, E., Ozaki, K., Sone, M., Hama, C., Tanifuji-Morimoto, T., et al. (2000). GAL4/UAS-WGA system as a powerful tool for tracing Drosophila transsynaptic neural pathways. *J Neurosci Res,* 59:94–99.

Takemura, S. Y., Lu, Z. and Meinertzhagen, I.A. (2008). Synaptic circuits of the *Drosophila* optic lobe: the input terminals to the medulla. *J Comp Neurol*, 509:493–513.

Takemura, S.Y., Karuppudurai, T., Ting, C.Y., Lu, Z., Lee, C.H., Meinertzhagen, I.A. (2011). Cholinergic circuits integrate neighboring visual signals in a *Drosophila* motion detection pathway. *Curr Biol*, 21:2077–2084.

Tan, L.C.S. (2013). Epidemiology of Parkinson's disease. *Neurol Asia*, 18(3):231-238.

Tatton, WG., Kwan, MM., Verrier, MC., Seniuk, NA., Theriault, E. (1990). MPTP produces reversible disappearance of tyrosine hydroxylase-containing retinal amacrine cells. *Brain Res,* 527: 21–31.

Tao-Cheng, J.H. (2006). Activity-related redistribution of presynaptic proteins at the active zone. *Neurosci,* 141:1217–1224.

Taylor, C.A., Yan, J., Howell, A.S., Dong, X., Shen, K. (2015). RAB-10 Regulates Dendritic Branching by Balancing Dendritic Transport. *PLoS Genet*, 11(12):e1005695.

Taymans, JM., Cookson, MR. (2010). Mechanisms in dominant parkinsonism: The toxic triangle of LRRK2, alpha-synuclein, and tau. *Bioessays*, 32(3):227-235.

Technau, GM. (2008). Brain Development in Drosophila Melanogaster. *Berlin: Springer Verlag*; 2008.

Thomas, B., Beal, MF. (2007). Parkinson's disease. *Hum Mol Genet*, 16(2):183-194.

Thum, A.S., Knapek, S., Rister, J., Dierichs-Schmitt, E., Heisenberg, M., Tanimoto, H. (2006). Differential potencies ofeffector genes in adult Drosophila. *J Comp Neurol*, 498(2):194-203.

Todd, AM., Staveley, BE. (2008). Pink1 suppresses alpha-synuclein-induced phenotypes in a *Drosophila* model of Parkinson's disease. *Genome*, 51(12):1040-1046.

Touchot, N., Chardin, P., Tavitian, A. (1987). Four additional members of the ras gene superfamily isolated by an oligonucleotide strategy: molecular cloning of YPT-related cDNAs from a rat brain library. *Proc Natl Acad Sci USA*, 84(23):8210-4.

Trimble, WS., Cowan, DM., Scheller, RH. (1988). VAMP-1: a synaptic vesicle-associated integral membrane protein. *PNAS*, 85(12): 4538–4542.

Tuthill, JC., Nern, A., Rubin, GM., Reiser, MB. (2014). Wide-field feedback neurons dynamically tune early visual processing. *Neuron*, 82:887-95.

Urwyler, P., Nef, T., Killen, A., Collerton, D., Thomas, A., Burn, D., McKeith, I., Mosimann, UP. (2014). Visual complaints and visual hallucinations in Parkinson's disease. *Parkinsonism Relat Disord*, 20:318–22.

Valente, EM., Abou-Sleiman, PM., Caputo, V., Muqit, MM., Harvey, K., Gispert, S., Ali, Z., Del Turco, D., Bentivoglio, AR., Healy, DG., Albanese, A., Nussbaum, R., González-Maldonado, R., Deller, T., Salvi, S., Cortelli, P., Gilks, WP., Latchman, DS., Harvey, RJ., Dallapiccola, B., Auburger, G., Wood, NW. (2004). Hereditary early-onset Parkinson's disease caused by mutations in PINK1. *Science*, 304(5674):1158-1160.

Vazquez-Martinez, R., Cruz-Garcia, D., Duran-Prado, M., Peinado, JR., Castaño, JP. Malagon, MM. (2007). Rab18 inhibits secretory activity in neuroendocrine cells by interacting with secretory granules. *Traffic*, 8(7):867-882.

Venderona, K., Kabbach, G., Abdel-Messih, E., Zhang, Y., Parks, RJ., Imai, Y., Gehrke, S., Ngsee, J., Lavoie, MJ., Slack, RS., Rao, Y., Zhang, Z., Lu, B., Haque, ME., Park, DS. (2009). Leucine-Rich Repeat Kinase 2 interacts with Parkin, DJ-1 and PINK-1 in a *Drosophila melanogaster* model of Parkinson's disease. *Hum Mol Genet*, 18(22):4390-4404.

Verhoeven, K., De Jonghe, P., Coen, K., Verpoorten, N., Auer-Grumbach, M., Kwon, J.M., FitzPatrick, D., Schmedding, E., De Vriendt, E., Jacobs, A., Van Gerwen, V., Wagner, K., Hartung, HP., Timmerman, V. (2003). Mutations in the small GTP-ase late endosomal protein RAB7 cause Charcot-Marie-Tooth type 2B neuropathy. *Am J Hum Genet*, 72:722-727.

Vigil, D., Cherfils, J., Rossman, KL., Der, CJ. (2010). Ras superfamily GEFs and GAPs: validated and tractable targets for cancer therapy? *Nat Rev Cancer*, 10(12):842-857.

Vilarino Guell, C., Wider, C., Ross, OA., Dachsel, JC., Kachergus, JM., Lincoln, SJ., Soto-Ortolaza, AI., Cobb, SA., Wilhoite, GJ., Bacon, JA., Behrouz, B., Melrose, HL., Hentati, E., Puschmann, A., Evans, DM., Conibear, E., Wasserman, WW., Aasly, JO., Burkhard, PR., Djaldetti, R., Ghika, J., Hentati, F., Krygowska-Wajs, A., Lynch, T., Melamed, E., Rajput, A., Rajput, AH., Solida, A., Wu, RM., Uitti, RJ., Wszolek, ZK., Vingerhoets, F., Farrer, MJ. (2011). VPS35 mutations in Parkinson disease. *Am J Hum Genet*, 89(1):162-167.

Vilinsky, I. and Johnson, K. (2012). Electroretinograms in *Drosophila*: A Robust and
Genetically Accessible Electrophysiological System for the Undergraduate Laboratory. *J Undergrad Neurosci Educ*, 11(1):149-157.

Vincent, A., Briggs, L., Chatwin, GF., Emery, E., Tomlins, R., Oswald, M., Middleton, CA., Evans, GJ., Sweeney, ST., Elliott, CJ. (2012). Parkin-Induced Defects in Neurophysiology and Locomotion Are Generated By Metabolic Dysfunction and Not Oxidative Stress. *Hum Mol Genet*, 21(8):1760–1769.

Vitte, J., Traver, S., Maues De Paula, A., Lesage, S., Rovelli, G., Corti, O., Duyckaerts, C., Brice, A. (2010). Leucine-rich repeat kinase 2 is associated with the endoplasmic reticulum in dopaminergic neurons and accumulates

in the core of Lewy bodies in Parkinson disease. *J Neuropathol Exp Neurol*, 69(9):959-972.

Volta, M., Milnerwood, AJ., Farrer, MJ. (2015). Insights from late-onset familial parkinsonism on the pathogenesis of idiopathic Parkinson's disease. *Lancet Neurol*, 14: 1054–64.

Walch-Solimena, C., Jahn, R., Südhof, TC. (1993). Synaptic vesicle proteins in exocytosis: what do we know? *Curr Opin Neurobiol*, 3(3):329-36.

Wang, D,. Qian, Li., Xiong, H., Liu, J., Neckameyer, WS., Oldham, S., Xia, K., Wang, J., Bodmer, R., Zhang, Z. (2006). Antioxidants protect PINK1-dependent dopaminergic neurons in *Drosophila*. *PNAS*, 103(36):13520-13525.

Wang, C., Lu, R., Ouyang, X., Ho, MW., Chia, W., Yu, F., Lim, KL. (2007). Drosophila overexpressing parkin R275W mutant exhibits dopaminergic neuron degeneration and mitochondrial abnormalities. *J Neurosci*, 27(32):8563-8570.

Wang, D., Tang, B., Zhao, G., Pan, Q., Xia, K., Bodmer, R., Zhang, Z. (2008). Dispensable role of *Drosophila* ortholog of LRRK2 kinase activity in survival of dopaminergic neurons. *Mol Neurodegener*, 3:3.

Waschbüsch, D., Michels, H., Strassheim, S., Ossendorf, E., Kessler, D., Gloeckner, CJ, Barnekow, A. (2014). LRRK2 transport is regulated by its novel interacting partner Rab32. *PLoS One*, 9(10):e111632.

Wasmeier, C., Romao, M., Plowright, L., Bennett, D.C., Raposo, G., Seabra M.C. (2006). Rab38 and Rab32 control post-Golgi trafficking of melanogenic enzymes. *J Cell Biol*, 175:271–281.

Webber, PJ., West, AB. (2009). LRRK2 in Parkinson's Disease: Function in Cells and Neurodegeneration. *FEBS J*, 276(22):6436-6444.

Weil, RS., Schrag, AE., Warren, JD., Crutch, SJ., Lees, AJ., Morris, HR. (2016). Visual dysfunction in Parkinson's disease. *Brain*, 139(11):2827-2843.

Weiner, WJ. (2004). Initial treatment of Parkinson disease: levodopa or dopamine agonists. *Arch Neurol*, 61:1966–9.

West, A.B., Moore, DJ., Biskup, S., Bugayenko, A., Smith, WW., Ross, CA., Dawson, VL., Dawson, TM. (2005). Parkinson's disease-associated mutations in leucine-rich repeat kinase 2 augment kinase activity. *PNAS*, 102(46): 16842-16847.

West, AB1., Moore, DJ., Choi, C., Andrabi, SA., Li, X., Dikeman, D., Biskup, S., Zhang, Z., Lim, KL., Dawson, VL., Dawson, TM. (2007). Parkinson's disease-associated mutations in LRRK2 link enhanced GTP-binding and kinase activities to neuronal toxicity. *Hum Mol Genet*, 16(2):223-232.

Winslow, AR1., Chen, CW., Corrochano, S., Acevedo-Arozena, A., Gordon, DE., Peden, AA., Lichtenberg, M., Menzies, FM., Ravikumar, B., Imarisio, S., Brown, S., O'Kane, CJ., Rubinsztein, DC. (2010). α-Synuclein impairs macroautophagy: implications for Parkinson's disease. *J Cell Biol*, 190(6):1023-1037.

Wintermeyer, P., Krüger, R., Kuhn, W., Müller, T., Woitalla, D., Berg, D., Becker, G., Leroy, E., Polymeropoulos, M., Berger, K., Przuntek, H., Schöls, L., Epplen, JT., Riess, O. (2000). Mutation analysis and association studies of the UCHL1 gene in German Parkinson's disease patients. *Neuroreport*, 11(10):2079-2082.

Witkovsky, P. (2004). Dopamine and retinal function. *Doc Ophthalmol*, 108:17-40.

Witkovsky, P., Arango-Gonzales, B., Haycock, JW., Kohler, K. (2005). Rat retinal dopaminergic neurons: differential maturation of somatodendritic and axonal compartments. *J Comp Neurol*, 481(4):352-362.

Woodman, PG. (2000). Biogenesis of the Sorting Endosome: The Role of Rab5. *Traffic*, 1:695-701.

Xiong, Y., Yuan, C., Chen, R., Dawson, TM., Dawson, VL. (2012). ArfGAP1 is a GTPase activating protein for LRRK2: reciprocal regulation of ArfGAP1 by LRRK2. *J Neurosci*, 32(11):3877-3886.

Yang, Y., Nishimura, I., Imai, Y., Takahashi, R., Lu, B. (2003). Parkin suppresses dopaminergic neuron-selective neurotoxicity induced by Pael-R in Drosophila. *Neuron*, 37(6):911-924.

Yang, Y., Gehrke, S., Haque, ME., Imai, Y., Kosek, J., Yang, L., Beal, MF., Nishimura, I., Wakamatsu, K., Ito, S., Takahashi, R., Lu, B. (2005) Inactivation of Drosophila DJ-1 leads to impairments of oxidative stress response and phosphatidylinositol 3-kinase/Akt signaling. *Proc Natl Acad Sci USA*, 102: 13670–13675.

Yang, Y,. Ouyang, Y., Beal, MF., McQuibban, A., Vogel, H., Lu, B. (2008). Pink1 regulates mitochondrial dynamics through interaction with the fission/fusion machinery. *Proc Natl Acad Sci USA*, 105(19):7070-7075.

Yang, Q. and Mao, Z. (2010). Parkinson disease: a role for autophagy? *Neuroscientist,* 16:335–341.

Yao, C., Johnson, WM., Gao, Y., Wang, W., Zhang, J., Deak, M., Alessi, DR., Zhu, X., Mieyal, JJ., Roder, H., Wilson-Delfosse, AL., Chen, SG. (2013). Kinase inhibitors arrest neurodegeneration in cell and c. elegans models of LRRK2 toxicity. *Hum Mol Genet*, 22:328–344.

Youdim, MBH., Edmondson, D., Tipton, KF. (2006). The therapeutic potential of monoamine oxidase inhibitors. *Nature Rev Neurosci,* 7:295-309.

Yu, Z., Ren, M., Wang, Z., Zhang, B., Rong, YS., Jiao, R., Gao, G. (2013). Highly Efficient Genome Modifications Mediated by CRISPR/Cas9 in *Drosophila*. *Genetics,* 195:289-291.

Yun, HJ., Park, J., Ho, DH., Kim, H., Kim, CH., Oh, H., Ga, I., Seo, H., Chang, S., Son, I., Seol, W. (2013). LRRK2 phosphorylates Snapin and inhibits interaction of Snapin with SNAP-25. *Exp Mol Med*, 45:e36.

Yun, HJ., Kim, H., Ga, I., Oh, H., Ho, DH., Kim, J., Seo, H., Son, I., Seol, W. (2015). An early endosome regulator, Rab5b, is a LRRK2 kinase substrate. *J Biochem*, 157(6):485-95.

Zerial, M., McBride, H. (2001). Rab proteins as membrane organizers. *Nature Rev Mol Cell Biol*, 2:107-117.

Zhang, J., Schulze, KL., Hiesinger, PR., Suyama, K., Wang, S., Fish, M., Acar, M., Hoskins, RA., Bellen, HJ., Scott, MP. (2007). Thirty-one flavors of Drosophila rab proteins. *Genetics*, 176(2):1307-22.

Zhang, D.Q., Wong, K.Y., Sollars, P.J., Berson, D.M., Pickard, G.E., McMahon, D.G. (2008). Intraretinal signaling by ganglion cell pgotoreceptors to dopaminergic amacrine neurons. *PNAS*, 105 (37): 14181-14186.

Zheng, L., De Polavieja, GG., Wolfram, V., Asyali, MH., Hardie, RC., Juusola, M. (2006). Feedback network controls photoreceptor output at the layer of first visual synapses in Drosophila. *J Gen Physiol*, 127:495-510.

Zheng, L., Nikolaev, A., Wardill, T.J., O'Kane, C.J., de Polavieja, G.G., Juusola, M. (2009). Network adaptation improves temporal representation of naturalistic stimuli in *Drosophila* eye: I. dynamics. *PLoS ONE,* 4(1):e4307.

Zhou, L., Schnitzler, A., Agapite, J., Schwartz, LM., Steller, H., Nambu, JR. (1997). Cooperative functions of the reaper and head involution defective

genes in the programmed cell death of *Drosophila* central nervous system midline cells. *Proc Natl Acad Sci USA,* 94(10):5131-6.

Zhu, Y., Hu, L., Zhou, Y., Yao, Q., Liu, L., Shao, F. (2010). Structural mechanism of host Rab1 activation by the bifunctional Legionella type IV effector SidM/DrrA. *Proc Natl Acad Sci USA,* 107(10):4699-4704.

Zhu, Y. (2013). The *Drosophila* visual system. *Cell Adh Migr,* 7(4):333-344.

Zou, W., Yadav, S., DeVault, L., Jan, Y.N., Sherwood, D.R. (2015). RAB-10-Dependent Membrane Transport Is Required for Dendrite Arborization. *PLoS Genet,* 11(9):e1005484.

Zimprich, A., Biskup, S., Leitner, P., Lichtner, P., Farrer, M., Lincoln, S., Kachergus, J., Hulihan, M., Uitti, RJ., Calne, DB., Stoessl, AJ., Pfeiffer, RF., Patenge, N., Carbajal, IC., Vieregge, P., Asmus, F., Müller-Myhsok, B., Dickson, DW., Meitinger, T., Strom, TM., Wszolek, ZK., Gasser, T. (2004). Mutations in *LRRK2* Cause Autosomal-Dominant Parkinsonism with Pleiomorphic Pathology. *Neuron,* 44: 601-607.